Chapter 1

Hydrodynamics

In this document, the hydrodynamic equations are derived that govern the tidal dynamics in estuaries and coastal seas. The three-dimensional shallow water equations are reduced in complexity by using a scaling analysis, perturbation method and harmonic decomposition.

The derivation starts from the three-dimensional shallow water equations. Using a scaling analysis, a small parameter is identified which is then used to determine the order of magnitude of each term. A perturbation method is used to establish which terms balance at leading, first and higher order. All non-linear terms are of first and higher order. The leading-order balances are therefore linear and much easier to solve then the original non-linear equations. The non-linear and higher-order terms are not neglected, but are instead included in the higher-order balances. The non-linearities act as forcing mechanisms in the linear higher-order balances. The linearity of the balances at each order allows the effect of individual forcing mechanisms to be identified. The time dependency of the water motion is resolved using harmonic decomposition.

Background

A considerable volume of literature has been published on estuarine dynamics. These models range from explanatory to complex (Murray, 2003). Explanatory models aim to simplify the dynamics as much as possible, while retaining the essential processes. They strive for a qualitative agreement with reality. On the other hand, complex models aim to include as much complexity as possible to represent reality as closely as possible. They strive for a quantitative agreement with reality. Explanatory models are often better suited to increase understanding of estuarine processes, whereas complex models are often better suited to provide forecasts of realistic estuaries.

Various explanatory models have been made. Among these models are perturbative models. The use of a perturbation method is motivated by two observations. Firstly, this approach allows for the identification and isolation of individual forcing mechanisms and, secondly, it reduces the complexity of the equations.

Below, the developments in this area of research are briefly summarized, but this overview is by no means exhaustive. Kreiss (1957) was the first to apply a perturbation approach to obtain the leading- and first-order water motion in a one-dimensional, depth-averaged model of constant width and depth. Later this approach was extended by Gallagher and Munk (1971); Li (1974); Kabbaj and Le Provost (1980); Uncles (1981); DiLorenzo (1988); Shetye and Gouviea (1992). Ianniello (1977) extended this approach to include the vertical structure of both the tide and residual currents generated by the non-linear tidal interactions. In 1979, Ianniello extended his model to include estuaries of variable width and depth. Other authors using this method to resolve the two-dimensional vertical structure are McCarthy (1993); Cheng *et al.* (2010); Chernetsky (2012); Dijkstra (2019) and to analyse the three-dimensional structure are Winant (2007, 2008); Waterhouse *et al.* (2011); Ensing *et al.* (2015); Wei (2017); Kumar (2018).

1.1 The hydrodynamic equations

The water motion is described by the three-dimensional, Reynolds-averaged shallow water equations. In these equations, the turbulent fluctuations are taken into account using the eddy viscosity formulation and the effects of Coriolis using the f-plane approximation. Moreover, the equations are expressed in (local) Cartesian coordinates because the characteristic length scales of the considered systems are much smaller than the radius of the Earth (LeBlond and Mysak, 1978, p. 17). We assume that the density variations are small compared to the average density and that the horizontal length scale is much larger than the vertical length scale allowing for the Boussinesq approximation and the hydrostatic balance, respectively. The equations that solve for the water level elevation $\zeta(x,y,t)$ and the three Cartesian velocity components $u(x,y,z,t)$, $v(x,y,z,t)$, $w(x,y,z,t)$ read (see, e.g., Cushman-Roisin and Beckers, 2009, p. 98)

$$\begin{cases} u_x + v_y + w_z = 0, & \text{(continuity)} \\ u_t + uu_x + vu_y + wu_z - fv = -g(R_x + \zeta_x) - g\displaystyle\int_z^{R+\zeta} \frac{\rho_x}{\rho_0}\, d\tilde{z} + (A_\mathrm{h} u_x)_x + (A_\mathrm{h} u_y)_y + (A_v u_z)_z, & \text{(x-momentum)} \\ v_t + uv_x + vv_y + wv_z + fu = -g(R_y + \zeta_y) - g\displaystyle\int_z^{R+\zeta} \frac{\rho_y}{\rho_0}\, d\tilde{z} + (A_\mathrm{h} v_x)_x + (A_\mathrm{h} v_y)_y + (A_v v_z)_z, & \text{(y-momentum)} \\ \zeta_t + \left(\displaystyle\int_{-H}^{R+\zeta} u\, dz\right)_x + \left(\displaystyle\int_{-H}^{R+\zeta} v\, dz\right)_y = 0. & \text{(depth-integrated continuity)} \end{cases}$$

Here, x, y and z are the three Cartesian coordinates in a right-handed coordinate system with z pointing upwards, t is the time, f is the Coriolis parameter, g the acceleration of gravity, ρ is the density with reference density ρ_0, R is a reference level and A_h, A_v are the horizontal and vertical eddy viscosities, respectively. The subscripts x, y, z and t denote taking the partial derivative with respect to these variables.

A sketch of the vertical geometry is shown in Figure 1.1b. Mean sea level (MSL) is located at $z = 0$. The bed level $z = -H(x,y)$ is defined relative to MSL, where the depth H is the signed distance from MSL to the bed. The surface level is located at $z = R(x,y) + \zeta(x,y,t)$ relative to MSL. Here, the reference level R is an estimate for the stationary mean part of the free surface and ζ is the (remaining) fluctuating part. This reference level is introduced by Dijkstra (2019, p. 40) to ensure that the mean water depth in the model, $R + H$, remains positive when, for example, the bed is above mean sea level over part of the domain and it provides an useful estimate for the mean water depth.

The next step in obtaining a well-posed mathematical problem is the formulation of the boundary conditions. The boundary conditions specify the behaviour of the fluid at the boundary while the equations govern the fluid behaviour inside the domain. The domain and boundary conditions depend on the problem under consideration. We will mostly study the tidal dynamics in estuaries and, therefore, a sketch of an estuary is shown in Figure 1.1a. The *lateral* boundaries of an estuary can be divided into three categories: boundaries that are connected with the sea $\partial\Omega_\mathrm{sea}$, impermeable bank boundaries $\partial\Omega_\mathrm{bank}$ and boundaries that are connected with rivers and tributaries $\partial\Omega_\mathrm{river}$.

For boundaries connected with the sea, the tidal amplitude is prescribed:

$$\zeta = A(x,y,t), \qquad \text{at} \quad \partial\Omega_\mathrm{sea}. \qquad \text{(tidal forcing)}$$

At the estuarine banks, a no-slip boundary condition is used (Pedlosky, 1987, p. 186):

$$u = v = w = 0, \qquad \text{at} \quad \partial\Omega_\mathrm{bank}. \qquad \text{(no-slip)}$$

Along the boundaries connected with a river or tributary, the riverine velocity is imposed:

$$\boldsymbol{u} = \boldsymbol{u}_\mathrm{river}(x,y,z,t), \qquad \text{at} \quad \partial\Omega_\mathrm{river}. \qquad \text{(riverine forcing)}$$

Here, the bold symbol $\boldsymbol{u}$ is shorthand notation for a velocity vector with components (u,v,w).

Formally speaking, the hydrostatic assumption implies that the z-momentum equation, a second-order differential equation, has been reduced to a zeroth-order differential equation with respect to the horizontal coodinates. Therefore, the vertical velocity w cannot satisfy the boundary conditions imposed at the lateral sides (Vreugdenhil, 1994, p. 22). Only by including the higher-order horizontal terms, which requires the use of non-hydrostatic models, can the vertical velocity w be required to satisfy the imposed lateral boundary conditions.

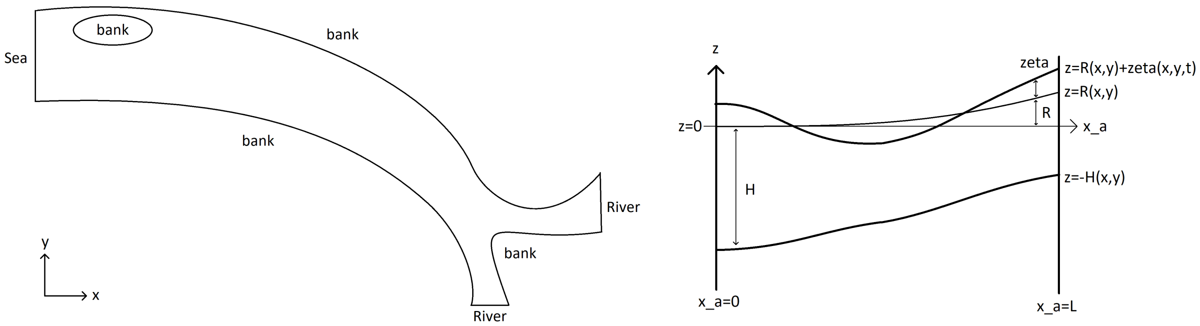

(a) Top-view (b) Side-view

Figure 1.1: Two schematic representations of an idealised estuary. The top-view in (a) shows an example of the lateral geometry of an estuary. For each section of lateral boundary, the corresponding boundary type is indicated. The side-view in (b) illustrates the relationship between the various vertical geometry components in an idealised, along-channel cross-section of an estuary.

The sea, bank and river boundary conditions specify the fluid behaviour at the lateral boundaries of the estuary. However, a body of water is also bounded in the vertical direction, namely at the free surface and the bed, respectively. Focussing on the free surface first, we impose that fluid particles on the free surface always remain part of the free surface. The corresponding condition is called a kinematic boundary condition (see, e.g., Lamb, 1932, p. 7). In addition, the shear stresses acting on the free surface by, for example, the wind are ignored. Therefore, a dynamic no-stress condition is imposed. The kinematic and dynamic boundary conditions read

$$
\begin{aligned}
w &= \zeta_t + u(R+\zeta)_x + v(R+\zeta)_y, && \text{at} \quad z = R+\zeta, && \text{(kinematic)} \\
A_v u_z &= A_v v_z = 0, && \text{at} \quad z = R+\zeta. && \text{(no-stress)}
\end{aligned}
$$

At the bed, a no-slip condition is prescribed:

$$
u = v = w = 0, \qquad \text{at} \quad z = -H. \qquad \text{(no-slip)}
$$

Strictly speaking, it is not necessary to include the depth-integrated continuity equation in the hydrodynamic equations as this equation can be derived from the continuity equation and boundary conditions.[1] The depth-integrated continuity equation is included in the hydrodynamic equations for completeness.

Nomenclature

Perhaps, it is helpful for future reference to briefly mention the physically motivated names used to indicate each term in the momentum equations before proceeding with the analysis of the equations. The x- and y-momentum equations describe the same physical phenomena, so it is sufficient to only consider the x-momentum equation. The terms are generally referred to as

$$
\underbrace{u_t}_{\text{local inertia}} + \underbrace{uu_x + vu_y + wu_z}_{\text{advection}} - \underbrace{fv}_{\text{Coriolis}} = \underbrace{-g(R_x + \zeta_x)}_{\text{barotropic pressure}} - \underbrace{g\int_z^{R+\zeta} \frac{\rho_x}{\rho_0}\, d\tilde{z}}_{\text{baroclinic pressure}} + \underbrace{(A_\mathrm{h} u_x)_x + (A_\mathrm{h} u_y)_y}_{\text{horizontal eddy viscosity}} + \underbrace{(A_v u_z)_z}_{\text{vertical eddy viscosity}} .
$$

1.2 Scaling analysis

A scaling analysis is a systematic mathematical procedure to determine the relative importance of the different terms in an equation. The first step in a scaling analysis is to introduce a typical scale for each variable in

[1] The depth-integrated continuity equation can be obtained by integrating the continuity equation over the depth. Then, applying Leibniz integral rule and the kinematic and no-slip boundary conditions yields the desired equation (see, e.g., Rozendaal, 2019, p. 14).

an equation. The next step is to non-dimensionalize the coefficients by dividing by the 'largest' dimensional coefficient. A key step in the scaling analysis is the identification of a small non-dimensional parameter. By relating the non-dimensional coefficients to this small parameter, the relative importance of each term can be identified. The most dominant terms are called *leading-order terms*. The terms that are significantly smaller than these leading-order terms are further categorised according to their relative importance. The most dominant terms, after removing the leading-order terms, are called *first-order terms*. This categorisation continues, with all terms of second- and higher-order referred to as *higher-order terms*.

When solving the resulting equations, one can choose to solve the *nondimensional* equations for the *nondimensional* variables or to solve the equivalent *dimensional* equations for the *dimensional* variables. Both methods have their merits. The dimensionless approach, on the one hand, yields equations in which the terms are of comparable order of magnitude. Therefore, the discretized equations and subsequent calculations are less prone to numerical round-off errors. Additionally, the nondimensional variables can be scaled to any specific application and are, therefore, very general. However, the nondimensional results themselves can appear quite artificial to some people. On the other hand, the dimensional approach yields equations that are easier to compare with those found in literature and the dimensional variables are naturally scaled to the specific case under consideration. This results in solutions that can be directly interpreted physically. The dimensional approach is pursued here because for our applications the benefits outweigh those of the nondimensional method.

The first step in a perturbation approach is the scaling of the equations. This scaling is used to identify which terms balance at leading order and which terms balance at higher order. The current scaling analysis is based upon five crucial assumptions:

1. It is assumed that the typical water level elevation is much smaller than the typical depth, such that their ratio is much smaller than unity:
$$\varepsilon = \frac{A_{M_2}}{H_0} \ll 1.$$
The small parameter ε is used to determine the order of the non-dimensional coefficients and, therefore, informally of the corresponding non-dimensional and dimensional terms. A term is called leading order if its typical magnitude is independent of ε and is denoted by $\mathcal{O}(1)$. A term is referred to as first order if its typical magnitude is of order ε compared to the leading-order terms and this is denoted by $\mathcal{O}(\varepsilon)$. Likewise, an nth order term is of order ε^n compared to the leading-order terms and this is denoted by $\mathcal{O}(\varepsilon^n)$.

2. It is assumed that the typical wave length scale, the typical bathymetric length scale and the typical convergence length scale are of the same order of magnitude as the length of the tidal influence into the estuary. This allows us to define a single estuarine length scale L. This assumption implies that all variations should be smooth over the length of the estuary. The result of this assumption is that the non-linear advective terms are first order in ε.

3. It is assumed that the length scale L_R on which the reference level changes is much larger than the estuarine length scale L, i.e., $L_R \gg L$. We assume that $L_R = 1/\varepsilon^2 L$. This assumption implies that the gradient of the reference level is a first-order contribution in the momentum equations.[2]

4. It is assumed that the horizontal density gradient ρ_∇ is small, such that, $\rho_\nabla L/\rho_0$ is of order ε^2. A consequence of this assumption is that the non-linear baroclinic pressure term is of order ε.

5. It is assumed that the horizontal eddy viscosity $\mathscr{A}_\mathrm{h}$ is small. We assume that $\mathscr{A}_\mathrm{h} T_{M_2}/L^2$ is of order ε^2. This assumption implies that the horizontal eddy viscosity terms are of order ε^2.

To determine the order of magnitude of each term, the equations are scaled using nine typical scales. These nine scales consist of six independent scales and three depended scales, which are shown in Table 1.1. The three dependent scales are based on three balances the flow is assumed to approximately satisfy. The three depended scales are derived below:

[2]The ordering of the reference level terms is sensitive to the chosen length scale of the reference level L_R. Provided that the reference level R scales with the average depth scale H_0, see Table 1.1, the reference level terms can either be dominant $\mathcal{O}(1/\varepsilon)$, leading-order $\mathcal{O}(1)$ or first-order $\mathcal{O}(\varepsilon)$ terms for $L_R = \mathcal{O}(1)L$, $L = \mathcal{O}(1/\varepsilon)L$ and $L_R = \mathcal{O}(1/\varepsilon^2)L$, respectively. Thus if the reference level is relatively large and changes on the estuarine length scale, then these terms can (locally) dominate the dynamics.

1. We derive a typical horizontal velocity scale U from the depth-integrated continuity equation. We introduce the characteristic scales into this equation to make it dimensionless. The superscript $*$ denotes a dimensionless variable. This results in the following balance:

$$\frac{A_{M_2}}{T_{M_2}} \underbrace{\zeta^*_{t^*}}_{\mathcal{O}(1)} + \frac{H_0 U}{L} \underbrace{\left(\int_{-H^*}^{R^*+\varepsilon\zeta^*} u^* \, dz^* \right)_{x^*}}_{\mathcal{O}(1)} + \frac{H_0 U}{L} \underbrace{\left(\int_{-H^*}^{R^*+\varepsilon\zeta^*} v^* \, dz^* \right)_{y^*}}_{\mathcal{O}(1)} = 0,$$

   using assumptions 1 and 2.

   Strictly speaking, the upper limit of integration still depends on ε and, therefore, contributes to the integral. However, using a Taylor expansion it can be shown that this leads to a marginal contribution and that the integral is, to leading order, a leading-order term. See below for a more elaborate discussion.

   We require an approximate balance between these three leading-order terms, yielding the horizontal velocity scale:

$$U = \frac{A_{M_2}}{H_0} \frac{L}{T_{M_2}}.$$

2. The typical vertical velocity W scale follows from the three-dimensional, continuity equation. The continuity equation in dimensionless form reads

$$\frac{U}{L} u^*_{x^*} + \frac{U}{L} v^*_{y^*} + \frac{W}{H_0} w^*_{z^*} = 0.$$

   Here, assumption 2 is used. We furthermore assume that that all three terms are of the same order of magnitude. The approximate vertical velocity scale is then given by

$$W = \frac{H_0}{L} U.$$

3. The vertical eddy viscosity term is not necessarily a leading-order term everywhere in the domain. However, since two boundary conditions need to be satisfied, it follows that there is a region in which this term becomes leading order. In addition, since the water is assumed to be shallow, this region can occupy a significant part of the water column. Hence, this term is included in the leading-order balance.

   A typical vertical eddy viscosity scale $\mathcal{A}_v$ can be derived from the non-dimensional, uniform, stationary, barotropic momentum balance:

$$\frac{\mathcal{A}_v U}{H_0^2} \left(A_v^* u^*_{z^*} \right)_{z^*} = \frac{g A_{M_2}}{L} \zeta^*_{x^*},$$

   such that the typical eddy viscosity scale reads as

$$\mathcal{A}_v = \frac{g T_{M_2} H_0^3}{L^2},$$

   where again assumption 2 has been used.

The next step in the scaling analysis is to introduce the typical scales into the equations of motion.

Scaling the continuity equation

The continuity equation is made dimensionless using the typical scales given in Table 1.1. The dimensionless continuity equation is obtained after multiplying by L/U and is given by

$$u^*_{x^*} + v^*_{y^*} + w^*_{z^*} = 0.$$

Hence, the order of magnitude of the terms in the *dimensional*, continuity equation reads

$$\underbrace{u_x}_{\mathcal{O}(1)} + \underbrace{v_y}_{\mathcal{O}(1)} + \underbrace{w_z}_{\mathcal{O}(1)} = 0.$$

Table 1.1: Typical scales of the variables. The dependent scales are derived in the text.

	Scale	Description	Dimensionless quantity
Independent	T_{M_2}	M_2 tidal period	$t = T_{M_2} t^*$ and $f = f^* / T_{M2}$
	A_{M_2}	M_2 tidal amplitude	$\zeta = A_{M_2} \zeta^*$ and $A = A_{M_2} A^*$
	H_0	Average depth	$z = H_0 z^*$, $R = H_0 R^*$ and $H = H_0 H^*$
	L	Length of estuary	$x = Lx^*$ and $y = Ly^*$
	ρ_∇	Typical density gradient	$\nabla\rho = \rho_\nabla \nabla^* \rho^*$
	$\mathscr{A}_\mathrm{h}$	Typical horizontal eddy viscosity	$A_\mathrm{h} = \mathscr{A}_\mathrm{h} A_\mathrm{h}^*$
Dependent	U	Typical horizontal velocity	$u = Uu^*$, $v = Uv^*$, $u_\mathrm{river} = Uu^*_\mathrm{river}$ and $v_\mathrm{river} = Uv^*_\mathrm{river}$
	W	Typical vertical velocity	$w = Ww^*$ and $w_\mathrm{river} = Ww^*_\mathrm{river}$
	$\mathscr{A}_v$	Typical vertical eddy viscosity	$A_v = \mathscr{A}_v A_v^*$

Scaling the x-momentum equation

The x-momentum equation can be made dimensionless upon substituting the typical scales. After multiplying by T_{M_2}/U and using the derived scales, we obtain

$$u^*_{t^*} + \frac{A_{M_2}}{H_0}\left(u^* u^*_{x^*} + v^* u^*_{y^*} + w^* u^*_{z^*}\right) - f^* v^* = -gH_0 \frac{T^2_{M_2}}{L^2}\left(\varepsilon R^*_{x^*} + \zeta^*_{x^*}\right) - gH_0 \frac{\rho_\nabla T^2_{M_2}}{\rho_0 L}\frac{H_0}{A_{M_2}} \int_{z^*}^{R^*+\varepsilon\zeta^*} \rho^*_{x^*}\, d\tilde{z}^*$$
$$+ \frac{\mathscr{A}_\mathrm{h} T_{M_2}}{L^2}\left(\left(A^*_\mathrm{h} u^*_{x^*}\right)_{x^*} + \left(A^*_\mathrm{h} u^*_{y^*}\right)_{y^*}\right) + gH_0 \frac{T^2_{M_2}}{L^2}\left(A^*_v u^*_{z^*}\right)_{z^*}.$$

Here, assumption 3 is used to determine the scaling of the reference level gradient.

The nondimensional factor A_{M_2}/H_0 in front of the momentum advection terms $u^* u^*_{x^*} + v^* u^*_{y^*} + w^* u^*_{z^*}$ denotes the ratio between the typical tidal amplitude and the typical depth. This parameter is called ε and is assumed to be much smaller than unity (assumption 1):

$$\varepsilon = \frac{A_{M_2}}{H_0} \ll 1.$$

This parameter is used to determine the ordering of the three other coefficients in the dimensionless momentum equation, which are discussed below.

The first factor is given by $gH_0 \cdot T^2_{M_2}/L^2$ and can be recognised as the square of the ratio between the barotropic shallow-water wave velocity $c_E = \sqrt{gH_0}$ and an estimation of this velocity $\tilde{c}_E = L/T_{M_2}$ (assumption 2):

$$gH_0 \frac{T^2_{M_2}}{L^2} = \left(\frac{c_E}{\tilde{c}_E}\right)^2 = \mathscr{O}(1).$$

We stress that this scaling is only valid for systems we are interested in.

The next factor to consider is $gH_0 \cdot \rho_\nabla T^2_{M_2}/(\rho_0 L) \cdot H_0/A_{M_2}$, which is the ratio between the internal baroclinic wave velocity $c_I = c_E \rho_\nabla L/\rho_0$ and the horizontal velocity U. This ratio is typically known as the reciprocal of the *densimetric Froude number* (Dyke, 2001, p. 153). Using the approximate barotropic wave velocity equality $c_E \approx \tilde{c}_E$ (assumption 2), the dimensionless number can be rewritten as

$$\frac{1}{\mathrm{Fr_d}} = \frac{c_I}{U} = gH_0 \frac{\rho_\nabla T^2_{M_2}}{\rho_0 L}\frac{H_0}{A_{M_2}} \approx \frac{\rho_\nabla L}{\rho_0}\frac{H_0}{A_{M_2}} = \mathscr{O}(\varepsilon),$$

where we have assumed that horizontal density gradient is small such that $\rho_\nabla L/\rho_0$ is of order ε^2 (assumptions 1 and 4). These assumptions imply that the internal baroclinic waves are much slower than the horizontal flow.

The limits of integration of the baroclinic term still depend on ε. We can linearise the integrand around $\tilde{z}^* = R^*$

using a Taylor expansion because ε is small (assumption 1) to obtain

$$\begin{aligned}
\int_{z^*}^{R^*+\varepsilon\zeta^*} \rho^*_{x^*}\,d\tilde{z}^* &= \int_{z^*}^{R^*} \rho^*_{x^*}\,d\tilde{z}^* + \int_{R^*}^{R^*+\varepsilon\zeta^*} \sum_{n=0}^{\infty} \frac{\rho^{*(n)}_{x^*}\big|_{\tilde{z}^*=R^*}}{n!}(\tilde{z}^*-R^*)^n\,d\tilde{z}^* \\
&= \int_{z^*}^{R^*} \rho^*_{x^*}\,d\tilde{z}^* + \sum_{n=0}^{\infty} \varepsilon^{n+1}\frac{\rho^{*(n)}_{x^*}\big|_{\tilde{z}^*=R^*}}{(n+1)!}(\zeta^*)^{n+1} \\
&= \int_{z^*}^{R^*} \rho^*_{x^*}\,d\tilde{z}^* + \varepsilon\rho^*_{x^*}\big|_{\tilde{z}^*=R^*}\zeta^* + \dots.
\end{aligned}$$

Another, possibly simpler, method to arrive at this result is to Taylor expand the integral itself around the upper limit of integration R^* and evaluate it at $R^*+\varepsilon\zeta^*$.

Lastly, we consider the horizontal viscosity factor $\mathscr{A}_\mathrm{h} T_{M_2}/L^2$. This factor is the ratio between the horizontal viscous velocity $c_V = \mathscr{A}_\mathrm{h}/L$ and the barotropic wave velocity $\tilde{c}_E$. The order of magnitude of this factor can be expressed as

$$\frac{\mathscr{A}_\mathrm{h} T_{M_2}}{L^2} = \frac{c_V}{\tilde{c}_E} = \mathscr{O}(\varepsilon^2),$$

which is small by assumption 5.

The terms in the *dimensional* x-momentum equation then have the following order of magnitude:

$$\underbrace{u_t}_{\mathscr{O}(1)} + \underbrace{uu_x + vu_y + wu_z}_{\mathscr{O}(\varepsilon)} - \underbrace{fv}_{\mathscr{O}(1)} = -g(\underbrace{R_x}_{\mathscr{O}(\varepsilon)} + \underbrace{\zeta_x}_{\mathscr{O}(1)}) - \underbrace{g\int_z^R \frac{\rho_x}{\rho_0}\,d\tilde{z}}_{\mathscr{O}(\varepsilon)} - \underbrace{g\frac{\rho_x|_{z=R}}{\rho_0}\zeta}_{\mathscr{O}(\varepsilon^2)} + \dots + \underbrace{(A_\mathrm{h}u_x)_x + (A_\mathrm{h}u_y)_y}_{\mathscr{O}(\varepsilon^2)} + \underbrace{(A_\mathrm{v}u_z)_z}_{\mathscr{O}(1)}.$$

Scaling the y-momentum equation

The x- and y-momentum equations describe exactly the same physical phenomena in two different spatial directions. Moreover, no distinction has been made between the characteristic scales in these two dimensions. As such, the scaling of the y-momentum equation is completely analogues to the scaling of the x-momentum equation and is omitted.

The order of magnitude of the dimensional y-momentum equation is given by

$$\underbrace{v_t}_{\mathscr{O}(1)} + \underbrace{uv_x + vv_y + wv_z}_{\mathscr{O}(\varepsilon)} + \underbrace{fu}_{\mathscr{O}(1)} = -g(\underbrace{R_y}_{\mathscr{O}(\varepsilon)} + \underbrace{\zeta_y}_{\mathscr{O}(1)}) - \underbrace{g\int_z^R \frac{\rho_y}{\rho_0}\,d\tilde{z}}_{\mathscr{O}(\varepsilon)} - \underbrace{g\frac{\rho_y|_{z=R}}{\rho_0}\zeta}_{\mathscr{O}(\varepsilon^2)} + \dots + \underbrace{(A_\mathrm{h}v_x)_x + (A_\mathrm{h}v_y)_y}_{\mathscr{O}(\varepsilon^2)} + \underbrace{(A_\mathrm{v}v_z)_z}_{\mathscr{O}(1)}.$$

Scaling the depth-integrated continuity equation

The depth-integrated continuity equation is made dimensionless by substituting the typical scales given in Table 1.1. After multiplying by T_{M_2}/A_{M_2} and using the derived scales, the following equation is obtained

$$\zeta^*_{t^*} + \left(\int_{-H^*}^{R^*+\varepsilon\zeta^*} u^*\,dz^*\right)_{x^*} + \left(\int_{-H^*}^{R^*+\varepsilon\zeta^*} v^*\,dz^*\right)_{y^*} = 0.$$

The limits of integration still depend on ε. We start with the first integral term. To determine its order, we can linearise the integrand around $z^*=R^*$ using a Taylor expansion to obtain

$$\begin{aligned}
\int_{-H^*}^{R^*+\varepsilon\zeta^*} u^*\,dz^* &= \int_{-H^*}^{R^*} u^*\,dz^* + \sum_{n=0}^{\infty} \varepsilon^{n+1}\frac{u^{*(n)}\big|_{z^*=R^*}}{(n+1)!}(\zeta^*)^{n+1} \\
&= \int_{-H^*}^{R^*} u^*\,dz^* + \varepsilon u^*|_{z^*=R^*}\zeta^* + \dots.
\end{aligned}$$

The linearisation of the second integral term follows analogously. The order of magnitude of the dimensional, depth-integrated continuity equation therefore reads

$$\underbrace{\zeta_t}_{\mathscr{O}(1)} + \underbrace{\left(\int_{-H}^{R} u\,dz\right)_x}_{\mathscr{O}(1)} + \underbrace{(u|_{z=R}\zeta)_x}_{\mathscr{O}(\varepsilon)} + \dots + \underbrace{\left(\int_{-H}^{R} v\,dz\right)_y}_{\mathscr{O}(1)} + \underbrace{(v|_{z=R}\zeta)_y}_{\mathscr{O}(\varepsilon)} + \dots = 0.$$

For the scaling analysis, the order of magnitude of the boundary conditions is required as well, which is the subject of the next section.

Scaling the boundary conditions

The lateral boundary conditions are made dimensionless by substituting their characteristic scales, which are given in Table 1.1. The oder of magnitude of the prescribed tidal amplitude is given by

$$\underbrace{\zeta}_{\mathcal{O}(1)} = \underbrace{A(x,y,t)}_{\mathcal{O}(1)}, \qquad \text{at} \quad \partial\Omega_{\text{sea}}. \qquad \text{(tidal forcing)}$$

The ordering of the no-slip boundary condition reads

$$\underbrace{u}_{\mathcal{O}(1)} = \underbrace{v}_{\mathcal{O}(1)} = \underbrace{w}_{\mathcal{O}(1)} = 0, \qquad \text{at} \quad \partial\Omega_{\text{bank}}, \qquad \text{(no-slip)}$$

and, lastly, the order of magnitude of the imposed riverine flow takes the form:

$$\underbrace{\boldsymbol{u}}_{\mathcal{O}(1)} = \underbrace{\boldsymbol{u}_{\text{river}}(x,y,z,t)}_{\mathcal{O}(1)}, \qquad \text{at} \quad \partial\Omega_{\text{river}}. \qquad \text{(riverine forcing)}$$

The boundary conditions imposed at the free surface need to be linearised to determine their order of magnitude. We illustrate the process for the kinematic boundary condition. The gradient of reference level is still assumed to be small. Using the typical scales, the dimensionless kinematic boundary condition is obtained:

$$w^* = \zeta^*_{t^*} + \varepsilon\big(u^*(\varepsilon R^* + \zeta^*)_{x^*} + v^*(\varepsilon R^* + \zeta^*)_{y^*}\big), \qquad \text{at} \quad z^* = R^* + \varepsilon\zeta^*.$$

This equation is evaluated at the free surface, making it nonlinear. All terms that depend on z^* are Taylor expanded around $z^* = R^*$ and evaluated at $z^* = R^* + \varepsilon\zeta^*$, resulting in

$$\sum_{n=0}^{\infty} \varepsilon^n \frac{w^{*(n)}\big|_{z^*=R^*}}{n!}(\zeta^*)^n = \zeta^*_{t^*} + \varepsilon\left[\left(\sum_{n=0}^{\infty} \varepsilon^n \frac{u^{*(n)}\big|_{z^*=R^*}}{n!}(\zeta^*)^n\right)(\varepsilon R^* + \zeta^*)_{x^*} + \left(\sum_{n=0}^{\infty} \varepsilon^n \frac{v^{*(n)}\big|_{z^*=R^*}}{n!}(\zeta^*)^n\right)(\varepsilon R^* + \zeta^*)_{y^*}\right].$$

Only leading- and first-order contributions are retained to obtain:

$$w^*|_{z^*=R^*} + \varepsilon w^*_{z^*}|_{z^*=R^*}\zeta^* + \ldots = \zeta^*_{t^*} + \varepsilon\big(u^*|_{z^*=R^*}\zeta^*_{x^*} + \ldots + v^*|_{z^*=R^*}\zeta^*_{y^*} + \ldots\big).$$

Thus, the order of magnitude of the linearized kinematic boundary condition is given by

$$\underbrace{w}_{\mathcal{O}(1)} + \underbrace{w_z\zeta}_{\mathcal{O}(\varepsilon)} + \ldots = \underbrace{\zeta_t}_{\mathcal{O}(1)} + \big(\underbrace{u\zeta_x}_{\mathcal{O}(\varepsilon)} + \ldots + \underbrace{v\zeta_y}_{\mathcal{O}(\varepsilon)} + \ldots\big), \qquad \text{at} \quad z = R. \qquad \text{(kinematic)}$$

Similarly, the ordering of the linearized dynamic boundary conditions is found to be

$$\underbrace{A_v u_z}_{\mathcal{O}(1)} + \underbrace{(A_v u_z)_z\zeta}_{\mathcal{O}(\varepsilon)} + \ldots = \underbrace{A_v v_z}_{\mathcal{O}(1)} + \underbrace{(A_v v_z)_z\zeta}_{\mathcal{O}(\varepsilon)} + \ldots = 0, \qquad \text{at} \quad z = R. \qquad \text{(no-stress)}$$

Finally, the order of magnitude of the no-slip condition at the bed reads

$$\underbrace{u}_{\mathcal{O}(1)} = \underbrace{v}_{\mathcal{O}(1)} = \underbrace{w}_{\mathcal{O}(1)} = 0, \qquad \text{at} \quad z = -H. \qquad \text{(no-slip)}$$

1.3 Perturbation approach

Instead of neglecting first- and higher-order non-linear effects, as is done when linearising the equations, the perturbation method expands these non-linearities into a series of linear estimates. To this end, the solution variables ζ, u, v and w are expanded in an asymptotic series ordered in the small parameter ε:

$$\begin{aligned}
\zeta &= \zeta^0 + \zeta^1 + \zeta^2 + \dots, \\
u &= u^0 + u^1 + u^2 + \dots, \\
v &= v^0 + v^1 + v^2 + \dots, \\
w &= w^0 + w^1 + w^2 + \dots,
\end{aligned}$$

where $[\cdot]^0$ denotes a quantity at leading order, $[\cdot]^1$ a quantity at order ε and, continuing this pattern, $[\cdot]^n$ denotes a quantity at order ε^n.

In addition, the known parameters in this model are also expanded in a similar manner. This yields the following asymptotic series for the eddy viscosity parameters, density, tidal forcing and riverine forcing:

$$\begin{aligned}
A_\mathrm{h} &= A_\mathrm{h}^0 + A_\mathrm{h}^1 + A_\mathrm{h}^2 + \dots, \\
A_v &= A_v^0 + A_v^1 + A_v^2 + \dots, \\
\rho &= \rho^0 + \rho^1 + \rho^2 + \dots, \\
A &= A^0 + A^1 + A^2 + \dots, \\
\boldsymbol{u}_\mathrm{river} &= \boldsymbol{u}_\mathrm{river}^0 + \boldsymbol{u}_\mathrm{river}^1 + \boldsymbol{u}_\mathrm{river}^2 + \dots.
\end{aligned}$$

These series are substituted into the equations and boundary conditions. The resulting equations are still equivalent to the original equations. The analysis so far has merely identified which terms are of leading order and which terms are of higher order.

The key step in the perturbation approach is the identification of the balances. The leading-order terms can only be balanced with other leading-order terms because the first- and higher-order terms are, by construction, too small to balance these terms (in the limit of ε to zero). Thus, these terms result in the leading-order or *dominant* balance. Using that the leading-order terms balance, only first- and higher-order terms remain in the system of equations. The most dominant terms are now the first-order terms, resulting in the *first-order balance*. This systematic identification of balances continues for the second- and higher-order terms resulting in an infinite number of balances.

An asymptotic expansion has the important property that the leading-order term is *approximately correct* and that higher-order terms are *corrections of decreasing size* (Hinch, 1991, p. 20). Once ε is sufficiently small, the leading-order term is virtually correct. The fully nonlinear solution can be approximated to any degree of accuracy by increasing the number of terms, provided that the asymptotic expansion convergences. In practice, it turns out that the qualitative properties of the solution are often well captured by only a limited number of asymptotic terms.

An asymptotic expansion is, in general, not a convergent series, where the answer can be reproduced as accurately as desired by increasing the number of terms. Instead, an asymptotic expansion is useful as a sequence of approximations. Each approximation provides a value close to the desired answer for a finite, often small, number of terms. In fact, an asymptotic expansion usually reaches its best approximation after a certain number of terms. If more terms are included, the approximation becomes worse and starts to diverge. A convergent series, in contrast, can require a large number of terms before a good approximation is obtained (Holmes, 2013, p. 13).

We turn our attention back to the balances. The balances at each order of ε are collected together for the different equations. This results in a system of equations at leading, first and higher orders. Because of the observation that in our model the non-linear interactions are of order ε and higher, each system of equations depends on physical terms of the *same* and *lower* order. This dependency requires one to solve the leading-order equations for the leading-order physical variables first. Likewise, the first-order equations depend both on the leading- and first-order variables. The leading-order variables are already obtained by solving the leading-order equations. Thus, the first-order equations are solved by the first-order variables. This process continues for the second- and higher-order equations.

The requirement that the leading-order equations need to be solved first is in-line with the interpretation that the leading-order variables form an approximate solution to the full system of equations. Moreover, the first-order variables can only be solved after the leading-order variables are obtained which reinforces the notion of correction on top of the approximate solution.

The leading- and first-order equations are discussed below together with their corresponding boundary conditions.

1.4 The leading-order hydrodynamic equations

Collecting leading-order terms in the continuity and momentum equations results in the leading-order hydrodynamic equations describing barotropic water motion. These equations, which solve for the leading-order water level elevation $\zeta^0(x,y,t)$ and velocity components $u^0(x,y,z,t)$, $v^0(x,y,z,t)$, $w^0(x,y,z,t)$, are given by

$$\begin{cases} u^0_x + v^0_y + w^0_z = 0, & \text{(continuity)} \\ u^0_t - f v^0 = -g\zeta^0_x + \left(A^0_v u^0_z\right)_z, & \text{(x-momentum)} \\ v^0_t + f u^0 = -g\zeta^0_y + \left(A^0_v v^0_z\right)_z, & \text{(y-momentum)} \\ \zeta^0_t + \left(\int_{-H}^{R} u^0\,dz\right)_x + \left(\int_{-H}^{R} v^0\,dz\right)_y = 0. & \text{(depth-integrated continuity)} \end{cases}$$

We remark that the horizontal eddy viscosity terms are not included in the leading-order balances. The consequences of this are disscused in the next sections.

The leading-order kinematic and no-stress boundary conditions imposed at the free surface read

$$\begin{aligned} w^0 &= \zeta^0_t, && \text{at} \quad z = R, && \text{(kinematic)} \\ A^0_v u^0_z &= A^0_v v^0_z = 0, && \text{at} \quad z = R. && \text{(no-stress)} \end{aligned}$$

Near the boundaries at the bed and lateral sides, where the no-slip conditions apply, there is usually a layer where the velocity rapidly decreases to zero, called a *boundary layer*. The boundary conditions associated with these layers depend on the equations used, the resolving power of a model and its typical applications. The boundary layers and their implementation are discussed next.

1.4.1 The bottom boundary layer

The tidal currents are influenced by the friction at the bed. In deep water with slow currents, the frictional boundary layer occupies a relatively thin region near the bed. In shallow water with faster currents, the boundary layer may occupy the entire water depth and dominate the tidal dynamics (Soulsby, 1983, p. 189).

The bottom boundary layer can be divided into three qualitatively different zones of flow: the bed layer, the logarithmic layer and the outer layer. The vertical structure of the three layers is shown schematically in Figure 1.2. We discuss the characteristics of each layer below:

1. The *bed layer* is a thin layer next to the bed and is typically a few centimetres thick in a sea. The flow in the bed layer can be classified into smooth, transitional rough and rough hydrodynamic regimes based on the roughness Reynolds number defined as

$$\mathrm{Re}_* = \frac{u_* D}{\nu}.$$

Here, u_* is the friction velocity, D is the roughness height and ν is the kinematic viscosity. Sternberg (1968) suggests the following classification of the regimes:

$$\begin{aligned} &\text{Smooth turbulent:} && \mathrm{Re}_* < 5.5, \\ &\text{Transitional:} && 5.5 < \mathrm{Re}_* < 165, \\ &\text{Rough turbulent:} && \mathrm{Re}_* > 165. \end{aligned}$$

The roughness Reynolds number can be interpreted as a comparison between particle size D and the viscous length scale ν/u_*. For example, if the roughness height is less than 5.5 times the viscous length scale, then the bed is smooth with respect to the viscous sublayer scale and the flow can be characterised as smooth.

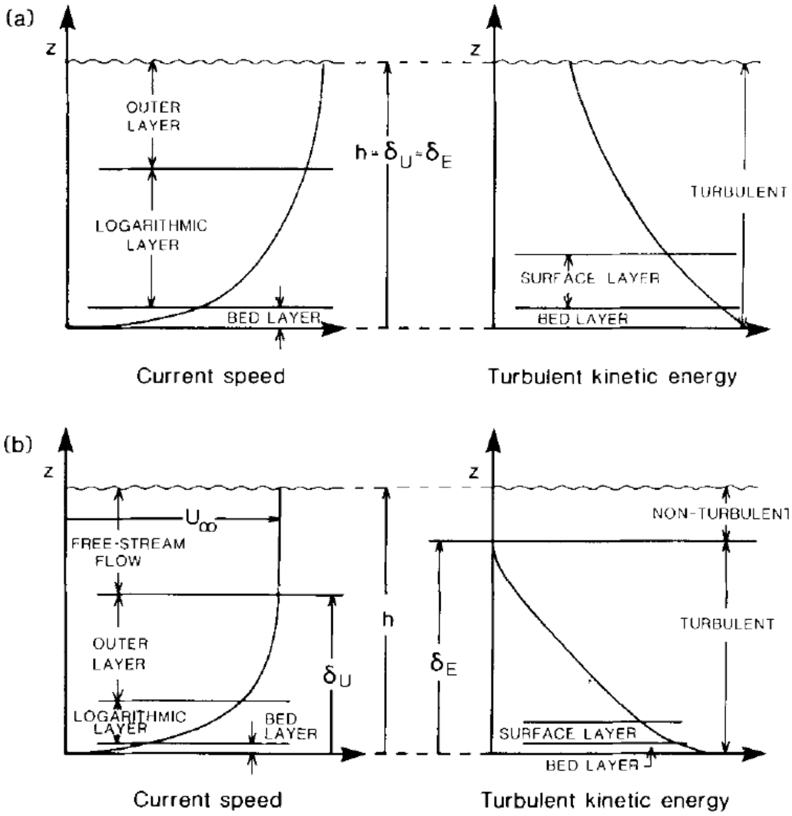

Figure 1.2: Schematic subdivision of the vertical boundary layer. (a) For a boundary layer that occupies the entire water depth and (b) for a boundary layer that occupies part of the water depth. The former is typical for shallow water and the latter for deep water. The layers are not drawn to scale. Taken from Soulsby (1983, p. 198).

In the smooth turbulent flow regime, i.e., when the bed is sufficiently smooth, the molecular viscosity dominates the dynamics. These dynamics are well studied and understood. If the bed is rough, turbulence dominates the dynamics. The dynamics in the transition region is more complicated and less well understood.

For hydrodynamically smooth flow, the velocity profile in the bed layer is given by

$$u(z) = \frac{u_*^2}{\nu} z,$$

where z is the distance from the bed. That is, for smooth flow there is a thin region close to the bed where the flow scales linearly with the distance from the bed.

2. The *logarithmic layer* is the layer just above the bed layer and is typically a few meters high in a sea. In this layer, neither the details of the bed nor the details of the free-stream flow affect the local dynamics. That is, the range of heights is simultaneously too great for the geometric details of the bed to affect the flow and too small for the flow to be influenced directly by the free-stream velocity at the top of the water column. The flow in the logarithmic layer is given by

$$u(z) = \frac{u_*}{\kappa} \ln\left(\frac{z - z_\mathrm{r}}{z_0}\right),$$

where κ is the von Kármán constant, z_r is a reference height, z_0 is the roughness length and z the distance from the bed. This result is known as the law of the wall in fluid dynamics. This result can either be derived by assuming constant shear stress and an eddy viscosity proportional to the distance from the bed or, more realistically, by assuming a linear shear stress and a quadratic eddy viscosity profile. For more details we refer the reader to Burchard (2002, p. 54).

3. The *outer layer* is the layer above the logarithmic layer and usually extends tens of metres into the vertical direction, often up to the free surface in shallow water. In this layer the velocity and turbulence strongly depend on the surface flow and, therefore, no universal description can be given.

Between two consecutive layers, there is a *transition layer*. In this layer, the processes of both layers are equally important. Mathematically, the solution of the lower layer is matched asymptotically to the solution of the upper layer.

If the body of water is deep enough, an extra layer exists on top of the bottom boundary layer, called the *free-stream layer*. In this layer, the flow is more or less independent of the flow in the bottom boundary layer and is mostly affected by the boundary conditions imposed at the free surface.

We note that there is no consensus about the names of these layers. The names depend on the field and, more importantly, on the convention applied by the author. For example, the bed and logarithmic layer are sometimes referred to as the bottom boundary layer, while the outer layer is not explicitly referred to as a boundary layer phenomenon.

Bottom boundary conditions

In shallow seas and estuaries, the bottom boundary layer usually extends all the way to the free surface. It is, therefore, important to include the bottom boundary layer in these types of models. Within the bottom boundary layer, the outer layer occupies most of the water depth, while the logarithmic and bed layer are thin compared to this layer. These thin layers introduce small length scales into the problem. Resolving these length scales requires additional computational power and time. The effects of these layers are, therefore, usually parametrised in oceanic and estuarine models (Vreugdenhil, 1994, p. 222). One of these parametrisations is the partial-slip formulation[3] (see, e.g., Schramkowski and De Swart, 2002, p. 3):

$$\underbrace{A_v u_z}_{\mathcal{O}(1)} = \underbrace{s_f u}_{\mathcal{O}(1)}, \quad \text{and} \quad \underbrace{A_v v_z}_{\mathcal{O}(1)} = \underbrace{s_f v}_{\mathcal{O}(1)}, \qquad \text{at} \quad z = -H. \qquad \text{(partial-slip)}$$

[3]This parametrisation has already been suggested by, for example, Sverdrup (1926, p. 43). However, Sverdrup ended up replacing it with a more mathematically traceable condition.

Here, s_f denotes the partial-slip roughness coefficient. For $s_f \to \infty$, this condition reduces to the no-slip condition: $u = v = 0$. If the partial-slip coefficient is made dependent on the magnitude of the local velocity, then this condition becomes a quadratic bottom friction law (see, e.g., Burchard and Baumert, 1998, p. 311). This condition should be applied at the top of the approximately constant stress layer instead of at the true bed where the no-slip condition applies.

Strictly speaking, the partial slip condition is imposed on the shear stresses *tangential* to the bed. That is, the stresses acting on, and directed in, the plane tangential to the bed are specified.[4]These shear stresses depend on the derivative of the along bed velocity components with respect to the distance to the bed. It is assumed that the gradient of the bed remains small over the whole domain, such that, the flow tangential to the bed can be approximated by the lateral velocity components and the distance to the bed by the vertical coordinate z. That is, we assume that the norm of the gradient of the bed H is much smaller than unity, i.e., $|\nabla H| \ll 1$. We note that this assumption is similar to the assumption that the typical bathymetric length scale is of the same order of magnitude as the estuarine length scale, that is assumption 2. We note that a similar assumption has been made for the kinematric and no-stress boundary conditions at the free surface.

The partial-slip formulation generally results in a non-zero tangential velocity at the bed. To ensure that fluid particles do not flow through the bed, a kinematic boundary condition has to be imposed:

$$\underbrace{w}_{\mathcal{O}(1)} = \underbrace{-uH_x - vH_y}_{\mathcal{O}(1)}, \qquad \text{at} \quad z = -H. \qquad \text{(kinematic)}$$

Here, it is assumed that the bed is stationary.

The order of magnitude of these boundary conditions is determined using their typical scales and the assumption that the partial-slip coefficient scales as $s_f = \mathscr{A}_v / H_0 s_f^*$. The partial-slip coefficient is expanded in an asymptotic series in ε, similar to the other parameters in the model. The leading-order partial-slip boundary conditions are given by

$$A_v^0 u_z^0 = s_f^0 u^0, \qquad \text{and} \qquad A_v^0 v_z^0 = s_f^0 v^0, \qquad \text{at} \quad z = -H, \qquad \text{(partial-slip)}$$

and the leading-order kinematic boundary condition reads

$$w^0 = -u^0 H_x - v^0 H_y, \qquad \text{at} \quad z = -H. \qquad \text{(kinematic)}$$

1.4.2 The lateral boundary layer

Next, we focus on the lateral boundary layer. Note that, in contrast to the bottom boundary layer where the vertical eddy viscosity coefficients were included, the horizontal eddy viscosity coefficients are not part of the leading-order hydrodynamics equations.

Using the perturbation approach, the hydrodynamic equations have been reduced from second- to first-order differential equations in the horizontal directions. If a leading-order equation is of lower order than the original equation then that indicates that the original equation is *singularly perturbed*. A singularly perturbed equation usually consists of multiple dominant balances, each valid in a different region of the domain. In case of small horizontal eddy viscosity, this typically manifests itself in a layer close to the lateral boundary where the effects of viscosity become important. This layer is here referred to as the *lateral boundary layer*. In the areas outside of this boundary layer, the horizontal eddy viscosity plays an insignificant role and can be omitted (Pedlosky, 1987, p. 194–200).

At this point one has two options: include or exclude the horizontal eddy viscosity coefficients and the lateral boundary layers. This decision usually depends on the system being studied. If the flow near the lateral boundaries is important, these terms should be included. Conversely, when the flow is studied far away from the lateral boundaries, these terms are usually neglected because they introduce very small length scales into the problem that would require additional computational efforts near the lateral boundaries. Allocating computational resources towards these small regions implies that these resources cannot be used to refine the solution in the domain of interest.

[4]For a detailed derivation and explanation of the stress tensor used in fluid dynamics we refer to Batchelor (1967, p. 141).

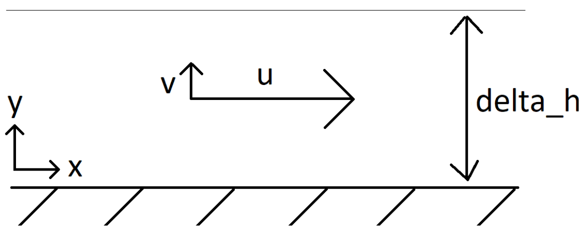

Figure 1.3: Schematic representation of the top-view of a lateral boundary layer.

Lateral boundary layer thickness

We predominantly study the tidal flow in estuaries. To determine if we need to include the horizontal eddy viscosity parameters in the leading-order equations, we compare the typical lateral boundary layer width with a typical estuarine width.

We derive a lateral boundary layer thickness scale following Mofjeld (1980, p. 1050), see Figure 1.3 for a schematic representation of the lateral boundary layer. Assume, without loss of generality, that the lateral wall is located at $y = 0$. The flow normal to the boundary vanishes because of the no-slip condition at the wall and just outside the boundary layer this flow is often small too. Therefore, it is not unreasonable to assume that the normal flow remains small inside the lateral boundary layer, that is $v = 0$. The tangential velocity u, on the other hand, needs to increase from zero at the wall to the free stream velocity or a fraction there of outside of the boundary layer. Thus, the tangential velocity is important in the boundary layer. The vertical velocity w is small in the whole domain because the horizontal length scale is assumed to be much larger than the vertical length scale. Thus, the magnitude of the velocity vector inside of the lateral boundary layer is small, such that the convective terms can be neglected. The last two assumptions are that the bottom boundary layer can be ignored and that the along boundary length scale is large compared to the boundary layer thickness. In the lateral boundary layer, the dominant balance is then between inertia and the lateral eddy viscosity:

$$u_t = (A_\mathrm{h} u_y)_y,$$

from which a lateral boundary layer thickness scale δ_h can be derived:

$$\delta_\mathrm{h} = \sqrt{\mathscr{A}_\mathrm{h} T_{M_2}}.$$

Defining a typical horizontal eddy viscosity near the lateral boundaries is complicated because the magnitude of the eddy viscosity parameter usually decreases rapidly towards the lateral sides (as the turbulent eddies become physically restricted). We estimate that a typical eddy viscosity scale near the lateral boundaries is about $\mathscr{A}_\mathrm{h} = 10^{-4}\,\mathrm{m^2\,s^{-1}}$. The typical time scale is given by $T_{M_2} = 12.42\,\mathrm{h}$. This yields a lateral boundary layer thickness of $\delta_\mathrm{h} = 6.7\,\mathrm{m}$. The width of an estuary is typically about 100–1000 m. We conclude that the lateral boundary layer is relatively thin compared to the estuarine width and, therefore, that the horizontal eddy viscosity terms can be neglected at leading order.

Reformulation of lateral boundary conditions

We have shown that the horizontal eddy viscosity terms can be neglected at leading order. As a consequence, the hydrodynamic equations have been reduced from second- to first-order differential equations in the horizontal direction. This implies that not all original lateral boundary conditions can be satisfied. The boundary conditions that can be imposed to obtain a well-posed mathematical problem are derived next.

The allowable boundary conditions depend on the remaining lateral derivatives in the leading-order hydrodynamic equations. First, we investigate the lateral boundary conditions that can be imposed for the free surface. Thereafter, we consider the allowable boundary conditions for the velocity at the lateral sides. To this end, the lateral derivatives are considered per equation. This section can be considered fairly technical, so buckle up!

Free surface boundary conditions The three-dimensional continuity equation does not depend on the free surface ζ or its lateral derivatives: ζ_x and ζ_y. This means that this equation cannot be used to determine the boundary conditions for the free surface.

The momentum equations depend on the lateral derivatives of the free surface. That is, they contain the terms ζ_x and ζ_y. Given the horizontal velocity components u and v, the free surface ζ can still satisfy lateral boundary conditions. Furthermore, the depth dependence of the horizontal velocity components does not affect the free surface ζ because it is independent of the depth z.

The last equation is the depth-averaged continuity equation. In this equation, no lateral derivatives of the free surface are present, only its variation in time. This shows that this equation cannot be used to determine boundary conditions for the free surface.

To summarize, the boundary conditions that can be prescribed for the free surface at the lateral sides are the same as for the original equations. That is, we can impose a free surface elevation.

Velocity boundary conditions The three-dimensional continuity equation contains lateral derivatives of the horizontal velocity components, namely u_x and v_y. This *may* indicate that lateral boundary conditions can be imposed on the horizontal velocity components: u and v. However, it turns out that this equation plays more of an auxiliary role in the current system of equations. The purpose of this equation is to specify the vertical velocity w given the horizontal velocity components. It cannot, directly, be used to determine the free surface or the horizontal velocity components. Indeed, the momentum equations and the depth-integrated continuity equation do not depend *explicitly* on w. They only depend on the behaviour of w at the boundaries, which is captured by the boundary conditions. As such the other equations are naturally decoupled from the vertical velocity w and the three-dimensional continuity equation. This decoupling allows one to first solve the other equations for ζ, u and v. Afterwards, the vertical velocity w can be obtained. To conclude, the three-dimensional, continuity equation cannot be used to determine which lateral boundary conditions can be specified. For this purpose, the other decoupled equations have to be considered.

The leading-order x- and y-momentum equations do *not* contain lateral derivatives of the horizontal velocity components. That is, these equations do not contain u_x, u_y, v_x or v_y. So for a given surface elevation $R+\zeta$ and vertical position z, it follows that the horizontal velocity components cannot satisfy lateral boundary conditions. Now, because the vertical position z was chosen arbitrary, it follows that the horizontal velocity components cannot satisfy lateral boundary conditions that depend on the vertical coordinate z.

The depth-integrated continuity equation contains lateral derivatives of the *depth-integrated*, horizontal velocity components, i.e., the terms $(\int u\,dz)_x$ and $(\int v\,dz)_y$. Therefore, it follows that the depth-integrated, velocity profiles can satisfy boundary conditions imposed at the lateral sides.

We have shown that, at the lateral sides, it is not possible to prescribe the horizontal velocity components in a depth dependent manner. They can solely be prescribed in a depth-integrated fashion. The depth-integrated horizontal velocity components are typically referred to as the lateral *transport of water*, see for example Huijts *et al.* (2011, p. 1069).

The depth-integrated continuity equation is integrated over a small control volume that encloses part of the boundary. If the thickness of this control volume goes to zero, while enclosing part of the boundary, it follows that the transport of water normal to the boundary just before and after the boundary is continuous. That is, the transport through the boundary is the same on both sides of the boundary. Therefore, it follows that the transport of water *normal* to the boundary must be prescribed at the lateral sides. This boundary condition reads

$$\left(\int_{-H}^{R} \boldsymbol{u}^0\,dz\right)\cdot\boldsymbol{n} = q^0(x,y,t),$$

with the prescribed, leading-order, normal transport of water given by

$$q^0(x,y,t) = \boldsymbol{q}^0\cdot\boldsymbol{n} = \left(\int_{-H}^{R} \boldsymbol{u}_\mathrm{k}^0\,dz\right)\cdot\boldsymbol{n}.$$

From now on, *each bold vector is a short hand notation for a two-dimensional vector.* In this case, the bold symbol $\boldsymbol{u}$ is a shorthand for the *horizontal* velocity vector (u,v), $\boldsymbol{u}_\mathrm{k}^0$ is a *known* horizontal velocity vector, $\boldsymbol{n}$ is the outward pointing unit normal and $\boldsymbol{q}^0$ is the prescribed horizontal transport of water. The velocity $\boldsymbol{u}_\mathrm{k}^0$ is called a known rather than a prescribed velocity because we have shown that for the current equations it is not allowed to prescribe depth-dependent horizontal velocity components.

Formally, one could also prescribe a linear combination of the free surface and velocity boundary conditions. This type of boundary condition is not used here and will not be pursued further.

Scaling the transport boundary condition

The transport boundary condition can also be derived from the non-perturbed, depth-integrated continuity equation. This derivation is necessary because the original boundary condition is required to determine the scaling of this condition. The non-linear, transport boundary condition reads

$$\left(\int_{-H}^{R+\zeta} \boldsymbol{u}\, dz\right) \cdot \boldsymbol{n} = q.$$

Taylor expanding the integrand and using the typical scales yields the following order of magnitude of the transport boundary condition:

$$\Bigg(\underbrace{\int_{-H}^{R} \boldsymbol{u}\, dz}_{\mathcal{O}(1)} + \underbrace{\boldsymbol{u}|_{z=R}\zeta}_{\mathcal{O}(\varepsilon)} + \ldots\Bigg) \cdot \boldsymbol{n} = \underbrace{q}_{\mathcal{O}(1)}.$$

The leading-order, lateral boundary conditions are presented next.

Lateral boundary conditions

The prescribed free surface boundary condition can be used without modifications. At the lateral boundaries connected to the sea, the leading-order tidal amplitude is imposed:

$$\zeta^0 = A^0(x, y, t), \qquad \text{at} \quad \partial\Omega_{\text{sea}}. \qquad \text{(tidal forcing)}$$

The transport normal to the boundary has to be prescribed. The most important property of the estuarine banks is that there is no net transport of water through these boundaries. At these boundaries, the leading-order transport of water is required to vanish:

$$\left(\int_{-H}^{R} \boldsymbol{u}^0\, dz\right) \cdot \boldsymbol{n} = 0, \qquad \text{at} \quad \partial\Omega_{\text{bank}}. \qquad \text{(no-transport)}$$

This condition should be imposed at the location where the transport of water between the outer and the lateral boundary layer solution vanishes, instead of at the true lateral sides (Schramkowski and De Swart, 2002, p. 3).

Similarly, the transport of water is prescribed at the riverine boundaries. The leading-order riverine boundary condition reads

$$\left(\int_{-H}^{R} \boldsymbol{u}^0\, dz\right) \cdot \boldsymbol{n} = -q^0_{\text{river}}(x, y, t), \qquad \text{at} \quad \partial\Omega_{\text{river}}, \qquad \text{(riverine forcing)}$$

where q^0_{river} is the prescribed leading-order riverine transport of water flowing into the domain.

1.4.3 Summary of the leading-order hydrodynamics equations

It might be beneficial to briefly summarize the leading-order hydrodynamics equations and the leading-order boundary conditions. The leading-order hydrodynamic equations read

$$\begin{cases} u^0_x + v^0_y + w^0_z = 0, & \text{(continuity)} \\ u^0_t - f v^0 = -g\zeta^0_x + \left(A^0_v u^0_z\right)_z, & \text{(x-momentum)} \\ v^0_t + f u^0 = -g\zeta^0_y + \left(A^0_v v^0_z\right)_z, & \text{(y-momentum)} \\ \zeta^0_t + \left(\int_{-H}^{R} u^0\, dz\right)_x + \left(\int_{-H}^{R} v^0\, dz\right)_y = 0. & \text{(depth-integrated continuity)} \end{cases}$$

We want to emphasize that in this section new boundary conditions have been derived which were not imposed on the orginal hydrodynamic equations. This is the case because the mathematical structure of the leading-order hydrodynamic equations has changed and because the original boundary conditions introduced small length scales into the problem. Furthermore, each bold symbol now denotes a two-dimensional vector.

At the lateral sea boundary, the tidal amplitude is prescribed:

$$\zeta^0 = A^0(x, y, t), \qquad \text{at} \quad \partial\Omega_{\text{sea}}. \qquad \text{(tidal forcing)}$$

At the estuarine banks, no-transport of water is imposed:

$$\left(\int_{-H}^{R} \boldsymbol{u}^0 \, dz\right) \cdot \boldsymbol{n} = 0, \qquad \text{at} \quad \partial\Omega_{\text{bank}}, \qquad \text{(no-transport)}$$

and at the riverine boundaries, the riverine transport of water is prescribed:

$$\left(\int_{-H}^{R} \boldsymbol{u}^0 \, dz\right) \cdot \boldsymbol{n} = -q^0_{\text{river}}(x, y, t), \qquad \text{at} \quad \partial\Omega_{\text{river}}. \qquad \text{(riverine forcing)}$$

At the free surface, a kinematic and no-stress boundary conditions are prescribed:

$$\begin{aligned} w^0 &= \zeta^0_t, && \text{at} \quad z = R, && \text{(kinematic)} \\ A^0_v \boldsymbol{u}^0_z &= \boldsymbol{0}, && \text{at} \quad z = R. && \text{(no-stress)} \end{aligned}$$

At the bed, a kinematic and partial-slip boundary condition are imposed:

$$\begin{aligned} w^0 &= -u^0 H_x - v^0 H_y, && \text{at} \quad z = -H, && \text{(kinematic)} \\ A^0_v \boldsymbol{u}^0_z &= s^0_f \boldsymbol{u}^0, && \text{at} \quad z = -H. && \text{(partial-slip)} \end{aligned}$$

Again, the bold symbol $\boldsymbol{u}$ is a shorthand for the horizontal velocity vector (u, v) and $\boldsymbol{n}$ is the outward pointing unit normal.

1.5 The first-order hydrodynamic equations

The collection of first-order terms in the continuity and momentum equations results in the first-order hydrodynamic equations. Each individual forcing mechanism in the first-order hydrodynamic equations is denoted with a Greek letter. The first-order body forcing terms are given by

$$\begin{aligned} \boldsymbol{\eta}^1(x, y, z, t) &= \boldsymbol{u}^0 \cdot \nabla \boldsymbol{u}^0 + w^0 \boldsymbol{u}^0_z = \begin{bmatrix} u^0 u^0_x + v^0 u^0_y + w^0 u^0_z \\ u^0 v^0_x + v^0 v^0_y + w^0 v^0_z \end{bmatrix}, && \text{(advection)} \\ \boldsymbol{\varsigma}^1(x, y, z, t) &= g \int_z^R \frac{\nabla \rho^0}{\rho_0} \, d\tilde{z} = \begin{bmatrix} g \int_z^R \rho^0_x / \rho_0 \, d\tilde{z} \\ g \int_z^R \rho^0_y / \rho_0 \, d\tilde{z} \end{bmatrix}, && \text{(baroclinic)} \\ \boldsymbol{\psi}^1(x, y, z, t) &= A^1_v \boldsymbol{u}^0_z = \begin{bmatrix} A^1_v u^0_z \\ A^1_v v^0_z \end{bmatrix}, && \text{(eddy viscosity)} \\ \boldsymbol{\xi}^1(x, y) &= \nabla R = \begin{bmatrix} R_x \\ R_y \end{bmatrix}, && \text{(reference level)} \end{aligned}$$

and the first-order surface and bottom forcing terms read

$$\boldsymbol{\gamma}^1(x,y,t) = \zeta^0\boldsymbol{u}^0 = \begin{bmatrix}\zeta^0 u^0\\ \zeta^0 v^0\end{bmatrix}, \qquad \text{at} \quad z=R, \qquad \text{(tidal return flow)}$$

$$\boldsymbol{\chi}^1(x,y,t) = \zeta^0\left(A_v^0\boldsymbol{u}_z^0\right)_z = \begin{bmatrix}\zeta^0\left(A_v^0 u_z^0\right)_z\\ \zeta^0\left(A_v^0 v_z^0\right)_z\end{bmatrix}, \qquad \text{at} \quad z=R, \qquad \text{(no-stress)}$$

$$\boldsymbol{\mu}^1(x,y,t) = s_f^1\boldsymbol{u}^0 = \begin{bmatrix}s_f^1 u^0\\ s_f^1 v^0\end{bmatrix}, \qquad \text{at} \quad z=-H. \qquad \text{(partial-slip)}$$

The symbol ∇ denotes the horizontal gradient, i.e, $\nabla = \begin{bmatrix}\partial_x & \partial_y\end{bmatrix}^T$. The forcing due to eddy viscosity $\boldsymbol{\psi}^1$ could be considered as one of the many contributions of the eddy viscosity-shear covariance, or ESCO for short (Dijkstra *et al.*, 2017).

The equations for the first-order water level elevation $\zeta^1(x,y,t)$ and velocity components $u^1(x,y,z,t)$, $v^1(x,y,z,t)$, $w^1(x,y,z,t)$ read

$$\begin{cases} u_x^1 + v_y^1 + w_z^1 = 0, & \text{(continuity)}\\ u_t^1 - f v^1 = -g\zeta_x^1 + \left(A_v^0 u_z^1\right)_z - g\xi_1^1 - \eta_1^1 - \varsigma_1^1 + \psi_{z,1}^1, & \text{(x-momentum)}\\ v_t^1 + f u^1 = -g\zeta_y^1 + \left(A_v^0 v_z^1\right)_z - g\xi_2^1 - \eta_2^1 - \varsigma_2^1 + \psi_{z,2}^1, & \text{(y-momentum)}\\ \zeta_t^1 + \left(\displaystyle\int_{-H}^{R} u^1\,dz\right)_x + \left(\displaystyle\int_{-H}^{R} v^1\,dz\right)_y = -\nabla\cdot\boldsymbol{\gamma}^1. & \text{(depth-integrated continuity)}\end{cases}$$

Here, the last subscript of a Greek letter denotes taking the corresponding component of that vector.

At the sea ward boundary, the first-order tidal amplitude is prescribed:

$$\zeta^1 = A^1(x,y,t), \qquad \text{at} \quad \partial\Omega_{\text{sea}}. \qquad \text{(tidal forcing)}$$

At the estuarine bank, no-transport of water is imposed:

$$\left(\int_{-H}^{R}\boldsymbol{u}^1\,dz\right)\cdot\boldsymbol{n} = -\boldsymbol{\gamma}^1\cdot\boldsymbol{n}, \qquad \text{at} \quad \partial\Omega_{\text{bank}}, \qquad \text{(no-transport)}$$

and at the riverine boundaries, the first-order riverine transport of water is prescribed:

$$\left(\int_{-H}^{R}\boldsymbol{u}^1\,dz\right)\cdot\boldsymbol{n} = -q_{\text{river}}^1(x,y,t) - \boldsymbol{\gamma}^1\cdot\boldsymbol{n}, \qquad \text{at} \quad \partial\Omega_{\text{river}}. \qquad \text{(riverine forcing)}$$

At the free surface, a kinematic and no-stress boundary conditions are prescribed:

$$\begin{aligned} w^1 &= \zeta_t^1 + \nabla\cdot\boldsymbol{\gamma}^1, && \text{at} \quad z=R, && \text{(kinematic)}\\ A_v^0\boldsymbol{u}_z^1 &= -\boldsymbol{\psi}^1 - \boldsymbol{\chi}^1, && \text{at} \quad z=R. && \text{(no-stress)}\end{aligned}$$

At the bed, a kinematic boundary and partial-slip condition are imposed:

$$\begin{aligned} w^1 &= -u^1 H_x - v^1 H_y, && \text{at} \quad z=-H, && \text{(kinematic)}\\ A_v^0\boldsymbol{u}_z^1 &= s_f^0\boldsymbol{u}^1 - \boldsymbol{\psi}^1 + \boldsymbol{\mu}^1, && \text{at} \quad z=-H. && \text{(partial-slip)}\end{aligned}$$

We remark that the original formulation of the first-order kinematic boundary condition at the free surface,

$$w^1 = \zeta_t^1 + \boldsymbol{u}^0\cdot\nabla\zeta^0 - w_z^0\zeta^0,$$

is written in a more convenient form using the leading-order three-dimensional continuity equation.

Table 1.2: Hydrodynamic forcing mechanisms and the order at which these mechanisms appear.

Symbol	Short name	Explanation	Order
External			
A	Tide	Tidal amplitude forced at the seaward boundaries	$0, 1, \ldots$
q_{river}	River	Depth-integrated riverine velocity at the riverine boundaries	$0, 1, \ldots$
$\boldsymbol{\varsigma}$	Baroclinic	Forcing by the baroclinic pressure gradient	$1, 2, \ldots$
$\boldsymbol{\xi}$	Reference	Forcing due to the gradient of the reference level	$1, 2, \ldots$
Internal			
$\boldsymbol{\eta}$	Advection	Advection of momentum	$1, 2, \ldots$
$\boldsymbol{\psi}$	Eddy viscosity	Effect of higher-order eddy viscosity contributions	$1, 2, \ldots$
$\boldsymbol{\gamma}$	Tidal return flow	The flow required to balance the mass flux induced by the tidal correlations between the velocity and water level elevation	$1, 2, \ldots$
$\boldsymbol{\chi}$	Velocity-depth asymmetry	Correction induced by applying the no-stress condition at $z = R$ instead of the true free surface at $z = R + \zeta$	$1, 2, \ldots$
$\boldsymbol{\mu}$	Partial-slip	Effect of higher-order partial-slip contributions	$1, 2, \ldots$

The forcing terms are summarised in Table 1.2. The forcing terms can be categorised based on their generation mechanism. Each term is either *externally prescribed* or *internally generated*. Externally prescribed terms are those terms that are prescribed explicitly. That is, they are *independent* of the current state of the system. Internally generated terms, on the other hand, are those terms that are generated by the system itself. They do depend on the current state of the system and cannot be prescribed.

The forcing mechanisms may also be classified based on their relationship with the leading-order solution variables. The tidal, riverine, baroclinic and reference level forcing are all independent of the leading-order solution variables, whereas the eddy viscosity and partial-slip forcing mechanisms have a linear dependence. The advective, tidal return flow and no-stress forcing mechanisms depend quadratically on the leading-order solution variables. Thus, the highest-order non-linearities included in the first-order hydrodynamic equations are of the quadratic type.

The hydrodynamic equations are linear at each order. This allows the principle of superposition to be used. The effect of each forcing mechanism can be evaluated independently and separately. The total solution is then obtained by summing all the contributions together.

1.6 Harmonic decomposition

The solution of any forced, linear differential equation that includes a temporal derivative can be decomposed into two parts: *a homogeneous solution* and *a particular solution*. The homogeneous solution satisfies the homogeneous differential equation with homogeneous boundary conditions resulting in a solution with undetermined coefficients without considering the initial conditions. A particular solution satisfies the inhomogeneous differential equation with inhomogeneous boundary conditions and does not necessarily satisfy the initial conditions. The coefficients of the homogenous solution are chosen such that the sum of the homogeneous and particular solution satisfy the initial conditions.

If there is some type of dissipation or energy loss in the system, by, for example, bed friction or viscosity, then it follows that both solutions lose energy overtime. However, the coefficients of the homogeneous solution are only non-zero because of the initial condition. Thus, it follows that the total energy of the homogeneous solution diminishes over time, such that the amplitude of the homogeneous solution eventually vanishes. The total energy of the particular solution is constantly replenished by the inhomogeneous forcing terms. Therefore, after a sufficiently long time the total solution only consists of the particular solution, whereas the homogeneous solution has vanished. The homogenous solution is therefore also referred to as the transient solution. A detailed analysis of transient behaviour of waves can be found in Gill (1982).

We propose that, instead of solving for both the homogeneous and the particular solution and waiting for the homogeneous solution to vanish, it would be faster to directly solve for the particular solution. Thus, we consider the particular part of the solution only. Another reason for this choice is that we are mainly interested in the equilibrium behaviour of the solution, i.e., the behaviour for very large values of the time t. (Mathematically speaking, the behaviour of the solution when the time t goes to infinity.)

It is assumed that the forcing is periodic with angular frequency ω. Since the equations are linear, it follows that the solution has the same periodicity as the forcing. As a consequence, the solution can be expressed as a Fourier series:

$$\begin{aligned}
\zeta^k(x,y,t) &= \sum_{n=0}^{\infty} \Re\Big(Z_n^k(x,y)e^{ni\omega t}\Big),\\
u^k(x,y,z,t) &= \sum_{n=0}^{\infty} \Re\Big(U_n^k(x,y,z)e^{ni\omega t}\Big),\\
v^k(x,y,z,t) &= \sum_{n=0}^{\infty} \Re\Big(V_n^k(x,y,z)e^{ni\omega t}\Big),\\
w^k(x,y,z,t) &= \sum_{n=0}^{\infty} \Re\Big(W_n^k(x,y,z)e^{ni\omega t}\Big).
\end{aligned}$$

Here, the superscript k denotes the order of the variables, so $k = 0,1,2,\ldots$, and the subscript n denotes the nth Fourier coefficient or component. The latter index can also be used to identify the angular frequency of a given quantity, assuming it has a Fourier expansion.

The assumed periodic forcing consists of the external tidal, riverine and baroclinic forcing, which are also expanded in a Fourier series:

$$\begin{aligned}
A^k(x,y,t) &= \sum_{n=0}^{\infty} \Re\Big(A_n^k(x,y)e^{ni\omega t}\Big),\\
q^k_{\text{river}}(x,y,t) &= \sum_{n=0}^{\infty} \Re\Big(q^k_{\text{river},n}(x,y)e^{ni\omega t}\Big),\\
\rho^k(x,y,z,t) &= \sum_{n=0}^{\infty} \Re\Big(\rho_n^k(x,y,z)e^{ni\omega t}\Big).
\end{aligned}$$

In addition, the *leading-order* eddy viscosity and partial slip parameters are assumed to be constant in time but their *higher-order* contributions may depend on time. They are assumed to have the same periodicity as the other periodic forcing mechanisms. Thus, the higher-order contributions are also expanded in a Fourier series:

$$\begin{aligned}
A^k_{\text{h}}(x,y,t) &= \sum_{n=0}^{\infty} \Re\Big(A^k_{\text{h},n}(x,y)e^{ni\omega t}\Big),\\
A^k_{\text{v}}(x,y,t) &= \sum_{n=0}^{\infty} \Re\Big(A^k_{\text{v},n}(x,y)e^{ni\omega t}\Big),\\
s^k_f(x,y,t) &= \sum_{n=0}^{\infty} \Re\Big(s^k_{f,n}(x,y)e^{ni\omega t}\Big),
\end{aligned}$$

for $k \geq 1$. Here, we have assumed that the eddy viscosity parameters are independent of the vertical coordinate z.

The other parameters in the model are assumed to be time independent.

The spatial dependency of the model parameters is expressed below.

1. The gravitational constant g, Coriolis parameter f, reference density ρ_0 and angular frequency ω are assumed to be constant.

2. The eddy viscosities A_{h}, A_v, partial slip parameter s_f, bed level H and reference level R are assumed to depend on the horizontal spatial coordinates (x,y) only. That is, they are independent of the vertical coordinate z.

3. The diagnostic density ρ may depend on all three spatial coordinates (x,y,z).

It is convenient to collect the parameters appearing in the leading-order equations and boundary conditions that depend on the horizontal coordinates (x, y) in a single vector:

$$\boldsymbol{\phi}^0 = \begin{bmatrix} A_v^0 & s_f^0 & H & R \end{bmatrix}^T.$$

This is convenient because the analytic quantities that are derived to solve the leading-order equations and boundary conditions may depend on these spatially dependent parameters. Therefore, a horizontal derivative of such a quantity can be expressed using the chain rule in terms of the horizontal derivatives of these parameters. This can be compactly expressed using vector notation.

1.6.1 Leading-order hydrodynamic equations

The Fourier expansions are substituted in the leading-order hydrodynamic equations. Using the orthogonality of the sine and cosine, the following equivalent system of complex equations is obtained for each frequency component n:

$$\begin{cases} U_{n,x}^0 + V_{n,y}^0 + W_{n,z}^0 = 0, & \text{(continuity)} \\ ni\omega U_n^0 - f V_n^0 = -g Z_{n,x}^0 + A_v^0 U_{n,zz}^0, & \text{(}x\text{-momentum)} \\ ni\omega V_n^0 + f U_n^0 = -g Z_{n,y}^0 + A_v^0 V_{n,zz}^0, & \text{(}y\text{-momentum)} \\ ni\omega Z_n^0 + \left(\int_{-H}^{R} U_n^0 \, dz\right)_x + \left(\int_{-H}^{R} V_n^0 \, dz\right)_y = 0. & \text{(depth-integrated continuity)} \end{cases}$$

The equivalent boundary conditions are obtained using similar techniques. At the lateral sea boundary, the complex tidal amplitude is prescribed:

$$Z_n^0 = A_n^0(x, y), \qquad \text{at} \quad \partial\Omega_{\text{sea}}. \qquad \text{(tidal forcing)}$$

At the estuarine banks, no-transport of water is imposed:

$$\left(\int_{-H}^{R} \boldsymbol{U}_n^0 \, dz\right) \cdot \boldsymbol{n} = 0, \qquad \text{at} \quad \partial\Omega_{\text{bank}}, \qquad \text{(no-transport)}$$

and at the riverine boundaries, the complex riverine transport of water is prescribed:

$$\left(\int_{-H}^{R} \boldsymbol{U}_n^0 \, dz\right) \cdot \boldsymbol{n} = -q_{\text{river},n}^0(x, y), \qquad \text{at} \quad \partial\Omega_{\text{river}}. \qquad \text{(riverine forcing)}$$

At the free surface, a kinematic and no-stress boundary conditions are prescribed:

$$\begin{aligned} W_n^0 &= ni\omega Z_n^0, & &\text{at} \quad z = R, & &\text{(kinematic)} \\ A_v^0 \boldsymbol{U}_{n,z}^0 &= \mathbf{0}, & &\text{at} \quad z = R. & &\text{(no-stress)} \end{aligned}$$

At the bed, a kinematic and partial-slip boundary condition are imposed:

$$\begin{aligned} W_n^0 &= -U_n^0 H_x - V_n^0 H_y, & &\text{at} \quad z = -H, & &\text{(kinematic)} \\ A_v^0 \boldsymbol{U}_{n,z}^0 &= s_f^0 \boldsymbol{U}_n^0, & &\text{at} \quad z = -H. & &\text{(partial-slip)} \end{aligned}$$

Here, the bold symbol $\boldsymbol{U}_n^0$ denotes the complex vector $\begin{bmatrix} U_n^0 & V_n^0 \end{bmatrix}^T$.

1.6.2 Solving the leading-order hydrodynamic equations

We first decouple the x- and y-momentum equations. To this end, we write the momentum equations in matrix vector form as

$$\mathbf{M}_n^0(z) \boldsymbol{U}_n^0(z) = g \nabla Z_n^0,$$

where we have defined

$$\mathbf{M}_n^0(z) = \begin{bmatrix} A_v^0\partial_{zz} - ni\omega & f \\ -f & A_v^0\partial_{zz} - ni\omega \end{bmatrix}.$$

To emphasize that some vectors and matrices depend on the vertical coordinate z, we explicitly denote their z dependence after the variable.

The matrix $\mathbf{M}_n^0(z)$ is normal, i.e., $\mathbf{M}_n^0(z)^*\mathbf{M}_n^0(z) = \mathbf{M}_n^0(z)\mathbf{M}_n^0(z)^*$. Thus the matrix $\mathbf{M}_n^0(z)$ is diagonalizable by a unitary matrix. The unitary diagonalization reads

$$\mathbf{M}_n^0(z) = \mathbf{P}\mathbf{\Lambda}_n^0(z)\mathbf{P}^*,$$

with

$$\mathbf{P} = \frac{1}{\sqrt{2}}\begin{bmatrix} 1 & 1 \\ -i & i \end{bmatrix}, \qquad \mathbf{\Lambda}_n^0(z) = \begin{bmatrix} A_v^0\partial_{zz} - i(n\omega+f) & 0 \\ 0 & A_v^0\partial_{zz} - i(n\omega-f) \end{bmatrix}, \qquad \text{and} \qquad \mathbf{P}^* = \frac{1}{\sqrt{2}}\begin{bmatrix} 1 & i \\ 1 & -i \end{bmatrix}.$$

We remark that the unitary diagonalization is not unique. Any matrix of the form $\hat{\mathbf{P}} = \exp(it)\,\mathbf{P}$ for $t \in \mathbb{R}$ is still an unitary matrix, as $\hat{\mathbf{P}}\hat{\mathbf{P}}^* = \mathbf{I}_2$, and can be used for the diagonalization. We have chosen the unitary matrix such that the diagonalization coincides with that of Kumar (2018), apart from a factor $1/\sqrt{2}$. In addition, we note that this diagonalization remains valid in the special case that $f = 0$, where the matrix $\mathbf{M}_n^0(z)$ is already diagonal. In this case, the diagonal matrix $\mathbf{\Lambda}_n^0(z)$ reduces to a scalar times the identity matrix. Then the matrices $\mathbf{P}$ and $\mathbf{P}^*$ cancel, leaving only the scaler times the identity matrix. This is precisely equal to the diagonal matrix $\mathbf{M}_n^0(z)$ for $f = 0$. Hence this special case is also captured with this diagonalization.

The diagonalization is substituted into the momentum equations and multiplied from the left with $\mathbf{P}^*$, to obtain

$$\mathbf{\Lambda}_n^0(z)\boldsymbol{R}_n^0(z) = g\,\mathbf{P}^*\nabla Z_n^0,$$

where we have defined the rotating flow variables vector[5] $\boldsymbol{R}_n^0(z) = \mathbf{P}^*\boldsymbol{U}_n^0(z)$. Since the matrix $\mathbf{\Lambda}_n^0(z)$ is diagonal, it follows that the momentum equation have been decoupled. The decoupled equations read

$$\boldsymbol{R}_{n,zz}^0(z) - \left(\boldsymbol{\alpha}_n^0\right)^2\boldsymbol{R}_n^0(z) = \frac{g}{A_v^0}\mathbf{P}^*\nabla Z_n^0,$$

where we have defined the diagonal matrix with vertical decay coefficients as

$$\boldsymbol{\alpha}_n^0(x,y) = \begin{bmatrix} \sqrt{i(n\omega+f)/A_v^0} & 0 \\ 0 & \sqrt{i(n\omega-f)/A_v^0} \end{bmatrix}.$$

These equations are ordinary differential equations in the vertical coordinate z. The corresponding boundary conditions are given by

$$\begin{aligned} A_v^0\boldsymbol{R}_{n,z}^0(z) &= \mathbf{0}, && \text{at} \quad z = R, \\ A_v^0\boldsymbol{R}_{n,z}^0(z) &= s_f^0\boldsymbol{R}_n^0(z), && \text{at} \quad z = -H. \end{aligned}$$

Since the coefficients and right-hand side are independent of z, an analytical solution can be found for the rotating flow variables. It consists of an exact depth profile multiplied by a linear combination of the components of the free surface gradient and it reads

$$\boldsymbol{R}_n^0(z) = \mathbf{c}_n^0(z)\,\mathbf{P}^*\nabla Z_n^0,$$

with diagonal matrices

$$\mathrm{c}_{n,ii}^0(z) = \frac{g}{A_v^0\left(\alpha_{n,ii}^0\right)^2}\left\{s_f^0\beta_{n,ii}^0\cosh\!\left(\alpha_{n,ii}^0(z-R)\right) - 1\right\}, \qquad \text{for} \quad -H \le z \le R,$$

and

$$\beta_{n,ii}^0(x,y) = \frac{1}{A_v^0\alpha_{n,ii}^0\sinh\!\left(\alpha_{n,ii}^0 D\right) + s_f^0\cosh\!\left(\alpha_{n,ii}^0 D\right)},$$

[5]For more information about the rotating flow variables, see for example Mofjeld (1980, p. 1041) and references therein, or Appendix B.5.

for $i = 1,2$. The subscript ii denotes the ith diagonal element of the matrix. The off-diagonal entries of a diagonal matrix are zero. Here, we have defined the local water depth as $D(x, y) = H(x, y) + R(x, y)$.

It is useful to define an intermediary variable known as the depth-integrated rotating flow variables:

$$\boldsymbol{\mathcal{R}}_n^0(z) = \int_{-H}^{z} \boldsymbol{R}_n^0(\tilde{z})\, d\tilde{z} = \mathbf{C}_n^0(z)\,\mathbf{P}^*\nabla Z_n^0,$$

where we have defined the depth-integrated diagonal matrix

$$\mathrm{C}_{n,ii}^0(z) = \int_{-H}^{z} \mathrm{c}_{n,ii}^0(\tilde{z})\, d\tilde{z} = \frac{g}{A_v^0\left(\alpha_{n,ii}^0\right)^2}\left\{\frac{s_f^0\beta_{n,ii}^0}{\alpha_{n,ii}^0}\left[\sinh\left(\alpha_{n,ii}^0(z-R)\right)+\sinh\left(\alpha_{n,ii}^0 D\right)\right]-(z+H)\right\}.$$

The last step in decoupling and solving of the momentum equations consists of transforming back to the horizontal velocity vector $\boldsymbol{U}_n^0(z)$. By inverting the definition of the rotating flow variables, $\boldsymbol{R}_n^0(z) = \mathbf{P}^*\boldsymbol{U}_n^0(z)$, we find

$$\boldsymbol{U}_n^0(z) = \mathbf{P}\,\boldsymbol{R}_n^0(z) = \mathbf{d}_n^0(z)\,\nabla Z_n^0,$$

with the matrix

$$\mathbf{d}_n^0(z) = \mathbf{P}\,\mathbf{c}_n^0(z)\,\mathbf{P}^*.$$

Similarly, we also define a depth-integrated horizontal velocity vector. This quantity is also known as the transport of water and can be expressed in terms of the depth-integrated rotating flow variables. It is given by

$$\boldsymbol{q}_n^0(z) = \int_{-H}^{z} \boldsymbol{U}_n^0(\tilde{z})\, d\tilde{z} = \mathbf{P}\,\boldsymbol{\mathcal{R}}_n^0(z) = \mathbf{D}_n^0(z)\,\nabla Z_n^0,$$

where we have defined the diffusion matrix

$$\mathbf{D}_n^0(z) = \mathbf{P}\,\mathbf{C}_n^0(z)\,\mathbf{P}^*.$$

The next step in solving the leading-order hydrodynamic equations is to construct a single differential equation for the free surface Z_n^0. Substituting the transport of water into the depth-integrated continuity equation results in an equation for the free surface elevation:[6]

$$\nabla\cdot\left[\mathbf{D}_n^0(R)\,\nabla Z_n^0\right] + ni\omega Z_n^0 = 0. \tag{1.6.1}$$

The corresponding boundary conditions read

$$\begin{aligned}
&Z_n^0 = A_n^0(x,y), && \text{at } \partial\Omega_{\text{sea}}, && \text{(tidal forcing)}\\
&\left[\mathbf{D}_n^0(R)\,\nabla Z_n^0\right]\cdot\boldsymbol{n} = 0, && \text{at } \partial\Omega_{\text{bank}}, && \text{(no-transport)}\\
&\left[\mathbf{D}_n^0(R)\,\nabla Z_n^0\right]\cdot\boldsymbol{n} = -q_{\text{river},n}^0(x,y), && \text{at } \partial\Omega_{\text{river}}. && \text{(riverine forcing)}
\end{aligned}$$

An equation for the vertical velocity $W_n^0(z)$ can be obtained by integrating the continuity equation over the depth and using the kinematic boundary condition at the bed, to obtain

$$W_n^0(z) = -\nabla\cdot\left[\mathbf{D}_n^0(z)\,\nabla Z_n^0\right].$$

[6] There seems to be a deeper mathematical connection between the $\mathbf{P}$ matrices, the gradient and the Wirtinger derivatives. For instance, $\mathbf{P}^*\nabla = \sqrt{2}\begin{bmatrix}\partial_{\bar{z}} & \partial_z\end{bmatrix}^T$ and $\nabla^T\mathbf{P} = \sqrt{2}\begin{bmatrix}\partial_z & \partial_{\bar{z}}\end{bmatrix}$, where we have defined the Wirtinger derivatives $\partial_z = (\partial_x - i\partial_y)/2$ and $\partial_{\bar{z}} = (\partial_x + i\partial_y)/2$ (see, e.g., Henrici, 1987, p. 287). The z used here differs from the main text. The exact details of such a formulation remain unknown, but it appears to be related to the use of complex coordinates, see for example Wiggins (2003, p. 280) and Lee *et al.* (2017). Upon further investigation, these matrices, Wirtinger calculus and complex coordinates are closely related, for a detailed overview, we refer to Kreutz-Delgado (2009).

Special case

The above derivation is valid whenever $|f| \neq n\omega$. However, if this condition is not satisfied, care must be taken as either of the $\alpha^0_{n,ii}$'s goes to zero, causing us to divide by zero in $\mathrm{c}^0_{n,ii}(z)$ and $\mathrm{C}^0_{n,ii}(z)$. These problems can be alleviated by considering the appropriate limit.

We assume that $|f|$ goes to $n\omega$. Then it follows that $\alpha^0_{n,ii} \to 0$ for $i = 1$ òr $i = 2$. Using L'Hospital's rule twice, we obtain

$$\lim_{\alpha^0_{n,ii} \to 0} \mathrm{c}^0_{n,ii}(z) = \frac{g}{2A^0_v}\left[(z-R)^2 - \left(D + 2A^0_v/s^0_f\right)D\right],$$

and by either computing the limit or integrating the previous result over the depth, one gets

$$\lim_{\alpha^0_{n,ii} \to 0} \mathrm{C}^0_{n,ii}(z) = \frac{g}{6A^0_v}\left[(z-R)^3 + D^3 - 3\left(D + 2A^0_v/s^0_f\right)D(z+H)\right].$$

The first result can also be obtained by re-solving the rotating flow differential equations with $\alpha^0_{n,ii} = 0$.

Expanding the vertical velocity term

To compute the vertical velocity term $W^0_n(z)$, the divergence of $\mathbf{D}^0_n(z)\,\nabla Z^0_n$ must be calculated with $\mathbf{D}^0_n(z) = \mathbf{P}\,\mathbf{C}^0_n(z)\,\mathbf{P}^*$. Here, the quantities $\mathbf{C}^0_n(z)$ and ∇Z^0_n depend on the horizontal coordinates and the matrices $\mathbf{P}$ and $\mathbf{P}^*$ do not. This suggests that the argument of the divergence operator may be simplified. Similar to taking an ordinary derivative of an expression, the constant factors with respect to the derivative operator may be factored out. However, matrix operators and matrices do not necessarily commute, as matrix multiplication is non-commutative. Hence, the 'factoring out' of the constant matrices requires a little more sophistication.

We want that the horizontal differential operator acts directly on $\mathbf{C}^0_n(z)$ and ∇Z^0_n since those are the only quantities depending on the horizontal coordinates. We have for the vertical velocity component that

$$\begin{aligned} W^0_n(z) &= -\nabla \cdot \left[\mathbf{P}\,\mathbf{C}^0_n(z)\,\mathbf{P}^*\nabla Z^0_n\right], \\ &= -\nabla^T\left[\mathbf{P}\,\mathbf{C}^0_n(z)\,\mathbf{P}^*\nabla Z^0_n\right], \\ &= -\breve{\boldsymbol{P}}^*\,\hat{\nabla}\left[\mathbf{C}^0_n(z)\,\hat{\nabla}^T Z^0_n\right]\breve{\boldsymbol{P}}, \end{aligned}$$

where we have used the 'commutation' relations $\nabla^T\mathbf{P} = \breve{\boldsymbol{P}}^*\,\hat{\nabla}$ and $\mathbf{P}^*\nabla Z^0_n = \hat{\nabla}^T Z^0_n\,\breve{\boldsymbol{P}}$ with operators

$$\hat{\nabla} = \begin{bmatrix} \partial_x & \partial_x \\ \partial_y & -\partial_y \end{bmatrix}, \qquad \hat{\nabla}^T = \begin{bmatrix} \partial_x & \partial_y \\ \partial_x & -\partial_y \end{bmatrix},$$

and vectors and matrix

$$\breve{\boldsymbol{P}}^* = \frac{1}{\sqrt{2}}\begin{bmatrix} 1 & -i \end{bmatrix}, \qquad \breve{\boldsymbol{P}} = \frac{1}{\sqrt{2}}\begin{bmatrix} 1 \\ i \end{bmatrix}, \qquad \hat{\nabla}^T Z^0_n = \begin{bmatrix} Z^0_{n,x} & Z^0_{n,y} \\ Z^0_{n,x} & -Z^0_{n,y} \end{bmatrix}.$$

The next step is to expand the horizontal operator, which can be written as

$$\begin{aligned} \hat{\nabla}\left[\mathbf{C}^0_n(z)\,\hat{\nabla}^T Z^0_n\right] &= \mathrm{C}^0_{n,11}(z)\,\mathbf{H}Z^0_n + \mathrm{C}^0_{n,22}(z)\,\tilde{\mathbf{H}}Z^0_n + \hat{\nabla}\mathbf{C}^0_n(z)\,\hat{\nabla}^T Z^0_n, \\ &= \boldsymbol{\mathcal{K}}\mathbf{C}^0_n(z)\,\boldsymbol{\mathcal{L}}Z^0_n, \end{aligned}$$

where we have defined the matrices

$$\mathbf{H}Z^0_n = \begin{bmatrix} Z^0_{n,xx} & Z^0_{n,xy} \\ Z^0_{n,yx} & Z^0_{n,yy} \end{bmatrix}, \qquad \tilde{\mathbf{H}}Z^0_n = \begin{bmatrix} Z^0_{n,xx} & -Z^0_{n,xy} \\ -Z^0_{n,yx} & Z^0_{n,yy} \end{bmatrix}, \qquad \hat{\nabla}\mathbf{C}^0_n(z) = \begin{bmatrix} \mathrm{C}^0_{n,11,x}(z) & \mathrm{C}^0_{n,22,x}(z) \\ \mathrm{C}^0_{n,11,y}(z) & -\mathrm{C}^0_{n,22,y}(z) \end{bmatrix},$$

$$\boldsymbol{\mathcal{K}}\mathbf{C}^0_n(z) = \begin{bmatrix} \mathrm{C}^0_{n,11}(z)\,\mathbf{I}_2 & \mathrm{C}^0_{n,22}(z)\,\mathbf{I}_2 & \hat{\nabla}\mathbf{C}^0_n(z) \end{bmatrix}, \qquad \boldsymbol{\mathcal{L}}Z^0_n = \begin{bmatrix} \mathbf{H}Z^0_n \\ \tilde{\mathbf{H}}Z^0_n \\ \hat{\nabla}^T Z^0_n \end{bmatrix}.$$

Here, $\mathbf{I}_2$ is the 2×2 identity matrix and $\mathbf{H}Z_n^0$ is the Hessian of Z_n^0. We assume that Z_n^0 is sufficiently smooth, such that $Z_{n,xy}^0 = Z_{n,yx}^0$. As a consequence, the matrices $\mathbf{H}Z_n^0$ and $\tilde{\mathbf{H}}Z_n^0$ are symmetric. Finally, the last line in this equation is just a regular matrix product.

In conclusion, we have derived that the leading-order vertical velocity can be computed using

$$W_n^0(z) = -\check{\boldsymbol{P}}^*\mathcal{K}\mathbf{C}_n^0(z)\,\boldsymbol{\mathcal{L}}Z_n^0\,\check{\boldsymbol{P}}.$$

This expression simplifies if the matrix operations working on the Hessians are written out and this yields

$$W_n^0(z) = -\frac{1}{2}\,\mathrm{tr}\big(\mathbf{C}_n^0(z)\big)\Delta Z_n^0 - \check{\boldsymbol{P}}^*\hat{\nabla}\mathbf{C}_n^0(z)\,\mathbf{P}^*\nabla Z_n^0.$$

Here, the 'commutation' relation $\hat{\nabla}^T Z_n^0\,\check{\boldsymbol{P}} = \mathbf{P}^*\nabla Z_n^0$ has been used to recover the gradient ∇Z_n^0 and the trace operator $\mathrm{tr}([\cdot])$ has been applied. The trace operator returns the sum of the elements on the main diagonal of a square matrix, e.g., in this case

$$\mathrm{tr}\big(\mathbf{C}_n^0(z)\big) = \mathrm{C}_{n,11}^0(z) + \mathrm{C}_{n,22}^0(z).$$

Moreover, this formula for the vertical velocity does not depend on each term of the Hessian individually but only depends on the Laplacian ΔZ_n^0 (i.e., the trace of the Hessian $\mathbf{H}Z_n^0$) and the gradient ∇Z_n^0. This formula may be interpreted as a specific application of the product rule.

For interpretation purposes, one can also use the 'commutation' relation $\check{\boldsymbol{P}}^*\hat{\nabla} = \nabla^T\mathbf{P}$ working on $\mathbf{C}_n^0(z)$. The following form of the vertical velocity is obtained

$$W_n^0(z) = -\frac{1}{2}\,\mathrm{tr}\big(\mathbf{C}_n^0(z)\big)\Delta Z_n^0 - \nabla\cdot\big[\mathbf{P}\,\mathbf{C}_n^0(z)\big]\,\mathbf{P}^*\nabla Z_n^0.$$

Here, we have used that $\nabla^T = \nabla\cdot$. The divergence of a matrix is defined as the divergence of the columns of the matrix and appended together to obtain a row vector, inline with the relationship $\nabla^T = \nabla\cdot$.

Depth-integrated vertical velocity

Sometimes it is useful to consider the depth-integrated vertical velocity. The vertical velocity can be integrated over the depth to obtain

$$\mathcal{W}_n^0(z) = \int_{-H}^{z} W_n^0(\tilde{z})\,d\tilde{z} = -\check{\boldsymbol{P}}^*\hat{\mathcal{K}}\mathbf{C}_n^0(z)\,\boldsymbol{\mathcal{L}}Z_n^0\,\check{\boldsymbol{P}}.$$

The depth-integrated operator $\hat{\mathcal{K}}$ working on $\mathbf{C}_n^0(z)$ is defined as

$$\hat{\mathcal{K}}\mathbf{C}_n^0(z) = \int_{-H}^{z}\mathcal{K}\mathbf{C}_n^0(\tilde{z})\,d\tilde{z} = \left[\int_{-H}^{z}\mathrm{C}_{n,11}^0(\tilde{z})\,d\tilde{z}\,\mathbf{I}_2 \quad \int_{-H}^{z}\mathrm{C}_{n,22}^0(\tilde{z})\,d\tilde{z}\,\mathbf{I}_2 \quad \int_{-H}^{z}\hat{\nabla}\mathbf{C}_n^0(\tilde{z})\,d\tilde{z}\right].$$

Alternatively, the depth-integrated vertical velocity may be expressed as

$$\mathcal{W}_n^0(z) = -\frac{1}{2}\left(\int_{-H}^{z}\mathrm{C}_{n,11}^0(\tilde{z})\,d\tilde{z} + \int_{-H}^{z}\mathrm{C}_{n,22}^0(\tilde{z})\,d\tilde{z}\right)\Delta Z_n^0 - \check{\boldsymbol{P}}^*\int_{-H}^{z}\hat{\nabla}\mathbf{C}_n^0(\tilde{z})\,d\tilde{z}\,\mathbf{P}^*\nabla Z_n^0.$$

In Appendix B.10, formulas to compute the horizontal derivatives of $\mathrm{C}_{n,ii}^0(z)$ are presented to construct the matrix $\hat{\nabla}\mathbf{C}_n^0(z)$ which is required to construct the matrix $\mathcal{K}\mathbf{C}_n^0(z)$. In addition, we also compute the depth-integral of $\mathrm{C}_{n,ii}^0(z)$ and of $\hat{\nabla}\mathbf{C}_n^0(z)$ in order to construct the matrix $\hat{\mathcal{K}}\mathbf{C}_n^0(z)$.

Depth-averaged flow variables

During the derivation of the leading-order free surface equation (1.6.1), the following complex flow vectors are introduced that depend on the vertical coordinate z:

$$\boldsymbol{R}_n^0(z), \qquad \boldsymbol{U}_n^0(z), \qquad W_n^0(z).$$

These depth-dependent flow vectors have also been depth-integrated to obtain

$$\boldsymbol{\mathcal{R}}_n^0(z), \qquad \boldsymbol{q}_n^0(z), \qquad \mathcal{W}_n^0(z),$$

respectively. Another useful quantity to define is the depth-averaged flow. The depth-averaged flow velocities are defined as

$$
\begin{aligned}
[\boldsymbol{R}]_n^0 &= \frac{1}{D}\int_{-H}^{R} \boldsymbol{R}_n^0(z)\,dz = \frac{1}{D}\boldsymbol{\mathcal{R}}_n^0(R) = \frac{1}{D}\mathbf{C}_n^0(R)\,\mathbf{P}^*\nabla Z_n^0,\\
[\boldsymbol{U}]_n^0 &= \frac{1}{D}\int_{-H}^{R} \boldsymbol{U}_n^0(z)\,dz = \frac{1}{D}\boldsymbol{q}_n^0(R) = \frac{1}{D}\mathbf{D}_n^0(R)\,\nabla Z_n^0,\\
[W]_n^0 &= \frac{1}{D}\int_{-H}^{R} W_n^0(z)\,dz = \frac{1}{D}\mathcal{W}_n^0(R) = -\frac{1}{D}\check{\boldsymbol{P}}^*\hat{\boldsymbol{\mathcal{K}}}\mathbf{C}_n^0(R)\,\boldsymbol{\mathcal{L}}Z_n^0\,\check{\boldsymbol{P}}.
\end{aligned}
$$

Here, $[\cdot]$ denotes a depth-averaged variable and $D = H+R$ is the local water depth. We will only use this notation to denote a single depth-averaged variable and *not* use these brackets to denote the depth-average operator in order to avoid potential confusion with the case where these brackets are used to group terms.

1.6.3 First-order hydrodynamic equations

The forcing mechanisms in the first-order hydrodynamic equations are also expanded in a Fourier series. The expansions of the first-order body forcing terms read

$$\boldsymbol{\eta}^1(x,y,z,t) = \sum_{n=0}^{\infty} \Re\mathfrak{e}\Big(\boldsymbol{\eta}^1_n(x,y,z)e^{ni\omega t}\Big), \qquad \text{(advection)}$$
$$\boldsymbol{\varsigma}^1(x,y,z,t) = \sum_{n=0}^{\infty} \Re\mathfrak{e}\Big(\boldsymbol{\varsigma}^1_n(x,y,z)e^{ni\omega t}\Big), \qquad \text{(baroclinic)}$$
$$\boldsymbol{\psi}^1(x,y,z,t) = \sum_{n=0}^{\infty} \Re\mathfrak{e}\Big(\boldsymbol{\psi}^1_n(x,y,z)e^{ni\omega t}\Big), \qquad \text{(eddy viscosity)}$$
$$\boldsymbol{\xi}^1(x,y) = \sum_{n=0}^{\infty} \Re\mathfrak{e}\Big(\boldsymbol{\xi}^1_n(x,y)e^{ni\omega t}\Big), \qquad \text{(reference level)}$$

and of the first-order surface and bottom forcing terms:

$$\boldsymbol{\gamma}^1(x,y,t) = \sum_{n=0}^{\infty} \Re\mathfrak{e}\Big(\boldsymbol{\gamma}^1_n(x,y)e^{ni\omega t}\Big), \qquad \text{at} \quad z = R, \qquad \text{(tidal return flow)}$$
$$\boldsymbol{\chi}^1(x,y,t) = \sum_{n=0}^{\infty} \Re\mathfrak{e}\Big(\boldsymbol{\chi}^1_n(x,y)e^{ni\omega t}\Big), \qquad \text{at} \quad z = R, \qquad \text{(no-stress)}$$
$$\boldsymbol{\mu}^1(x,y,t) = \sum_{n=0}^{\infty} \Re\mathfrak{e}\Big(\boldsymbol{\mu}^1_n(x,y)e^{ni\omega t}\Big), \qquad \text{at} \quad z = -H. \qquad \text{(partial-slip)}$$

Here, the forcing terms have been expanded in Fourier series. An explicit formula for the Fourier coefficients of a Fourier series consisting of the product of two other Fourier series is derived in appendix B.2. In contrast, the reference level forcing $\boldsymbol{\xi}^1$ consists of a single Fourier component since the reference level is assumed to be stationary. That is to say, only the first term in the Fourier expansion is non-zero.

Similar to the leading-order hydrodynamic equations, the Fourier expansions are substituted in the first-order hydrodynamic equations. Using the orthogonality of the sine and cosine, the following equivalent system of complex equations is obtained for each frequency component n:

$$\begin{cases} U^1_{n,x} + V^1_{n,y} + W^1_{n,z} = 0, & \text{(continuity)} \\ ni\omega U^1_n - fV^1_n = -gZ^1_{n,x} + A^0_v U^1_{n,zz} - g\xi^1_{n,1} - \eta^1_{n,1} - \varsigma^1_{n,1} + \psi^1_{n,1,z}, & (x\text{-momentum}) \\ ni\omega V^1_n + fU^1_n = -gZ^1_{n,y} + A^0_v V^1_{n,zz} - g\xi^1_{n,2} - \eta^1_{n,2} - \varsigma^1_{n,2} + \psi^1_{n,2,z}, & (y\text{-momentum}) \\ ni\omega Z^1_n + \left(\int_{-H}^{R} U^1_n\,dz\right)_x + \left(\int_{-H}^{R} V^1_n\,dz\right)_y = -\nabla\cdot\boldsymbol{\gamma}^1_n. & \text{(depth-integrated continuity)} \end{cases}$$

Here, the last subscript of a Greek letter denotes taking the specified component of that vector.

The corresponding boundary conditions are derived in a similar manner. At the seaward boundary, the complex first-order tidal amplitude is prescribed:

$$Z^1_n = A^1_n(x,y), \qquad \text{at} \quad \partial\Omega_{\text{sea}}. \qquad \text{(tidal forcing)}$$

At the estuarine bank, no-transport of water is imposed:

$$\left(\int_{-H}^{R} \boldsymbol{U}^1_n\,dz\right)\cdot\boldsymbol{n} = -\boldsymbol{\gamma}^1_n\cdot\boldsymbol{n}, \qquad \text{at} \quad \partial\Omega_{\text{bank}}, \qquad \text{(no-transport)}$$

and at the riverine boundaries, the first-order complex riverine transport of water is prescribed:

$$\left(\int_{-H}^{R} \boldsymbol{U}^1_n\,dz\right)\cdot\boldsymbol{n} = -q^1_{\text{river},n}(x,y) - \boldsymbol{\gamma}^1_n\cdot\boldsymbol{n}, \qquad \text{at} \quad \partial\Omega_{\text{river}}. \qquad \text{(riverine forcing)}$$

At the free surface, a kinematic and no-stress boundary condition are prescribed:

$$\begin{aligned} W_n^1 &= ni\omega Z_n^1 + \nabla\cdot\boldsymbol{\gamma}_n^1, && \text{at} \quad z = R, && \text{(kinematic)} \\ A_v^0 \boldsymbol{U}_{n,z}^1 &= -\boldsymbol{\psi}_n^1 - \boldsymbol{\chi}_n^1, && \text{at} \quad z = R. && \text{(no-stress)} \end{aligned}$$

At the bed, a kinematic boundary and partial-slip condition are imposed:

$$\begin{aligned} W_n^1 &= -U_n^1 H_x - V_n^1 H_y, && \text{at} \quad z = -H, && \text{(kinematic)} \\ A_v^0 \boldsymbol{U}_{n,z}^1 &= s_f^0 \boldsymbol{U}_n^1 - \boldsymbol{\psi}_n^1 + \boldsymbol{\mu}_n^1, && \text{at} \quad z = -H. && \text{(partial-slip)} \end{aligned}$$

1.6.4 Solving the first-order hydrodynamic equations

The first-order hydrodynamic equations are linear. Thus, the solution of each forcing mechanism may be considered separately and added together to obtain the total solution. To this end, the solution variables are written as a sum over the forcing mechanisms:

$$Z_n^1 = \sum_f Z_n^{1,f}, \qquad U_n^1(z) = \sum_f U_n^{1,f}(z), \qquad V_n^1(z) = \sum_f V_n^{1,f}(z), \qquad W_n^1(z) = \sum_f W_n^{1,f}(z),$$

where the forcing mechanism index f runs through the set containing all forcing mechanisms:

$$\mathscr{F} = \{\xi, \chi, \mu, \eta, \varsigma, \psi, \gamma, A, q\}.$$

Here, ξ is the reference level forcing, χ is the no-stress forcing, μ is the partial-slip forcing, η is the advective forcing, ς is the baroclinic forcing, ψ is the eddy viscosity forcing, γ is the tidal return flow forcing, A is the amplitude forcing and q is the riverine forcing.

The momentum equations can be written in matrix vector form for forcing mechanisms f as

$$\mathbf{M}_n^0(z)\boldsymbol{U}_n^{1,f}(z) = g\nabla Z_n^{1,f} + \boldsymbol{\Sigma}_n^{1,f}(z),$$

with the boundary conditions given by

$$\begin{aligned} A_v^0 \boldsymbol{U}_{n,z}^{1,f}(z) &= \boldsymbol{\Sigma}_{n,R}^{1,f}, && \text{at} \quad z = R, \\ A_v^0 \boldsymbol{U}_{n,z}^{1,f}(z) &= s_f^0 \boldsymbol{U}_n^{1,f}(z) + \boldsymbol{\Sigma}_{n,-H}^{1,f}, && \text{at} \quad z = -H. \end{aligned}$$

Here, we have defined the momentum matrix (with Coriolis f)

$$\mathbf{M}_n^0(z) = \begin{bmatrix} A_v^0\partial_{zz} - ni\omega & f \\ -f & A_v^0\partial_{zz} - ni\omega \end{bmatrix},$$

and the body and boundary forcing vectors

$$\boldsymbol{\Sigma}_n^{1,f}(z) = \begin{cases} g\boldsymbol{\xi}_n^1, & f = \xi, \\ \boldsymbol{\eta}_n^1(z), & f = \eta, \\ \boldsymbol{\varsigma}_n^1(z), & f = \varsigma, \\ -\boldsymbol{\psi}_{n,z}^1(z), & f = \psi, \\ \mathbf{0}, & \text{otherwise}, \end{cases}, \quad \boldsymbol{\Sigma}_{n,R}^{1,f} = \begin{cases} -\boldsymbol{\psi}_n^1(R), & f = \psi, \\ -\boldsymbol{\chi}_n^1, & f = \chi, \\ \mathbf{0}, & \text{otherwise}, \end{cases}, \quad \boldsymbol{\Sigma}_{n,-H}^{1,f} = \begin{cases} -\boldsymbol{\psi}_n^1(-H), & f = \psi, \\ \boldsymbol{\mu}_n^1, & f = \mu, \\ \mathbf{0}, & \text{otherwise}. \end{cases}$$

To emphasize that some vectors and matrices depend on the depth z, we explicitly denote their depth dependence after the variable.

We decouple the momentum equations. The matrix $\mathbf{M}_n^0(z)$ is again normal, i.e., $\mathbf{M}_n^0(z)^*\mathbf{M}_n^0(z) = \mathbf{M}_n^0(z)\mathbf{M}_n^0(z)^*$. Thus the matrix $\mathbf{M}_n^0(z)$ is diagonalizable by a unitary matrix. The unitary diagonalization reads

$$\mathbf{M}_n^0(z) = \mathbf{P}\boldsymbol{\Lambda}_n^0(z)\mathbf{P}^*,$$

with

$$\mathbf{P} = \frac{1}{\sqrt{2}}\begin{bmatrix} 1 & 1 \\ -i & i \end{bmatrix}, \qquad \boldsymbol{\Lambda}_n^0(z) = \begin{bmatrix} A_v^0\partial_{zz} - i(n\omega + f) & 0 \\ 0 & A_v^0\partial_{zz} - i(n\omega - f) \end{bmatrix}, \qquad \text{and} \qquad \mathbf{P}^* = \frac{1}{\sqrt{2}}\begin{bmatrix} 1 & i \\ 1 & -i \end{bmatrix}.$$

This diagonalization is substituted into the momentum equations and multiplied from the left with $\mathbf{P}^*$, to obtain

$$\mathbf{\Lambda}_n^0(z)\boldsymbol{R}_n^{1,f}(z) = \mathbf{P}^*\left[g\nabla Z_n^{1,f} + \mathbf{\Sigma}_n^{1,f}(z)\right],$$

where we have defined the rotating flow variables vector per forcing mechanism f: $\boldsymbol{R}_n^{1,f}(z) = \mathbf{P}^*\boldsymbol{U}_n^{1,f}(z)$. Similarly, multiplying the no-stress and partial-slip boundary conditions from the left with $\mathbf{P}^*$ yields the corresponding boundary conditions:

$$\begin{aligned} A_v^0\boldsymbol{R}_{n,z}^{1,f}(z) &= \mathbf{P}^*\mathbf{\Sigma}_{n,R}^{1,f}, && \text{at} \quad z = R, \\ A_v^0\boldsymbol{R}_{n,z}^{1,f}(z) &= s_f^0\boldsymbol{R}_n^{1,f}(z) + \mathbf{P}^*\mathbf{\Sigma}_{n,-H}^{1,f}, && \text{at} \quad z = -H. \end{aligned}$$

For each forcing mechanism f, the solution of the rotating flow variables consist of two parts: a *forced* and *forcing* part. Starting with the latter, the forcing part is either generated by nonlinear interactions of the leading-order hydrodynamics or is externally prescribed. From the point of view of the first-order hydrodynamics, the forcing part is a known fixed quantity that cannot be changed. In response to this forcing part or externally prescribed forcing mechanisms, a first-order hydrodynamic response is generated: the forced part. The forced part is the hydrodynamic response to a specific forcing mechanism, it is the corresponding first-order flow as a consequence of the forcing. Roughly speaking, a forcing mechanism generates a specific setup of the first-order free surface. The gradient of this specific free surface setup consequently drives a flow. The free surface setup and flow together constitute the forced hydrodynamic response to a forcing. The decomposition into a *forced* and *forcing* part reads

$$\boldsymbol{R}_n^{1,f}(z) = \hat{\boldsymbol{R}}_n^{1,f}(z) + \check{\boldsymbol{R}}_n^{1,f}(z).$$

They satisfy the following decoupled ordinary differential equations in the vertical coordinate z:

$$\hat{\boldsymbol{R}}_{n,zz}^{1,f}(z) - \left(\boldsymbol{\alpha}_n^0\right)^2\hat{\boldsymbol{R}}_n^{1,f}(z) = \frac{g}{A_v^0}\mathbf{P}^*\nabla Z_n^{1,f}, \qquad \check{\boldsymbol{R}}_{n,zz}^{1,f}(z) - \left(\boldsymbol{\alpha}_n^0\right)^2\check{\boldsymbol{R}}_n^{1,f}(z) = \frac{1}{A_v^0}\mathbf{P}^*\mathbf{\Sigma}_n^{1,f}(z),$$

with corresponding homogeneous and inhomogeneous boundary conditions given by

$$\begin{aligned} A_v^0\hat{\boldsymbol{R}}_{n,z}^{1,f}(z) &= \mathbf{0}, & A_v^0\check{\boldsymbol{R}}_{n,z}^{1,f}(z) &= \mathbf{P}^*\mathbf{\Sigma}_{n,R}^{1,f} && \text{at} \quad z = R, \\ A_v^0\hat{\boldsymbol{R}}_{n,z}^{1,f}(z) &= s_f^0\hat{\boldsymbol{R}}_n^{1,f}(z), & A_v^0\check{\boldsymbol{R}}_{n,z}^{1,f}(z) &= s_f^0\check{\boldsymbol{R}}_n^{1,f}(z) + \mathbf{P}^*\mathbf{\Sigma}_{n,-H}^{1,f} && \text{at} \quad z = -H. \end{aligned}$$

Here, we have defined the diagonal matrix

$$\boldsymbol{\alpha}_n^0(x,y) = \begin{bmatrix} \sqrt{i(n\omega + f)/A_v^0} & 0 \\ 0 & \sqrt{i(n\omega - f)/A_v^0} \end{bmatrix}.$$

The problem for the forced rotating flow variables is the same as that for the leading-order rotating flow variables. Hence, we can reuse that solution. Regarding the solution of the forcing rotating flow variables, we denote the solution as the inverse of the second-order ode operator. This solution can also be obtained analytically using, for example, variation of parameters.

The *forced* and *forcing* solution for each forcing mechanism f are given by

$$\hat{\boldsymbol{R}}_n^{1,f}(z) = \mathbf{c}_n^0(z)\mathbf{P}^*\nabla Z_n^{1,f}, \qquad \check{\boldsymbol{R}}_n^{1,f}(z) = \mathbf{\Lambda}_n^0(z)^{-1}\left\{\mathbf{P}^*\mathbf{\Sigma}_n^{1,f}(z), \mathbf{P}^*\mathbf{\Sigma}_{n,R}^{1,f}, \mathbf{P}^*\mathbf{\Sigma}_{n,-H}^{1,f}\right\}.$$

The known *forcing* part simplifies if we evaluate the index f:

$$\begin{aligned} \check{\boldsymbol{R}}_n^{1,\xi}(z) &= \mathbf{c}_n^0(z)\mathbf{P}^*\boldsymbol{\xi}_n^1, & \check{\boldsymbol{R}}_n^{1,\chi}(z) &= \mathbf{c}_n^{1,\chi}(z)\mathbf{P}^*\boldsymbol{\chi}_n^1, & \check{\boldsymbol{R}}_n^{1,\mu}(z) &= \mathbf{c}_n^{1,\mu}(z)\mathbf{P}^*\boldsymbol{\mu}_n^1, \\ \check{\boldsymbol{R}}_n^{1,\eta}(z) &= \mathbf{\Lambda}_n^0(z)^{-1}\left\{\mathbf{P}^*\boldsymbol{\eta}_n^1(z), \mathbf{0}, \mathbf{0}\right\}, & \check{\boldsymbol{R}}_n^{1,\varsigma}(z) &= \mathbf{\Lambda}_n^0(z)^{-1}\left\{\mathbf{P}^*\boldsymbol{\varsigma}_n^1(z), \mathbf{0}, \mathbf{0}\right\}, & \check{\boldsymbol{R}}_n^{1,\psi}(z) &= -\mathbf{\Lambda}_n^0(z)^{-1}\left\{\mathbf{P}^*\boldsymbol{\psi}_{n,z}^1(z),\right. \\ &&&&& \left.\mathbf{P}^*\boldsymbol{\psi}_n^1(R), \mathbf{P}^*\boldsymbol{\psi}_n^1(-H)\right\}, \\ \check{\boldsymbol{R}}_n^{1,\gamma}(z) &= \mathbf{0}, & \check{\boldsymbol{R}}_n^{1,A}(z) &= \mathbf{0}, & \check{\boldsymbol{R}}_n^{1,q}(z) &= \mathbf{0}. \end{aligned}$$

Here, the analytic solution of the no-stress forcing $f = \chi$ and partial-slip forcing $f = \mu$ are used. These analytic solutions are derived in Section 1.7.3, but are, in fact, valid for any n. Explicit solutions for the forcing rotating flow variables under the standard forcing conditions can be found in Section 1.7.3.

Again, it is useful to integrate the rotating flow variables over the depth. Decomposing the depth-integrated flow variables into a *forced* and *forcing* component yields

$$\boldsymbol{\mathcal{R}}_n^{1,f}(z) = \hat{\boldsymbol{\mathcal{R}}}_n^{1,f}(z) + \check{\boldsymbol{\mathcal{R}}}_n^{1,f}(z),$$

where we have defined the depth-integrated *forced* and *forcing* rotating flow variables for each forcing mechanism f:

$$\hat{\boldsymbol{\mathcal{R}}}_n^{1,f}(z) = \int_{-H}^{z} \hat{\boldsymbol{R}}_n^{1,f}(\tilde{z})\, d\tilde{z} = \mathbf{C}_n^0(z)\,\mathbf{P}^*\nabla Z_n^{1,f}, \qquad \check{\boldsymbol{\mathcal{R}}}_n^{1,f}(z) = \int_{-H}^{z} \check{\boldsymbol{R}}_n^{1,f}(\tilde{z})\, d\tilde{z}.$$

The known *forcing* part simplifies upon evaluating the index f:

$$\begin{aligned}
&\check{\boldsymbol{\mathcal{R}}}_n^{1,\xi}(z) = \mathbf{C}_n^0(z)\,\mathbf{P}^*\boldsymbol{\xi}_n^1, &&\check{\boldsymbol{\mathcal{R}}}_n^{1,\chi}(z) = \mathbf{C}_n^{1,\chi}(z)\,\mathbf{P}^*\boldsymbol{\chi}_n^1, &&\check{\boldsymbol{\mathcal{R}}}_n^{1,\mu}(z) = \mathbf{C}_n^{1,\mu}(z)\,\mathbf{P}^*\boldsymbol{\mu}_n^1,\\
&\check{\boldsymbol{\mathcal{R}}}_n^{1,\eta}(z) = \int_{-H}^{z} \check{\boldsymbol{R}}_n^{1,\eta}(\tilde{z})\, d\tilde{z}, &&\check{\boldsymbol{\mathcal{R}}}_n^{1,\varsigma}(z) = \int_{-H}^{z} \check{\boldsymbol{R}}_n^{1,\varsigma}(\tilde{z})\, d\tilde{z}, &&\check{\boldsymbol{\mathcal{R}}}_n^{1,\psi}(z) = \int_{-H}^{z} \check{\boldsymbol{R}}_n^{1,\psi}(\tilde{z})\, d\tilde{z},\\
&\check{\boldsymbol{\mathcal{R}}}_n^{1,\gamma}(z) = \mathbf{0}, &&\check{\boldsymbol{\mathcal{R}}}_n^{1,A}(z) = \mathbf{0}, &&\check{\boldsymbol{\mathcal{R}}}_n^{1,q}(z) = \mathbf{0}.
\end{aligned}$$

The next step in the decoupling and solving of the momentum equations consists of transforming back to the horizontal velocity vector $\boldsymbol{U}_n^{1,f}(z)$. This can be done by inverting the definition of the rotating flow variables, $\boldsymbol{R}_n^{1,f}(z) = \mathbf{P}^*\boldsymbol{U}_n^{1,f}(z)$. The horizontal velocity vector can be split into a *forced* and *forcing* part:

$$\boldsymbol{U}_n^{1,f}(z) = \hat{\boldsymbol{U}}_n^{1,f}(z) + \check{\boldsymbol{U}}_n^{1,f}(z).$$

where, we have defined the *forced* and *forcing* horizontal velocity as

$$\hat{\boldsymbol{U}}_n^{1,f}(z) = \mathbf{P}\,\hat{\boldsymbol{R}}_n^{1,f}(z) = \mathbf{d}_n^0(z)\nabla Z_n^{1,f}, \qquad \check{\boldsymbol{U}}_n^{1,f}(z) = \mathbf{P}\,\check{\boldsymbol{R}}_n^{1,f}(z).$$

The known *forcing* horizontal velocities simplify when we evaluate the index f:

$$\begin{aligned}
&\check{\boldsymbol{U}}_n^{1,\xi}(z) = \mathbf{d}_n^0(z)\,\boldsymbol{\xi}_n^1, &&\check{\boldsymbol{U}}_n^{1,\chi}(z) = \mathbf{d}_n^{1,\chi}(z)\,\boldsymbol{\chi}_n^1, &&\check{\boldsymbol{U}}_n^{1,\mu}(z) = \mathbf{d}_n^{1,\mu}(z)\,\boldsymbol{\mu}_n^1,\\
&\check{\boldsymbol{U}}_n^{1,\eta}(z) = \mathbf{P}\,\check{\boldsymbol{R}}_n^{1,\eta}(z), &&\check{\boldsymbol{U}}_n^{1,\varsigma}(z) = \mathbf{P}\,\check{\boldsymbol{R}}_n^{1,\varsigma}(z), &&\check{\boldsymbol{U}}_n^{1,\psi}(z) = \mathbf{P}\,\check{\boldsymbol{R}}_n^{1,\psi}(z),\\
&\check{\boldsymbol{U}}_n^{1,\gamma}(z) = \mathbf{0}, &&\check{\boldsymbol{U}}_n^{1,A}(z) = \mathbf{0}, &&\check{\boldsymbol{U}}_n^{1,q}(z) = \mathbf{0}.
\end{aligned}$$

Here, we have defined the matrices

$$\mathbf{d}_n^0(z) = \mathbf{P}\,\mathbf{c}_n^0(z)\,\mathbf{P}^*, \qquad \mathbf{d}_n^{1,\chi}(z) = \mathbf{P}\,\mathbf{c}_n^{1,\chi}(z)\,\mathbf{P}^*, \qquad \mathbf{d}_n^{1,\mu}(z) = \mathbf{P}\,\mathbf{c}_n^{1,\mu}(z)\,\mathbf{P}^*.$$

The next step in solving the first-order hydrodynamic equations is to construct a single differential equation for the free surface Z_n^1. This can be done by considering the depth-integrated continuity equation:

$$\nabla\cdot\left[\int_{-H}^{R}\boldsymbol{U}_n^1\,dz\right] + ni\omega Z_n^1 = -\nabla\cdot\boldsymbol{\gamma}_n^1.$$

This equation depends on the horizontal velocity vector integrated over depth, which is also known as the horizontal transport of water. Here, the $f = \gamma$ forcing introduces itself.

By integrating the horizontal velocity vector over the depth, the transport of water is found for each forcing mechanism f. The transport of water can be decomposed into a *forced* and *forcing* contribution

$$\boldsymbol{q}_n^{1,f}(z) = \hat{\boldsymbol{q}}_n^{1,f}(z) + \check{\boldsymbol{q}}_n^{1,f}(z),$$

which are defined as

$$\hat{\boldsymbol{q}}_n^{1,f}(z) = \int_{-H}^{z} \hat{\boldsymbol{U}}_n^{1,f}(\tilde{z})\, d\tilde{z} = \mathbf{D}_n^0(z)\,\nabla Z_n^{1,f}, \qquad \check{\boldsymbol{q}}_n^{1,f}(z) = \int_{-H}^{z} \check{\boldsymbol{U}}_n^{1,f}(\tilde{z})\, d\tilde{z} = \mathbf{P}\,\check{\boldsymbol{\mathcal{R}}}_n^{1,f}(z),$$

except for the forcing transport of water for the $f = \gamma$ forcing mechanism, which is defined below.

If we evaluate the index f, the known *forcing* terms simplify:

$$\check{\boldsymbol{q}}_n^{1,\xi}(z) = \mathbf{D}_n^0(z)\,\boldsymbol{\xi}_n^1, \qquad \check{\boldsymbol{q}}_n^{1,\chi}(z) = \mathbf{D}_n^{1,\chi}(z)\,\boldsymbol{\chi}_n^1, \qquad \check{\boldsymbol{q}}_n^{1,\mu}(z) = \mathbf{D}_n^{1,\mu}(z)\,\boldsymbol{\mu}_n^1,$$
$$\check{\boldsymbol{q}}_n^{1,\eta}(z) = \mathbf{P}\,\check{\boldsymbol{\mathcal{R}}}_n^{1,\eta}(z), \qquad \check{\boldsymbol{q}}_n^{1,\varsigma}(z) = \mathbf{P}\,\check{\boldsymbol{\mathcal{R}}}_n^{1,\varsigma}(z), \qquad \check{\boldsymbol{q}}_n^{1,\psi}(z) = \mathbf{P}\,\check{\boldsymbol{\mathcal{R}}}_n^{1,\psi}(z),$$
$$\check{\boldsymbol{q}}_n^{1,\gamma}(z) = \mathbb{1}_R(x,y,z)\,\boldsymbol{\gamma}_n^1, \qquad \check{\boldsymbol{q}}_n^{1,A}(z) = \mathbf{0}, \qquad \check{\boldsymbol{q}}_n^{1,q}(z) = \mathbf{0},$$

where we have defined the matrices

$$\mathbf{D}_n^0(z) = \mathbf{P}\mathbf{C}_n^0(z)\mathbf{P}^*, \qquad \mathbf{D}_n^{1,\chi}(z) = \mathbf{P}\mathbf{C}_n^{1,\chi}(z)\mathbf{P}^*, \qquad \mathbf{D}_n^{1,\mu}(z) = \mathbf{P}\mathbf{C}_n^{1,\mu}(z)\mathbf{P}^*.$$

Here, we have defined the reference level indicator function

$$\mathbb{1}_R(x,y,z) = \begin{cases} 1, & \text{if } z = R(x,y), \\ 0, & \text{else.} \end{cases}$$

Substituting this transport expression evaluated at the reference level $z = R$ into the depth-integrated continuity equation results in an equation for the first-order free surface elevation for each forcing mechanism f in $\mathscr{F}$:

$$\nabla\cdot\left[\mathbf{D}_n^0(R)\,\nabla Z_n^{1,f}\right] + ni\omega Z_n^{1,f} = -\nabla\cdot\left[\check{\boldsymbol{q}}_n^{1,f}(R)\right], \tag{1.6.2}$$

with the boundary conditions given by

$$\begin{aligned} Z_n^{1,f} &= A_n^{1,f}(x,y), && \text{at} \quad \partial\Omega_{\text{sea}}, \\ \left[\mathbf{D}_n^0(R)\,\nabla Z_n^{1,f}\right]\cdot\boldsymbol{n} &= \tilde{q}_{\text{bank},n}^{1,f}(x,y), && \text{at} \quad \partial\Omega_{\text{bank}}, \\ \left[\mathbf{D}_n^0(R)\,\nabla Z_n^{1,f}\right]\cdot\boldsymbol{n} &= \dot{q}_{\text{river},n}^{1,f}(x,y), && \text{at} \quad \partial\Omega_{\text{river}}. \end{aligned}$$

Here, we have defined the amplitude forcing at $\partial\Omega_{\text{sea}}$ and the transport of water forcing mechanisms at $\partial\Omega_{\text{bank}}$ and $\partial\Omega_{\text{river}}$:

$$A_n^{1,f}(x,y) = \begin{cases} A_n^1(x,y) & \text{if } f = A, \\ 0 & \text{otherwise,} \end{cases} \qquad \tilde{q}_{\text{bank},n}^{1,f}(x,y) = \begin{cases} -\boldsymbol{\gamma}_n^1\cdot\boldsymbol{n} & \text{if } f = \gamma, \\ 0 & \text{otherwise,} \end{cases} \qquad \dot{q}_{\text{river},n}^{1,f}(x,y) = \begin{cases} -\boldsymbol{\gamma}_n^1\cdot\boldsymbol{n} & \text{if } f = \gamma, \\ -q_{\text{river},n}^1 & \text{if } f = q, \\ 0 & \text{otherwise.} \end{cases}$$

Here, the amplitude forcing $f = A$ and the river riverine forcing $f = q$ are introduced and $\boldsymbol{n}$ is the outward pointing unit normal. This means, for example, that when the inner product between the transport of water and the outward pointing unit normal is positive, the transport of water is directed out of the domain and vice versa, when it is negative, the transport of water is directed into the domain.

An equation for the vertical velocity $W_n^1(z)$ is obtained by integrating the continuity equation over the depth and using the kinematic boundary condition at the bed, to obtain

$$W_n^1(z) = -\nabla\cdot\left[\int_{-H}^{z}\boldsymbol{U}_n^1(\tilde{z})\,d\tilde{z}\right].$$

The vertical velocity can be decomposed into a *forced* and *forcing* vertical velocity for each forcing mechanism f:

$$W_n^{1,f}(z) = \hat{W}_n^{1,f}(z) + \check{W}_n^{1,f}(z).$$

where we have defined the *forced* and *forcing* vertical velocities as

$$\hat{W}_n^{1,f}(z) = -\nabla\cdot\left[\mathbf{D}_n^0(z)\,\nabla Z_n^{1,f}\right], \qquad \check{W}_n^{1,f}(z) = -\nabla\cdot\left[\check{\boldsymbol{q}}_n^{1,f}(z)\right].$$

Strictly speaking, these equations are only valid for $-H(x,y) < z < R(x,y)$. Hence, they may not be evaluated at $z = R(x,y)$ or $z = -H(x,y)$. However, these equations can be evaluated at these levels by considering the appropriate limit. Using this limiting procedure, one may also show that the tidal return flow forcing $\check{\boldsymbol{q}}_n^{1,\gamma}(z)$, which vanishes in the internal z domain, does not appear in the limit of z to $R(x,y)$.[7]

[7]This result can also be obtained by integrating the full three-dimensional continuity equation over the depth, linearising around $z = R(x,y)$, scaling, substituting the asymptotic expansions and, finally, collecting the first-order terms.

Expanding the vertical velocity terms

We expand the first-order vertical velocity $W_n^{1,f}(z)$. It consists of a forced and forcing vertical velocity. These velocities can be expanded as

$$\hat{W}_n^{1,f}(z) = -\check{\boldsymbol{P}}^* \boldsymbol{\mathcal{K}} \mathbf{C}_n^0(z)\, \boldsymbol{\mathcal{L}} Z_n^{1,f} \check{\boldsymbol{P}}, \qquad \check{W}_n^{1,f}(z) = -\nabla \cdot \left[\mathbf{P} \int_{-H}^{z} \check{\boldsymbol{R}}_n^{1,f}(\tilde{z})\, d\tilde{z} \right] = -\check{\boldsymbol{P}}^* \hat{\nabla} \left[\int_{-H}^{z} \check{\boldsymbol{R}}_n^{1,f}(\tilde{z})\, d\tilde{z} \right],$$

where we have reused the matrices and operators that were defined for the expansion of the leading-order vertical velocity, see Section 1.6.2 for details.

The forced vertical velocity is written as a product of matrices of base quantities (or atoms). Thus this term cannot be simplified further. The forcing vertical velocity, on the other hand, may be simplified under certain conditions. It might be possible to exchange the differentiation and integration using Leibniz integral rule, but this is not done here. One can also numerically evaluate the divergence for fixed z levels. However, the depth-integral must then be evaluated numerically too using a certain number of numerically computed z levels. We simplify this expression in the special case where the forcing transport of water can be written in the form $\check{\boldsymbol{q}}_n^{1,f}(z) = \mathbf{P}\, \mathbf{C}_n^{m,f}(z)\, \mathbf{P}^* \boldsymbol{f}_n^1$ for $m = 0$ or $m = 1$. It follows that

$$\begin{aligned} \check{W}_n^{1,f}(z) &= -\check{\boldsymbol{P}}^* \hat{\nabla} \left[\mathbf{C}_n^{m,f}(z)\, \mathbf{P}^* \boldsymbol{f}_n^1 \right], \\ &= -\check{\boldsymbol{P}}^* \hat{\nabla} \left[\mathbf{C}_n^{m,f}(z)\, \hat{\mathbf{1}} \boldsymbol{f}_n^{1,\mathcal{D}} \right] \check{\boldsymbol{P}}, \end{aligned}$$

where we have defined a compact notation for the diagonalization of a vector and the constant matrix:

$$\boldsymbol{f}_n^{1,\mathcal{D}} = \boldsymbol{\mathcal{D}}\{\boldsymbol{f}_n^1\} = \begin{bmatrix} f_{n,1}^1 & 0 \\ 0 & f_{n,2}^1 \end{bmatrix}, \qquad \hat{\mathbf{1}} = \begin{bmatrix} 1 & 1 \\ 1 & -1 \end{bmatrix}.$$

The next step is to expand the horizontal operator, which can be written as

$$\begin{aligned} \hat{\nabla} \left[\mathbf{C}_n^{m,f}(z)\, \hat{\mathbf{1}} \boldsymbol{f}_n^{1,\mathcal{D}} \right] &= \mathrm{C}_{n,11}^{m,f}(z)\, \check{\nabla} \boldsymbol{f}_n^{1,\mathcal{D}} + \mathrm{C}_{n,22}^{m,f}(z)\, \tilde{\nabla} \boldsymbol{f}_n^{1,\mathcal{D}} + \hat{\nabla} \mathbf{C}_n^{m,f}(z)\, \hat{\mathbf{1}} \boldsymbol{f}_n^{1,\mathcal{D}}, \\ &= \boldsymbol{\mathcal{K}} \mathbf{C}_n^{m,f}(z)\, \hat{\boldsymbol{\mathcal{L}}} \boldsymbol{f}_n^{1,\mathcal{D}}, \end{aligned}$$

where we have defined the differential operators

$$\check{\nabla} = \begin{bmatrix} \partial_x & \partial_x \\ \partial_y & \partial_y \end{bmatrix}, \qquad \tilde{\nabla} = \begin{bmatrix} \partial_x & -\partial_x \\ -\partial_y & \partial_y \end{bmatrix}, \qquad \hat{\nabla} = \begin{bmatrix} \partial_x & \partial_x \\ \partial_y & -\partial_y \end{bmatrix}, \qquad \hat{\boldsymbol{\mathcal{L}}} = \begin{bmatrix} \check{\nabla} \\ \tilde{\nabla} \\ \hat{\mathbf{1}} \end{bmatrix}.$$

Furthermore, we have defined the matrices

$$\check{\nabla} \boldsymbol{f}_n^{1,\mathcal{D}} = \begin{bmatrix} f_{n,1,x}^1 & f_{n,2,x}^1 \\ f_{n,1,y}^1 & f_{n,2,y}^1 \end{bmatrix}, \qquad \tilde{\nabla} \boldsymbol{f}_n^{1,\mathcal{D}} = \begin{bmatrix} f_{n,1,x}^1 & -f_{n,2,x}^1 \\ -f_{n,1,y}^1 & f_{n,2,y}^1 \end{bmatrix}, \qquad \hat{\nabla} \mathbf{C}_n^m(z) = \begin{bmatrix} \mathrm{C}_{n,11,x}^m(z) & \mathrm{C}_{n,22,x}^m(z) \\ \mathrm{C}_{n,11,y}^m(z) & -\mathrm{C}_{n,22,y}^m(z) \end{bmatrix},$$

$$\boldsymbol{\mathcal{K}} \mathbf{C}_n^{m,f}(z) = \begin{bmatrix} \mathrm{C}_{n,11}^{m,f}(z)\, \mathbf{I}_2 & \mathrm{C}_{n,22}^{m,f}(z)\, \mathbf{I}_2 & \hat{\nabla} \mathbf{C}_n^{m,f}(z) \end{bmatrix}, \qquad \hat{\boldsymbol{\mathcal{L}}} \boldsymbol{f}_n^{1,\mathcal{D}} = \begin{bmatrix} \check{\nabla} \boldsymbol{f}_n^{1,\mathcal{D}} \\ \tilde{\nabla} \boldsymbol{f}_n^{1,\mathcal{D}} \\ \hat{\mathbf{1}} \boldsymbol{f}_n^{1,\mathcal{D}} \end{bmatrix}.$$

In conclusion, we have for this case with $m = 0, 1$ that

$$\check{W}_n^{1,f}(z) = -\check{\boldsymbol{P}}^* \boldsymbol{\mathcal{K}} \mathbf{C}_n^{m,f}(z)\, \hat{\boldsymbol{\mathcal{L}}} \boldsymbol{f}_n^{1,\mathcal{D}}\, \check{\boldsymbol{P}}.$$

Finally, we note the operator $\hat{\boldsymbol{\mathcal{L}}}$ is a generalization of the operator $\boldsymbol{\mathcal{L}}$. To see this, let the generalized operator $\hat{\boldsymbol{\mathcal{L}}}$ work on $\nabla Z_n^{0,\mathcal{D}}$. Then we have

$$\hat{\boldsymbol{\mathcal{L}}} \nabla Z_n^{0,\mathcal{D}} = \begin{bmatrix} \check{\nabla} \nabla Z_n^{0,\mathcal{D}} \\ \tilde{\nabla} \nabla Z_n^{0,\mathcal{D}} \\ \hat{\mathbf{1}} \nabla Z_n^{0,\mathcal{D}} \end{bmatrix} = \begin{bmatrix} \mathbf{H} Z_n^0 \\ \tilde{\mathbf{H}} Z_n^0 \\ \hat{\nabla}^T Z_n^0 \end{bmatrix} = \boldsymbol{\mathcal{L}} Z_n^0.$$

Table 1.3: Table summarising the forcing mechanisms of the leading- and first-order water motion under the standard forcing conditions. The rows show which forcing generates which tidal constituents through which mechanism. The columns depict all the forcing mechanisms for a certain tidal constituent.

		$\mathcal{O}(1)$	$\mathcal{O}(\varepsilon)$	$\mathcal{O}(\varepsilon)$
		M_2	M_0	M_4
	External	A	q, ς, ξ	A
$\mathcal{O}(1)$	Internal M_2		η, γ, χ, μ	η, γ, χ, μ

1.7 Standard forcing conditions

The frequency components of the solution form a particularly well-analysable set under certain *external forcing conditions*. These assumptions are referred to as *standard forcing conditions*. These conditions can be considered as a slight extension of those considered by Kumar (2018) and are given by

1. The leading-order water motion is forced by an M_2 tidal constituent at the seaward boundaries (A).
2. The first-order water motion is forced by a constant river discharge at the riverine boundaries (q) and an M_4 constituent at the seaward boundaries (A).
3. The first-order water motion is forced by a baroclinic forcing for which the density gradient is independent of the vertical coordinate z and consists of a subtidal M_0 component only (ς).
4. The first-order water motion is forced by a subtidal reference level forcing (ξ).
5. The first-order water motion is internally forced by a partial-slip forcing for which the first-order partial slip parameter consists of an M_2 component only. In combination with the leading-order M_2 water motion, this mechanisms generates an M_0 and M_4 tidal signal (μ).
6. The first-order water motion is *not* forced by the eddy viscosity forcing, since the eddy viscosity parameter is assumed to consist of a leading-order component only, (i.e., $\psi \notin \mathscr{F}$).

Under these assumptions, the leading-order water motion consists of a single frequency component, namely the M_2 constituent. The externally forced first-order water motion consists of the M_0 and M_4 constituents and the internally generated first-order water motion consist of the same constituents, e.g., η, γ and χ. Hence, the first-order water motion consists of two frequency components: the M_0 and M_4 constituents. The forcing mechanisms and the forced water motion components are summarised in Table 1.3. The forcing mechanisms under the standard forcing conditions can be collected into a single list:

$$\tilde{\mathscr{F}} = \{\xi, \chi, \mu, \eta, \varsigma, \gamma, A, q\}.$$

1.7.1 Leading-order hydrodynamics

The leading-order hydrodynamic equations and boundary conditions are presented under the standard forcing conditions. The water motion consists of a single frequency component. Let ω be the the M_2 angular frequency, then the leading-order water motion only consists of the $n = 1$ frequency component.

The equation for the leading-order free surface elevation $Z_1^0(x, y)$ reads

$$\nabla \cdot \left[\mathbf{D}_1^0(R)\,\nabla Z_1^0\right] + i\omega Z_1^0 = 0, \tag{1.7.1}$$

with boundary conditions:

$$\begin{aligned}
&Z_1^0 = A_1^0(x, y), && \text{at} \quad \partial\Omega_{\text{sea}}, && \text{(tidal forcing)}\\
&\left[\mathbf{D}_1^0(R)\,\nabla Z_1^0\right] \cdot \boldsymbol{n} = 0, && \text{at} \quad \partial\Omega_{\text{bank}}, && \text{(no-transport)}\\
&\left[\mathbf{D}_1^0(R)\,\nabla Z_1^0\right] \cdot \boldsymbol{n} = 0, && \text{at} \quad \partial\Omega_{\text{river}}. && \text{(no-transport)}
\end{aligned}$$

Once the leading-order free surface elevation Z_1^0 is known, all leading-order flow variables are known too, since they can be expressed in terms of the leading-order free surface elevation, its gradient and hessian. For example,

Table 1.4: Leading-order flow variables depending on the leading-order free surface elevation Z_1^0.

	Horizontal rotating velocity	Horizontal velocity	Vertical velocity
Normal	$\boldsymbol{R}_1^0(z)$	$\boldsymbol{U}_1^0(z)$	$W_1^0(z)$
Depth-integrated	$\boldsymbol{\mathcal{R}}_1^0(z)$	$\boldsymbol{q}_1^0(z)$	$\mathcal{W}_1^0(z)$
Depth-averaged	$[\boldsymbol{R}]_1^0$	$[\boldsymbol{U}]_1^0$	$[W]_1^0$

Table 1.5: Leading-order tidal ellipse parameters depending on the leading-order free surface elevation Z_1^0.

	Major-axis	Minor-axis	Orientation	Phase	Ellipticity
Normal	$M_1^0(z)$	$m_1^0(z)$	$\theta_1^0(z)$	$\psi_1^0(z)$	$\varepsilon_1^0(z)$
Depth-integrated	$\hat{M}_1^0(z)$	$\hat{m}_1^0(z)$	$\hat{\theta}_1^0(z)$	$\hat{\psi}_1^0(z)$	$\hat{\varepsilon}_1^0(z)$
Depth-averaged	$[M]_1^0$	$[m]_1^0$	$[\theta]_1^0$	$[\psi]_1^0$	$[\varepsilon]_1^0$

the leading-order equation for the horizontal velocity vector $\boldsymbol{U}_1^0(x,y,z)$ depends on the gradient ∇Z_1^0:

$$\boldsymbol{U}_1^0(z) = \mathbf{d}_1^0(z)\,\nabla Z_1^0,$$

whereas leading-order equation for the vertical velocity $W_1^0(x,y,z)$ depends on both the gradient and Laplacian of Z_1^0:

$$W_1^0(z) = -\frac{1}{2}\,\mathrm{tr}\big(\mathbf{C}_1^0(z)\big)\Delta Z_1^0 - \check{\boldsymbol{P}}^*\hat{\nabla}\mathbf{C}_1^0(z)\,\mathbf{P}^*\nabla Z_1^0.$$

In Table 1.4, an overview of the leading-order flow variables can be found. The horizontal velocity vectors trace out an ellipse over the tidal cycle. The tidal ellipse parameter can conveniently be computed using the rotating flow variables, see Appendix B.5 for details, and they can be found in Table 1.5. Thus once the leading-order free surface is known, the leading-order tidal ellipse parameters are known too.

1.7.2 First-order hydrodynamics

The first-order hydrodynamic equations and boundary conditions are derived under the standard forcing conditions. The first-order water motion consists of two frequency components, namely the M_0 and M_4 constituents. Again, assuming that ω is the angular frequency of the semidiurnal M_2 constituent, the frequency components of the first-order water motion are given by $n = 0$ for M_0 and $n = 2$ for M_4.

The differential equations for the first-order forcing rotating flow variables were not explicitly solved in Section 1.6.4. Instead, the abstract notation of the inverse operator was used. Here, we derive explicit analytical solutions for $n = 0, 2$.

We first derive an explicit expression for the Fourier coefficients of the first-order forcing mechanisms. Under the standard forcing conditions, the eddy viscosity forcing $\boldsymbol{\psi}^1$ vanishes. For the remaining forcing mechanisms, we obtain the following coefficients for $n = 0, 2$:

$$\begin{aligned}\boldsymbol{\eta}^1(x,y,z,t) &= \mathfrak{Re}\left\{\frac{1}{2}\left[\overline{\boldsymbol{U}}_1^0\cdot\nabla\boldsymbol{U}_1^0 + W_1^0\overline{\boldsymbol{U}}_{1,z}^0\right]\right\} + \mathfrak{Re}\left\{\frac{1}{2}\left[\boldsymbol{U}_1^0\cdot\nabla\boldsymbol{U}_1^0 + W_1^0\boldsymbol{U}_{1,z}^0\right]e^{2i\omega t}\right\}, \qquad \text{(advection)}\\ &= \mathfrak{Re}\left\{\frac{1}{2}\begin{bmatrix}\overline{U}_1^0U_{1,x}^0 + \overline{V}_1^0U_{1,y}^0 + W_1^0\overline{U}_{1,z}^0\\ \overline{U}_1^0V_{1,x}^0 + \overline{V}_1^0V_{1,y}^0 + W_1^0\overline{V}_{1,z}^0\end{bmatrix}\right\} + \mathfrak{Re}\left\{\frac{1}{2}\begin{bmatrix}U_1^0U_{1,x}^0 + V_1^0U_{1,y}^0 + W_1^0U_{1,z}^0\\ U_1^0V_{1,x}^0 + V_1^0V_{1,y}^0 + W_1^0V_{1,z}^0\end{bmatrix}e^{2i\omega t}\right\},\end{aligned}$$

$$\boldsymbol{\varsigma}^1(x,y,z,t) = \mathfrak{Re}\left\{\frac{g}{\rho_0}\nabla\rho_0^0(R-z)\right\} = \mathfrak{Re}\left\{\frac{g}{\rho_0}\begin{bmatrix}\rho_{0,x}^0\\ \rho_{0,y}^0\end{bmatrix}(R-z)\right\}, \qquad \text{(baroclinic)}$$

$$\boldsymbol{\xi}^1(x,y) = \mathfrak{Re}\{\nabla R\} = \mathfrak{Re}\left\{\begin{bmatrix}R_x\\ R_y\end{bmatrix}\right\}, \qquad \text{(reference level)}$$

and for the first-order surface and bottom forcing terms, we have

$$\begin{aligned}
\boldsymbol{\gamma}^1(x,y,t) &= \mathfrak{Re}\left\{\frac{1}{2}\overline{Z}_1^0\,\boldsymbol{U}_1^0\right\} + \mathfrak{Re}\left\{\frac{1}{2}Z_1^0\,\boldsymbol{U}_1^0\,e^{2i\omega t}\right\}, && \text{at} \quad z=R, && \text{(tidal return flow)}\\
&= \mathfrak{Re}\left\{\frac{1}{2}\overline{Z}_1^0\begin{bmatrix}U_1^0\\V_1^0\end{bmatrix}\right\} + \mathfrak{Re}\left\{\frac{1}{2}Z_1^0\begin{bmatrix}U_1^0\\V_1^0\end{bmatrix}e^{2i\omega t}\right\}, && \text{at} \quad z=R, &&\\
\boldsymbol{\chi}^1(x,y,t) &= \mathfrak{Re}\left\{\frac{1}{2}\overline{Z}_1^0 A_v^0\,\boldsymbol{U}_{1,zz}^0\right\} + \mathfrak{Re}\left\{\frac{1}{2}Z_1^0 A_v^0\,\boldsymbol{U}_{1,zz}^0\,e^{2i\omega t}\right\}, && \text{at} \quad z=R, && \text{(no-stress)}\\
&= \mathfrak{Re}\left\{\frac{1}{2}\overline{Z}_1^0 A_v^0\begin{bmatrix}U_{1,zz}^0\\V_{1,zz}^0\end{bmatrix}\right\} + \mathfrak{Re}\left\{\frac{1}{2}Z_1^0 A_v^0\begin{bmatrix}U_{1,zz}^0\\V_{1,zz}^0\end{bmatrix}e^{2i\omega t}\right\}, && \text{at} \quad z=R, &&\\
\boldsymbol{\mu}^1(x,y,t) &= \mathfrak{Re}\left\{\frac{1}{2}\overline{s}_{f,1}^1\,\boldsymbol{U}_1^0\right\} + \mathfrak{Re}\left\{\frac{1}{2}s_{f,1}^1\,\boldsymbol{U}_1^0\,e^{2i\omega t}\right\}, && \text{at} \quad z=-H, && \text{(partial slip)}\\
&= \mathfrak{Re}\left\{\frac{1}{2}\overline{s}_{f,1}^1\begin{bmatrix}U_1^0\\V_1^0\end{bmatrix}\right\} + \mathfrak{Re}\left\{\frac{1}{2}s_{f,1}^1\begin{bmatrix}U_1^0\\V_1^0\end{bmatrix}e^{2i\omega t}\right\}, && \text{at} \quad z=-H. &&
\end{aligned}$$

We note that the real part of a complex number is invariant under complex conjugation. That is, the real part of a complex number remains the same when we take its complex conjugate, i.e., $\mathfrak{Re}\{z\} = \mathfrak{Re}\{\overline{z}\}$ for z in $\mathbb{C}$. This property allows us, for example, to let the complex conjugate work on the quantities that do *not* depend on the horizontal derivatives in the advective forcing.

The Fourier coefficients of the first-order tidal and riverine forcing under the standard forcing conditions read

$$\begin{aligned}
A^1(x,y,t) &= \mathfrak{Re}\left\{A_2^1(x,y)\,e^{2i\omega t}\right\}, && \text{at} \quad \partial\Omega_{\text{sea}}, && \text{(tidal forcing)}\\
q_{\text{river}}^1(x,y,t) &= \mathfrak{Re}\left\{q_{\text{river},0}^1(x,y)\right\}, && \text{at} \quad \partial\Omega_{\text{river}}. && \text{(riverine forcing)}
\end{aligned}$$

The equation solving for the first-order free surface elevation $Z_n^{1,f}$ for the frequency component $n=1,2$ and forcing mechanism f in $\tilde{\mathscr{F}}$ is given by

$$\nabla\cdot\left[\mathbf{D}_n^0(R)\,\nabla Z_n^{1,f}\right] + ni\omega Z_n^{1,f} = -\nabla\cdot\left[\check{\boldsymbol{q}}_n^{1,f}(R)\right], \tag{1.7.2}$$

with the boundary conditions:

$$\begin{aligned}
Z_n^{1,f} &= A_n^{1,f}(x,y), && \text{at} \quad \partial\Omega_{\text{sea}},\\
\left[\mathbf{D}_n^0(R)\,\nabla Z_n^{1,f}\right]\cdot\boldsymbol{n} &= \tilde{q}_{\text{bank},n}^{1,f}(x,y), && \text{at} \quad \partial\Omega_{\text{bank}},\\
\left[\mathbf{D}_n^0(R)\,\nabla Z_n^{1,f}\right]\cdot\boldsymbol{n} &= \dot{q}_{\text{river},n}^{1,f}(x,y), && \text{at} \quad \partial\Omega_{\text{river}}.
\end{aligned}$$

To solve this equation for the first-order free surface elevation $Z_n^{1,f}$, the forcing terms $\check{\boldsymbol{q}}_n^{1,f}(R)$, $A_n^{1,f}$, $\tilde{q}_{\text{bank},n}^{1,f}$ and $\dot{q}_{\text{river},n}^{1,f}$ need to be known. The forcing terms acting on the boundary are readily expressed in terms of known quantities. The body forcing mechanisms $\check{\boldsymbol{q}}_n^{1,f}(R)$ are a little more difficult to express. The body forcing mechanisms can be computed using two equivalent routes (since the depth-integral and the multiplication with the constant matrix $\mathbf{P}$ commute), as the diagram below illustrates:

$$\begin{tikzcd}
\check{\boldsymbol{R}}_n^{1,f}(z) \arrow[r, "\int_{-H}^{z}[\cdot]\,dz"] \arrow[d, "\mathbf{P}\,[\cdot]"'] & \check{\boldsymbol{\mathcal{R}}}_n^{1,f}(z) \arrow[d, "\mathbf{P}\,[\cdot]"] \\
\check{\boldsymbol{U}}_n^{1,f}(z) \arrow[r, "\int_{-H}^{z}[\cdot]\,dz"'] & \check{\boldsymbol{q}}_n^{1,f}(z)
\end{tikzcd} .$$

Both routes start at the forcing rotating flow variables $\check{\boldsymbol{R}}_n^{1,f}(z)$. Thus for each forcing mechanism f in $\tilde{\mathscr{F}}$, we derive $\check{\boldsymbol{R}}_n^{1,f}(z)$ and integrate it over the depth to obtain $\check{\boldsymbol{\mathcal{R}}}_n^{1,f}(z)$, then the forcing horizontal velocity $\check{\boldsymbol{U}}_n^{1,f}(z)$ and forcing transport of water $\check{\boldsymbol{q}}_n^{1,f}(z)$ are found by left multiplying by the matrix $\mathbf{P}$.

Once the first-order free surface elevation $Z_n^{1,f}$ is known, all first-order forced flow variables are known too, analogous to the leading-order case. The net response to a forcing mechanisms is found by adding the forced and forcing contributions together. For each of these flow variables, the tidal ellipse parameters can be computed.

1.7.3 Solving the equation for the forcing rotating flow variables

In this section, we derive analytical solutions for the forcing rotating flow variables and their depth-integral. They satisfy the following decoupled ordinary differential equations in the vertical coordinate z for $n = 0, 2$ and f in $\tilde{\mathscr{F}}$:

$$\check{\boldsymbol{R}}_{n,zz}^{1,f}(z) - \left(\boldsymbol{\alpha}_n^0\right)^2 \check{\boldsymbol{R}}_n^{1,f}(z) = \frac{1}{A_v^0}\mathbf{P}^*\boldsymbol{\Sigma}_n^{1,f}(z),$$

with corresponding boundary conditions given by

$$\begin{aligned} A_v^0\check{\boldsymbol{R}}_{n,z}^{1,f}(z) &= \mathbf{P}^*\boldsymbol{\Sigma}_{n,R}^{1,f} && \text{at} \quad z = R, \\ A_v^0\check{\boldsymbol{R}}_{n,z}^{1,f}(z) &= s_f^0\check{\boldsymbol{R}}_n^{1,f}(z) + \mathbf{P}^*\boldsymbol{\Sigma}_{n,-H}^{1,f} && \text{at} \quad z = -H. \end{aligned}$$

For the forcing mechanisms, the tidal return flow $f = \gamma$, the amplitude forcing $f = A$ and the riverine forcing $f = q$, all forcing terms in the above differential equation vanish. Hence, the solution to the homogenous equation with homogenous boundary conditions is the trivial solution:

$$\check{\boldsymbol{R}}_n^{1,\gamma}(z) = \mathbf{0}, \qquad \check{\boldsymbol{R}}_n^{1,A}(z) = \mathbf{0}, \qquad \check{\boldsymbol{R}}_n^{1,q}(z) = \mathbf{0}.$$

Integrating over depth yields the corresponding depth-integrated rotating flow variables:

$$\check{\boldsymbol{\mathcal{R}}}_n^{1,\gamma}(z) = \mathbf{0}, \qquad \check{\boldsymbol{\mathcal{R}}}_n^{1,A}(z) = \mathbf{0}, \qquad \check{\boldsymbol{\mathcal{R}}}_n^{1,q}(z) = \mathbf{0}.$$

For the reference level forcing $f = \xi$, only the depth-independent body forcing term remains. This is the same problem as considered for the forced problem. Therefore, the solution is this given by

$$\check{\boldsymbol{R}}_n^{1,\xi}(z) = \mathbf{c}_n^0(z)\,\mathbf{P}^*\boldsymbol{\xi}_n^1,$$

with the depth-integrated rotating flow variable:

$$\check{\boldsymbol{\mathcal{R}}}_n^{1,\xi}(z) = \mathbf{C}_n^0(z)\,\mathbf{P}^*\boldsymbol{\xi}_n^1.$$

The remaining forcing mechanisms are the no-stress forcing $f = \chi$, the partial-slip forcing $f = \mu$, the baroclinic forcing $f = \varsigma$ and the advective forcing $f = \eta$. We consider these forcing mechanism in detail below. We solve the corresponding equations for forcing rotating flow variables and integrate over the depth to obtain the depth-integrated rotating flow variables.

The analytical solution for the advective forcing $f = \eta$ can be found in Appendix B.11, since the solution procedure is quite elaborate.

The no-stress analytic solution

We consider the no-stress forcing $f = \chi$ separately. The differential equations for $n = 0, 2$ become

$$\check{\boldsymbol{R}}_{n,zz}^{1,\chi}(z) - \left(\boldsymbol{\alpha}_n^0\right)^2 \check{\boldsymbol{R}}_n^{1,\chi}(z) = \mathbf{0},$$

with boundary conditions

$$\begin{aligned} A_\nu^0 \check{\boldsymbol{R}}_{n,z}^{1,\chi}(z) &= -\mathbf{P}^* \boldsymbol{\chi}_n^1, && \text{at} \quad z = R, \\ A_\nu^0 \check{\boldsymbol{R}}_{n,z}^{1,\chi}(z) &= s_f^0 \check{\boldsymbol{R}}_n^{1,\chi}(z), && \text{at} \quad z = -H. \end{aligned}$$

The solution of this differential equation reads

$$\check{\boldsymbol{R}}_n^{1,\chi}(z) = \mathbf{c}_n^{1,\chi}(z)\, \mathbf{P}^* \boldsymbol{\chi}_n^1,$$

with the elements of the diagonal matrices given by

$$\mathrm{c}_{n,ii}^{1,\chi}(z) = -\frac{1}{A_\nu^0 \alpha_{n,ii}^0} \left\{ \sinh\!\left(\alpha_{n,ii}^0 (z-R)\right) + \mathrm{A}_{n,ii}^{0,\chi} \beta_{n,ii}^0 \cosh\!\left(\alpha_{n,ii}^0 (z-R)\right) \right\},$$

and

$$\mathrm{A}_{n,ii}^{0,\chi}(x,y) = A_\nu^0 \alpha_{n,ii}^0 \cosh\!\left(\alpha_{n,ii}^0 D\right) + s_f^0 \sinh\!\left(\alpha_{n,ii}^0 D\right),$$

and

$$\beta_{n,ii}^0(x,y) = \frac{1}{A_\nu^0 \alpha_{n,ii}^0 \sinh\!\left(\alpha_{n,ii}^0 D\right) + s_f^0 \cosh\!\left(\alpha_{n,ii}^0 D\right)}.$$

We integrate this solution over the depth to obtain the depth-integrated rotating flow variable

$$\check{\boldsymbol{\mathcal{R}}}_n^{1,\chi}(z) = \mathbf{C}_n^{1,\chi}(z)\, \mathbf{P}^* \boldsymbol{\chi}_n^1,$$

with the elements of the diagonal matrix $\mathbf{C}_n^{0,\chi}(z)$ given by

$$\begin{aligned} \mathrm{C}_{n,ii}^{1,\chi}(z) &= \int_{-H}^{z} \mathrm{c}_{n,ii}^{1,\chi}(\tilde{z})\, d\tilde{z}, \\ &= -\frac{1}{A_\nu^0 (\alpha_{n,ii}^0)^2} \Big\{ \quad \mathrm{A}_{n,ii}^{0,\chi} \beta_{n,ii}^0 \left[\sinh\!\left(\alpha_{n,ii}^0 (z-R)\right) + \sinh\!\left(\alpha_{n,ii}^0 D\right) \right] \\ &\qquad + \cosh\!\left(\alpha_{n,ii}^0 (z-R)\right) - \cosh\!\left(\alpha_{n,ii}^0 D\right) \Big\}. \end{aligned}$$

In case $n = 0$ and we take the limit of f to 0, the following coefficients are obtained

$$\lim_{f \to 0} \mathrm{c}_{0,ii}^{1,\chi}(z) = -\frac{z+H}{A_\nu^0} - \frac{1}{s_f^0},$$

and for the depth-integrated variant:

$$\lim_{f \to 0} \mathrm{C}_{0,ii}^{1,\chi}(z) = -(z+H)\left(\frac{z+H}{2A_\nu^0} + \frac{1}{s_f^0} \right),$$

The partial-slip analytic solution

We consider the partial-slip forcing $f = \mu$ separately. The differential equations for $n = 0,2$ become

$$\check{\boldsymbol{R}}^{1,\mu}_{n,zz}(z) - \left(\boldsymbol{\alpha}^0_n\right)^2 \check{\boldsymbol{R}}^{1,\mu}_n(z) = \mathbf{0},$$

with boundary conditions

$$\begin{aligned} A^0_\nu \check{\boldsymbol{R}}^{1,\mu}_{n,z}(z) &= \mathbf{0}, && \text{at} \quad z = R, \\ A^0_\nu \check{\boldsymbol{R}}^{1,\mu}_{n,z}(z) &= s^0_f \check{\boldsymbol{R}}^{1,\mu}_n(z) + \mathbf{P}^* \boldsymbol{\mu}^1_n, && \text{at} \quad z = -H. \end{aligned}$$

We solve this differential equation analytically. The solution reads

$$\check{\boldsymbol{R}}^{1,\mu}_n(z) = \mathbf{c}^{1,\mu}_n(z)\,\mathbf{P}^*\boldsymbol{\mu}^1_n,$$

with the elements of the diagonal matrices given by

$$\mathrm{c}^{1,\mu}_{n,ii}(z) = -\beta^0_{n,ii}\cosh\!\left(\alpha^0_{n,ii}(z-R)\right),$$

and

$$\beta^0_{n,ii}(x,y) = \frac{1}{A^0_\nu \alpha^0_{n,ii}\sinh\!\left(\alpha^0_{n,ii}D\right) + s^0_f\cosh\!\left(\alpha^0_{n,ii}D\right)}.$$

The partial-slip solution is integrated over the depth and this yields

$$\check{\boldsymbol{\mathcal{R}}}^{1,\mu}_n(z) = \mathbf{C}^{1,\mu}_n(z)\,\mathbf{P}^*\boldsymbol{\mu}^1_n,$$

with the elements of the diagonal matrix given by

$$\begin{aligned} \mathrm{C}^{1,\mu}_{n,ii}(z) &= \int_{-H}^{z} \mathrm{c}^{1,\mu}_{n,ii}(\tilde{z})\,d\tilde{z}, \\ &= -\frac{\beta^0_{n,ii}}{\alpha^0_{n,ii}}\left[\sinh\!\left(\alpha^0_{n,ii}(z-R)\right) + \sinh\!\left(\alpha^0_{n,ii}D\right)\right]. \end{aligned}$$

The baroclinic analytic solution

We consider the baroclinic forcing $f=\varsigma$ separately. The differential equations for $n=0$ become

$$\check{\boldsymbol{R}}^{1,\varsigma}_{n,zz}(z)-\left(\boldsymbol{\alpha}^0_n\right)^2\check{\boldsymbol{R}}^{1,\varsigma}_n(z)=\frac{g}{A^0_v\rho_0}(R-z)\,\mathbf{P}^*\nabla\rho^0_n,$$

with boundary conditions

$$\begin{aligned}
A^0_v\check{\boldsymbol{R}}^{1,\varsigma}_{n,z}(z)&=\mathbf{0}, && \text{at} \quad z=R,\\
A^0_v\check{\boldsymbol{R}}^{1,\varsigma}_{n,z}(z)&=s^0_f\check{\boldsymbol{R}}^{1,\varsigma}_n(z), && \text{at} \quad z=-H.
\end{aligned}$$

The solution of this differential equation reads

$$\check{\boldsymbol{R}}^{1,\varsigma}_n(z)=\mathbf{c}^{1,\varsigma}_n(z)\,\mathbf{P}^*\nabla\rho^0_n,$$

with the elements of the diagonal matrices given by

$$\mathrm{c}^{1,\varsigma}_{n,ii}(z)=-\frac{g}{A^0_v\rho_0(\alpha^0_{n,ii})^3}\left\{\sinh\left(\alpha^0_{n,ii}(z-R)\right)+\mathrm{A}^{0,\varsigma}_{n,ii}\beta^0_{n,ii}\cosh\left(\alpha^0_{n,ii}(z-R)\right)-\alpha^0_{n,ii}(z-R)\right\},$$

and

$$\mathrm{A}^{0,\varsigma}_{n,ii}(x,y)=A^0_v\alpha^0_{n,ii}\left[\cosh\left(\alpha^0_{n,ii}D\right)-1\right]+s^0_f\left[\sinh\left(\alpha^0_{n,ii}D\right)-\alpha^0_{n,ii}D\right],$$

and

$$\beta^0_{n,ii}(x,y)=\frac{1}{A^0_v\alpha^0_{n,ii}\sinh\left(\alpha^0_{n,ii}D\right)+s^0_f\cosh\left(\alpha^0_{n,ii}D\right)}.$$

We integrate this solution over the depth to obtain

$$\check{\boldsymbol{\mathcal{R}}}^{1,\varsigma}_n(z)=\mathbf{C}^{1,\varsigma}_n(z)\,\mathbf{P}^*\nabla\rho^0_n,$$

with the elements of the diagonal matrix given by

$$\begin{aligned}
\mathrm{C}^{1,\varsigma}_{n,ii}(z)&=\int_{-H}^{z}\mathrm{c}^{1,\varsigma}_{n,ii}(\tilde{z})\,d\tilde{z},\\
&=-\frac{g}{A^0_v\rho_0(\alpha^0_{n,ii})^3}\left\{\frac{\mathrm{A}^{0,\varsigma}_{n,ii}\beta^0_{n,ii}}{\alpha^0_{n,ii}}\left[\sinh\left(\alpha^0_{n,ii}(z-R)\right)+\sinh\left(\alpha^0_{n,ii}D\right)\right]\right.\\
&\qquad+\frac{1}{\alpha^0_{n,ii}}\left[\cosh\left(\alpha^0_{n,ii}(z-R)\right)-\cosh\left(\alpha^0_{n,ii}D\right)\right]\\
&\qquad\left.-\frac{\alpha^0_{n,ii}}{2}\left((z-R)^2-D^2\right)\right\}.
\end{aligned}$$

In case $n=0$ and the limit f goes 0, the α's go to zero again causing us to divide by zero. Taking the limit of the above coefficient matrix elements yields

$$\lim_{f\to0}\mathrm{c}^{1,\varsigma}_{0,ii}(z)=-\frac{g}{6A^0_v\rho_0}\left[(z+H)(z-R)(z-R-D)+\left(z+H+3A^0_v/s^0_f\right)D^2\right],$$

and similarly, for the depth-integrated coefficient, we get

$$\lim_{f\to0}\mathrm{C}^{1,\varsigma}_{0,ii}(z)=-\frac{g}{24A^0_v\rho_0}(z+H)\left[(z+H)\left(2(z-R)^2-(z+H)^2\right)+4\left(z+H+3A^0_v/s^0_f\right)D^2\right].$$

Both terms have become independent of the index i.

Chapter 2

Numerical implementation

In this chapter, the numerical solution method is presented that is used to solve the hydrodynamic equations. The vertical dimension z can be solved analytically, thus only the horizontal dimensions (x, y) have to be solved numerically. A finite element method is chosen because it can be used to solve complex two-dimensional geometries.

2.1 General form of the free surface equation

In this section, the general form of the free surface equation is discussed. We focus on the standard forcing conditions, see Section 1.7.

The leading- and first-order equations for the free surface (1.6.1) and (1.6.2) have a highly similar structure. This allows us to derive their weak forms simultaneously. Therefore, we will consider the general problem of order k, frequency component n and forcing mechanism f:

$$\nabla \cdot \left[\mathbf{D}_n^0(R)\,\nabla Z_n^{k,f}\right] + ni\omega Z_n^{k,f} = -\nabla \cdot \left[\check{\boldsymbol{q}}_n^{k,f}(R)\right], \tag{2.1.1}$$

with boundary conditions

$$\begin{aligned}
Z_n^{k,f} &= A_n^{k,f}(x, y), && \text{at} \quad \partial\Omega_{\text{sea}},\\
\left[\mathbf{D}_n^0(R)\,\nabla Z_n^{k,f}\right] \cdot \boldsymbol{n} &= \tilde{q}_{\text{bank},n}^{k,f}(x, y), && \text{at} \quad \partial\Omega_{\text{bank}},\\
\left[\mathbf{D}_n^0(R)\,\nabla Z_n^{k,f}\right] \cdot \boldsymbol{n} &= \dot{q}_{\text{river},n}^{k,f}(x, y), && \text{at} \quad \partial\Omega_{\text{river}}.
\end{aligned}$$

Next, we will show that this general form reduces to the leading- and first-order equations under the standard forcing conditions.

This general equation reduces to the leading-order equation for the M_2 tidal constituent forced at the seaward boundary under the standard forcing conditions (1.7.1), if we choose leading-order $k = 0$, M_2 frequency $n = 1$, tide forcing $f = A$ with $A_n^{k,f} = A_1^0(x, y)$ and if all other forcing mechanisms vanish: $\check{\boldsymbol{q}}_n^{k,f}(R) = \mathbf{0}$, $\tilde{q}_{\text{bank},n}^{k,f} = 0$ and $\dot{q}_{\text{river},n}^{k,f} = 0$, yielding

$$\nabla \cdot \left[\mathbf{D}_1^0(R)\,\nabla Z_1^{0A}\right] + i\omega Z_1^{0A} = 0,$$

with leading-order boundary conditions

$$\begin{aligned}
Z_1^{0A} &= A_1^0(x, y), && \text{at} \quad \partial\Omega_{\text{sea}},\\
\left[\mathbf{D}_1^0(R)\,\nabla Z_1^{0A}\right] \cdot \boldsymbol{n} &= 0, && \text{at} \quad \partial\Omega_{\text{bank}},\\
\left[\mathbf{D}_1^0(R)\,\nabla Z_1^{0A}\right] \cdot \boldsymbol{n} &= 0, && \text{at} \quad \partial\Omega_{\text{river}}.
\end{aligned}$$

Here, we have omitted the comma separating the order 0 and forcing mechanism A.

The general equation reduces to the first-order equation for the free surface for the M_0 and M_4 tidal constituents generated by forcing mechanism f under the standard forcing conditions (1.7.2), if we choose first-order $k = 1$, M_0 and M_4 frequencies $n \in \{0,2\}$ and the corresponding standard forcing mechanism $f \in \tilde{\mathscr{F}} = \{\xi, \chi, \mu, \eta, \varsigma, \gamma, A, q\}$:

$$\nabla \cdot \left[\mathbf{D}_n^0(R)\nabla Z_n^{1,f}\right] + ni\omega Z_n^{1,f} = -\nabla \cdot \left[\check{\boldsymbol{q}}_n^{1,f}(R)\right],$$

with the first-order boundary conditions

$$\begin{aligned}
&Z_n^{1,f} = A_n^{1,f}(x,y), && \text{at } \partial\Omega_{\text{sea}},\\
&\left[\mathbf{D}_n^0(R)\nabla Z_n^{1,f}\right]\cdot\boldsymbol{n} = \tilde{q}_{\text{bank},n}^{1,f}(x,y), && \text{at } \partial\Omega_{\text{bank}},\\
&\left[\mathbf{D}_n^0(R)\nabla Z_n^{1,f}\right]\cdot\boldsymbol{n} = \dot{q}_{\text{river},n}^{1,f}(x,y), && \text{at } \partial\Omega_{\text{river}}.
\end{aligned}$$

2.2 Weak form of general free surface equation

In this section, the weak form is presented that is solved using the finite element method.

We define the finite element spaces where the test functions and the solution reside in. Let Ω be the two-dimensional domain with the boundary consisting of segments of $\partial\Omega_{\text{sea}}$, $\partial\Omega_{\text{bank}}$ and $\partial\Omega_{\text{river}}$. Define the standard $L^2(\Omega)$ space and Sobolev space $H^1(\Omega)$ as

$$\begin{aligned}
L^2(\Omega) &= \left\{\varphi : \Omega \mapsto \mathbb{C} \mid \|\varphi\|_2 < \infty\right\},\\
H^1(\Omega) &= \left\{\varphi \in L^2(\Omega) \mid \varphi_x \in L^2(\Omega),\, \varphi_y \in L^2(\Omega)\right\},
\end{aligned}$$

where we have defined the L^2-norm as

$$\|\varphi\|_2 = \sqrt{\int_\Omega |\varphi|^2\, d\Omega}.$$

The essential boundary conditions for this problem are located at $\partial\Omega_{\text{sea}}$. Thus we seek test functions in the homogeneous space

$$\Sigma_0(\Omega) = \left\{\varphi \in H^1(\Omega) \mid \varphi = 0 \text{ at } \partial\Omega_{\text{sea}}\right\}.$$

The weak form can be compactly expressed using a bilinear and linear form. These are derived in Appendix B.7. Define the bilinear form as

$$a_n\left(Z_n^{k,f},\varphi\right) = \int_\Omega -\left[\mathbf{D}_n^0(R)\nabla Z_n^{k,f}\right]\cdot\nabla\varphi + ni\omega Z_n^{k,f}\varphi\, d\Omega,$$

and the linear form as

$$b_n^{k,f}(\varphi) = \int_\Omega \left[\check{\boldsymbol{q}}_n^{k,f}(R)\right]\cdot\nabla\varphi\, d\Omega - \int_{\partial\Omega_{\text{bank}}} \breve{q}_{\text{bank},n}^{1,f}\varphi\, d\Gamma - \int_{\partial\Omega_{\text{river}}} \acute{q}_{\text{river},n}^{1,f}\varphi\, d\Gamma.$$

Then, the weak formulation can be compactly stated as follows:

Find $Z_n^{k,f} \in H^1(\Omega)$ with $Z_n^{k,f} = A_n^{k,f}(x,y)$ at $\partial\Omega_{\text{sea}}$ such that for all test functions $\varphi \in \Sigma_0(\Omega)$ it holds that

$$a_n\left(Z_n^{k,f},\varphi\right) = b_n^{k,f}(\varphi).$$

2.3 Implementation

In this section, we given an overview of the structure of the numerical model.

2.3.1 Hydrodynamic classes

In Fig. 2.1, the classes defined to solve the ordered hydrodynamics are shown.

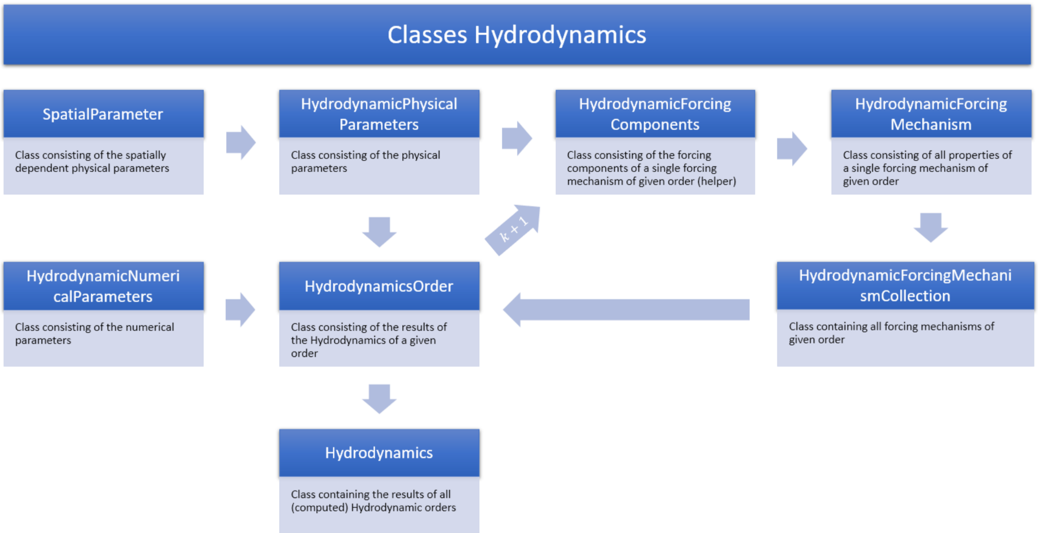

Figure 2.1: Classes defined to solve the hydrodynamics

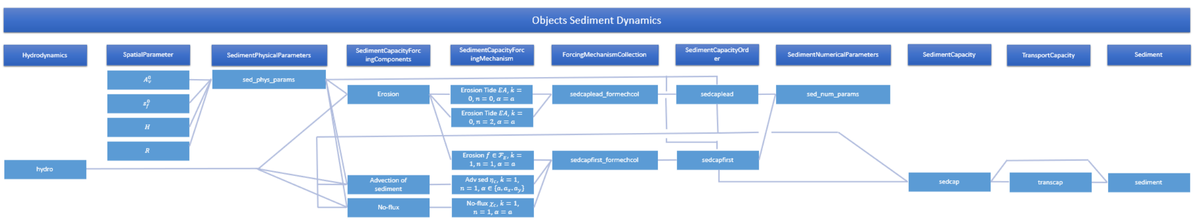

Figure 2.2: Objects defined to solve the hydrodynamics

2.3.2 hydrodynamic objects

In Fig. 2.2, the hydrodynamic objects and their relations are shown.

2.3.3 Description of the hydrodynamic classes and objects

We provide an overview of the files used and their input and output.

We use the colour `script` to indicate python scripts or pseudo code. We use the colour `object` to denote objects.

`main_hydrodynamics.py`

- Input:
  - geometry
  - physicalparameters(geometry)
  - numericalparameters(geometry)
- Generate mesh
- `NumericalParametersHydroLead`
- `PhysicalParametersHydroLead`
- `ForcingMechanismsHydroLead`
- `compute_hydrolead.py`
  - Input:
    * `NumericalParametersHydroLead`
    * `PhysicalParametersHydroLead`
    * `ForcingMechanismsHydroLead`
  - Output: `HydroLead`[1]['tide']
- `NumericalParametersHydroFirst`
- `ForcingMechanimsHydroFirst`
- `compute_hydrofirst.py`
  - Input:
    * `NumericalParametersHydroFirst`
    * `PhysicalParametersHydroLead`
    * `ForcingMechanimsHydroFirst`
  - Output: `HydroFirst`
- Post-processing
- Save output
- Plots

The general hydrodynamic scripts

The spatial parameters are assumed to be prescribed in terms of ξ and η coordinates, which both dependent internally on the Cartesian (x, y) coordinates, such that we may say $\xi(x, y)$, $\eta(x, y)$.

For example, for a spatially varying bathymetry $H(\xi,\eta)$. We have using the chain rule that

$$H_x = H_\xi \xi_x + H_\eta \eta_x, \qquad H_y = H_\xi \xi_y + H_\eta \eta_y.$$

This can be represented more compactly using the gradient as follows

$$\nabla H = H_\xi \nabla \xi + H_\eta \nabla \eta.$$

With this in mind, we define the spatial parameter class as follows:

`SpatialParameter`

- Input: Sympy function handle fh, xi_gf, eta_gf
- Use sympy to determine the gradient of fh
- Output: gridfunction fh, gridfunction gradient of fh

For each forcing mechanism a forcing mechanism class is made. Later these forcing mechanisms are collected together in a forcing mechanisms class.

`ForcingMechanism`

- Input:
  - symbol
  - frequency_component
  - `ForcingComponents`
  - A_sea
  - q_R_wallup
  - q_R_walldown
  - q_R_river

`ForcingComponents`

- Input:
  - $\check{\boldsymbol{R}}_n^{1,f}(z)$
  - $\check{\boldsymbol{\mathcal{R}}}_n^{1,f}(z)$
  - `PhysicalParametersHydroLead`
- Returns:
  - $\check{\boldsymbol{R}}_n^{1,f}(z)$
  - $\check{\boldsymbol{\mathcal{R}}}_n^{1,f}(z)$
  - $\check{\boldsymbol{U}}_n^{1,f}(z)$
  - $\check{\boldsymbol{q}}_n^{1,f}(z)$
  - $\check{\boldsymbol{q}}_n^{1,f}(R)$
  - $\check{W}_n^{1,f}(z)$
  - $\mathcal{W}_n^{1,f}(z)$

The leading-order hydrodynamic scripts

The leading-order hydrodynamic computation is shown below:

`compute_hydrolead.py`

- Input:
  - `NumericalParametersHydroLead`

    - PhysicalParametersHydrolead
    - ForcingMechanismsHydroLead
- Solve leading-order weak form for $Z_1^{0,A}$
- Generate HydroLead object
- Output HydroLead object (e.g.: $Z_1^{0,A}$, $\boldsymbol{U}_1^{0,A}(z)$, $W_1^{0,A}(z)$, $[\boldsymbol{U}]_1^{0,A}$, $\boldsymbol{R}_1^{0,A}(z)$, $\boldsymbol{\mathcal{R}}_1^{0,A}(z)$, $\boldsymbol{q}_1^{0,A}(z)$.)

PhysicalParametersHydroLead

- Input:
    - The spatially constant parameters occurring in the leading-order equations and boundary conditions at the free surface and bed: the gravitational constant g, Coriolis parameter f and angular frequency ω.
    - The horizontal spatially varying parameters occurring in the leading-order equations and boundary conditions at the free surface and bed as SpatialParameter: the vertical eddy viscosity $A_v^0(x,y)$, partial slip parameter $s_f^0(x,y)$, bed level $H(x,y)$ and reference level $R(x,y)$.
- Generates the leading order coefficients and matrices with these parameters, such as the collection of the leading-order horizontally variable parameters

$$\boldsymbol{\phi}^0 = \begin{bmatrix} A_v^0 & s_f^0 & H & R \end{bmatrix}^T.$$

  and their gradient

$$\nabla\boldsymbol{\phi}^0 = \begin{bmatrix} \nabla A_v^0 & \nabla s_f^0 & \nabla H & \nabla R \end{bmatrix}^T.$$

For the numerical parameters, we assume that we do not use any adaptive refinement.

NumericalParametersHydroLead

- geometrydata
- boundary parameter partitition dict
- boundary maxh dict
- degree spline geometry
- degree curved geometry
- smoothness spline geometry
- order
- maxh

Then each forcing mechanism is collected in a special dictionary called PhysicalParametersHydroLead.

ForcingMechanismsHydroLead

- Input:
    - list of ForcingMechanism
- creates special dictionary with all the forcing mechanisms subscriptable using the symbol.

We define an output object to capture the results from the leading- and first-order hydrodynamic equations. We create this object because for the leading-order hydrodynamics there are already 41 possible variables returned. For the first-order hydrodynamic results there are possibly 9 forcing mechanisms, 2 frequency components and 41 output variables, yielding 738 possible output variables. To capture these variables effectively, we define a hydrodynamic result object:

Hydro

- Output free surface: $Z_n^{k,f}$
- Output flow variables: $\boldsymbol{R}_n^{k,f}(z)$, $\boldsymbol{U}_n^{k,f}(z)$, $W_n^{k,f}(z)$,
  - Their components: $R_{n,1}^{k,f}(z)$, $R_{n,2}^{k,f}(z)$, $U_n^{k,f}(z)$, $V_n^{k,f}(z)$
- Output depth-integrated flow variables: $\boldsymbol{\mathcal{R}}_n^{k,f}(z)$, $\boldsymbol{q}_n^{k,f}(z)$, $\mathcal{W}_n^{k,f}(z)$
  - Their components: $\mathcal{R}_{n,1}^{k,f}(z)$, $\mathcal{R}_{n,2}^{k,f}(z)$, $q_{n,1}^{k,f}(z)$, $q_{n,2}^{k,f}(z)$,
- Output depth-integrated flow variables evaluated at $z = R$: $\boldsymbol{\mathcal{R}}_n^{k,f}(R)$, $\boldsymbol{q}_n^{k,f}(R)$, $\mathcal{W}_n^{k,f}(R)$
  - Their components: $\mathcal{R}_{n,1}^{k,f}(R)$, $\mathcal{R}_{n,2}^{k,f}(R)$, $q_{n,1}^{k,f}(R)$, $q_{n,2}^{k,f}(R)$,
- Output depth-averaged flow variables: $[\boldsymbol{R}]_n^{k,f}$, $[\boldsymbol{U}]_n^{k,f}$, $[W]_n^{k,f}$,
  - Their components: $[R]_{n,1}^{k,f}$, $[R]_{n,2}^{k,f}$, $[U]_n^{k,f}$, $[V]_n^{k,f}$
- Output tidal ellipse parameters of the flow: $M_n^k(z)$, $m_n^k(z)$, $\theta_n^k(z)$, $\psi_n^k(z)$, $\varepsilon_n^k(z)$
- Output tidal ellipse parameters of the depth-integrated flow: $\hat{M}_n^k(z)$, $\hat{m}_n^k(z)$, $\hat{\theta}_n^k(z)$, $\hat{\psi}_n^k(z)$, $\hat{\varepsilon}_n^k(z)$
- Output tidal ellipse parameters of the depth-averaged flow: $[M]_n^k$, $[m]_n^k$, $[\theta]_n^k$, $[\psi]_n^k$, $[\varepsilon]_n^k$.
- If the along- and across-channel coordinates (ξ, η) are defined, it is also possible to generate along- and across-channel velocities (U_ξ, U_η):
  - The along- and across-channel velocities: $U_{\xi,n}^{k,f}(z)$, $U_{\eta,n}^{k,f}(z)$
  - The depth-averaged along- and across-channel velocities: $[U]_{\xi,n}^{k,f}$, $[U]_{\eta,n}^{k,f}$.

Here, the brackets $[\cdot]$ denote the depth-average and $M_n^k(z)$, $m_n^k(z)$, $\theta_n^k(z)$, $\psi_n^k(z)$ and $\varepsilon_n^k(z)$ denote, respectively, the major-axis, minor-axis, orientation, phase and ellipticity of the tidal ellipse. For more information about the tidal ellipse parameters, we refer to Appendix B.5. The along- and across-channel velocity are defined in Appendix B.4.

The objects `HydroLead` and `HydroFirst` are specific instances of this more general `Hydro` object.

The first-order hydrodynamic scripts

`compute_hydrofirst.py`

- Input:
  - `NumericalParametersHydroFirst`
  - `PhysicalParametersHydroFirst`
  - `ForcingMechanimsHydroFirst`
  - `PhysicalParametersHydroLead`
- For each frequency component n:
  - Compute $a_n(\cdot, \varphi)$
  - For each forcing mechanisms f:
    - Compute $b_n^{1,f}(\varphi)$
    - Solve $a_n\left(Z_n^{1,f}, \varphi\right) = b_n^{1,f}(\varphi)$ for $Z_n^{1,f}$.
- Generate `HydroFirst`($(Z_n^{1,f})_{n=0,2}^{f\in\mathscr{F}}$)
- Output: `HydroFirst`

`NumericalParametersHydroFirst`

Chapter 3

Sediment dynamics

The sediment dynamics in estuaries has been studied extensively. These dynamics are particularly well analysable using a perturbation method and harmonic decomposition. Schuttelaars (1997) has shown that the leading-order suspended sediment concentration in short tidal embayments consists primarily of an M_0 and M_4 component. Friedrichs *et al.* (1998) have extended these ideas to strongly frictional, funnel-shaped embayments and computed the first-order suspended sediment concentration. Using the concept of tidally averaged suspended sediment transport, they note that solely the M_2 component of the first-order suspended sediment results in net sediment transport, assuming the leading-order water motion consists solely of an M_2 component. Using the concept of morphodynamic equilibrium, they were able to capture the qualitative features of an Estuarine Turbidity Maxima (ETM). In Huijts *et al.* (2006) the concept of morphodynamic equilibrium is used to study the sediment dynamics in an estuarine cross-section. Chernetsky (2012) has created a width-averaged model (2DV) of an estuary in which the individual along-channel sediment transport mechanisms can be identified and analysed. Dijkstra (2019) is the first to model the regime shift of the Ems to a hyperturbid state using solely channel deepening. He used a 2DV model (iFlow) with the erodibility formulation from Brouwer *et al.* (2018). Kumar (2018) was the first to create a three-dimensional model to study the sediment dynamics in estuaries using a perturbation method and harmonic decomposition. He used this model to study the effects of bathymetric changes on the location of the ETM.

3.1 The suspended sediment equation

The sediment is assumed to consists of non-cohesive, fine particles with uniform grain size (i.e., constant settling velocity) that are primarily transported as suspended load. The dynamics of the suspended sediment concentration $c(x, y, z, t)$ is described using a three-dimensional advection-diffusion equation including the effects of settling (for details, see, e.g., Kumar, 2018; Schuttelaars and Zitman, 2022)

$$\underbrace{c_t}_{\text{local inertia}} + \underbrace{uc_x + vc_y + wc_z}_{\text{advection}} = \underbrace{w_s c_z}_{\text{settling}} + \underbrace{(K_\mathrm{h} c_x)_x + (K_\mathrm{h} c_y)_y + (K_v c_z)_z}_{\text{diffusion}}.$$

Here, w_s denotes the settling velocity and K_h, K_v are the horizontal and vertical eddy diffusivity. The advective terms have been written in non-conservative form using the continuity equation.

At the free surface, a no sediment flux is prescribed

$$w_s c + K_v c_z - K_\mathrm{h} c_x (R+\zeta)_x - K_\mathrm{h} c_y (R+\zeta)_y = 0, \qquad \text{at} \quad z = R+\zeta,$$

whereas near the bed, the diffusive flux equals the erosion E:

$$-K_v c_z - K_\mathrm{h} c_x H_x - K_\mathrm{h} c_y H_y = E, \qquad \text{at} \quad z = -H.$$

Here, it is assumed that the free surface and bottom slope are sufficiently small.

The erosion flux E is parametrised as $E = w_s c_\star$ with reference concentration $c_\star$, which can be further expressed as

$$E = w_s \rho_s \frac{|\boldsymbol{\tau}_b|}{\rho_0 g' d_s} \Phi(a). \tag{3.1.1}$$

Here, ρ_s is the density of sediment, $\boldsymbol{\tau}_b = \rho_0 A_v \boldsymbol{u}_z$ is the bed shear stress, $g' = g(\rho_s - \rho_0)/\rho_0$ is the reduced gravity, d_s is the mean grain size, $a = a(x, y)$ the availability of easily erodible sediment on the bed and $\Phi(\cdot)$ is the erodability function. The deposition near the bed is defined as $D = w_s c_b$, with c_b is the sediment concentration near the bed, i.e., $c_b = c|_{z=-H}$. In general, the subscript b is used to refer to quantities evaluated near the bed.

An alternative formulation of the erosion flux (3.1.1) is given by (see, e.g., Dijkstra, 2019)

$$E = M|\boldsymbol{\tau}_b|\Phi(a), \tag{3.1.2}$$

with M an erosion parameter, which is typically used as a calibration parameter. The two formulations are the same if $M = w_s\rho_s/(\rho_0 g' d_s)$. We use this formulation for the erosion flux E.

3.2 Scaling

3.2.1 Scaling the erosion flux

Remember that the horizontal flow is ordered in ε as follows

$$\boldsymbol{u} = \boldsymbol{u}^0 + \boldsymbol{u}^1 + \boldsymbol{u}^2 + \ldots.$$

The norm squared of the horizontal flow is expanded to second order using the inner product as

$$|\boldsymbol{u}|^2 = \boldsymbol{u}\cdot\boldsymbol{u} = \left(\boldsymbol{u}^0 + \boldsymbol{u}^1 + \boldsymbol{u}^2 + \ldots\right)\cdot\left(\boldsymbol{u}^0 + \boldsymbol{u}^1 + \boldsymbol{u}^2 + \ldots\right) = \underbrace{\left|\boldsymbol{u}^0\right|^2}_{\mathcal{O}(1)} + \underbrace{2\boldsymbol{u}^0\cdot\boldsymbol{u}^1}_{\mathcal{O}(\varepsilon)} + \underbrace{2\boldsymbol{u}^0\cdot\boldsymbol{u}^2 + \left|\boldsymbol{u}^1\right|^2}_{\mathcal{O}(\varepsilon^2)} + \ldots.$$

This expansion can also be determined using the table

	$\boldsymbol{u}^0$	$\boldsymbol{u}^1$	$\boldsymbol{u}^2$
$\boldsymbol{u}^0$	1	ε	ε^2
$\boldsymbol{u}^1$	ε	ε^2	ε^3
$\boldsymbol{u}^2$	ε^2	ε^3	ε^4

The bed shear stress is also expanded to second order using the partial-slip formulation and assuming that $2\boldsymbol{u}_b^0\cdot\boldsymbol{u}_b^1 + 2\boldsymbol{u}_b^0\cdot\boldsymbol{u}_b^2 + \left|\boldsymbol{u}_b^1\right|^2 \ll \left|\boldsymbol{u}_b^0\right|^2$ as

$$\begin{aligned}
|\boldsymbol{\tau}_b| &= \rho_0|A_v\boldsymbol{u}_z|,\\
&= \rho_0 s_f|\boldsymbol{u}_b|,\\
&= \rho_0 s_f\sqrt{\boldsymbol{u}_b\cdot\boldsymbol{u}_b},\\
&= \rho_0 s_f\sqrt{\left|\boldsymbol{u}_b^0\right|^2 + 2\boldsymbol{u}_b^0\cdot\boldsymbol{u}_b^1 + 2\boldsymbol{u}_b^0\cdot\boldsymbol{u}_b^2 + \left|\boldsymbol{u}_b^1\right|^2 + \ldots},\\
&= \rho_0 s_f\left|\boldsymbol{u}_b^0\right|\sqrt{1 + \frac{2\boldsymbol{u}_b^0\cdot\boldsymbol{u}_b^1 + 2\boldsymbol{u}_b^0\cdot\boldsymbol{u}_b^2 + \left|\boldsymbol{u}_b^1\right|^2 + \ldots}{\left|\boldsymbol{u}_b^0\right|^2}},\\
&= \rho_0 s_f\left|\boldsymbol{u}_b^0\right|\left[1 + \frac{1}{2}\left(2\frac{\boldsymbol{u}_b^0\cdot\boldsymbol{u}_b^1}{|\boldsymbol{u}_b^0|^2} + 2\frac{\boldsymbol{u}_b^0\cdot\boldsymbol{u}_b^2}{|\boldsymbol{u}_b^0|^2} + \frac{\left|\boldsymbol{u}_b^1\right|^2}{|\boldsymbol{u}_b^0|^2} + \ldots\right) - \frac{1}{8}\left(4\frac{(\boldsymbol{u}_b^0\cdot\boldsymbol{u}_b^1)^2}{|\boldsymbol{u}_b^0|^4} + \ldots\right) + \ldots\right],\\
&= \underbrace{\rho_0 s_f\left|\boldsymbol{u}_b^0\right|}_{\mathcal{O}(1)} + \underbrace{\rho_0 s_f\frac{\boldsymbol{u}_b^0\cdot\boldsymbol{u}_b^1}{\left|\boldsymbol{u}_b^0\right|}}_{\mathcal{O}(\varepsilon)} + \underbrace{\rho_0 s_f\left(\frac{\boldsymbol{u}_b^0\cdot\boldsymbol{u}_b^2}{\left|\boldsymbol{u}_b^0\right|} + \frac{1}{2}\frac{\left|\boldsymbol{u}_b^1\right|^2}{\left|\boldsymbol{u}_b^0\right|} - \frac{1}{2}\frac{(\boldsymbol{u}_b^0\cdot\boldsymbol{u}_b^1)^2}{\left|\boldsymbol{u}_b^0\right|^3}\right)}_{\mathcal{O}(\varepsilon^2)} + \ldots,\\
&= \underbrace{\rho_0 s_f\left|\boldsymbol{u}_b^0\right|}_{\mathcal{O}(1)} + \underbrace{\rho_0 s_f\,\boldsymbol{n}_b^0\cdot\boldsymbol{u}_b^1}_{\mathcal{O}(\varepsilon)} + \underbrace{\rho_0 s_f\left(\boldsymbol{n}_b^0\cdot\boldsymbol{u}_b^2 + \frac{1}{2}\left(\left|\boldsymbol{r}_b^1\right|^2 - (\boldsymbol{n}_b^0\cdot\boldsymbol{r}_b^1)^2\right)\right)}_{\mathcal{O}(\varepsilon^2)} + \ldots, \qquad \text{at } z=-H,
\end{aligned}$$

where we have defined the unit vector pointing into the leading-order velocity direction and the vector pointing into the first-order velocity direction:

$$\boldsymbol{n}_b^0 = \frac{\boldsymbol{u}_b^0}{\left|\boldsymbol{u}_b^0\right|}, \qquad \boldsymbol{r}_b^1 = \frac{\boldsymbol{u}_b^1}{\sqrt{\left|\boldsymbol{u}_b^0\right|}}. \tag{3.2.1}$$

The erosion parameter can be ordered in the small parameter ε as

$$E = \underbrace{E^0}_{\mathcal{O}(1)} + \underbrace{E^1}_{\mathcal{O}(\varepsilon)} + \ldots.$$

Using erosion flux formulation (3.1.2), it follows that the leading- and first-order contributions are given by

$$\begin{aligned} E^0 &= \rho_0 s_f M \left|\boldsymbol{u}_b^0\right| \Phi(a), \\ E^1 &= \rho_0 s_f M\, \boldsymbol{n}_b^0 \cdot \boldsymbol{u}_b^1 \Phi(a). \end{aligned}$$

These expressions are non-linear in the velocity, thereby generating overtides in the forcing of suspended sediment concentration.

3.2.2 Scaling the equations

These equations are scaled using characteristic scales (see, e.g., Kumar, 2018). The following ordering is obtained for the suspended sediment equation

$$\underbrace{c_t}_{\mathcal{O}(1)} + \underbrace{uc_x + vc_y + wc_z}_{\mathcal{O}(\varepsilon)} = \underbrace{w_s c_z}_{\mathcal{O}(1)} + \underbrace{(K_\mathrm{h} c_x)_x + (K_\mathrm{h} c_y)_y}_{\mathcal{O}(\varepsilon^2)} + \underbrace{(K_v c_z)_z}_{\mathcal{O}(1)}.$$

At the free surface, the ordering of the terms is given by

$$\underbrace{w_s c + K_v c_z}_{\mathcal{O}(1)} + \underbrace{(w_s c + K_v c_z)_z \zeta}_{\mathcal{O}(\varepsilon)} + \ldots + \underbrace{-K_\mathrm{h} c_x (R+\zeta)_x - K_\mathrm{h} c_y (R+\zeta)_y}_{\mathcal{O}(\varepsilon^3)} + \cdots = 0, \qquad \text{at} \quad z = R,$$

whereas near the bed, we have

$$\underbrace{-K_v c_z}_{\mathcal{O}(1)} \underbrace{-K_\mathrm{h} c_x H_x - K_\mathrm{h} c_y H_y}_{\mathcal{O}(\varepsilon^2)} = \underbrace{E^0}_{\mathcal{O}(1)} + \underbrace{E^1}_{\mathcal{O}(\varepsilon)}, \qquad \text{at} \quad z = -H.$$

3.3 Perturbation method

The suspended sediment concentration is expanded in the small parameter ε, similar to the water motion variables ζ, u, v and w:

$$c = c^0 + c^1 + c^2 + \ldots.$$

Again, the superscripts denote the order in ε.

3.3.1 Leading-order suspended sediment equation

Collecting terms of leading-order, the suspended sediment equation at leading-order is obtained as

$$c_t^0 = w_s c_z^0 + \left(K_v c_z^0\right)_z. \tag{3.3.1}$$

Similarly, for the boundary conditions, ones gets

$$w_s c^0 + K_v c_z^0 = 0, \qquad \text{at} \quad z = R,$$

and near the bed

$$-K_v c_z^0 = E^0, \qquad \text{at} \quad z = -H.$$

3.3.2 First-order suspended sediment equation

Collecting the first-order terms results in the first-order sediment equation. The forcing mechanisms of this equation are denoted with a Greek letter. The advective body forcing term is given by

$$\eta_c^1(x,y,z,t) = u^0 c_x^0 + v^0 c_y^0 + w^0 c_z^0, \qquad \text{(advection of sediment)}$$

and the no-flux forcing at the surface read

$$\chi_c^1(x,y,t) = \zeta^0 c_t^0 \qquad \text{at} \quad z = R, \qquad \text{(no flux)}$$

where we have used the leading-order suspended sediment balance to write $\left(w_s c^0 + K_v c_z^0\right)_z = c_t^0$.

The first-order suspended sediment equation is given by

$$c_t^1 = w_s c_z^1 + \left(K_v c_z^1\right)_z - \eta_c^1. \tag{3.3.2}$$

The first-order boundary conditions read

$$w_s c^1 + K_v c_z^1 = -\chi_c^1, \qquad \text{at} \quad z = R,$$

and near the bed, we have

$$-K_v c_z^1 = E^1, \qquad \text{at} \quad z = -H.$$

3.3.3 Second-order suspended sediment equation

The full second-order suspended sediment equation is not considered. However, near the riverine boundary, the velocity of each tidal constituent vanishes due to the no-transport of water boundary condition, except for the sub-tidal river flow, which is explicitly imposed there. This implies that the sediment transport due to the tidal constituents near the riverine side is marginal, whereas the river flow might still be large enough to erode sediments and subsequently transport it down stream. This transport mechanism is due to the first-order river-induced velocity and the second-order river-induced sediment resuspension. This net sediment transport mechanisms can be important and is therefore included in the second-order balance of net sediment transport mechanisms of the morphodynamic equilibrium condition, whereas according to scaling this term is only a fourth-order term.

The corresponding second-order forced suspended sediment equation reads

$$c_{\text{river},t}^2 = w_s c_{\text{river},z}^2 + (K_v c_{\text{river},z}^2)_z,$$

with boundary conditions

$$\begin{aligned} w_s c_{\text{river}}^2 + K_v c_{\text{river},z}^2 &= 0, &&\text{at} \quad z = R,\\ -K_v c_{\text{river},z}^2 &= E_{\text{river}}^2, &&\text{at} \quad z = -H. \end{aligned}$$

3.3.4 Morphodynamic equilibrium condition

The morphodynamic equilibrium condition is the crux of this model. It is the last piece of the puzzle that brings everything together. It connects how the harmonic components of the hydrodynamics interact with those of sediment dynamics in such a way that a certain equilibrium state is achieved.

The *morphodynamic equilibrium condition* states that the total amount of sediment in the estuary varies on a timescale that is much longer than the timescale at which the easily erodible sediment is redistributed over the system. That is, the total amount of sediment in the system is constant and the equilibrium distribution of sediment in the estuary is sought.

In morphodynamic equilibrium, the tidally-averaged erosion and deposition are in balance:

$$\langle E - D \rangle = 0,$$

Table 3.1: Summary of the harmonic components of the leading- and first-order water and sediment dynamics.

	Hydrodynamics	Sediment dynamics
Leading order $\mathcal{O}(1)$	$\boldsymbol{u}_1^0$	c_0^0, c_2^0
First order $\mathcal{O}(\varepsilon)$	$\boldsymbol{u}_0^1$, $\boldsymbol{u}_2^1$	c_1^1

where $\langle\cdot\rangle$ denotes the tidal average.

Integrating the (conservative) suspended sediment equation over the depth and using the boundary conditions for the water motion and sediment at the free surface and bed yields

$$\left(\int_{-H}^{R+\zeta} c\,dz\right)_t + \left(\int_{-H}^{R+\zeta} uc - K_\mathrm{h} c_x\,dz\right)_x + \left(\int_{-H}^{R+\zeta} vc - K_\mathrm{h} c_y\,dz\right)_y = E - D.$$

Averaging this equation over the tidal period and using that the tidally-averaged erosion and deposition balance yields the condition:

$$\left\langle \left(\int_{-H}^{R+\zeta} uc - K_\mathrm{h} c_x\,dz\right)_x + \left(\int_{-H}^{R+\zeta} vc - K_\mathrm{h} c_y\,dz\right)_y \right\rangle = 0.$$

The morphodynamic equilibrium condition is equivalent to requiring that the divergence of the tidally-averaged suspended sediment transport vanishes:

$$\nabla\cdot\mathcal{T} = 0, \tag{3.3.3}$$

which states that in morphodynamic equilibrium there is no net transport of sediments. The suspended sediment transport $\mathcal{T}$ is defined as the sum of the advective and diffusive transport integrated over the depth and averaged over the tidal cycle:

$$\mathcal{T} = \left\langle \int_{-H}^{R+\zeta} \underbrace{\boldsymbol{u}c}_{\text{advection}} - \underbrace{K_\mathrm{h}\nabla c}_{\text{diffusion}}\,dz \right\rangle.$$

3.3.5 Scaling the morphodynamic equilibrium condition

Under the standard forcing conditions, the water motion and suspended sediment concentration consist of several harmonic components. The most important for net sediment transport are the subtidal M_0, semi-diurnal M_2 and the first overtide M_4 tidal constituents (Chernetsky, 2012; Kumar, 2018; Dijkstra, 2019). The hydrodynamics and sediment dynamics are therefore truncated after the M_4 tidal component, neglecting the higher-order overtides (e.g., the M_6, M_8, M_{10} etc. tidal components).

The leading-order water motion $\boldsymbol{u}^0$ consists of an M_2 component, denoted by $\boldsymbol{u}_1^0$, whereas the leading-order suspended sediment concentration c^0 consists of both a subtidal M_0 and M_4 signal, denoted by c_0^0 and c_2^0, (in which the superscript denotes the order in ε and the subscript denotes the harmonic component, where 0 denotes the subtidal component, 1 the M_2 component and 2 the M_4 component):

$$\boldsymbol{u}^0 = \underbrace{\boldsymbol{u}_1^0}_{M_2}, \qquad c^0 = \underbrace{c_0^0}_{M_0} + \underbrace{c_2^0}_{M_4}.$$

The first-order water motion $\boldsymbol{u}^1$ consists of both a subtidal M_0 and M_4 component, denoted by $\boldsymbol{u}_0^1$ and $\boldsymbol{u}_2^1$, and the first-order suspended sediment concentration c^1 consists of an M_2 component, denoted by c_1^1:

$$\boldsymbol{u}^1 = \underbrace{\boldsymbol{u}_0^1}_{M_0} + \underbrace{\boldsymbol{u}_2^1}_{M_4}, \qquad c^1 = \underbrace{c_1^1}_{M_2}.$$

In Table 3.1, the harmonic components of the leading- and first-order water and sediment motion are summarised.

Substitution of the above relations into the net sediment transport vector shows that only certain correlations between the water motion and sediment concentration may lead to net transport at second order (for a full derivation, see, Kumar, 2018):

$$
\begin{aligned}
\mathscr{T} &= \left\langle \int_{-H}^{R+\zeta} \boldsymbol{u} c - K_\mathrm{h} \nabla c \, dz \right\rangle, \\
&= \left\langle \int_{-H}^{R} \boldsymbol{u}^0 c^0 + \boldsymbol{u}^0 c^1 + \boldsymbol{u}^1 c^0 - K_\mathrm{h} \nabla c^0 \, dz + \boldsymbol{\zeta}^0 \boldsymbol{u}^0 c^0|_{z=R} \right\rangle + \mathscr{O}(\varepsilon^3), \\
&= \left\langle \int_{-H}^{R} \underbrace{\boldsymbol{u}_1^0 c_1^1 + \boldsymbol{u}_0^1 c_0^0 + \boldsymbol{u}_2^1 c_2^0}_{\text{advection}} - \underbrace{K_\mathrm{h} \nabla c_0^0}_{\text{diffusion}} \, dz + \underbrace{\zeta_1^0 \boldsymbol{u}_1^0 c^0|_{z=R}}_{\text{stokes}} \right\rangle + \mathscr{O}(\varepsilon^3),
\end{aligned} \tag{3.3.4}
$$

Regarding the advective transport, only the M_0–M_0, M_2–M_2 and M_4–M_4 interactions result in tidally-averaged sediment transport. For the diffusive transport, only the M_0 component of the leading-order suspended sediment concentration leads to tidally-averaged transport. The other interactions do not lead to net transport since the sine and cosine are orthogonal (for more details, see Appendix B.1).

3.3.6 Equation for the erodability function

To solve the equations governing sediment dynamics, the erodability function $\Phi(a)$ must be determined as it is an unknown in the current model. Thus, the goal is to construct a single equation for the erodability function $\Phi(a)$. If the erodability function is linear in the sediment availability, e.g., $\Phi(a) = a$, then this is equivalent to constructing a single equation for the sediment availability $a(x, y)$ (see, for example, Kumar, 2018). In Section 3.3.5, the frequency components of the leading- and first-order suspended sediment concentration have been introduced and they are summarised in Table 3.1. In this section, the origin of these harmonic components is presented as part of the derivation.

The leading-order suspended sediment equation (3.3.1) is only forced by the leading-order erosion flux E^0. Harmonic analysis shows that this forcing mechanism consists of only the even multiples of the M_2 signal (see Appendix B.8 for details). Using that the leading-order erosion flux E^0 is linear in the erodability function $\Phi(a)$ and truncating after the M_4 component, we may write:

$$
E^0 = E^{0a}\,\Phi(a) = \left(E_0^{0a} + E_2^{0a}\right)\Phi(a),
$$

where we have defined

$$
E^{0a} = \rho_0 s_f M \left|\boldsymbol{u}_b^0\right|. \tag{3.3.5}
$$

Since the leading-order suspended sediment equation is linear, it follows that this linear dependency of the forcing on $\Phi(a)$ and on M_0 and M_4, also applies to the leading-order suspended sediment concentration c^0. We denote this with both a hat and a superscript a as

$$
c^0 = \hat{c}^{0a}\,\Phi(a) = \left(\hat{c}_0^{0a} + \hat{c}_2^{0a}\right)\Phi(a).
$$

We call $\hat{c}^{ka}$ the sediment capacity of order k.

Next, we extend this idea to the first-order suspended sediment concentration. The forcing mechanisms of the first-order suspended sediment concentration consists of only the odd harmonics of the M_2 frequency (see Appendix B.9 for details regarding the first-order erosion forcing). Using that these forcing mechanisms are linear in the erodability function $\Phi(a)$ and truncating after the M_4 constituent, we obtain

$$
\begin{aligned}
\eta_c^1(x,y,z,t) &= \left(\eta_c^{1a} + \boldsymbol{\eta}_c^{1\nabla a}\cdot\nabla\right)\Phi(a) = \left(\eta_{c,1}^{1a} + \boldsymbol{\eta}_{c,1}^{1\nabla a}\cdot\nabla\right)\Phi(a), && \text{(advection of sediment)} \\
\chi_c^1(x,y,t) &= \chi_c^{1a}\,\Phi(a) = \chi_{c,1}^{1a}\,\Phi(a), && \text{(no flux)} \\
E^1(x,y,t) &= E^{1a}\,\Phi(a) = E_1^{1a}\,\Phi(a). && \text{(erosion flux)}
\end{aligned} \tag{3.3.6}
$$

Here, we have defined the forcing mechanisms

$$
\begin{aligned}
\eta_c^{1a}(x,y,z,t) &= \boldsymbol{u}^0\cdot\nabla\hat{c}^{0a} + w^0\hat{c}_z^{0a}, \\
\boldsymbol{\eta}_c^{1\nabla a}(x,y,z,t) &= \boldsymbol{u}^0\hat{c}^{0a}, \\
\chi_c^{1a}(x,y,t) &= \zeta^0\hat{c}_t^{0a}, && \text{at} \quad z = R, \\
E^{1a}(x,y,t) &= \rho_0 s_f M\,\boldsymbol{n}_b^0\cdot\boldsymbol{u}_b^1, && \text{at} \quad z = -H.
\end{aligned} \tag{3.3.7}
$$

Since the first-order forcing mechanisms depend linearly on $\Phi(a)$ and its gradient $\nabla\Phi(a)$, and since the first-order equation is linear, it follows that we may express the first-order suspended sediment equation as

$$c^1 = \left(\hat{c}^{1a} + \hat{\boldsymbol{c}}^{1\nabla a}\cdot\nabla\right)\Phi(a) = \left(\hat{c}_1^{1a} + \hat{\boldsymbol{c}}_1^{1\nabla a}\cdot\nabla\right)\Phi(a).$$

Here, we have defined the vector $\hat{\boldsymbol{c}}_1^{1\nabla a} = \begin{bmatrix}\hat{c}_1^{1a_x} & \hat{c}_1^{1a_y}\end{bmatrix}^T$ containing the contributions of $\hat{c}_1^1$ scaling with $\partial_x\Phi(a)$ and $\partial_y\Phi(a)$, respectively.

Substituting the above expressions for c^0 and c^1 into the net sediment transport vector (3.3.4) and using that it is linear in the sediment concentration shows that

$$\begin{aligned}
\mathscr{T} &= \left\langle \int_{-R}^{H} \boldsymbol{u}_1^0 \left(\hat{\boldsymbol{c}}_1^{1\nabla a}\right)^T \nabla - K_\mathrm{h}\hat{c}_0^{0a}\nabla\, dz + \int_{-H}^{R} \boldsymbol{u}_1^0\hat{c}_1^{1a} + \boldsymbol{u}_0^1\hat{c}_0^{0a} + \boldsymbol{u}_2^1\hat{c}_2^{0a} - K_\mathrm{h}\nabla\left(\hat{c}_0^{0a}\right) dz + \zeta_1^0\boldsymbol{u}_1^0\hat{c}^{0a}\Big|_{z=R}\right\rangle \Phi(a),\\
&= \left(\int_{-R}^{H}\left\langle \boldsymbol{u}_1^0\left(\hat{\boldsymbol{c}}_1^{1\nabla a}\right)^T\right\rangle - K_\mathrm{h}\hat{c}_0^{0a}\, dz\nabla + \int_{-H}^{R}\left\langle \boldsymbol{u}_1^0\hat{c}_1^{1a}\right\rangle + \boldsymbol{u}_0^1\hat{c}_0^{0a} + \left\langle \boldsymbol{u}_2^1\hat{c}_2^{0a}\right\rangle - K_\mathrm{h}\nabla\left(\hat{c}_0^{0a}\right) dz + \left\langle \zeta_1^0\boldsymbol{u}_1^0\hat{c}^{0a}\Big|_{z=R}\right\rangle\right)\Phi(a),\\
&= \left(\int_{-R}^{H}\left\langle \boldsymbol{u}_1^0\left(\hat{\boldsymbol{c}}_1^{1\nabla a}\right)^T\right\rangle - K_\mathrm{h}\hat{c}_0^{0a}\, dz\right)\nabla\Phi + \left(\int_{-H}^{R}\left\langle \boldsymbol{u}_1^0\hat{c}_1^{1a}\right\rangle + \boldsymbol{u}_0^1\hat{c}_0^{0a} + \left\langle \boldsymbol{u}_2^1\hat{c}_2^{0a}\right\rangle - K_\mathrm{h}\nabla\left(\hat{c}_0^{0a}\right) dz + \left\langle \zeta_1^0\boldsymbol{u}_1^0\hat{c}^{0a}\Big|_{z=R}\right\rangle\right)\Phi,\\
&= \mathbf{D}^{\nabla a}\nabla\Phi + \boldsymbol{T}^a\Phi.
\end{aligned} \tag{3.3.8}$$

Here, the operator ∇ works on everything to the right of it and we write Φ rather than $\Phi(a)$ for conciseness. Furthermore, we have defined the sediment availability diffusion matrix $\mathbf{D}^{\nabla a}$ and sediment availability transport vector $\boldsymbol{T}^a$ as

$$\begin{aligned}
\mathbf{D}^{\nabla a} &= \underbrace{\mathbf{D}_{M_2}^{\nabla a}}_{M_2-M_2} + \underbrace{\mathbf{D}_\mathrm{diff}^{\nabla a}}_{\text{diffusion}},\\
\boldsymbol{T}^a &= \underbrace{\boldsymbol{T}_{M_2}^a}_{M_2-M_2} + \underbrace{\boldsymbol{T}_{M_0}^a}_{M_0-M_0} + \underbrace{\boldsymbol{T}_{M_4}^a}_{M_4-M_4} + \underbrace{\boldsymbol{T}_\mathrm{diff}^a}_{\text{diffusion}} + \underbrace{\boldsymbol{T}_\mathrm{stokes}^a}_{\text{stokes}}.
\end{aligned}$$

For the advective terms, the first harmonic component of the under brace relates to the harmonic of the velocity and the second to the harmonic of the sediment concentration. The contributions to the availability matrix are given by

$$\begin{aligned}
\mathbf{D}_{M_2}^{\nabla a} &= \int_{-H}^{R}\left\langle \boldsymbol{u}_1^0\left(\hat{\boldsymbol{c}}_1^{1\nabla a}\right)^T\right\rangle dz = \int_{-H}^{R}\left\langle \boldsymbol{u}_1^0\otimes\hat{\boldsymbol{c}}_1^{1\nabla a}\right\rangle dz = \int_{-H}^{R}\left\langle \begin{bmatrix} u_1^0\hat{c}_1^{1a_x} & u_1^0\hat{c}_1^{1a_y}\\ v_1^0\hat{c}_1^{1a_x} & v_1^0\hat{c}_1^{1a_y}\end{bmatrix}\right\rangle dz,\\
\mathbf{D}_\mathrm{diff}^{\nabla a} &= -K_\mathrm{h}\int_{-H}^{R}\hat{c}_0^{0a}\, dz\,\mathbf{I}_2,
\end{aligned}$$

with $\otimes$ (here) denoting the outer product between two vectors and $\mathbf{I}_2$ the 2×2 identity matrix. For the availability transport vector, we have the contributions

$$\boldsymbol{T}_{M_2}^a = \int_{-H}^{R}\left\langle \boldsymbol{u}_1^0\hat{c}_1^{1a}\right\rangle dz, \qquad \boldsymbol{T}_{M_0}^a = \int_{-H}^{R}\boldsymbol{u}_0^1\hat{c}_0^{0a}\, dz, \qquad \boldsymbol{T}_{M_4}^a = \int_{-H}^{R}\left\langle \boldsymbol{u}_2^1\hat{c}_2^{0a}\right\rangle dz,$$

$$\boldsymbol{T}_\mathrm{diff}^a = -K_\mathrm{h}\int_{-H}^{R}\nabla\hat{c}_0^{0a}\, dz, \qquad \boldsymbol{T}_\mathrm{stokes}^a = \left\langle \zeta_1^0\boldsymbol{u}_1^0\left(\hat{c}_0^{0a}+\hat{c}_2^{0a}\right)\Big|_{z=R}\right\rangle.$$

The sediment availability transport vector is also referred to as the *transport capacity* (see, e.g., Dijkstra, 2019): the sediment transport $\mathscr{T}$ that would occur if there were an abundance of sediment on the bed everywhere in the domain, assuming the resulting hydrodynamic and sediment dynamic conditions remain approximately constant.

Combining the morphodynamic equilibrium condition (3.3.3) and the sediment availability formulation (3.3.8), a single equation for the erodability function $\Phi(x, y)$ is obtained:

$$\nabla\cdot\left[\mathbf{D}^{\nabla a}\nabla\Phi + \boldsymbol{T}^a\Phi\right] = 0. \tag{3.3.9}$$

To solve this equation, boundary conditions have to be imposed. At the seaward boundary, the depth- and tidally-averaged suspended sediment concentration is prescribed (similar to Wei, 2017):

$$\frac{1}{D}\int_{-H}^{R}\langle c\rangle\, dz = [\langle c\rangle]_\mathrm{sea}(x, y), \qquad \text{at} \quad \partial\Omega_\mathrm{sea},$$

at the banks, a no-transport condition is imposed (similar to Wei, 2017; Kumar, 2018):

$$\left[\mathbf{D}^{\nabla a}\nabla\Phi + \boldsymbol{T}^{a}\Phi\right]\cdot\boldsymbol{n} = 0, \qquad \text{at} \quad \partial\Omega_{\text{bank}},$$

at the riverine boundary, the sediment transport is prescribed (similar to Dijkstra, 2019):

$$\left[\mathbf{D}^{\nabla a}\nabla\Phi + \boldsymbol{T}^{a}\Phi\right]\cdot\boldsymbol{n} = -\mathscr{F}_{\text{river}}(x,y), \qquad \text{at} \quad \partial\Omega_{\text{river}}.$$

The riverine sediment transport is typically directed into the domain. Since $\boldsymbol{n}$ is the outward pointing unit vector, minus this vector ($-\boldsymbol{n}$) points into the domain. Thus $\mathscr{F}_{\text{river}}(x,y) > 0$ is the sediment transport pointing into the domain.

The prescribed depth- and tidally-averaged suspended sediment concentration can be transformed to a Dirichlet boundary condition for Φ as

$$\Phi = \frac{[\langle c\rangle]_{\text{sea}}}{[\hat{c}]_0^{0a}}, \qquad \text{at} \quad \partial\Omega_{\text{sea}}. \tag{3.3.10}$$

Table 3.2: The hydrodynamic and sediment dynamic variables generated by each forcing mechanism.

Mechanism	Tide A	Riv. q	Bar. ς	Ref. ξ	Adv. η	Sto. γ	N.str. χ	P.slip μ	Adv.s. η_c	N.flux χ_c
$\mathcal{O}(1)$ M_2 $\boldsymbol{u}_1^0$	$\boldsymbol{u}_1^{0A}$									
$\mathcal{O}(\varepsilon)$ M_0 $\boldsymbol{u}_0^1$		$\boldsymbol{u}_0^{1q}$	$\boldsymbol{u}_0^{1\varsigma}$	$\boldsymbol{u}_0^{1\xi}$	$\boldsymbol{u}_0^{1\eta}$	$\boldsymbol{u}_0^{1\gamma}$	$\boldsymbol{u}_0^{1\chi}$	$\boldsymbol{u}_0^{1\mu}$		
$\mathcal{O}(\varepsilon)$ M_4 $\boldsymbol{u}_2^1$	$\boldsymbol{u}_2^{1A}$				$\boldsymbol{u}_2^{1\eta}$	$\boldsymbol{u}_2^{1\gamma}$	$\boldsymbol{u}_2^{1\chi}$	$\boldsymbol{u}_2^{1\mu}$		
$\mathcal{O}(1)$ M_0 c_0^0	c_0^{0EA}									
$\mathcal{O}(1)$ M_4 c_2^0	c_2^{0EA}									
$\mathcal{O}(\varepsilon)$ M_2 c_1^1	c_1^{1EA}	c_1^{1Eq}	$c_1^{1E\varsigma}$	$c_1^{1E\xi}$	$c_1^{1E\eta}$	$c_1^{1E\gamma}$	$c_1^{1E\chi}$	$c_1^{1E\mu}$	$c_1^{1\eta_c}$	$c_1^{1\chi_c}$

3.3.7 Decomposition of transport mechanisms

The sediment transport vector consist of several contributions that can be combined in different ways to obtain different sediment transport decompositions.

Focusing on the net sediment transport vector. The net sediment transport vector consists of three physical transport mechanisms: advection, diffusion and Stokes return flow. These three physical mechanisms can also be expressed in terms of the sediment availability matrix and vector as follows

$$
\begin{aligned}
\mathcal{T}_{\text{advection}} &= \mathbf{D}_{M_2}^{\nabla a}\,\nabla\Phi + \left(\boldsymbol{T}_{M_2}^a + \boldsymbol{T}_{M_0}^a + \boldsymbol{T}_{M_4}^a\right)\Phi,\\
\mathcal{T}_{\text{diffusion}} &= \mathbf{D}_{\text{diff}}^{\nabla a}\,\nabla\Phi + \boldsymbol{T}_{\text{diff}}^a\,\Phi,\\
\mathcal{T}_{\text{stokes}} &= \boldsymbol{T}_{\text{stokes}}^a\,\Phi.
\end{aligned}
$$

Another decomposition is based on the transport capacity and the underlying physical mechanisms. The leading- and first-order hydrodynamic variables under the standard forcing conditions are decomposed into the underlying physical mechanism using Table 1.3. In Table 3.2, the hydrodynamic and sediment dynamic variables generated by each forcing mechanism are depicted. The superscript E denotes that the physical mechanism acts through the erosion at the bed. Using this decomposition, the variables that are generated by a single physical mechanism can be substituted directly into the transport capacity terms, yielding

$$
\boldsymbol{T}_{M_2}^a = \int_{-H}^{R} \left\langle \boldsymbol{u}_1^{0A}\hat{c}_1^{1a}\right\rangle dz, \qquad \boldsymbol{T}_{M_0}^a = \int_{-H}^{R} \boldsymbol{u}_0^1\hat{c}_0^{0EAa}\,dz, \qquad \boldsymbol{T}_{M_4}^a = \int_{-H}^{R} \left\langle \boldsymbol{u}_2^1\hat{c}_2^{0EAa}\right\rangle dz,
$$

$$
\boldsymbol{T}_{\text{diff}}^a = -K_{\text{h}}\int_{-H}^{R} \nabla\hat{c}_0^{0EAa}\,dz, \qquad \boldsymbol{T}_{\text{stokes}}^a = \left\langle \zeta_1^{0A}\boldsymbol{u}_1^{0A}\left(\hat{c}_0^{0EAa} + \hat{c}_2^{0EAa}\right)\Big|_{z=R}\right\rangle.
$$

The advective transport capacity terms $\boldsymbol{T}_{M_2}^a$, $\boldsymbol{T}_{M_0}^a$ and $\boldsymbol{T}_{M_4}^a$ still contain a single unexpanded variable, $\hat{c}_1^{1a}$, $\boldsymbol{u}_0^1$ and $\boldsymbol{u}_2^1$, respectively. We use the physical mechanism of these unexpanded variables to refer to their contributions in the resulting transport. The decomposition of the advective transport capacity terms can be found in Table 3.3 where we have used Table 3.2.

We can do the same for the diffusion matrix contributions:

$$
\begin{aligned}
\mathbf{D}_{M_2}^{\nabla a} &= \int_{-H}^{R} \left\langle \boldsymbol{u}_1^{0A}\left(\hat{\boldsymbol{c}}_1^{1\eta_c\nabla a}\right)^T\right\rangle dz = \int_{-H}^{R} \left\langle \begin{bmatrix} u_1^{0A}\hat{c}_1^{1\eta_c a_x} & u_1^{0A}\hat{c}_1^{1\eta_c a_y} \\ v_1^{0A}\hat{c}_1^{1\eta_c a_x} & v_1^{0A}\hat{c}_1^{1\eta_c a_y} \end{bmatrix}\right\rangle dz,\\
\mathbf{D}_{\text{diff}}^{\nabla a} &= -K_{\text{h}}\int_{-H}^{R} \hat{c}_0^{0EAa}\,dz\,\mathbf{I}_2,
\end{aligned}
$$

3.3.8 Fourier coefficients of availability vector and matrix

Using the Fourier expansion of the variables and Appendix B.1, the transport terms can be expressed as

$$
\boldsymbol{T}_{M_2}^a = \int_{-H}^{R} \frac{1}{2}\mathfrak{Re}\left(\boldsymbol{U}_1^{0A}\left(\hat{C}_1^{1a}\right)^*\right) dz, \qquad \boldsymbol{T}_{M_0}^a = \int_{-H}^{R} \boldsymbol{U}_0^1\hat{C}_0^{0EAa}\,dz, \qquad \boldsymbol{T}_{M_4}^a = \int_{-H}^{R} \frac{1}{2}\mathfrak{Re}\left(\boldsymbol{U}_2^1\left(\hat{C}_2^{0EAa}\right)^*\right) dz,
$$

Table 3.3: Decomposition of the advective transport capacity terms.

	Tide A	River q	Baroc. ς	Ref. ξ	Adv. η	Stokes γ	N.str. χ	P.slip μ	Adv.s. η_c	N.fl. χ_c
$\boldsymbol{T}^a_{M_2}$	$\boldsymbol{u}_1^{0A}\hat{c}_1^{1EAa}$	$\boldsymbol{u}_1^{0A}\hat{c}_1^{1Eqa}$	$\boldsymbol{u}_1^{0A}\hat{c}_1^{1E\varsigma a}$	$\boldsymbol{u}_1^{0A}\hat{c}_1^{1E\xi a}$	$\boldsymbol{u}_1^{0A}\hat{c}_1^{1E\eta a}$	$\boldsymbol{u}_1^{0A}\hat{c}_1^{1E\gamma a}$	$\boldsymbol{u}_1^{0A}\hat{c}_1^{1E\chi a}$	$\boldsymbol{u}_1^{0A}\hat{c}_1^{1E\mu a}$	$\boldsymbol{u}_1^{0A}\hat{c}_1^{1\eta_c a}$	$\boldsymbol{u}_1^{0A}\hat{c}_1^{1\chi_c a}$
$\boldsymbol{T}^a_{M_0}$		$\boldsymbol{u}_0^{1q}\hat{c}_0^{0EAa}$	$\boldsymbol{u}_0^{1\varsigma}\hat{c}_0^{0EAa}$	$\boldsymbol{u}_0^{1\xi}\hat{c}_0^{0EAa}$	$\boldsymbol{u}_0^{1\eta}\hat{c}_0^{0EAa}$	$\boldsymbol{u}_0^{1\gamma}\hat{c}_0^{0EAa}$	$\boldsymbol{u}_0^{1\chi}\hat{c}_0^{0EAa}$	$\boldsymbol{u}_0^{1\mu}\hat{c}_0^{0EAa}$		
$\boldsymbol{T}^a_{M_4}$	$\boldsymbol{u}_2^{1A}\hat{c}_2^{0EAa}$				$\boldsymbol{u}_2^{1\eta}\hat{c}_2^{0EAa}$	$\boldsymbol{u}_2^{1\gamma}\hat{c}_2^{0EAa}$	$\boldsymbol{u}_2^{1\chi}\hat{c}_2^{0EAa}$	$\boldsymbol{u}_2^{1\mu}\hat{c}_2^{0EAa}$		

$$\boldsymbol{T}^a_{\text{diff}} = -K_{\text{h}}\int_{-H}^{R}\nabla\hat{C}_0^{0EAa}\,dz, \qquad \boldsymbol{T}^a_{\text{stokes}} = \mathfrak{Re}\left(\frac{1}{2}\left(Z_1^{0A}\right)^*\boldsymbol{U}_1^{0A}\hat{C}_0^{0EAa} + \frac{1}{4}Z_1^{0A}\boldsymbol{U}_1^{0A}\left(\hat{C}_2^{0EAa}\right)^*\right)\Bigg|_{z=R}.$$

Here, we assumed that we have defined the M_0 components as strictly real:

$$\boldsymbol{U}_0^1 = \mathfrak{Re}\left(\boldsymbol{U}_0^1\right), \qquad C_0^{0EAa} = \mathfrak{Re}\left(\hat{C}_0^{0EAa}\right).$$

For the diffusion matrix, we find

$$\mathbf{D}^{\nabla a}_{M_2} = \int_{-H}^{R}\frac{1}{2}\mathfrak{Re}\left(\boldsymbol{U}_1^{0A}\left(\hat{\boldsymbol{C}}_1^{1\eta_c\nabla a}\right)^*\right)dz = \int_{-H}^{R}\frac{1}{2}\mathfrak{Re}\left(\begin{bmatrix} U_1^{0A}\left(\hat{C}_1^{1\eta_c a_x}\right)^* & U_1^{0A}\left(\hat{C}_1^{1\eta_c a_y}\right)^* \\ V_1^{0A}\left(\hat{C}_1^{1\eta_c a_x}\right)^* & V_1^{0A}\left(\hat{C}_1^{1\eta_c a_y}\right)^* \end{bmatrix}\right)dz,$$

$$\mathbf{D}^{\nabla a}_{\text{diff}} = -K_{\text{h}}\int_{-H}^{R}\hat{C}_0^{0EAa}\,dz\,\mathbf{I}_2,$$

Here, $*$ denotes the conjugate transpose operator.

3.3.9 General suspended sediment equation

The leading- and first-order suspended sediment equations have a highly similar structure. We define a general equation that captures both cases. We extend this idea to other similarities as well. We create decompositions based on the order, harmonics, forcing mechanisms and availability.

Order decomposition

Define the suspended sediment equation of order $k \in \{0,1\}$ as

$$c_t^k = w_s c_z^k + \left(K_v c_z^k\right)_z - \eta_c^k.$$

The boundary conditions imposed at the free surface and near the bed read

$$\begin{aligned} w_s c^k + K_v c_z^k &= -\chi_c^k, && \text{at} \quad z = R, \\ -K_v c_z^k &= E^k, && \text{at} \quad z = -H. \end{aligned}$$

Here, we have defined the k-th order forcing mechanisms as

$$\eta_c^k = \begin{cases} \eta_c^1 & \text{if } k = 1, \\ 0 & \text{otherwise,} \end{cases}, \qquad \chi_c^k = \begin{cases} \chi_c^1 & \text{if } k = 1, \\ 0 & \text{otherwise,} \end{cases} \qquad E^k = \begin{cases} E^0 & \text{if } k = 0, \\ E^1 & \text{if } k = 1, \\ 0 & \text{otherwise.} \end{cases}$$

For $k = 0$, the equations reduce to the leading-order suspended sediment equation (3.3.1), whereas for $k = 1$, the first-order suspended sediment equation (3.3.2) is recovered.

Harmonic decomposition

We define the Fourier series expansion of the k-th order suspended sediment concentration as

$$c^k(x,y,z,t) = \sum_{n=0}^{\infty} c_n^k(x,y,z,t) = \sum_{n=0}^{\infty} \mathfrak{Re}\left(C_n^k(x,y,z)e^{ni\omega t}\right).$$

Similarly, for the k-th order forcing mechanisms, we have the expansions

$$\begin{aligned} \eta_c^k(x,y,z,t) &= \sum_{n=0}^{\infty} \eta_{c,n}^k(x,y,z,t) = \sum_{n=0}^{\infty} \mathfrak{Re}\left(\hat{\eta}_{c,n}^k(x,y,z)e^{ni\omega t}\right), \\ \chi_c^k(x,y,z,t) &= \sum_{n=0}^{\infty} \chi_{c,n}^k(x,y,z,t) = \sum_{n=0}^{\infty} \mathfrak{Re}\left(\hat{\chi}_{c,n}^k(x,y,z)e^{ni\omega t}\right), \\ E^k(x,y,z,t) &= \sum_{n=0}^{\infty} E_n^k(x,y,z,t) = \sum_{n=0}^{\infty} \mathfrak{Re}\left(\hat{E}_n^k(x,y,z)e^{ni\omega t}\right). \end{aligned}$$

Using the orthogonality of the sine and cosine, we define the suspended sediment equation of order k and frequency component n as

$$ni\omega C_n^k = w_s C_{n,z}^k + \left(K_v C_{n,z}^k\right)_z - \hat{\eta}_{c,n}^k.$$

The boundary conditions read

$$\begin{aligned} w_s C_n^k + K_v C_{n,z}^k &= -\hat{\chi}_{c,n}^k, && \text{at} \quad z = R, \\ -K_v C_{n,z}^k &= \hat{E}_n^k, && \text{at} \quad z = -H. \end{aligned}$$

The subscript n denotes the n-th Fourier coefficient of the forcing:

$$\hat{\eta}_{c,n}^k = \begin{cases} \hat{\eta}_{c,1}^1 & \text{if } k = 1 \text{ and } n = 1, \\ 0 & \text{otherwise,} \end{cases} \qquad \hat{\chi}_{c,n}^k = \begin{cases} \hat{\chi}_{c,1}^1 & \text{if } k = 1 \text{ and } n = 1, \\ 0 & \text{otherwise,} \end{cases} \qquad \hat{E}_n^k = \begin{cases} \hat{E}_0^0 & \text{if } k = 0 \text{ and } n = 0, \\ \hat{E}_2^0 & \text{if } k = 0 \text{ and } n = 2, \\ \hat{E}_1^1 & \text{if } k = 1 \text{ and } n = 1, \\ 0 & \text{otherwise.} \end{cases}$$

Forcing decomposition

Define the set of all suspended sediment concentration forcing mechanisms as

$$\mathscr{F}_c = \mathscr{F}_E \cup \{\eta_c,\ \chi_c\},$$

where we have defined the set containing all erosion forcing mechanisms as

$$\mathscr{F}_E = \{EA,\ Eq,\ E\varsigma,\ E\xi,\ E\eta,\ E\gamma,\ E\chi,\ E\mu\}.$$

The general suspended sediment equation of order $k \in \{0,1\}$, frequency $n \in \{0,1,2\}$ and forcing mechanism $f \in \mathscr{F}_c$ is given by

$$ni\omega C_n^{k,f} = w_s C_{n,z}^{k,f} + \left(K_v C_{n,z}^{k,f}\right)_z - \hat{\eta}_{c,n}^{k,f}.$$

The boundary conditions imposed at the free surface and bed read

$$\begin{aligned} w_s C_n^{k,f} + K_v C_{n,z}^{k,f} &= -\hat{\chi}_{c,n}^{k,f}, && \text{at} \quad z = R, \\ -K_v C_{n,z}^{k,f} &= \hat{E}_n^{k,f}, && \text{at} \quad z = -H. \end{aligned}$$

The forcing mechanisms are defined as

$$\hat{\eta}_{c,n}^{k,f} = \begin{cases} \hat{\eta}_{c,1}^1 & \text{if } k=1,\ n=1 \text{ and } f=\eta_c, \\ 0 & \text{otherwise,} \end{cases} \qquad \hat{\chi}_{c,n}^{k,f} = \begin{cases} \hat{\chi}_{c,1}^1 & \text{if } k=1,\ n=1 \text{ and } f=\chi_c, \\ 0 & \text{otherwise,} \end{cases} \tag{3.3.11}$$

$$\hat{E}_n^{k,f} = \begin{cases} \hat{E}_0^0 & \text{if } k=0,\ n=0, \text{ and } f=EA, \\ \hat{E}_2^0 & \text{if } k=0,\ n=2, \text{ and } f=EA, \\ \hat{E}_1^1 & \text{if } k=1,\ n=1, \text{ and } f\in\mathscr{F}_E, \\ 0 & \text{otherwise.} \end{cases}$$

Availability decomposition

To construct a single equation for the erodability $\Phi(a)$ (i.e., equation (3.3.9)), we have used the availability decomposition of the suspended sediment concentration, which yielded the sediment capacity.

The general sediment capacity equation of order $k \in \{0,1\}$, frequency $n \in \{0,1,2\}$, forcing mechanism $f \in \mathscr{F}_c$ and availability $\alpha \in \{a,\ a_x,\ a_y\}$ is given by

$$ni\omega \hat{C}_n^{k,f,\alpha} = w_s \hat{C}_{n,z}^{k,f,\alpha} + \left(K_v \hat{C}_{n,z}^{k,f,\alpha}\right)_z - \hat{\eta}_{c,n}^{k,f,\alpha}.$$

The boundary conditions imposed at the free surface and bed read

$$\begin{aligned} w_s \hat{C}_n^{k,f,\alpha} + K_v \hat{C}_{n,z}^{k,f,\alpha} &= -\hat{\chi}_{c,n}^{k,f,\alpha}, && \text{at} \quad z = R, \\ -K_v \hat{C}_{n,z}^{k,f,\alpha} &= \hat{E}_n^{k,f,\alpha}, && \text{at} \quad z = -H. \end{aligned}$$

The forcing mechanisms are defined as

$$\hat{\eta}_{c,n}^{k,f,\alpha} = \begin{cases} \hat{\eta}_{c,1}^{1\alpha} & \text{if } k=1,\ n=1,\ f=\eta_c \text{ and } \alpha\in\{a,a_x,a_y\}, \\ 0 & \text{otherwise,} \end{cases} \qquad \hat{\chi}_{c,n}^{k,f,\alpha} = \begin{cases} \hat{\chi}_{c,1}^{1a} & \text{if } k=1,\ n=1,\ f=\chi_c \text{ and } \alpha=a, \\ 0 & \text{otherwise,} \end{cases}$$

$$\tag{3.3.12}$$

$$\hat{E}_n^{k,f,\alpha} = \begin{cases} \hat{E}_0^{0a} & \text{if } k=0,\ n=0,\ f=EA \text{ and } \alpha=a, \\ \hat{E}_2^{0a} & \text{if } k=0,\ n=2,\ f=EA \text{ and } \alpha=a, \\ \hat{E}_1^{1a} & \text{if } k=1,\ n=1,\ f\in\mathscr{F}_E \text{ and } \alpha=a, \\ 0 & \text{otherwise.} \end{cases}$$

We have abstracted the notation for the leading- and first-order suspended sediment equation in order to identity their similarities. In the next sections, we will solve the abstract equation for each forcing mechanism and directly obtain the solution for all orders k, frequency components n and availabilities α.

3.3.10 Explicit formulas of the Fourier coefficients of the forcing

No-flux forcing

For the no-flux forcing, we obtain the Fourier coefficients:

$$\hat{\chi}^{1}_{c,1} = i\omega \left(Z^{0A}_1\right)^* C^{0EA}_2, \qquad \text{at} \quad z = R,$$

and for the availability

$$\hat{\chi}^{1a}_{c,1} = i\omega \left(Z^{0A}_1\right)^* \hat{C}^{0EAa}_2, \qquad \text{at} \quad z = R.$$

Advection of sediment forcing

Using equation (3.3.6), the Fourier coefficients of the advection of sediment forcing are given by

$$\hat{\eta}^{1}_{c,1} = \left(\hat{\eta}^{1a}_{c,1} + \hat{\boldsymbol{\eta}}^{1\nabla a}_{c,1} \cdot \nabla\right) \Phi(a).$$

These contributions can be further decomposed into

$$\begin{aligned} \hat{\eta}^{1a}_{c,1} &= \mathscr{P}_1\left(\boldsymbol{u}^0 \cdot \nabla \hat{c}^{0a} + w^0 \hat{c}^{0a}_z\right), \\ \hat{\boldsymbol{\eta}}^{1\nabla a}_{c,1} &= \mathscr{P}_1\left(\boldsymbol{u}^0 \hat{c}^{0a}\right). \end{aligned}$$

Here, we have defined the Fourier coefficient projection operator $\mathscr{P}_n(\cdot)$ that projects the argument on the n Fourier basis function. Hence, using linearity and the harmonic components, we find

$$\begin{aligned} \hat{\eta}^{1a}_{c,1} &= \sum_{n\in\{0,2\}} \mathscr{P}_1\left(\boldsymbol{u}^0_1 \cdot \nabla \hat{c}^{0a}_n\right) + \mathscr{P}_1\left(w^0_1 \hat{c}^{0a}_{n,z}\right), \\ \hat{\boldsymbol{\eta}}^{1\nabla a}_{c,1} &= \sum_{n\in\{0,2\}} \mathscr{P}_1\left(\boldsymbol{u}^0_1 \hat{c}^{0a}_n\right), \end{aligned}$$

where, we have defined the contributions

$$\begin{aligned} \mathscr{P}_1\left(\boldsymbol{u}^0_1 \cdot \nabla \hat{c}^{0a}_n\right) &= \frac{1}{2}\Xi_n \left(\boldsymbol{U}^0_1\right)^{n*} \cdot \nabla \hat{C}^{0EAa}_n, \\ \mathscr{P}_1\left(w^0_1 \hat{c}^{0a}_{n,z}\right) &= \frac{1}{2}\Xi_n \left(W^0_1\right)^{n*} \hat{C}^{0EAa}_{n,z}, \\ \mathscr{P}_1\left(\boldsymbol{u}^0_1 \hat{c}^{0a}_n\right) &= \frac{1}{2}\Xi_n \left(\boldsymbol{U}^0_1\right)^{n*} \hat{C}^{0EAa}_n. \end{aligned}$$

Here, we have defined the conjugate operator and the factor:

$$n* = \begin{cases} \text{id} & \text{if } n = 0, \\ * & \text{if } n = 2, \end{cases}, \qquad \Xi_n = \begin{cases} 2 & \text{if } n = 0, \\ 1 & \text{otherwise,} \end{cases}$$

and we assumed that the subtidal frequency component of the suspended sediment is defined as strictly real:

$$\hat{C}^{0a}_0 = \mathfrak{Re}\left(\hat{C}^{0a}_0\right).$$

Component wise, we have the contributions

$$\begin{aligned} \mathscr{P}_1\left(\boldsymbol{u}^0_1 \cdot \nabla \hat{c}^{0a}_0\right) &= \boldsymbol{U}^0_1 \cdot \nabla \hat{C}^{0EAa}_0, & \mathscr{P}_1\left(w^0_1 \hat{c}^{0a}_{0,z}\right) &= W^0_1 \hat{C}^{0EAa}_{0,z}, \\ \mathscr{P}_1\left(\boldsymbol{u}^0_1 \cdot \nabla \hat{c}^{0a}_2\right) &= \frac{1}{2}\left(\boldsymbol{U}^0_1\right)^* \cdot \nabla \hat{C}^{0EAa}_2, & \mathscr{P}_1\left(w^0_1 \hat{c}^{0a}_{2,z}\right) &= \frac{1}{2}\left(W^0_1\right)^* \hat{C}^{0EAa}_{2,z}, \end{aligned}$$

and

$$\begin{aligned} \mathscr{P}_1\left(\boldsymbol{u}^0_1 \hat{c}^{0a}_0\right) &= \boldsymbol{U}^0_1 \hat{C}^{0EAa}_0, \\ \mathscr{P}_1\left(\boldsymbol{u}^0_1 \hat{c}^{0a}_2\right) &= \frac{1}{2}\left(\boldsymbol{U}^0_1\right)^* \hat{C}^{0EAa}_2. \end{aligned}$$

Erosion forcing

Lastly, the Fourier coefficients of the erosion forcing are considered. Combining the leading-order erosion flux (3.3.5) with the results from Appendix B.8.1, we obtain for the leading-order erosion flux coefficients that

$$\begin{aligned} \hat{E}_0^{0EAa} &= \rho_0 s_f M A_0^{EA}, && \text{at} \quad z=-H, \\ \hat{E}_2^{0EAa} &= \rho_0 s_f M A_2^{EA}, && \text{at} \quad z=-H. \end{aligned}$$

Thus, the leading-order erosion forcing is only forced by the erosion tide forcing EA.

Combining the first-order erosion flux (3.3.7) together with Appendix B.9.1, we obtain for the first-order erosion Fourier coefficients that

$$\hat{E}_1^{1,f,a} = \rho_0 s_f M B_1^f, \qquad \text{at} \quad z=-H,$$

for erosion forcing mechanism f in $\mathscr{F}_E$.

3.3.11 Contribution due to erosion forcing

In this section, we assume that forcing mechanism f is one of the erosion forcing mechanisms, i.e., $f \in \mathscr{F}_E$. Then we have $\alpha = a$ and we obtain the equation:

$$ni\omega \hat{C}_n^{k,f,a} = w_s \hat{C}_{n,z}^{k,f,a} + \left(K_v \hat{C}_{n,z}^{k,f,a}\right)_z, \tag{3.3.13}$$

with boundary conditions

$$\begin{aligned} w_s \hat{C}_n^{k,f,a} + K_v \hat{C}_{n,z}^{k,f,a} &= 0, && \text{at} \quad z=R, \\ -K_v \hat{C}_{n,z}^{k,f,a} &= \hat{E}_n^{k,f,a}, && \text{at} \quad z=-H. \end{aligned}$$

This is a second-order ordinary differential equation in the vertical coordinate z with constant coefficients that is forced at the bed $z=-H$. The solution is found as

$$\hat{C}_n^{k,f,a} = \hat{E}_n^{k,f,a} K_n \exp\bigl(-\sigma(z+H)\bigr)\left[-\sigma \sinh\bigl(\lambda_n(z-R)\bigr) + \lambda_n \cosh\bigl(\lambda_n(z-R)\bigr)\right],$$

where we have defined

$$\begin{aligned} \sigma &= \frac{w_s}{2K_v}, \\ \lambda_n &= \frac{1}{2K_v}\sqrt{w_s^2 + 4ni\omega K_v}, \end{aligned}$$

and

$$K_n = \frac{1}{K_v\left(\lambda_n^2+\sigma^2\right)\sinh\bigl(\lambda_n D\bigr) + w_s\lambda_n\cosh\bigl(\lambda_n D\bigr)}.$$

Here, $D = H + R$ is the local depth. Averaging over the depth yields the depth-averaged sediment capacity:

$$[\hat{C}]_n^{k,f,a} = \hat{E}_n^{k,f,a} K_n \frac{\sinh\bigl(\lambda_n D\bigr)}{D}.$$

Taking the vertical derivative of the z-depended solution yields

$$\hat{C}_{n,z}^{k,f,a} = \hat{E}_n^{k,f,a} K_n \exp\bigl(-\sigma(z+H)\bigr)\left[\left(\lambda_n^2+\sigma^2\right)\sinh\bigl(\lambda_n(z-R)\bigr) - 2\sigma\lambda_n \cosh\bigl(\lambda_n(z-R)\bigr)\right].$$

For $n=0$, the z-dependent solution reduces to

$$\hat{C}_0^{k,f,a} = \hat{E}_0^{k,f,a} \frac{1}{w_s} \exp\left(-2\sigma(z+H)\right),$$

and the depth-average to

$$[\hat{C}]_0^{k,f,a} = \hat{E}_0^{k,f,a} \frac{1}{2w_s\sigma D}\left(1-\exp\left(-2\sigma D\right)\right).$$

For spatially uniform K_v and w_s, it follows that λ_n is also spatially uniform, i.e., their gradients vanish. We obtain the expression:

$$\begin{aligned}\nabla\hat{C}_n^{k,f,a} =& \nabla\left[\hat{E}_n^{k,f,a}K_n\right]\exp\bigl(-\sigma(z+H)\bigr)\left[-\sigma\sinh\bigl(\lambda_n(z-R)\bigr)+\lambda_n\cosh\bigl(\lambda_n(z-R)\bigr)\right]\\ &+\hat{E}_n^{k,f,a}K_n\exp\bigl(-\sigma(z+H)\bigr)\Bigl\{\left(-\lambda_n^2\nabla R+\sigma^2\nabla H\right)\sinh\bigl(\lambda_n(z-R)\bigr)\\ &\qquad+\sigma\lambda_n\left(\nabla R-\nabla H\right)\cosh\bigl(\lambda_n(z-R)\bigr)\Bigr\}.\end{aligned}$$

3.3.12 Contribution due to no-flux forcing

In this section, we assume that forcing mechanism f is the no-flux forcing: $f=\chi_c$. Then we have $\alpha=a$ and the equations become

$$ni\omega\hat{C}_n^{k,\chi_c,a}=w_s\hat{C}_{n,z}^{k,\chi_c,a}+\left(K_v\hat{C}_{n,z}^{k,\chi_c,a}\right)_z,$$

with boundary condition at the free surface is given by

$$w_s\hat{C}_n^{k,\chi_c,a}+K_v\hat{C}_{n,z}^{k,\chi_c,a}=-\hat{\chi}_{c,n}^{k,a},\qquad\text{at}\quad z=R,$$

and the near-bed boundary condition reads

$$K_v\hat{C}_{n,z}^{k,\chi_c,a}=0,\qquad\text{at}\quad z=-H.$$

This is a constant coefficient second-order ordinary differential equation in the vertical coordinate z that is forced at the free surface $z=R$. The solution is given by

$$\hat{C}_n^{k,\chi_c,a}=-\hat{\chi}_{c,n}^{k,a}K_n\exp\bigl(-\sigma(z-R)\bigr)\left[\sigma\sinh\bigl(\lambda_n(z+H)\bigr)+\lambda_n\cosh\bigl(\lambda_n(z+H)\bigr)\right],$$

with the same K_n and λ_n as in the erosion contribution section. The depth-averaged sediment capacity reads

$$[\hat{C}]_n^{k,\chi_c,a}=-\hat{\chi}_{c,n}^{k,a}\frac{1}{ni\omega D}\left(1-w_s\lambda_nK_n\exp\left(\sigma D\right)\right).$$

3.3.13 Contribution due to advection of sediment forcing

In this section, we assume that the forcing mechanism is due to advection of sediment $f=\eta_c$. Using equation (3.3.11), we identify that the advection of sediment forcing occurs only for $k=1$ and $n=1$. The equations read

$$i\omega\hat{C}_1^{1,\eta_c,\alpha}=w_s\hat{C}_{1,z}^{1,\eta_c,\alpha}+\left(K_v\hat{C}_{1,z}^{1,\eta_c,\alpha}\right)_z-\hat{\eta}_{c,1}^{1,\alpha},$$

with the boundary conditions given by

$$\begin{aligned}w_s\hat{C}_1^{1,\eta_c,\alpha}+K_v\hat{C}_{1,z}^{1,\eta_c,\alpha}&=0,&&\text{at}\quad z=R,\\ K_v\hat{C}_{1,z}^{1,\eta_c,\alpha}&=0,&&\text{at}\quad z=-H.\end{aligned}$$

This is a second-order ordinary differential equation in z with constant coefficients, except for the advection of sediment forcing that depends on the vertical coordinate z, with homogenous boundary conditions. We use the method of variation of parameters to solve this equation.

We first write the differential equation in standard form:

$$\hat{C}_{1,zz}^{1,\eta_c,\alpha}+\frac{w_s}{K_v}\hat{C}_{1,z}^{1,\eta_c,\alpha}-\frac{i\omega}{K_v}\hat{C}_1^{1,\eta_c,\alpha}=\frac{1}{K_v}\hat{\eta}_{c,1}^{1,\alpha}.$$

Using the two homogeneous solutions $\hat{C}_1^{1,1}(z)$ and $\hat{C}_1^{1,2}(z)$, the Wronskian $W(z)$ can be computed. A particular solution to the forced equation is then found as

$$\hat{C}_1^{1,p,\alpha}(z)=A^{\alpha}(z)\hat{C}_1^{1,1}(z)+B^{\alpha}(z)\hat{C}_1^{1,2}(z),$$

where we have defined

$$A^{\alpha}(z) = \frac{1}{K_v}\int_z^R \frac{1}{W(\tilde{z})}\hat{C}_1^{1,2}(\tilde{z})\,\hat{\eta}_{c,1}^{1,\alpha}(\tilde{z})\,d\tilde{z},$$
$$B^{\alpha}(z) = -\frac{1}{K_v}\int_z^R \frac{1}{W(\tilde{z})}\hat{C}_1^{1,1}(\tilde{z})\,\hat{\eta}_{c,1}^{1,\alpha}(\tilde{z})\,d\tilde{z}.$$

Using variation of parameters you are free to choose one of the limits of integration. We have chosen to start from the top to eliminate the term $w_s\hat{C}_1^{1,p,\alpha}$ from the no-flux boundary condition imposed at the free surface.

The total advection of sediment solution for a given α consists of the homogenous and particular solution:

$$\hat{C}_1^{1,\eta_c,\alpha}(z) = \hat{C}_1^{1,h,\alpha}(z) + \hat{C}_1^{1,p,\alpha}(z).$$

Assuming we have constructed the particular solution according to the procedure above, the homogenous boundary conditions imposed on the total solution become inhomogeneous boundary conditions for the homogenous solution as

$$w_s\hat{C}_1^{1,h,\alpha} + K_v\hat{C}_{1,z}^{1,h,\alpha} = -h_s^{\alpha}, \qquad \text{at} \quad z = R,$$
$$K_v\hat{C}_{1,z}^{1,h,\alpha} = -h_b^{\alpha}, \qquad \text{at} \quad z = -H.$$

where, we have defined the forcing mechanisms at the surface and bed as

$$h_s^{\alpha} = K_v\hat{C}_{1,z}^{1,p,\alpha}\big|_{z=R},$$
$$h_b^{\alpha} = K_v\hat{C}_{1,z}^{1,p,\alpha}\big|_{z=-H}.$$

We note that by construction of variation of parameters (or by direct computation), we have that

$$A_z^{\alpha}(z)\hat{C}_1^{1,1}(z) + B_z^{\alpha}(z)\hat{C}_1^{1,2}(z) = 0,$$

such that the z derivative of the particular solution is given by

$$\hat{C}_{1,z}^{1,p,\alpha}(z) = A^{\alpha}(z)\hat{C}_{1,z}^{1,1}(z) + B^{\alpha}(z)\hat{C}_{1,z}^{1,2}(z),$$

Evaluating this expression at the free surface reveals that the forcing at the free surface vanishes:

$$h_s^{\alpha} = K_v\hat{C}_{1,z}^{1,p,\alpha}(z)\big|_{z=R} = 0,$$

since $A^{\alpha}(R) = B^{\alpha}(R) = 0$ and assuming the homogenous solution remains bounded. Thus the particular solution automatically satisfies the boundary condition imposed at the free surface.

Near the bed, we have the expression:

$$h_b^{\alpha} = K_v\hat{C}_{1,z}^{1,p,\alpha}(-H) = A^{\alpha}(-H)\hat{C}_{1,z}^{1,1}(-H) + B^{\alpha}(-H)\hat{C}_{1,z}^{1,2}(-H).$$

We may use the previously found solution forced at bed to satisfy the remaining inhomogeneous boundary condition:

$$\hat{C}_1^{1,h,\alpha}(z) = \hat{C}_1^{1,EAa}\big|_{\hat{E}_{c,1}^{1a} = h_b^{\alpha}}.$$

The total solution is given by

$$\hat{C}_1^{1,\eta_c,\alpha}(z) = \hat{C}_1^{1,h,\alpha}(z) + \hat{C}_1^{1,p,\alpha}(z).$$

Computing the Wronskian

We choose a specific basis for the homogeneous solution used to compute the particular solution. For example, we can choose the basis

$$\hat{C}_1^{1,1}(z) = \exp\left(-\sigma(z+H)\right)\sinh\big(\lambda_n(z-R)\big),$$
$$\hat{C}_1^{1,2}(z) = \exp\left(-\sigma(z+H)\right)\cosh\big(\lambda_n(z-R)\big).$$

The Wronskian is given by

$$W = -\lambda_n \exp\left(-2\sigma(z+H)\right).$$

Under this basis, we have

$$\begin{aligned}
A^{\alpha}(z) &= -\frac{1}{K_v\lambda_n}\int_z^R \exp\left(\sigma(\tilde{z}+H)\right)\cosh\bigl(\lambda_n(\tilde{z}-R)\bigr)\,\hat{\eta}_{c,1}^{1,\alpha}(\tilde{z})\,d\tilde{z},\\
B^{\alpha}(z) &= \frac{1}{K_v\lambda_n}\int_z^R \exp\left(\sigma(\tilde{z}+H)\right)\sinh\bigl(\lambda_n(\tilde{z}-R)\bigr)\,\hat{\eta}_{c,1}^{1,\alpha}(\tilde{z})\,d\tilde{z}.
\end{aligned}$$

The particular solution becomes

$$\begin{aligned}
\hat{C}_1^{1,p,\alpha}(z) =& A^{\alpha}(z)\hat{C}_1^{1,1}(z) + B^{\alpha}(z)\hat{C}_1^{1,2}(z),\\
=& \frac{1}{K_v\lambda_n}\exp\left(-\sigma(z+H)\right)\\
&\times\biggl(-\sinh\bigl(\lambda_n(z-R)\bigr)\int_z^R \exp\left(\sigma(\tilde{z}+H)\right)\cosh\bigl(\lambda_n(\tilde{z}-R)\bigr)\,\hat{\eta}_{c,1}^{1,\alpha}(\tilde{z})\,d\tilde{z}\\
&\quad+\cosh\bigl(\lambda_n(z-R)\bigr)\int_z^R \exp\left(\sigma(\tilde{z}+H)\right)\sinh\bigl(\lambda_n(\tilde{z}-R)\bigr)\,\hat{\eta}_{c,1}^{1,\alpha}(\tilde{z})\,d\tilde{z}\biggr).
\end{aligned}$$

3.3.14 Contribution due to advection of sediment forcing, integration from the bed

In this section, we assume that the forcing mechanism is due to advection of sediment $f = \eta_c$. Using equation (3.3.11), we identify that the advection of sediment forcing occurs only for $k = 1$ and $n = 1$. The equations read

$$i\omega\hat{C}_1^{1,\eta_c,\alpha} = w_s\hat{C}_{1,z}^{1,\eta_c,\alpha} + \left(K_v\hat{C}_{1,z}^{1,\eta_c,\alpha}\right)_z - \hat{\eta}_{c,1}^{1,\alpha},$$

with the boundary conditions given by

$$\begin{aligned}
w_s\hat{C}_1^{1,\eta_c,\alpha} + K_v\hat{C}_{1,z}^{1,\eta_c,\alpha} &= 0, &&\text{at}\quad z = R,\\
K_v\hat{C}_{1,z}^{1,\eta_c,\alpha} &= 0, &&\text{at}\quad z = -H.
\end{aligned}$$

This is a second-order ordinary differential equation in z with constant coefficients, except for the advection of sediment forcing that depends on the vertical coordinate z, with homogenous boundary conditions. We use the method of variation of parameters to solve this equation.

We first write the differential equation in standard form:

$$\hat{C}_{1,zz}^{1,\eta_c,\alpha} + \frac{w_s}{K_v}\hat{C}_{1,z}^{1,\eta_c,\alpha} - \frac{i\omega}{K_v}\hat{C}_1^{1,\eta_c,\alpha} = \frac{1}{K_v}\hat{\eta}_{c,1}^{1,\alpha}.$$

Using the two homogeneous solutions $\hat{C}_1^{1,1}(z)$ and $\hat{C}_1^{1,2}(z)$ satisfying the homogeneous equation, the Wronskian $W(z)$ can be computed. A particular solution to the forced equation is then found as

$$\hat{C}_1^{1,p,\alpha}(z) = A^{\alpha}(z)\hat{C}_1^{1,1}(z) + B^{\alpha}(z)\hat{C}_1^{1,2}(z),$$

where we have defined

$$\begin{aligned}
A^{\alpha}(z) &= -\frac{1}{K_v}\int_{-H}^{z}\frac{1}{W(\tilde{z})}\hat{C}_1^{1,2}(\tilde{z})\,\hat{\eta}_{c,1}^{1,\alpha}(\tilde{z})\,d\tilde{z},\\
B^{\alpha}(z) &= \frac{1}{K_v}\int_{-H}^{z}\frac{1}{W(\tilde{z})}\hat{C}_1^{1,1}(\tilde{z})\,\hat{\eta}_{c,1}^{1,\alpha}(\tilde{z})\,d\tilde{z}.
\end{aligned}$$

Using variation of parameters you are free to choose one of the limits of integration. We have chosen to start from the bed for simplicity.

The total advection of sediment solution for a given α consists of the homogenous and particular solution:

$$\hat{C}_1^{1,\eta_c,\alpha}(z) = \hat{C}_1^{1,h,\alpha}(z) + \hat{C}_1^{1,p,\alpha}(z).$$

Assuming we have constructed the particular solution according to the procedure above, the homogenous boundary conditions imposed on the total solution become inhomogeneous boundary conditions for the homogenous solution as

$$\begin{aligned} w_s \hat{C}_1^{1,h,\alpha} + K_v \hat{C}_{1,z}^{1,h,\alpha} &= -h_s^\alpha, && \text{at} \quad z = R, \\ K_v \hat{C}_{1,z}^{1,h,\alpha} &= -h_b^\alpha, && \text{at} \quad z = -H. \end{aligned}$$

where, we have defined the forcing mechanisms at the surface and bed as

$$\begin{aligned} h_s^\alpha &= \left[w_s \hat{C}_1^{1,p,\alpha} + K_v \hat{C}_{1,z}^{1,p,\alpha} \right]_{z=R}, \\ h_b^\alpha &= K_v \hat{C}_{1,z}^{1,p,\alpha} \big|_{z=-H}. \end{aligned}$$

We note that by construction of variation of parameters (or by direct computation), we have that

$$A_z^\alpha(z) \hat{C}_1^{1,1}(z) + B_z^\alpha(z) \hat{C}_1^{1,2}(z) = 0,$$

such that the z derivative of the particular solution is given by

$$\hat{C}_{1,z}^{1,p,\alpha}(z) = A^\alpha(z) \hat{C}_{1,z}^{1,1}(z) + B^\alpha(z) \hat{C}_{1,z}^{1,2}(z).$$

Evaluating this expression at the bed reveals that the forcing at the bed vanishes:

$$h_b^\alpha = K_v \hat{C}_{1,z}^{1,p,\alpha} \big|_{z=-H} = 0,$$

since $A^\alpha(-H) = B^\alpha(-H) = 0$ and assuming the homogenous solution remains bounded. Thus the particular solution does not force the homogenous solution at the bed.

Near the free surface, we have the expression:

$$\begin{aligned} h_s^\alpha = \left[w_s \hat{C}_1^{1,p,\alpha} + K_v \hat{C}_{1,z}^{1,p,\alpha} \right]_{z=R} &= w_s \left(A^\alpha(R) \hat{C}_1^{1,1}(R) + B^\alpha(R) \hat{C}_1^{1,2}(R) \right) + K_v \left(A^\alpha(R) \hat{C}_{1,z}^{1,1}(R) + B^\alpha(R) \hat{C}_{1,z}^{1,2}(R) \right), \\ &= A^\alpha(R) \left(w_s \hat{C}_1^{1,1}(R) + K_v \hat{C}_{1,z}^{1,1}(R) \right) + B^\alpha(R) \left(w_s \hat{C}_1^{1,2}(R) + K_v \hat{C}_{1,z}^{1,2}(R) \right). \end{aligned}$$

We may use a previously found solution forced which is forced at the free surface, but not at the bed or inside the water column. We can use the no-flux solution as it satisfies these requirements. Hence the homogenous solution satisfying the theses conditions is given by

$$\hat{C}_1^{1,h,\alpha}(z) = \hat{C}_1^{1\chi_c a} \big|_{\hat{\chi}_{c,1}^{1a} = h_s^\alpha}.$$

The total solution is given by

$$\hat{C}_1^{1,\eta_c,\alpha}(z) = \hat{C}_1^{1,h,\alpha}(z) + \hat{C}_1^{1,p,\alpha}(z).$$

Computing the Wronskian

We choose a specific basis for the homogeneous solution used to compute the particular solution. For example, we can choose the basis

$$\begin{aligned} \hat{C}_1^{1,1}(z) &= \exp\big(-\sigma(z+H)\big) \sinh\big(\lambda_n(z-R)\big), \\ \hat{C}_1^{1,2}(z) &= \exp\big(-\sigma(z+H)\big) \cosh\big(\lambda_n(z-R)\big). \end{aligned}$$

The vertical derivates are given by

$$\begin{aligned} \hat{C}_{1,z}^{1,1}(z) &= \exp\big(-\sigma(z+H)\big) \big(-\sigma \sinh\big(\lambda_n(z-R)\big) + \lambda_n \cosh\big(\lambda_n(z-R)\big)\big), \\ \hat{C}_{1,z}^{1,2}(z) &= \exp\big(-\sigma(z+H)\big) \big(\lambda_n \sinh\big(\lambda_n(z-R)\big) - \sigma \cosh\big(\lambda_n(z-R)\big)\big). \end{aligned}$$

The Wronskian is given by

$$W = -\lambda_n \exp\big(-2\sigma(z+H)\big).$$

Under this basis, we have

$$A^{\alpha}(z) = \frac{1}{K_v\lambda_n}\int_{-H}^{z} \exp\bigl(\sigma(\tilde{z}+H)\bigr)\cosh\bigl(\lambda_n(\tilde{z}-R)\bigr)\,\hat{\eta}_{c,1}^{1,\alpha}(\tilde{z})\,d\tilde{z},$$
$$B^{\alpha}(z) = -\frac{1}{K_v\lambda_n}\int_{-H}^{z} \exp\bigl(\sigma(\tilde{z}+H)\bigr)\sinh\bigl(\lambda_n(\tilde{z}-R)\bigr)\,\hat{\eta}_{c,1}^{1,\alpha}(\tilde{z})\,d\tilde{z}.$$

The forcing at the surface simplifies to

$$h_s^{\alpha} = \exp\bigl(-\sigma D\bigr)\left(A^{\alpha}(R)K_v\lambda_n + B^{\alpha}(R)\,(w_s-\sigma K_v)\right).$$

Chapter 4

Numerical implementation

In this section, the numerical implementation of the sediment dynamics and the erodability function is discussed.

4.1 Summary of erodability equation

The erodability equation (3.3.9) is given by

$$\nabla \cdot \left[\mathbf{D}^{\nabla a} \nabla \Phi + \boldsymbol{T}^{a} \Phi \right] = 0. \tag{4.1.1}$$

The imposed boundary conditions at the sea, banks and river read

$$\begin{aligned} \Phi &= \Phi_{\text{sea}}(x, y), && \text{at} \quad \partial\Omega_{\text{sea}}, \\ \left[\mathbf{D}^{\nabla a} \nabla \Phi + \boldsymbol{T}^{a} \Phi \right] \cdot \boldsymbol{n} &= 0, && \text{at} \quad \partial\Omega_{\text{bank}}, \\ \left[\mathbf{D}^{\nabla a} \nabla \Phi + \boldsymbol{T}^{a} \Phi \right] \cdot \boldsymbol{n} &= -\mathscr{F}_{\text{river}}(x, y), && \text{at} \quad \partial\Omega_{\text{river}}. \end{aligned}$$

Here, we have defined the erodability at sea as

$$\Phi_{\text{sea}}(x, y) = \frac{[\langle c \rangle]_{\text{sea}}}{[\hat{c}]_0^{0a}}, \qquad \text{at} \quad \partial\Omega_{\text{sea}},$$

where we have used equation (3.3.10).

4.2 Weak form

In this section, we derive the weak form that is used by the finite element method.

We use the same function spaces as in Section 2.2. The essential boundary condition for this problem is located at $\partial\Omega_{\text{sea}}$. Thus we seek test functions in the homogeneous space $\Sigma_0(\Omega)$.

Multiply equation (4.1.1) by a test function ψ in $\Sigma_0(\Omega)$ and integrate over the domain, to find

$$\int_{\Omega} \psi \nabla \cdot \left[\mathbf{D}^{\nabla a} \nabla \Phi + \boldsymbol{T}^{a} \Phi \right] d\Omega = 0. \tag{4.2.1}$$

Using integration by parts and decomposing the integral over the boundary into its components yields

$$\begin{aligned}
&\int_{\Omega} -\nabla\psi \cdot \left[\mathbf{D}^{\nabla a}\nabla\Phi + \boldsymbol{T}^{a}\Phi\right] d\Omega \\
&+ \int_{\partial\Omega_{\text{sea}}} \psi \left[\mathbf{D}^{\nabla a}\nabla\Phi + \boldsymbol{T}^{a}\Phi\right] \cdot \boldsymbol{n}\, d\Gamma \\
&+ \int_{\partial\Omega_{\text{bank}}} \psi \left[\mathbf{D}^{\nabla a}\nabla\Phi + \boldsymbol{T}^{a}\Phi\right] \cdot \boldsymbol{n}\, d\Gamma \\
&+ \int_{\partial\Omega_{\text{river}}} \psi \left[\mathbf{D}^{\nabla a}\nabla\Phi + \boldsymbol{T}^{a}\Phi\right] \cdot \boldsymbol{n}\, d\Gamma = 0.
\end{aligned}$$

Using that all test functions ψ in $\Sigma_0(\Omega)$ vanish at $\partial\Omega_{\text{sea}}$, the no-transport boundary condition imposed at $\partial\Omega_{\text{bank}}$ and the riverine boundary condition, shows that

$$\int_{\Omega} -\nabla\psi \cdot \left[\mathbf{D}^{\nabla a}\nabla\Phi + \boldsymbol{T}^{a}\Phi\right] d\Omega - \int_{\partial\Omega_{\text{river}}} \psi\, \mathscr{F}_{\text{river}}\, d\Gamma = 0.$$

Bringing all knowns to the right, gives

$$\int_{\Omega} -\nabla\psi \cdot \left[\mathbf{D}^{\nabla a}\nabla\Phi + \boldsymbol{T}^{a}\Phi\right] d\Omega = \int_{\partial\Omega_{\text{river}}} \psi\, \mathscr{F}_{\text{river}}\, d\Gamma.$$

Define the bilinear and linear forms as

$$\begin{aligned}
a_c(\Phi,\psi) &= \int_{\Omega} -\left[\mathbf{D}^{\nabla a}\nabla\Phi + \boldsymbol{T}^{a}\Phi\right] \cdot \nabla\psi\, d\Omega, \\
b_c(\psi) &= \int_{\partial\Omega_{\text{river}}} \mathscr{F}_{\text{river}}\, \psi\, d\Gamma.
\end{aligned}$$

Then the weak formulation can be posed as follows:

Find $\Phi \in H^1(\Omega)$ with $\Phi = \Phi_{\text{sea}}(x,y)$ at $\partial\Omega_{\text{sea}}$ such that for all test functions $\psi \in \Sigma_0(\Omega)$ it holds that

$$a_c\big(\Phi,\psi\big) = b_c(\psi).$$

4.3 Implementation

In this section, we given an overview of the structure of the numerical model concerning the sediment dynamics.

4.3.1 Sediment classes

In Fig. 4.1, the classes defined to solve the ordered hydrodynamics are shown.

4.3.2 Sediment objects

In Fig. 4.2, the hydrodynamic objects and their relations are shown.

4.3.3 Details of the classes and objects

We provide an overview of the files used and their input and output.

We use the colour `script` to indicate python scripts or pseudo code. We use the colour `object` to denote objects.

`main_sedimentdynamics.py`

- `compute_sedimentcapacity.py`
  - Input:

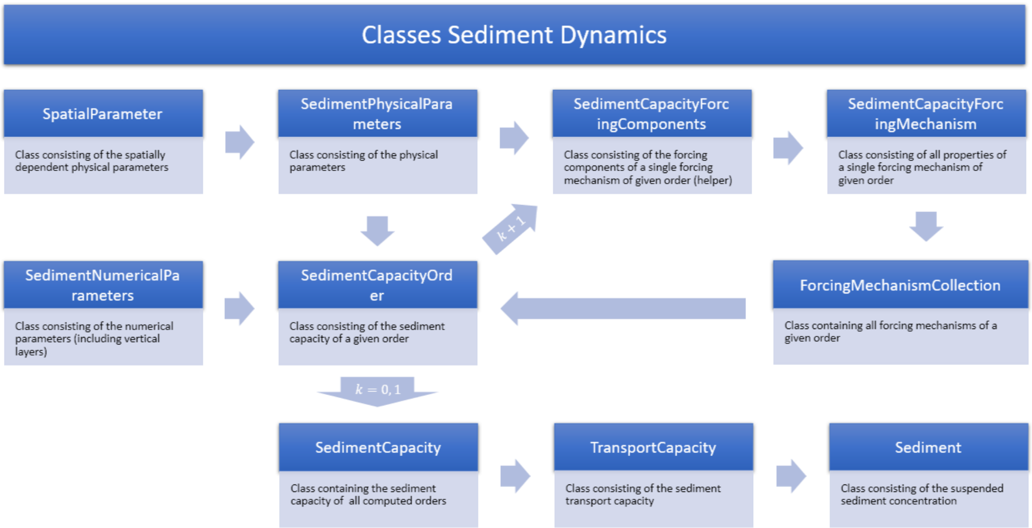

Figure 4.1: Classes defined to solve the sediment dynamics.

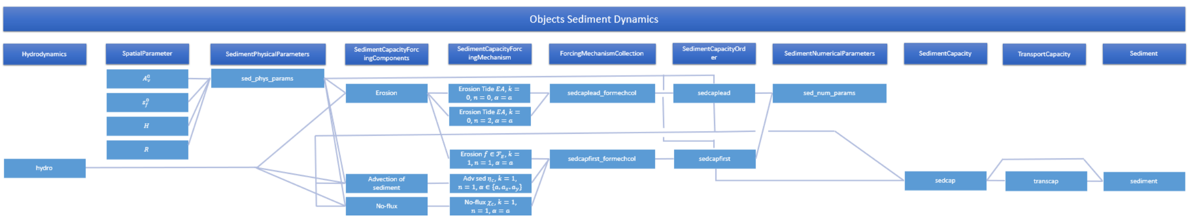

Figure 4.2: Objects defined to solve the sediment dynamics.

        * ?
        * ?
        * ?
    - Output: SedimentCapacity
- compute_transportcapacity.py
    - Input:
        * ?
        * ?
        * ?
    - Output: TransportCapacity
- compute_sediment.py
    - Input:
        * ?
        * ?
        * ?
    - Output: Sediment

4.3.4 Sediment Capacity

The sediment capacity scripts.

compute_sedimentcapacity.py

Computes the suspended sediment concentration without the erodability function $\Phi(a)$.

- Input:
    - ?
- Output: SedimentCapacity

SedimentCapacity

Object to store the suspended sediment capacity terms

- Property: $\hat{C}[k][n][f][\alpha]$

4.3.5 Transport Capacity

The transport capacity scripts.

compute_transportcapacity.py

Computes the diffusivity matrix and transport capacity vector (without the erodability function $\Phi(a)$*).*

- Input:
    - ?
- Output: TransportCapacity

TransportCapacity

Object to store the transport capacity terms

- Property: $D[f]$

- Property: $T[f]$

4.3.6 Sediment

The sediment scripts.

`compute_sediment.py`

Computes the erodability function $\Phi(a)$. *Using this function the true suspended sediment concentrations can be constructed.*

- Input:
  - `?`
- Output: `Sediment`

`Sediment`

Object to store the suspended sediment concentration terms

- Property: $C[k][n][f]$
- Property: $\Phi(a)$

Appendix A

Numerical derivations

A.1 Trapezoidal integration rule

Numerically projecting a solution from one basis to another may introduce additional numerical inaccuracies. Moreover, projecting from a high to a low degree of freedom basis by definition reduces the information stored in the solution and typically leads to larger errors. For example, projecting the solution from a high-order modal basis to a low-order nodal basis can drastically increase the error and is highly undesirable. In order to retain the high-order basis functions, we manually implement the composite trapezoidal method to numerically integrate over the vertical dimension.

The composite trapezoidal method states that

$$\int_{-H}^{R} f(z)\,dz \approx \sum_{k=1}^{N} \frac{1}{2}\left(f_{k-1} + f_k\right)\Delta_k,$$

where we have defined the shorthand notation for function evaluations $f_k = f(z_k)$, backwards difference $\Delta_k = \Delta z_k = z_k - z_{k-1}$ and defined the vectors $z = [z_0,\ z_1,\ \ldots,\ z_N]$, $f = [f_0,\ f_1,\ \ldots,\ f_N]$ and $\Delta = [\Delta_1,\ \Delta_2,\ \ldots,\ \Delta_N]$.

We want to minimize the number of function calls as this is an expensive operation. One method is to pre-compute the function evaluations and lookup these values during the algorithm, i.e., using the vectors defined above. This is not possible in our case, so we modify the algorithm such that the number of function evaluations is kept to a minimum. After some rearranging, we arrive at a form in which the function evaluations play a central role rather then the intervals:

$$\int_{-H}^{R} f(z)\,dz \approx \frac{1}{2}\sum_{k=0}^{N} f_k \Delta_k^c, \tag{A.1.1}$$

where we have defined the central difference as $\Delta_k^c = z_{k+1} - z_{k-1}$ for $0 < k < N$ and at the boundaries we have $\Delta_0^c = \Delta_1 = z_1 - z_0$ and $\Delta_N^c = \Delta_N = z_N - z_{N-1}$. The length the used numeric vectors is given by $|\Delta^c| = |f| = N+1$.

A.2 Iterated integration

Sometimes an iterated integral must be evaluated. If both integrals are evaluated numerically using the trapezoidal rule then this can lead to a significant number of function calls. Since, we are unable to pre-compute the function values, we derive a formula in which the number of function calls is minimized.

For example, define the integral dependent on z as

$$I(z) = \int_{-H}^{z} f(z')\,dz' \approx \frac{1}{2}\sum_{m=0}^{n(z)} f_m \Delta_m^c,$$

and the depth-integral as

$$J = \int_{-H}^{R} I(z)\,dz \approx \frac{1}{2}\sum_{k=0}^{N} I_k \Delta_k^c.$$

Here, we have used the function call minimizing form of the trapezoidal rule, see Eq. (A.1.1). The goal is to find an equation for the iterated integral that minimizes the number of function calls of the equation given by

$$J = \int_{-H}^{R} \int_{-H}^{z} f(z')\, dz'\, dz.$$

We use the same numerical grid for both integrals, hence we may replace $n(z)$ by k. Substitution yields

$$J \approx \frac{1}{4} \sum_{k=0}^{N} \sum_{m=0}^{k} f_m \Delta_m^c \Delta_k^c.$$

From this formula it is clear that the fast variable m repeatedly calls f_m, which is highly undesirable as this is an expensive operation. We introduce the index function $I\{m \le k\}$ and simplify

$$J \approx \frac{1}{4} \sum_{m=0}^{N} f_m \Delta_m^c \sum_{k=0}^{N} I\{m \le k\} \Delta_k^c.$$

We use the index function to conclude that $k \ge m$, thus

$$J \approx \frac{1}{4} \sum_{m=0}^{N} f_m \Delta_m^c \sum_{k=m}^{N} \Delta_k^c.$$

Now the fast variable runs over the cheap Δ_k^c rather than the expensive f_m. The function is now called at most $N+1$ times rather than order $\mathcal{O}(N^2)$, which is a big improvement when the function calls are expensive. We can simplify this further. We define

$$\Delta_m^s = \sum_{k=m}^{N} \Delta_k^c.$$

We recognise that the sum Δ_m^s forms a telescoping series and can therefore be simplified. We have for $0 < m < N$ that $\Delta_m^s = 2z_N - z_{m-1} - z_m$. For $m = 0$, we obtain $\Delta_0^s = 2(z_N - z_0)$ and for $m = N$, we have $\Delta_N^s = z_N - z_{N-1}$. Hence, the iterated integral can be written as a single sum:

$$J \approx \frac{1}{4} \sum_{m=0}^{N} f_m \Delta_m^c \Delta_m^s.$$

Appendix B

Miscellaneous derivations

B.1 Product of Fourier series consisting of a single harmonic

We derive the Fourier coefficients of the product of two Fourier series that both consist of a single harmonic. Assume, we have the following two single component Fourier series for $n > 0$ and $m > 0$:

$$u_n = \mathfrak{Re}\left(U_n e^{ni\omega t}\right), \qquad v_m = \mathfrak{Re}\left(V_m e^{mi\omega t}\right).$$

Their product equals

$$\begin{aligned} u_n v_m &= \mathfrak{Re}\left(U_n e^{ni\omega t}\right)\mathfrak{Re}\left(V_m e^{mi\omega t}\right), \\ &= \mathfrak{Re}\left(U_n e^{ni\omega t}\,\mathfrak{Re}\left(V_m e^{mi\omega t}\right)\right), \\ &= \mathfrak{Re}\left(U_n e^{ni\omega t}\frac{1}{2}\left(V_m e^{mi\omega t} + V_m^* e^{-mi\omega t}\right)\right), \\ &= \mathfrak{Re}\left(\frac{1}{2}U_n V_m e^{(n+m)i\omega t} + \frac{1}{2}U_n V_m^* e^{(n-m)i\omega t}\right), \\ &= \mathfrak{Re}\left(\psi_{n+m} e^{(n+m)i\omega t}\right) + \mathfrak{Re}\left(\psi_{n-m} e^{(n-m)i\omega t}\right). \end{aligned}$$

Thus, their product consists of two terms with different frequency. These frequencies are equal to the sum and difference of the frequency of their factors. The corresponding Fourier coefficient are given by

$$\psi_{n+m} = \frac{1}{2}U_n V_m, \qquad \psi_{n-m} = \frac{1}{2}U_n V_m^*.$$

Taking the tidal average of this product yields

$$\langle u_n v_m \rangle = \begin{cases} 0 & \text{if } m \neq n, \\ \mathfrak{Re}\left(\psi_0\right) = \frac{1}{2}\mathfrak{Re}\left(U_n V_n^*\right) & \text{if } m = n > 0. \end{cases}$$

B.2 Product of Fourier series

The Fourier coefficients are derived for a product of Fourier series. Assume we have the Fourier expansions:

$$u^0 = \sum_{n=0}^{\infty} \mathfrak{Re}\left(U_n^0 e^{ni\omega t}\right), \qquad \text{and} \qquad v^0 = \sum_{n=0}^{\infty} \mathfrak{Re}\left(V_n^0 e^{ni\omega t}\right),$$

and we want to compute the Fourier coefficients ψ_n^0 of their product:

$$\psi^0 = u^0 v^0,$$

defined as

$$\psi^0 = \sum_{n=0}^{\infty} \mathfrak{Re}\Big(\psi_n^0 e^{ni\omega t}\Big).$$

The solution of this problem reads

$$\psi^0 = \sum_{n=0}^{\infty} \mathfrak{Re}\left\{\frac{1}{2}\left[\sum_{k=0}^{n} U_k^0 V_{n-k}^0 + \sum_{k=0}^{\infty} U_{k+n}^0 \overline{V_k^0} + \sum_{k=0}^{\infty} U_k^0 \overline{V_{k+n}^0}\right] e^{ni\omega t}\right\} - \mathfrak{Re}\left\{\frac{1}{2}\sum_{k=0}^{\infty} U_k^0 \overline{V_k^0}\right\},$$

or written out explicitly for the coefficients:

$$\psi_n^0 = \begin{cases} \dfrac{1}{2}\left[U_0^0 V_0^0 + \displaystyle\sum_{k=0}^{\infty} U_k^0 \overline{V_k^0}\right] & \text{if } n = 0, \\ \dfrac{1}{2}\left[\displaystyle\sum_{k=0}^{n} U_k^0 V_{n-k}^0 + \sum_{k=0}^{\infty} U_{k+n}^0 \overline{V_k^0} + \sum_{k=0}^{\infty} U_k^0 \overline{V_{k+n}^0}\right] & \text{else.} \end{cases}$$

Here, the overline represents the complex conjugate.

Proof. We show how to derive the previously stated result.

The given Fourier expansions are substituted into the relation $\psi^0 = u^0 v^0$. Using that for any complex number $\mathfrak{Re}\{z\} = (z + \overline{z})/2$ and changing summation indices to k and m yields

$$\psi^0 = \sum_{k=0}^{\infty}\sum_{m=0}^{\infty} \mathfrak{Re}\left\{\frac{1}{2} U_k^0 V_m^0 e^{(k+m)i\omega t}\right\} + \sum_{k=0}^{\infty}\sum_{m=0}^{\infty} \mathfrak{Re}\left\{\frac{1}{2} U_k^0 \overline{V_m^0} e^{(k-m)i\omega t}\right\}.$$

Define the new summation index $n = k+m$ for the left double sum and $n = k-m$ for the right one. The indicator functions $1_{\{k\leq n\}}$ and $1_{\{k\geq n\}}$ are used to swap the summations. Simplifying the resulting summation bounds yields

$$\psi^0 = \sum_{n=0}^{\infty}\sum_{k=0}^{n} \mathfrak{Re}\left\{\frac{1}{2} U_k^0 V_{n-k}^0 e^{ni\omega t}\right\} + \sum_{n=-\infty}^{\infty}\ \sum_{k=\max(0,n)}^{\infty} \mathfrak{Re}\left\{\frac{1}{2} U_k^0 \overline{V_{k-n}^0} e^{ni\omega t}\right\}.$$

The second double sum contains both positive as 'negative' frequencies. Splitting this sum and introducing a new index results in

$$\left(\sum_{n=0}^{\infty} \mathfrak{Re}\left\{\frac{1}{2}\left[\sum_{k=0}^{\infty} U_{k+n}^0 \overline{V_k^0} + \sum_{k=0}^{\infty} U_k^0 \overline{V_{k+n}^0}\right] e^{ni\omega t}\right\}\right) - \mathfrak{Re}\left\{\frac{1}{2}\sum_{k=0}^{\infty} U_k^0 \overline{V_k^0}\right\}.$$

Combining the previous two displays yields the shown result. □

B.3 Analytical solutions for selected geometries

In this section, the leading-order free surface equation is solved for certain geometries to test the numerical code.

B.3.1 Assumptions

To make solving the leading-order free surface equation (1.6.1) mathematically traceable, certain simplifying assumptions are made:

- *No Coriolis:* $f = 0$. Under this assumption the elements of the $\boldsymbol{\alpha}_n^0$ matrix coincide: $\alpha_{n,11}^0 = \alpha_{n,22}^0$. As a consequence, the elements of the $\boldsymbol{\beta}_n^0$, $\mathbf{c}_n^0(z)$, $\mathbf{C}_n^0(z)$ matrices coincide as well. This allows us to write: $\mathbf{C}_n^0(z) = \mathrm{C}_{n,11}^0(z)\,\mathbf{I}_2$. Using this, we may simply the diffusion matrix to a scalar times the identity matrix:

$$\mathbf{D}_n^0(z) = \mathbf{P}\,\mathbf{C}_n^0(z)\,\mathbf{P}^* = \mathrm{C}_{n,11}^0(z)\,\mathbf{I}_2.$$

- *Spatially constant parameters.* If we further assume that the leading-order parameters do not depend on the spatial coordinates x, y and z, then the leading-order free surface equation simplifies to the Helmholtz equation:

$$\Delta Z_n^0 + \left(\kappa_n^0\right)^2 Z_n^0 = 0,$$

where we have defined the complex wavenumber

$$\kappa_n^0 = \sqrt{\frac{ni\omega}{\mathrm{C}_{n,11}^0(R)}}.$$

B.3.2 Rectangular geometry amplitude forcing

We consider a rectangular geometry and assume no Coriolis force and spatially constant parameter values subject to an amplitude forcing. We consider the following Helmholtz equation:

$$\Delta Z_n^0 + \left(\kappa_n^0\right)^2 Z_n^0 = 0, \tag{B.3.1}$$

with boundary conditions

$$\begin{aligned}
&Z_n^0 = A_n^0(y), && \text{at} \quad x = 0, && \text{(tidal forcing)}\\
&Z_{n,y}^0 = 0, && \text{at} \quad y = \pm B/2, && \text{(no-transport)}\\
&Z_{n,x}^0 = 0, && \text{at} \quad x = L. && \text{(no-transport)}
\end{aligned}$$

This problem can be solved analytically using separation of variables. We obtain the following solution

$$Z_n^0(x,y) = \sum_{k=0}^{\infty} a_k \cos\big(\mu_{n,k}(x-L)\big)\cos\big(\lambda_k(y-B/2)\big),$$

with the eigenvalues

$$\lambda_k = \frac{k\pi}{B}, \qquad \mu_{n,k} = \sqrt{\left(\kappa_n^0\right)^2 - \lambda_k^2}.$$

The coefficients are found using the orthogonality of the cosines:

$$a_k = \frac{2}{B\big(1+\mathrm{sinc}(\mathrm{k}\pi)\big)\cos\big(\mu_{n,k}L\big)} \int_{-B/2}^{B/2} A_n^0(y)\cos\big(\lambda_k(y-B/2)\big)\,dy.$$

Laterally constant amplitude forcing

For a laterally constant amplitude forcing $A_n^0(y) = A_n^0$, we obtain the following coefficients:

$$a_k = \begin{cases} \dfrac{A_n^0}{\cos\left(\kappa_n^0 L\right)}, & \text{if } k = 0,\\ 0, & \text{else.}\end{cases}$$

Henceforth, the solution consists of a single component:

$$Z_n^0(x,y) = \frac{A_n^0}{\cos\left(\kappa_n^0 L\right)}\cos\big(\kappa_n^0(x-L)\big).$$

Evanescent waves

The parameter $\mu_{n,k}$ exhibits some interesting behaviour. Since the eigenvalue λ_k increases linearly with k for k in $\mathbb{N}_0$, there will always be an $\hat{k}$ for which $\lambda_{\hat{k}} > |\kappa_n^0|$. For $k \geq \hat{k}$, we have to a good approximation:

$$\mu_{n,k} = \lambda_k\sqrt{-1+\frac{\left(\kappa_n^0\right)^2}{\lambda_k^2}} \approx -i\lambda_k,$$

if the argument of the square root lays in the lower half plane, else the sign is flipped. That is, the complex wavenumber for the along-channel direction has a vanishingly small real part and has a very large imaginary part for $k \geq \hat{k}$. The real part of the wavenumber is inversely proportional to the wavelength and the imaginary part is related to the decay length scale (for travelling waves). Thus since these waves have nearly zero real part, they have a nearly infinite wavelength and since they have a large imaginary part they decay rather quickly. The larger k, the quicker the decay. Thus the very large wavelength is not observed in practice as the waves are already damped out. These waves with very large imaginary parts are here referred to as evanescent waves.

For relatively 'narrow' estuaries something interesting happens. For these estuaries, the width B is small enough that λ_k can quickly grow larger than $|\kappa_n^0|$, i.e., $\lambda_{\hat{k}} > |\kappa_n^0|$ for relatively small $\hat{k}$. For typical estuarine widths, this inequality is already satisfied at $\hat{k} = 1$. This means that there is only one travelling wave ($k = 0$) and all other waves are evanescent ($k \geq 1$).

B.3.3 Rectangular geometry river discharge forcing

We consider a rectangular geometry and assume no Coriolis force and spatially constant parameter values subject to a river discharge forcing. We consider the following Helmholtz equation:

$$\Delta Z_n^0 + \left(\kappa_n^0\right)^2 Z_n^0 = 0, \tag{B.3.2}$$

with boundary conditions

$$\begin{aligned}
&Z_n^0 = 0, && \text{at} \quad x = 0, && \text{(tidal forcing)}\\
&Z_{n,y}^0 = 0, && \text{at} \quad y = \pm B/2, && \text{(no-transport)}\\
&\mathrm{C}_{n,11}^0(R)\, Z_{n,x}^0 = q_n^0(y), && \text{at} \quad x = L. && \text{(river)}
\end{aligned}$$

This problem can similarly be solved analytically using separation of variables. We obtain the following solution

$$Z_n^0(x,y) = \sum_{k=0}^{\infty} b_k \sin\left(\mu_{n,k} x\right) \cos\left(\lambda_k (y - B/2)\right),$$

with the same eigenvalues

$$\lambda_k = \frac{k\pi}{B}, \qquad \mu_{n,k} = \sqrt{\left(\kappa_n^0\right)^2 - \lambda_k^2}.$$

The coefficients are found using the orthogonality of the cosines:

$$b_k = \frac{2}{B\left(1 + \mathrm{sinc}(\mathrm{k}\pi)\right)\mu_{n,k} \cos\left(\mu_{n,k} L\right) \mathrm{C}_{n,11}^0(R)} \int_{-B/2}^{B/2} q_n^0(y) \cos\left(\lambda_k (y - B/2)\right) dy.$$

Laterally constant river discharge forcing

For a laterally constant river discharge forcing $q_n^0(y) = q_n^0$, we obtain the following coefficients, since only one eigenmode is exited:

$$b_k = \begin{cases} \dfrac{q_n^0}{\kappa_n^0 \cos\left(\kappa_n^0 L\right) \mathrm{C}_{n,11}^0(R)}, & \text{if } k = 0,\\ 0, & \text{else.} \end{cases}$$

Thus, the solution consists of a single component:

$$Z_n^0(x,y) = \frac{q_n^0}{\kappa_n^0 \cos\left(\kappa_n^0 L\right) \mathrm{C}_{n,11}^0(R)} \sin\left(\kappa_n^0 x\right).$$

For $n = 0$, this further simplifies to a linear function in x:

$$Z_0^0(x,y) = \frac{q_0^0}{\mathrm{C}_{0,11}^0(R)} x.$$

B.3.4 Rectangular geometry with baroclinic forcing

We consider a rectangular geometry with a subtidal baroclinic forcing, $n = 0$. We assume no Coriolis force and spatially constant leading-order parameter values, except the density gradient which may change along channel. We obtain the following equation:

$$\mathrm{C}^{0}_{0,11}(R)\Delta Z^{1,\varsigma}_{0} = -\nabla\cdot\left[\check{\boldsymbol{q}}^{1,\varsigma}_{0}(R)\right], \tag{B.3.3}$$

with boundary conditions

$$\begin{aligned} Z^{1,\varsigma}_{0} &= 0, && \text{at} \quad x = 0, && \text{(no-amplitude)}\\ Z^{1,\varsigma}_{0,y} &= 0, && \text{at} \quad y = \pm B/2, && \text{(no-transport)}\\ Z^{1,\varsigma}_{0,x} &= 0, && \text{at} \quad x = L. && \text{(no-transport)} \end{aligned}$$

Assuming a laterally uniform solution yields the equation

$$\mathrm{C}^{0}_{0,11}(R)Z^{1,\varsigma}_{0,xx} = -\check{q}^{1,\varsigma}_{0,1,x}(x,R),$$

with boundary conditions

$$\begin{aligned} Z^{1,\varsigma}_{0} &= 0, && \text{at} \quad x = 0, && \text{(no-amplitude)}\\ Z^{1,\varsigma}_{0,x} &= 0, && \text{at} \quad x = L. && \text{(no-transport)} \end{aligned}$$

The general solution of this equation with boundary conditions reads

$$Z^{1,\varsigma}_{0}(x,y) = \frac{1}{\mathrm{C}^{0}_{0,11}(R)}\left[\check{q}^{1,\varsigma}_{0,1}(L,R)\,x - \int_0^x \check{q}^{1,\varsigma}_{0,1}(\tilde{x},R)\,d\tilde{x}\right].$$

Next, we want to choose a specific $\check{q}^{1,\varsigma}_{0,1}(\tilde{x},R)$. We have

$$\check{\boldsymbol{q}}^{1,\varsigma}_{0}(R) = \mathbf{P}\check{\boldsymbol{\mathcal{R}}}^{1,\varsigma}_{0}(R), \qquad \check{\boldsymbol{\mathcal{R}}}^{1,\varsigma}_{0}(R) = \mathbf{C}^{1,\varsigma}_{0}(R)\,\mathbf{P}^{*}\nabla\rho^{0}_{0}.$$

Similar as before for $n = 0$ and $f = 0$, the depth-integrated vertical structure matrix $\mathbf{C}^{1,\varsigma}_{0}(R)$ can be written as $\mathrm{C}^{1,\varsigma}_{0,11}(R)\,\mathbf{I}_2$, such that the above equations reduce to

$$\check{\boldsymbol{q}}^{1,\varsigma}_{0}(R) = \mathrm{C}^{1,\varsigma}_{0,11}(R)\,\nabla\rho^{0}_{0}$$

Baroclinic forcing

In order to use a diagnostic baroclinic forcing the gradient of the density must be known. We derive a simple relationship in this section.

Assuming the estuary to be well-mixed, the diagnostic density can be expressed as (Kumar, 2018, p. 77)

$$\rho = \rho_0[1 + \beta_s s(\xi)],$$

with $s(\xi)$ the prescribed tidally- and depth-averaged salinity distribution along the estuary and $\beta_s = 7.6\cdot 10^{-4}\,\mathrm{psu}^{-1}$. The density gradient can be expressed as

$$\nabla\rho^{0}_{0} = \rho_0\beta_s\nabla s.$$

Hyperbolic tangent In Dijkstra (2019, p. 55), the subtidal and vertically uniform salinity is given by

$$s(\xi) = \frac{s_{\mathrm{sea}}}{2}\left(1 - \tanh\left(\frac{\xi - \xi_c}{\xi_L}\right)\right).$$

The following values are suggested $S_{\mathrm{sea}} = 30\,\mathrm{psu}$, $\xi_c = 0.713$ and $\xi_L = 0.235$ in dimensionless units.

Quadratic profile

We assume that the salinity profile has the following quadratic shape

$$s(x) = s_{\text{sea}} \left(1 - \frac{x}{L}\right)^2.$$

Using this simple quadratic salinity profile, yields the following solution for the forced baroclinic free surface

$$Z_0^{1,\varsigma}(x, y) = \frac{\rho_0 \beta_s s_{\text{sea}}}{L^2} \frac{\mathrm{C}_{0,11}^{1,\varsigma}(R)}{\mathrm{C}_{0,11}^{0}(R)} x(2L - x).$$

In a similar vein as before, the forcing velocity profile is given by

$$\check{\boldsymbol{U}}_0^{1,\varsigma}(z) = \mathrm{c}_{0,11}^{1,\varsigma}(z)\,\nabla\rho_0^0 = -2\frac{\rho_0 \beta_s s_{\text{sea}}}{L^2} \mathrm{c}_{0,11}^{1,\varsigma}(z)\,(L - x)\begin{bmatrix}1\\0\end{bmatrix}.$$

B.4 Along- and across-channel velocity

The along- and across channel coordinates (ξ, η) can be used to compute the velocity along- and across the channel.

The unit normal vectors in the ξ and η direction are given by

$$\boldsymbol{n}_\xi = \frac{\nabla \xi}{|\nabla \xi|}, \qquad \boldsymbol{n}_\eta = \frac{\nabla \eta}{|\nabla \eta|}.$$

Using these unit normal vectors, the velocity in the ξ and η direction are computed as

$$U_\xi = \boldsymbol{U} \cdot \boldsymbol{n}_\xi, \qquad U_\eta = \boldsymbol{U} \cdot \boldsymbol{n}_\eta.$$

B.5 Rotating flow variables and tidal ellipse parameters

The rotating flow variables play a key role in decoupling the momentum equations. In the x-y plane the velocity vector traces out an ellipse over the tidal cycle. We consider the computation of the parameters of this tidal ellipse.

B.5.1 Ellipse parameters

We follow the ideas of Butman (1975) to derive the tidal ellipse parameters. These parameters can conveniently expressed in terms of the rotating flow variables.

With each point (x, y) in the x-y plane we associate a point in the complex plane using the complex coordinate: $\breve{z} = x + iy$. Then any vector in the x-y plane can be expressed as $\breve{w} = u + iv$ in the complex plane, with u and v real-valued Cartesian components of the vector.

Using harmonic analysis, we assumed that we can write the horizontal velocity components for each order k as

$$u^k(x, y, z, t) = \sum_{n=0}^{\infty} \mathfrak{Re}\Big(U_n^k(x, y, z)e^{ni\omega t}\Big),$$
$$v^k(x, y, z, t) = \sum_{n=0}^{\infty} \mathfrak{Re}\Big(V_n^k(x, y, z)e^{ni\omega t}\Big).$$

We restrict our attention to the leading-order velocity components for a single harmonic component n:

$$u_n^0(x, y, z, t) = \mathfrak{Re}\Big(U_n^0(x, y, z)e^{ni\omega t}\Big),$$
$$v_n^0(x, y, z, t) = \mathfrak{Re}\Big(V_n^0(x, y, z)e^{ni\omega t}\Big).$$

During the derivation of the leading-order hydrodynamics, we have defined the rotating flow variables as $\boldsymbol{R}_n^0(z) = \mathbf{P}^*\boldsymbol{U}_n^0(z)$, thus $\boldsymbol{U}_n^0(z) = \mathbf{P}\boldsymbol{R}_n^0(z)$. Elements wise this reads

$$U_n^0(z) = \frac{1}{\sqrt{2}}\big(R_{n,1}^0(z) + R_{n,2}^0(z)\big), \qquad V_n^0(z) = \frac{i}{\sqrt{2}}\big(-R_{n,1}^0(z) + R_{n,2}^0(z)\big).$$

The next step is to substitute the rotating flow variables into the complex plane vector to obtain (a similar calculation has been carried out by, e.g., Visser *et al.* (1994))

$$\begin{aligned}
\breve{w}_n^0 &= u_n^0 + i v_n^0,\\
&= \mathfrak{Re}\Big(U_n^0 e^{ni\omega t}\Big) + i\,\mathfrak{Re}\Big(V_n^0 e^{ni\omega t}\Big),\\
&= \mathfrak{Re}\Big(R_{n,1}^0 \frac{e^{ni\omega t}}{\sqrt{2}}\Big) + i\,\mathfrak{Im}\Big(R_{n,1}^0 \frac{e^{ni\omega t}}{\sqrt{2}}\Big) + \overline{\mathfrak{Re}\Big(R_{n,2}^0 \frac{e^{ni\omega t}}{\sqrt{2}}\Big) + i\,\mathfrak{Im}\Big(R_{n,2}^0 \frac{e^{ni\omega t}}{\sqrt{2}}\Big)},\\
&= R_{n,1}^0 \frac{1}{\sqrt{2}} e^{ni\omega t} + \overline{R_{n,2}^0} \frac{1}{\sqrt{2}} e^{-ni\omega t}.
\end{aligned}$$

Both rotating flow variables are multiplied by a scaled complex exponential. The first rotating flow variable is multiplied by the complex exponential $\exp ni\omega t$, which traces out a counter-clockwise circle in the complex plane as t increases for $n, \omega > 0$. The second rotating flow variable is multiplied by the complex exponential $\exp -ni\omega t$, which traces out a clockwise circle in the complex plane as t increases for $n, \omega > 0$. Thus the amplitude of the first rotating flow variable $|R_{n,1}^0|$ indicates the importance of anticlockwise rotation, whereas the amplitude of the second rotating flow variable $|R_{n,2}^0|$ indicates the importance of the clockwise rotation.

The circular rotations do not necessarily need to start at the positive x axis for $t = 0$. Different starting locations along the circle are included using the phases of the complex rotating flow variables. The first rotating flow variable starts at an angle $\phi_{n,1}^0 = \arg(R_{n,1}^0)$ along the circle, whereas the second rotating flow variable starts at an angle $\phi_{n,2}^0 = -\arg(R_{n,2}^0)$. Importantly, note the minus sign here, which is a consequence of the complex conjugation for the second rotating flow variable.

An ellipse can be characterised using 4 parameters, see also Figure B.1. We also include the ellipticity:

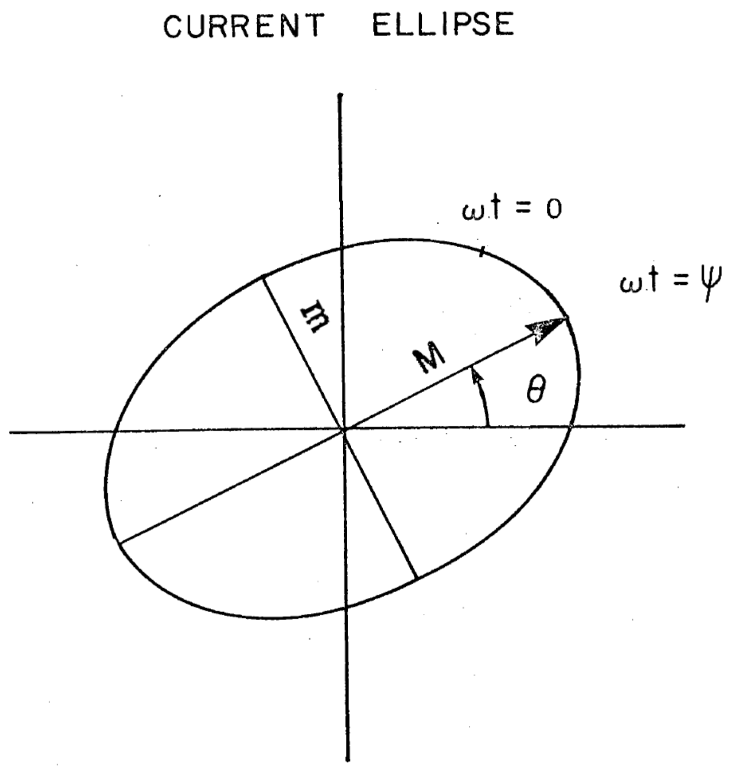

Figure B.1: Sketch of the 4 parameters that specify the tidal ellipse. Adapted from Butman (1975).

- the magnitude of the semi-major axis: M;
- the signed magnitude of the semi-minor axis (positive if the tidal ellipse rotates anticlockwise and negative if the tidal ellipse rotates clockwise): m;
- the orientation of the ellipse (the angle of the semi-major axis with respect to the x-axis): θ;
- the phase of the ellipse (the phase difference between reaching the maximal tidal current and $\omega t = 0$): ψ;
- the signed ratio between the semi-minor and semi-major axis called the signed ellipticity (positive if rotating anticlockwise and negative if rotating clockwise): $\varepsilon = m/M$.

The tidal ellipse parameters can be expressed in terms of the rotating flow variables $\boldsymbol{R}_n^0(z)$ as (see, e.g., Butman, 1975; Maas and van Haren, 1987; Souza and Simpson, 1996; Pugh, 1996):

$$
\begin{aligned}
M_n^0(z) &= \frac{1}{\sqrt{2}}\Big(\big|R_{n,1}^0(z)\big| + \big|R_{n,2}^0(z)\big|\Big),\\
m_n^0(z) &= \frac{1}{\sqrt{2}}\Big(\big|R_{n,1}^0(z)\big| - \big|R_{n,2}^0(z)\big|\Big),\\
\theta_n^0(z) &= \frac{1}{2}\big(\phi_{n,1}^0(z) + \phi_{n,2}^0(z)\big),\\
\psi_n^0(z) &= -\frac{1}{2}\big(\phi_{n,1}^0(z) - \phi_{n,2}^0(z)\big),\\
\varepsilon_n^0(z) &= \frac{m_n^0(z)}{M_n^0(z)},
\end{aligned}
$$

where we have defined the phases

$$
\phi_{n,1}^0(z) = \arg\big(R_{n,1}^0(z)\big), \qquad \phi_{n,2}^0(z) = -\arg\big(R_{n,2}^0(z)\big).
$$

B.5.2 Tidal ellipse parameters of the depth-integrated and depth-averaged rotating flow variables

The tidal parameters in the previous section are derived for the depth-dependent rotating flow variables $\boldsymbol{R}_n^0(z)$. These tidal parameter can also be constructed for the depth-integrated rotating flow variables $\boldsymbol{\mathcal{R}}_n^0(z)$ and the depth-averaged rotating flow variables $[\boldsymbol{R}]_n^0$.

The tidal ellipse parameters of depth-integrated rotating flow variables $\boldsymbol{\mathcal{R}}_n^0(z)$ are given by

$$\begin{aligned}
\hat{M}_n^0(z) &= \frac{1}{\sqrt{2}}\left(\left|\mathcal{R}_{n,1}^0(z)\right| + \left|\mathcal{R}_{n,2}^0(z)\right|\right),\\
\hat{m}_n^0(z) &= \frac{1}{\sqrt{2}}\left(\left|\mathcal{R}_{n,1}^0(z)\right| - \left|\mathcal{R}_{n,2}^0(z)\right|\right),\\
\hat{\theta}_n^0(z) &= \frac{1}{2}\left(\hat{\phi}_{n,1}^0(z) + \hat{\phi}_{n,2}^0(z)\right),\\
\hat{\psi}_n^0(z) &= -\frac{1}{2}\left(\hat{\phi}_{n,1}^0(z) - \hat{\phi}_{n,2}^0(z)\right),\\
\hat{\varepsilon}_n^0(z) &= \frac{\hat{m}_n^0(z)}{\hat{M}_n^0(z)}.
\end{aligned}$$

Here, we have defined the phases of the depth-integrated rotating flow variables as

$$\hat{\phi}_{n,1}^0(z) = \arg\left(\mathcal{R}_{n,1}^0(z)\right), \qquad \hat{\phi}_{n,2}^0(z) = -\arg\left(\mathcal{R}_{n,2}^0(z)\right).$$

The tidal ellipse parameters of the depth-averaged rotating flow variables $[\boldsymbol{R}]_n^0$ can be expressed in terms of the tidal ellipse parameters of the depth-integrated rotating flow variables and read

$$\begin{aligned}
[M]_n^0 &= \frac{1}{D}\hat{M}_n^0(R),\\
[m]_n^0 &= \frac{1}{D}\hat{m}_n^0(R),\\
[\theta]_n^0 &= \hat{\theta}_n^0(R),\\
[\psi]_n^0 &= \hat{\psi}_n^0(R),\\
[\varepsilon]_n^0 &= \frac{[m]_n^0}{[M]_n^0} = \frac{\hat{m}_n^0(R)}{\hat{M}_n^0(R)}.
\end{aligned}$$

Here, we have used that the argument of a complex number does not change if its multiplied by a real constant, such as the reciprocal of the local depth $1/D$.

B.6 Vorticity

We assume the flow is mainly horizontal, i.e., we assume the vertical velocity is much smaller than the horizontal velocities. The vorticity of a two-dimensional horizontal flow is a scalar quantify defined as

$$\omega \equiv \nabla \times \boldsymbol{u} = \begin{vmatrix} \partial_x & \partial_y \\ u & v \end{vmatrix} = v_x - u_y.$$

Another interpretation is that we only consider the z-component of the vorticity vector $\boldsymbol{\omega}$.

The taking the x derivative of the leading-order y-momentum equation and subtracting the y derivative of the leading-order x-momentum equation yields an equation for the leading-order vorticity:

$$\omega_t^0 - f w_z^0 = A_v^0 \omega_{zz}^0 + \nabla A_v^0 \times \boldsymbol{u}_{zz}^0.$$

For the leading-order x- and y-momentum equations, see Section 1.4.3.

B.6.1 Expanding the leading-order vorticity

The vorticity has the same time dependency as the leading-order solution since the vorticity is linear in $\boldsymbol{u}$. Thus, we may expand it in a Fourier series:

$$\omega^0(x,y,z,t) = \sum_{n=0}^{\infty} \mathfrak{Re}\Big(\Omega_n^0(x,y,z) e^{ni\omega t}\Big),$$

with $\Omega_n^0(x,y,z)$ the complex n-th Fourier coefficient. Here, the non-superscripted ω is the angular frequency of, for example, the M_2 constituent.

For the leading-order n-th vorticity component $\Omega_n^0(z)$, it follows using orthogonality that

$$\Omega_n^0(z) = V_{n,x}^0(z) - U_{n,y}^0(z) = \nabla \times \boldsymbol{U}_n^0(z).$$

When solving the leading-order hydrodynamic equations, we have derived that

$$\boldsymbol{U}_n^0(z) = \mathbf{P}\,\mathbf{c}_n^0(z)\,\mathbf{P}^*\,\nabla Z_n^0.$$

We can rewrite the curl in matrix vector form as

$$\begin{aligned}
\Omega_n^0(z) &= \nabla \times \boldsymbol{U}_n^0(z), \\
&= \dot{\nabla}^T \boldsymbol{U}_n^0(z), \\
&= \dot{\nabla}^T \big[\mathbf{P}\,\mathbf{c}_n^0(z)\,\mathbf{P}^*\,\nabla Z_n^0\big], \\
&= -i\check{\boldsymbol{P}}^*\check{\nabla}\big[\mathbf{c}_n^0(z)\,\hat{\nabla}^T Z_n^0\big]\check{\boldsymbol{P}}.
\end{aligned}$$

Here, we have used the 'commutation' relations $\dot{\nabla}^T\mathbf{P} = -i\check{\boldsymbol{P}}^*\check{\nabla}$ and $\mathbf{P}^*\nabla Z_n^0 = \hat{\nabla}^T Z_n^0\,\check{\boldsymbol{P}}$, where have defined the operators

$$\dot{\nabla}^T = \begin{bmatrix} -\partial_y & \partial_x \end{bmatrix}, \qquad \check{\nabla} = \begin{bmatrix} \partial_x & -\partial_x \\ \partial_y & \partial_y \end{bmatrix}, \qquad \hat{\nabla}^T = \begin{bmatrix} \partial_x & \partial_y \\ \partial_x & -\partial_y \end{bmatrix},$$

and vectors and matrix

$$\check{\boldsymbol{P}}^* = \frac{1}{\sqrt{2}}\begin{bmatrix} 1 & -i \end{bmatrix}, \qquad \check{\boldsymbol{P}} = \frac{1}{\sqrt{2}}\begin{bmatrix} 1 \\ i \end{bmatrix}, \qquad \hat{\nabla}^T Z_n^0 = \begin{bmatrix} Z_{n,x}^0 & Z_{n,y}^0 \\ Z_{n,x}^0 & -Z_{n,y}^0 \end{bmatrix}.$$

The next step is to evaluate the inner operator $\check{\nabla}$, we have

$$\begin{aligned}
\check{\nabla}\big[\mathbf{c}_n^0(z)\,\hat{\nabla}^T Z_n^0\big] &= \mathrm{c}_{n,11}^0(z)\,\mathbf{H} Z_n^0 - \mathrm{c}_{n,22}^0(z)\,\tilde{\mathbf{H}} Z_n^0 + \check{\nabla}\mathbf{c}_n^0(z)\,\hat{\nabla}^T Z_n^0, \\
&= \check{\mathcal{K}}\mathbf{c}_n^0(z)\,\boldsymbol{\mathcal{L}} Z_n^0,
\end{aligned}$$

where we have defined the matrices

$$\mathbf{H}Z_n^0 = \begin{bmatrix} Z_{n,xx}^0 & Z_{n,xy}^0 \\ Z_{n,yx}^0 & Z_{n,yy}^0 \end{bmatrix}, \qquad \tilde{\mathbf{H}}Z_n^0 = \begin{bmatrix} Z_{n,xx}^0 & -Z_{n,xy}^0 \\ -Z_{n,yx}^0 & Z_{n,yy}^0 \end{bmatrix}, \qquad \check{\nabla}\mathbf{c}_n^0(z) = \begin{bmatrix} \mathrm{c}_{n,11,x}^0(z) & -\mathrm{c}_{n,22,x}^0(z) \\ \mathrm{c}_{n,11,y}^0(z) & \mathrm{c}_{n,22,y}^0(z) \end{bmatrix},$$

$$\check{\mathcal{K}}\mathbf{c}_n^0(z) = \begin{bmatrix} \mathrm{c}_{n,11}^0(z)\,\mathbf{I}_2 & -\mathrm{c}_{n,22}^0(z)\,\mathbf{I}_2 & \check{\nabla}\mathbf{c}_n^0(z) \end{bmatrix}, \qquad \mathcal{L}Z_n^0 = \begin{bmatrix} \mathbf{H}Z_n^0 \\ \tilde{\mathbf{H}}Z_n^0 \\ \hat{\nabla}^T Z_n^0 \end{bmatrix}.$$

Here, $\mathbf{I}_2$ is the 2×2 identity matrix and $\mathbf{H}Z_n^0$ is the Hessian of Z_n^0. We assume that Z_n^0 is sufficiently smooth, such that $Z_{n,xy}^0 = Z_{n,yx}^0$. As a consequence, the matrices $\mathbf{H}Z_n^0$ and $\tilde{\mathbf{H}}Z_n^0$ are symmetric. Finally, the last line in this equation is just a regular matrix product.

Thus, the leading-order vorticity can be computed using

$$\Omega_n^0(z) = -i\check{\boldsymbol{P}}^*\check{\mathcal{K}}\mathbf{c}_n^0(z)\,\mathcal{L}Z_n^0\,\check{\boldsymbol{P}}.$$

One can also expand the above formula, the off-diagonal terms of the Hessian cancel yielding a simplified expression:

$$\Omega_n^0(z) = -\frac{i}{2}\big(\mathrm{c}_{n,11}^0(z) - \mathrm{c}_{n,22}^0(z)\big)\,\Delta Z_n^0 - i\check{\boldsymbol{P}}^*\check{\nabla}\mathbf{c}_n^0(z)\,\mathbf{P}^*\nabla Z_n^0.$$

Here, $\Delta Z_n^0 = Z_{n,xx}^0 + Z_{n,yy}^0$ is the Laplacian of Z_n^0 and the 'commutation' relation $\hat{\nabla}^T Z_n^0\,\check{\boldsymbol{P}} = \mathbf{P}^*\nabla Z_n^0$ has been used.

For interpretation purposes, the 'commutation' relation $-i\check{\boldsymbol{P}}^*\check{\nabla} = \dot{\nabla}^T\mathbf{P}$ applied to $\mathbf{c}_n^0(z)$ yields

$$-i\check{\boldsymbol{P}}^*\check{\nabla}\mathbf{c}_n^0(z) = \dot{\nabla}^T\big[\mathbf{P}\,\mathbf{c}_n^0(z)\big] = \nabla\times\big[\mathbf{P}\,\mathbf{c}_n^0(z)\big],$$

where, we have used that $\dot{\nabla}^T = \nabla\times$. Here, the curl operator works on a matrix. This is defined such that the previous relations hold and gives back a row vector. In particular, it computes the curl of each column of the matrix and appends them together. Combing this with the previous result yields the following expression for the complex vorticity:

$$\Omega_n^0(z) = -\frac{i}{2}\big(\mathrm{c}_{n,11}^0(z) - \mathrm{c}_{n,22}^0(z)\big)\,\Delta Z_n^0 + \nabla\times\big[\mathbf{P}\,\mathbf{c}_n^0(z)\big]\,\mathbf{P}^*\nabla Z_n^0.$$

In the absence of the Coriolis force, $f = 0$, the elements of the diagonal matrix $\mathbf{c}_n^0(z)$ are equal. Allowing us to write $\mathbf{c}_n^0(z) = \mathrm{c}_{n,11}^0(z)\,\mathbf{I}_2$. Then we get for the vorticity that

$$\Omega_n^0(z) = \nabla\times\big[\mathrm{c}_{n,11}^0(z)\,\mathbf{I}_2\big]\nabla Z_n^0 = \nabla\times\big[\mathrm{c}_{n,11}^0(z)\big]\,\nabla Z_n^0.$$

Here, the vorticity of a scalar is defined as the row vector:

$$\nabla\times\big[\mathrm{c}_{n,11}^0(z)\big] = \begin{bmatrix} -\mathrm{c}_{n,11,y}^0(z) & \mathrm{c}_{n,11,x}^0(z) \end{bmatrix}.$$

B.7 Deriving the weak form of the general hydrodynamic equation

We define the finite element spaces where the test functions and the solution reside in. Let Ω be the two-dimensional domain with the boundary consisting of segments of $\partial\Omega_{\text{sea}}$, $\partial\Omega_{\text{bank}}$ and $\partial\Omega_{\text{river}}$. Define the standard $L^2(\Omega)$ space and Sobolev space $H^1(\Omega)$ as

$$L^2(\Omega) = \{\varphi : \Omega \mapsto \mathbb{C} \,|\, \|\varphi\|_2 < \infty\},$$
$$H^1(\Omega) = \{\varphi \in L^2(\Omega) \,|\, \varphi_x \in L^2(\Omega), \varphi_y \in L^2(\Omega)\},$$

where we have defined the L^2-norm as

$$\|\varphi\|_2 = \sqrt{\int_\Omega |\varphi|^2 \, d\Omega}.$$

The essential boundary conditions for this problem are located at $\partial\Omega_{\text{sea}}$. Thus we seek test functions in the homogeneous space

$$\Sigma_0(\Omega) = \{\varphi \in H^1(\Omega) \,|\, \varphi = 0 \text{ at } \partial\Omega_{\text{sea}}\}.$$

We will use the higher-dimensional analogue of integration by parts. It states that for a scalar-valued function φ and vector-valued function $\boldsymbol{V}$ that

$$\int_\Omega \varphi \nabla \cdot \boldsymbol{V} \, d\Omega = \int_\Gamma \varphi \boldsymbol{V} \cdot \boldsymbol{n} \, d\Gamma - \int_\Omega \nabla\varphi \cdot \boldsymbol{V} \, d\Omega,$$

with $\boldsymbol{n}$ the outward pointing unit normal vector.

We multiply the general free surface equation (2.1.1) with the test function $\varphi \in \Sigma_0(\Omega)$ and integrate over the domain Ω to obtain

$$\int_\Omega \varphi \nabla \cdot \left[\mathbf{D}_n^0(R)\nabla Z_n^{k,f}\right] + ni\omega\varphi Z_n^{k,f} \, d\Omega = \int_\Omega -\varphi\nabla \cdot \left[\check{\boldsymbol{q}}_n^{k,f}(R)\right] d\Omega.$$

We consider the first and last term separately. Evoking the integration by parts formula on the first term, we find

$$\begin{aligned}\int_\Omega \varphi \nabla \cdot \left[\mathbf{D}_n^0(R)\nabla Z_n^{k,f}\right] d\Omega = &\int_{\partial\Omega_{\text{sea}}} \varphi\left[\mathbf{D}_n^0(R)\nabla Z_n^{k,f}\right] \cdot \boldsymbol{n} \, d\Gamma + \int_{\partial\Omega_{\text{bank}}} \varphi\left[\mathbf{D}_n^0(R)\nabla Z_n^{k,f}\right] \cdot \boldsymbol{n} \, d\Gamma \\ &+ \int_{\partial\Omega_{\text{river}}} \varphi\left[\mathbf{D}_n^0(R)\nabla Z_n^{k,f}\right] \cdot \boldsymbol{n} \, d\Gamma - \int_\Omega \nabla\varphi \cdot \left[\mathbf{D}_n^0(R)\nabla Z_n^{k,f}\right] d\Omega.\end{aligned}$$

Using that φ vanishes on the boundary $\partial\Omega_{\text{sea}}$ and substituting the natural boundary conditions yields

$$\int_\Omega \varphi \nabla \cdot \left[\mathbf{D}_n^0(R)\nabla Z_n^{k,f}\right] d\Omega = \int_{\partial\Omega_{\text{bank}}} \varphi \tilde{q}_{\text{bank},n}^{k,f} \, d\Gamma + \int_{\partial\Omega_{\text{river}}} \varphi \dot{q}_{\text{river},n}^{k,f} \, d\Gamma - \int_\Omega \nabla\varphi \cdot \left[\mathbf{D}_n^0(R)\nabla Z_n^{k,f}\right] d\Omega.$$

Using the integration by parts formula for the second term and using that $\varphi = 0$ at $\partial\Omega_{\text{sea}}$ yields similarly,

$$\int_\Omega -\varphi\nabla \cdot \left[\check{\boldsymbol{q}}_n^{k,f}(R)\right] d\Omega = -\int_{\partial\Omega_{\text{bank}}} \varphi\left[\check{\boldsymbol{q}}_n^{k,f}(R)\right] \cdot \boldsymbol{n} \, d\Gamma - \int_{\partial\Omega_{\text{river}}} \varphi\left[\check{\boldsymbol{q}}_n^{k,f}(R)\right] \cdot \boldsymbol{n} \, d\Gamma + \int_\Omega \nabla\varphi \cdot \left[\check{\boldsymbol{q}}_n^{k,f}(R)\right] d\Omega.$$

Combing the above two results and bringing all unknown $Z_n^{k,f}$ terms to the left and bringing all known terms to the right results in

$$\begin{aligned}\int_\Omega -\nabla\varphi \cdot \left[\mathbf{D}_n^0(R)\nabla Z_n^{k,f}\right] + ni\omega\varphi Z_n^{k,f} \, d\Omega = &\int_\Omega \nabla\varphi \cdot \left[\check{\boldsymbol{q}}_n^{k,f}(R)\right] d\Omega - \int_{\partial\Omega_{\text{bank}}} \varphi\left(\tilde{q}_{\text{bank},n}^{k,f} + \left[\check{\boldsymbol{q}}_n^{k,f}(R)\right] \cdot \boldsymbol{n}\right) d\Gamma \\ &- \int_{\partial\Omega_{\text{river}}} \varphi\left(\dot{q}_{\text{river},n}^{k,f} + \left[\check{\boldsymbol{q}}_n^{k,f}(R)\right] \cdot \boldsymbol{n}\right) d\Gamma.\end{aligned}$$

Cancellation

The tidal return flow forcing, $f=\gamma$, occurs in all three possible locations in the above equation: $\check{\boldsymbol{q}}_n^{k,f}(R)$, $\tilde{q}_{\text{bank},n}^{k,f}$ and $\dot{q}_{\text{river},n}^{k,f}$. This suggest that perhaps some terms can be simplified. We evaluate the indices $k=1$ and $f=\gamma$ to obtain $\check{\boldsymbol{q}}_n^{1,\gamma}(R)=\boldsymbol{\gamma}_n^1$, $\tilde{q}_{\text{bank},n}^{1,\gamma}=-\boldsymbol{\gamma}_n^1\cdot\boldsymbol{n}$ and $\dot{q}_{\text{river},n}^{1,\gamma}=-\boldsymbol{\gamma}_n^1\cdot\boldsymbol{n}$ such that the weak form simplifies to

$$\int_\Omega -\nabla\varphi\cdot\left[\mathbf{D}_n^0(R)\,\nabla Z_n^{1,\gamma}\right]+ni\omega\varphi Z_n^{1,\gamma}\,d\Omega=\int_\Omega \nabla\varphi\cdot\boldsymbol{\gamma}_n^1\,d\Omega.$$

We define two new boundary forcing functions that reflect this cancellation. We also use that the current boundary forcing functions are sparse in the index f, i.e., $\tilde{q}_{\text{bank},n}^{k,f}$ is only non-zero for $f=\gamma$ and $\dot{q}_{\text{river},n}^{k,f}$ is only non-zero for $f=\gamma,q$, and that $\check{\boldsymbol{q}}_n^{k,f}(R)$ vanishes for $f=q$. This leads to the following two new boundary forcing functions at $\partial\Omega_{\text{bank}}$ and $\partial\Omega_{\text{river}}$:

$$\breve{q}_{\text{bank},n}^{1,f}(x,y)=\begin{cases}0 & \text{if } f=\gamma,\\ \left[\check{\boldsymbol{q}}_n^{k,f}(R)\right]\cdot\boldsymbol{n} & \text{otherwise,}\end{cases}\qquad \acute{q}_{\text{river},n}^{1,f}(x,y)=\begin{cases}0 & \text{if } f=\gamma,\\ -q_{\text{river},n}^{1}(x,y) & \text{if } f=q,\\ \left[\check{\boldsymbol{q}}_n^{k,f}(R)\right]\cdot\boldsymbol{n} & \text{otherwise.}\end{cases}$$

We define the weak form as: find $Z_n^{k,f}\in H^1(\Omega)$ with $Z_n^{k,f}=A_n^{k,f}(x,y)$ at $\partial\Omega_{\text{sea}}$ such that for all test functions $\varphi\in\Sigma_0(\Omega)$ it holds that

$$\int_\Omega -\left[\mathbf{D}_n^0(R)\,\nabla Z_n^{k,f}\right]\cdot\nabla\varphi+ni\omega Z_n^{k,f}\varphi\,d\Omega=\int_\Omega\left[\check{\boldsymbol{q}}_n^{k,f}(R)\right]\cdot\nabla\varphi\,d\Omega-\int_{\partial\Omega_{\text{bank}}}\breve{q}_{\text{bank},n}^{1,f}\varphi\,d\Gamma-\int_{\partial\Omega_{\text{river}}}\acute{q}_{\text{river},n}^{1,f}\varphi\,d\Gamma.$$

In this derivation, we have removed the divergence of the right-hand side forcing function at the expense of introducing additional boundary forcing terms.

Bilinear and linear form

The weak form can also be written in abstract variational form using a bilinear and linear form. We define the bilinear form as

$$a_n\big(Z_n^{k,f},\varphi\big)=\int_\Omega -\left[\mathbf{D}_n^0(R)\,\nabla Z_n^{k,f}\right]\cdot\nabla\varphi+ni\omega Z_n^{k,f}\varphi\,d\Omega,$$

and the linear form as

$$b_n^{k,f}(\varphi)=\int_\Omega\left[\check{\boldsymbol{q}}_n^{k,f}(R)\right]\cdot\nabla\varphi\,d\Omega-\int_{\partial\Omega_{\text{bank}}}\breve{q}_{\text{bank},n}^{1,f}\varphi\,d\Gamma-\int_{\partial\Omega_{\text{river}}}\acute{q}_{\text{river},n}^{1,f}\varphi\,d\Gamma.$$

Then the above weak form can be compactly stated as follows: find $Z_n^{k,f}\in H^1(\Omega)$ with $Z_n^{k,f}=A_n^{k,f}(x,y)$ at $\partial\Omega_{\text{sea}}$ such that for all test functions $\varphi\in\Sigma_0(\Omega)$ it holds that

$$a_n\big(Z_n^{k,f},\varphi\big)=b_n^{k,f}(\varphi).$$

B.8 Expanding the leading-order erosion flux coefficients into a Fourier series

To obtain the Fourier coefficients of the leading-order erosion flux (3.3.5), it follows that the norm of the velocity vector needs to be expanded into a Fourier series. Thus, we want to find the A_n's such that

$$|\boldsymbol{u}_b^0| = \sum_{n=0}^{\infty} \mathfrak{Re}\left(A_n e^{in\omega t}\right).$$

The norm is an even function of $\boldsymbol{u}_b^0$, since

$$|-\boldsymbol{u}_b^0| = \sqrt{(-\boldsymbol{u}_b^0)\cdot(-\boldsymbol{u}_b^0)} = \sqrt{\boldsymbol{u}_b^0\cdot\boldsymbol{u}_b^0} = |\boldsymbol{u}_b^0|.$$

This means that for a pure M_2 signal with angular frequency ω, the norm of the near-bed velocity $|\boldsymbol{u}_b^0|$ consists of only even harmonics of the M_2 signal, i.e., the frequencies 0ω, 2ω, 4ω, 6ω, 8ω, ..., which correspond to the tidal constituents M_0, M_4, M_8, M_{12}, M_{16}, ... Thus, all the odd frequencies vanish and, in particular, we find that the norm of a velocity vector that consists solely of an M_2 component does not generate an M_2 signal.

We compute the Fourier coefficients A_n of the complex polar form. The real part operator makes finding the coefficients of this form a little more tricky than for a two sided complex Fourier series. One method to obtain an expression for these coefficients is as follows. Multiply both sides by $\mathfrak{Re}(c_m \exp -im\omega t)$ for $m \geq 0$, simplify and integrate over the period $T = 2\pi/\omega$, to obtain

$$\int_0^T |\boldsymbol{u}_b^0|\,\mathfrak{Re}\left(c_m e^{-im\omega t}\right) dt = \frac{1}{2}\mathfrak{Re}\left[\sum_{n=0}^{\infty} A_n\left(c_m\int_0^T e^{i(n-m)\omega t}\,dt + c_m^*\int_0^T e^{i(n+m)\omega t}\,dt\right)\right].$$

The integrals on the right-hand side are equal to

$$c_m\int_0^T e^{i(n-m)\omega t}\,dt + c_m^*\int_0^T e^{i(n+m)\omega t}\,dt = T\left(c_m\delta_{n,m} + c_m^*\delta_{m,n,0}\right).$$

Here, $\delta_{n,m}$ is the Kronecker delta that is one if its arguments match, $n = m$, and zero otherwise, and $\delta_{n,m,0}$ is the three argument Kronecker delta that is one if all three arguments match, $n = m = 0$, and zero otherwise. Using the Kronecker delta property and relabelling $m \mapsto n$ yields

$$\int_0^T |\boldsymbol{u}_b^0|\,\mathfrak{Re}\left(c_n e^{-in\omega t}\right) dt = \frac{1}{2}T\,\mathfrak{Re}\left[A_n\left(c_n + c_0^*\delta_{n,0}\right)\right].$$

We obtain the conditions for $n = 0$ and $n > 0$:

$$\mathfrak{Re}[A_0] = \frac{1}{T}\int_0^T |\boldsymbol{u}_b^0|\,dt, \qquad \mathfrak{Re}[A_n] = \frac{2}{T}\int_0^T |\boldsymbol{u}_b^0|\,\mathfrak{Re}\left(c_n e^{-in\omega t}\right) dt.$$

We choose $\mathfrak{Im}[A_0] = 0$. For $n > 0$, we are free to choose c_n however we want. By first choosing $c_n = 1$ and then $c_n = -i$, we are able to remove the real part operator and find expressions for the complex Fourier coefficients for $n > 0$. We combine the two expressions to find a single formula for all Fourier coefficients:

$$A_n = \xi_n \frac{1}{T}\int_0^T |\boldsymbol{u}_b^0|\,e^{-in\omega t}\,dt,$$

where, we have defined the n dependent factor:

$$\xi_n = 2 - \delta_{n,0} = \begin{cases} 1 & \text{if } n = 0, \\ 2 & \text{otherwise.} \end{cases}$$

This formula can generally be used for any real-valued function.

We can express the leading-order horizontal velocity vector evaluated near the bed as

$$\boldsymbol{u}_b^0(t) = \mathfrak{Re}\left(\boldsymbol{U}_b^0 e^{i\omega t}\right).$$

Here, we have used that the leading-order hydrodynamics consist of only an M_2 component, thus we can write $\boldsymbol{U}^0_{1,b} = \boldsymbol{U}^0_b$ for conciseness.

We introduce the nondimensional coordinate $\theta = \omega t$. Using this coordinate transformation, we obtain the integral

$$A_n = \xi_n \frac{1}{2\pi} \int_0^{2\pi} \left| \mathfrak{Re}\left(\boldsymbol{U}^0_b e^{i\theta} \right) \right| e^{-in\theta}\, d\theta.$$

We define the complex coordinate $z = e^{i\theta}$, which traces out an unit circle in the complex z-plane for $0 \leq \theta \leq 2\pi$. We obtain the contour integral

$$A_n = \xi_n \frac{1}{2\pi i} \oint_{|z|=1} \left| \mathfrak{Re}\left(\boldsymbol{U}^0_b z \right) \right| \frac{1}{z^{n+1}}\, dz. \tag{B.8.1}$$

This contour integral form of the Fourier coefficients plays a crucial role in the subsequent analysis.

Symmetry argument Using the contour integral formulation of the Fourier coefficients (B.8.1), we will show that all the odd harmonics of ω vanish, i.e., $A_n = 0$ for odd n.

Proof. Assume n is odd, then it can be expressed as $n = 2k+1$ for some integer k. The integrand can be written as

$$E_k(z) = \xi_{2k+1} \frac{1}{2\pi i} \left| \mathfrak{Re}\left(\boldsymbol{U}^0_b z \right) \right| \frac{1}{z^{2(k+1)}}.$$

We apply the mapping $z \mapsto -z$ to the integrand $E_k(z)$ and simplify:

$$E_k(-z) = \xi_{2k+1} \frac{1}{2\pi i} \left| \mathfrak{Re}\left(\boldsymbol{U}^0_b (-z) \right) \right| \frac{1}{(-z)^{2(k+1)}} = \xi_{2k+1} \frac{1}{2\pi i} \left| \mathfrak{Re}\left(\boldsymbol{U}^0_b z \right) \right| \frac{1}{z^{2(k+1)}} = E_k(z).$$

Comparing the extreme left to the extreme right shows that $E_k(-z) = E_k(z)$ for all z. Thus, the integrand $E_k(z)$ is an even function of z. Hence, the name $E_k(z)$.

The unit circle contour is symmetric around the origin. Thus, we can decompose the unit circle into two semicircular contours γ_1 and γ_2, such that

$$\int_{\gamma_2} E_k(z)\, dz = \int_{\gamma_1} E_k(-z)\, d(-z) = -\int_{\gamma_1} E_k(z)\, dz.$$

Henceforth, we have the following chain of equalities:

$$A_n = \oint_{|z|=1} E_k(z)\, dz = \left(\int_{\gamma_1} + \int_{\gamma_2} \right) E_k(z)\, dz = \left(\int_{\gamma_1} - \int_{\gamma_1} \right) E(z)\, dz = 0.$$

Thus, showing that A_n vanishes for odd n and, therefore, finishing the proof. □

Continuing the derivation We simplify the function $\left| \mathfrak{Re}\left(\boldsymbol{U}^0_b z \right) \right|$ found in the integrand. We define the complex unit vector

$$\boldsymbol{\alpha} = \frac{\boldsymbol{U}^0_b}{|\boldsymbol{U}^0_b|}.$$

This is an unit vector since it has unit length:

$$|\boldsymbol{\alpha}| = \frac{|\boldsymbol{U}^0_b|}{|\boldsymbol{U}^0_b|} = 1.$$

Here, we have defined the norm of a complex vector as

$$\left|\boldsymbol{U}^0_b\right| = \sqrt{\boldsymbol{U}^0_b \cdot \boldsymbol{U}^{0*}_b} = \sqrt{\left|U^0_b\right|^2 + \left|V^0_b\right|^2},$$

with $*$ denoting complex conjugation.

Using this complex unit vector, we can write the complex vector containing the Fourier coefficients of the horizontal velocity as

$$\boldsymbol{U}^0_b = \left|\boldsymbol{U}^0_b\right| \frac{\boldsymbol{U}^0_b}{\left|\boldsymbol{U}^0_b\right|} = \left|\boldsymbol{U}^0_b\right| \boldsymbol{\alpha}. \tag{B.8.2}$$

It then follows that we can write

$$
\begin{aligned}
\left|\mathfrak{Re}\left(\boldsymbol{U}_b^0 z\right)\right| &= \left|\boldsymbol{U}_b^0\right| \left|\mathfrak{Re}\left(\boldsymbol{\alpha} z\right)\right|, \\
&= \frac{1}{2}\left|\boldsymbol{U}_b^0\right| \left|\boldsymbol{\alpha} z + \boldsymbol{\alpha}^* z^*\right|.
\end{aligned} \tag{B.8.3}
$$

On the unit circle, it follows that

$$
|z| = 1 \qquad \Longrightarrow \qquad |z|^2 = 1 \qquad \Longrightarrow \qquad zz^* = 1 \qquad \Longrightarrow \qquad z^* = \frac{1}{z}.
$$

On the unit circle $|z| = 1$, the norm is expanded using the complex vector norm, which reduces to the real vector norm for real arguments:

$$
\begin{aligned}
\left|\boldsymbol{\alpha} z + \boldsymbol{\alpha}^* z^*\right| &= \sqrt{(\boldsymbol{\alpha} z + \boldsymbol{\alpha}^* z^*) \cdot (\boldsymbol{\alpha} z + \boldsymbol{\alpha}^* z^*)^*}, \\
&= \sqrt{(\boldsymbol{\alpha} z + \boldsymbol{\alpha}^* z^*) \cdot (\boldsymbol{\alpha} z + \boldsymbol{\alpha}^* z^*)}, \\
&= \sqrt{(\boldsymbol{\alpha} \cdot \boldsymbol{\alpha})\, z^2 + 2\,(\boldsymbol{\alpha} \cdot \boldsymbol{\alpha}^*)\, zz^* + (\boldsymbol{\alpha}^* \cdot \boldsymbol{\alpha}^*)\, (z^*)^2}, \\
&= \sqrt{(\boldsymbol{\alpha})^2\, z^2 + 2\,|\boldsymbol{\alpha}|^2\, |z|^2 + (\boldsymbol{\alpha}^*)^2\, \frac{1}{z^2}}, \\
&= \sqrt{\boldsymbol{\alpha}^2 z^2 + 2 + \left(\boldsymbol{\alpha}^2\right)^* \frac{1}{z^2}}, \\
&= \sqrt{a z^2 + 2 + a^* \frac{1}{z^2}}.
\end{aligned} \tag{B.8.4}
$$

To simplify notation, we have defined the complex number a as the square of the complex vector $\boldsymbol{\alpha}$, which we have defined as the innerproduct with itself:

$$
a = \boldsymbol{\alpha}^2 = \boldsymbol{\alpha} \cdot \boldsymbol{\alpha}.
$$

Using the triangle inequality, it follows that a lays inside an unit disk inside of the complex a-plane (i.e., $|a| \leq 1$), since

$$
|a| = \left|\boldsymbol{\alpha}^2\right| = \left|\alpha_1^2 + \alpha_2^2\right| \leq |\alpha_1|^2 + |\alpha_2|^2 = |\boldsymbol{\alpha}|^2 = 1,
$$

where α_1 and α_2 denote the first and second component of the complex unit vector $\boldsymbol{\alpha}$. Equality is achieved (i.e., $|a| = 1$), if the components of $\boldsymbol{\alpha}$ point in the same direction (i.e., have the same phase):

$$
\begin{aligned}
&|a| = \left|\boldsymbol{\alpha}^2\right| = \left|r_1^2 e^{i2\theta} + r_2^2 e^{i2\theta}\right| = \left|(r_1^2 + r_2^2) e^{i2\theta}\right| = r_1^2 + r_2^2 = \boldsymbol{\alpha} \cdot \boldsymbol{\alpha}^* = |\boldsymbol{\alpha}|^2 = 1, \\
&\Longrightarrow |a| = 1,
\end{aligned}
$$

where $\alpha_1 = r_1 e^{i\theta}$ and $\alpha_2 = r_2 e^{i\theta}$, or in the degenerate case when one of the components vanishes, i.e., $r_1 = 0$ or $r_2 = 0$.

Combing equations (B.8.1), (B.8.3) and (B.8.4), we obtain for the contour integral that

$$
A_n = \xi_n \frac{1}{2\pi i} \frac{1}{2} \left|\boldsymbol{U}_b^0\right| \oint_{|z|=1} \sqrt{a z^2 + 2 + a^* \frac{1}{z^2}}\, \frac{1}{z^{n+1}}\, dz. \tag{B.8.5}
$$

Since a is a complex scalar in the unit disk ($|a| \leq 1$), it can be parametrised in polar form as

$$
a = r e^{i\theta},
$$

for $0 \leq r \leq 1$ and $-\pi \leq \theta \leq \pi$. We can remove the θ dependence of the integrand by defining the rotated complex coordinate $w = e^{i\theta/2} z$. The contour integral (B.8.5) becomes

$$
A_n = \xi_n \frac{1}{2\pi i} \frac{1}{2} \left|\boldsymbol{U}_b^0\right| e^{in\theta/2} \oint_{|w|=1} \sqrt{2 + r\left(w^2 + \frac{1}{w^2}\right)}\, \frac{1}{w^{n+1}}\, dw.
$$

We have successfully reduced the integral from a four parameter integral to an one parameter integral. We go back to the real domain and parametrise the unit circle contour as $w = e^{i\theta}$ with dummy variable θ for $-\pi \le \theta \le \pi$. The Fourier coefficients become

$$A_n = \xi_n \frac{1}{2\pi}\frac{1}{2}\left|\boldsymbol{U}_b^0\right| e^{in\theta/2}\int_{-\pi}^{\pi}\sqrt{2+2r\cos 2\theta}\, e^{-in\theta}\, d\theta.$$

For $n = 0$, this integral can be expressed in terms of the complete elliptic integral of the second kind as

$$A_0 = \frac{1}{\pi}\sqrt{2+2r}\, E(k)\left|\boldsymbol{U}_b^0\right|,$$

where, we have defined the complete elliptic integral of the second kind as

$$E(k) = \int_0^{\pi/2}\sqrt{1-k^2\sin^2\theta}\, d\theta,$$

with the parameter

$$k = \sqrt{\frac{2r}{r+1}}.$$

For $r = 1$, we get $k = 1$ and $E(k) = 1$. The Fourier coefficient reduces to the one velocity component case:

$$A_0 = \frac{2}{\pi}\left|\boldsymbol{U}_b^0\right|.$$

Using even and oddness arguments, we get the following integral expression for the Fourier coefficients for $n > 0$:

$$A_n = \frac{1}{\pi}\left|\boldsymbol{U}_b^0\right| e^{in\theta/2}\int_0^{\pi}\sqrt{2+2r\cos 2\theta}\cos n\theta\, d\theta.$$

Next, we focus on the $n = 2$ coefficient of A_n. We get the expression

$$A_2 = \frac{2}{\pi}\left|\boldsymbol{U}_b^0\right| e^{i\theta}\int_0^{\pi/2}\sqrt{2+2r\cos 2\theta}\cos 2\theta\, d\theta,$$

where we have used the evenness of the integrand again.

This integral can be written in terms of the complete first and second elliptic integrals as

$$A_2 = \frac{2}{3\pi}\frac{\sqrt{2+2r}}{r}\left[E(k) + (r-1)K(k)\right]\left|\boldsymbol{U}_b^0\right| e^{i\theta}$$

where, we have defined the complete elliptic integral of the first kind as

$$K(k) = \int_0^{\pi/2}\frac{1}{\sqrt{1-k^2\sin^2\theta}}\, d\theta.$$

This calculation can also be performed for horizontal flow consisting of a single velocity component. For example, $U_b^0 = |U_b^0|\exp i\varphi \neq 0$ and $V_b^0 = 0$. The exact Fourier coefficient reads

$$\hat{A}_2 = \frac{4}{3\pi}\left|U_b^0\right| e^{i2\varphi}.$$

We check this limit with the two component horizontal flow case. In the limit $r = 1$, we get

$$A_2 = \frac{4}{3\pi}\left|\boldsymbol{U}_b^0\right| e^{i\theta}.$$

We express θ in terms of the complex velocity vector. Expanding the definitions, we find

$$a = \boldsymbol{\alpha}\cdot\boldsymbol{\alpha} = \frac{\boldsymbol{U}_b^0}{\left|\boldsymbol{U}_b^0\right|}\cdot\frac{\boldsymbol{U}_b^0}{\left|\boldsymbol{U}_b^0\right|} = \frac{1}{\left|\boldsymbol{U}_b^0\right|^2}\boldsymbol{U}_b^0\cdot\boldsymbol{U}_b^0 = \frac{1}{\left|\boldsymbol{U}_b^0\right|^2}\left(\left(U_b^0\right)^2 + \left(V_b^0\right)^2\right).$$

Therefore, we obtain

$$\theta = \operatorname{Arg} a = \operatorname{Arg}\left(\left(U_b^0\right)^2 + \left(V_b^0\right)^2\right).$$

For $r = 1$, we have $|a| = 1$ and so U_b^0 and V_b^0 have the same phase, say $\varphi = \operatorname{Arg} U_b^0$. We get

$$\theta = \operatorname{Arg}\left(\left|U_b^0\right|^2 + \left|V_b^0\right|^2\right) e^{i2\varphi} = 2\varphi. \tag{B.8.6}$$

Hence, we find the same result as the one flow component case:

$$A_2 = \frac{4}{3\pi} \left|\boldsymbol{U}_b^0\right| e^{i2\varphi}.$$

B.8.1 Practical approximations

The exact solutions of the Fourier coefficients can be expensive to evaluate. Using the minimax approximation algorithm, cheap and accurate approximations of these functions can be constructed as

$$\begin{aligned}
A_0 &\approx f_0(r)\left|\boldsymbol{U}_b^0\right|, \\
A_1 &= 0, \\
A_2 &\approx f_2(r)\left|\boldsymbol{U}_b^0\right| e^{i\theta}, \\
A_3 &= 0,
\end{aligned}$$

where, we have defined the Padé approximants:

$$\begin{aligned}
f_0(r) &= \frac{1.319675833 - 1.241923267r}{1.865818996 + (-1.740781287 + (0.0304939468 + (0.0583267878 - 0.09176029038r)\,r)\,r)\,r}, \\
f_2(r) &= \frac{0.0011553994 + (0.6392220857 - 0.5711563408r)\,r}{1.876856269 + (-1.874289441 + 0.1607692043r)\,r}.
\end{aligned}$$

The maximal error on the interval $0 \le r \le 1$ for $f_0(r)$ and $f_2(r)$ is, respectively, 0.0009188625 and 0.0006172602.

Table B.1: Multiplication table of the harmonic components generated by multiplying the harmonics of $\boldsymbol{n}_b^0$ (top row) by the M_0 and M_4 harmonic components of the first-order velocity $\boldsymbol{u}_b^1 = \boldsymbol{u}_{0b}^1 + \boldsymbol{u}_{2b}^1$ (first column). The generated harmonic components are the sum and difference of the multiplied harmonic components.

	M_2	M_6	M_{10}	M_{14}
M_0	M_2	M_6	M_{10}	M_{14}
M_4	M_6, M_2	M_{10}, M_2	M_{14}, M_6	M_{18}, M_{10}

B.9 Expanding the first-order erosion flux into a Fourier series

To obtain the Fourier coefficients of the first-order erosion flux (3.3.7), Brouwer's method is used, where first the relevant harmonic components are identified before carrying out the computations, making the process more streamlined. Direct computation would give the same result but make the process more mathematical.

The goal is to find the Fourier coefficients B_n that measure for each frequency component how much the first-order velocity points in the same direction as the leading-order velocity. Mathematically, we want to compute the Fourier coefficients of the innerproduct between the leading-order unit vector and the first-order velocity vector:

$$\boldsymbol{n}_b^0 \cdot \boldsymbol{u}_b^1 = \sum_{n=0}^{\infty} \mathfrak{Re}\left(B_n e^{in\omega t}\right).$$

The unit vector pointing in the leading-order velocity direction $\boldsymbol{n}_b^0$ is odd in the leading-order velocity $\boldsymbol{u}_b^0$, since

$$\boldsymbol{n}_b^0\left(-\boldsymbol{u}_b^0\right) = \frac{-\boldsymbol{u}_b^0}{\left|-\boldsymbol{u}_b^0\right|} = -\frac{\boldsymbol{u}_b^0}{\left|\boldsymbol{u}_b^0\right|} = -\boldsymbol{n}_b^0\left(\boldsymbol{u}_b^0\right),$$

where, we have used the definition of $\boldsymbol{n}_b^0$ given by equation (3.2.1). Using that the leading-order flow consists only of an M_2 component, it follows that the leading-order unit vector $\boldsymbol{u}_b^0$ consists of only the odd harmonics of the M_2 frequency. Thus, we have the following expansion:

$$\boldsymbol{n}_b^0(t) = \sum_{n=0}^{\infty} \mathfrak{Re}\left(\boldsymbol{D}_n e^{in\omega t}\right) = \mathfrak{Re}\left(\boldsymbol{D}_1 e^{i\omega t} + \boldsymbol{D}_3 e^{i3\omega t} + \ldots\right).$$

The first-order velocity $\boldsymbol{u}_b^1$ consist of an M_0 and M_4 harmonic component. The harmonics generated by the inner product between $\boldsymbol{n}_b^0$ and the first-order velocity $\boldsymbol{u}_b^1$ are shown in Table B.1. From this table, we see that the even harmonics of their product vanishes. Hence, B_n consists of only the odd harmonics of M_2:

$$\boldsymbol{n}_b^0 \cdot \boldsymbol{u}_b^1 = \sum_{n=0}^{\infty} \mathfrak{Re}\left(B_n e^{in\omega t}\right) = \mathfrak{Re}\left(B_1 e^{i\omega t} + B_3 e^{i3\omega t} + \ldots\right).$$

In other words, since $\boldsymbol{n}_b^0$ consists of only odd harmonics and $\boldsymbol{u}_b^1$ of only even harmonics, we may say that 'odd times even is odd'.

Furthermore, Table B.1 shows which combinations of harmonic components of $\boldsymbol{n}_b^0$ and $\boldsymbol{u}_b^1$, contribute to which harmonic component of their product. Focusing on the generated M_2 signal, it follows that only the M_2 and M_6 components of $\boldsymbol{n}_b^0$ contribute to the M_2 signal of their product. Hence, we are only interested in the Fourier coefficients $\boldsymbol{D}_1$ and $\boldsymbol{D}_3$ of the near-bed unit vector $\boldsymbol{n}_b^0$. Next, we determine the exact dependence of B_1 on the Fourier coefficients $\boldsymbol{D}_1$ and $\boldsymbol{D}_3$.

We can separately consider the $\boldsymbol{n}_b^0 \cdot \boldsymbol{u}_{0b}^1$ and $\boldsymbol{n}_b^0 \cdot \boldsymbol{u}_{2b}^1$ contributions to the M_2 signal and combine the results afterwards. Hence

$$\boldsymbol{n}_b^0 \cdot \boldsymbol{u}_{0b}^1 = \mathfrak{Re}\left(\boldsymbol{D}_1 \cdot \mathfrak{Re}\left(\boldsymbol{U}_{0b}^1\right) e^{i\omega t} + \ldots\right),$$

and

$$\begin{aligned}
\boldsymbol{n}_b^0 \cdot \boldsymbol{u}_{2b}^1 &= \mathfrak{Re}\left\{\boldsymbol{D}_1 e^{i\omega t} + \boldsymbol{D}_3 e^{i3\omega t} + \ldots\right\} \cdot \mathfrak{Re}\left(\boldsymbol{U}_{2b}^1 e^{i2\omega t}\right), \\
&= \mathfrak{Re}\left\{\left(\boldsymbol{D}_1 e^{i\omega t} + \boldsymbol{D}_3 e^{i3\omega t} + \ldots\right) \cdot \mathfrak{Re}\left(\boldsymbol{U}_{2b}^1 e^{i2\omega t}\right)\right\}, \\
&= \mathfrak{Re}\left\{\frac{1}{2}\left(\boldsymbol{D}_1 e^{i\omega t} + \boldsymbol{D}_3 e^{i3\omega t}\right) \cdot \left(\boldsymbol{U}_{2b}^1 e^{i2\omega t} + \left(\boldsymbol{U}_{2b}^1\right)^* e^{-i2\omega t}\right) + \ldots\right\}, \\
&= \mathfrak{Re}\left\{\frac{1}{2}\left(\boldsymbol{D}_1 \cdot \left(\boldsymbol{U}_{2b}^1\right)^* e^{-i\omega t} + \boldsymbol{D}_3 \cdot \left(\boldsymbol{U}_{2b}^1\right)^* e^{i\omega t}\right) + \ldots\right\}, \\
&= \mathfrak{Re}\left\{\frac{1}{2}\left((\boldsymbol{D}_1)^* \cdot \boldsymbol{U}_{2b}^1 e^{i\omega t} + \boldsymbol{D}_3 \cdot \left(\boldsymbol{U}_{2b}^1\right)^* e^{i\omega t}\right) + \ldots\right\}, \\
&= \mathfrak{Re}\left\{\frac{1}{2}\left[(\boldsymbol{D}_1)^* \cdot \boldsymbol{U}_{2b}^1 + \boldsymbol{D}_3 \cdot \left(\boldsymbol{U}_{2b}^1\right)^*\right] e^{i\omega t} + \ldots\right\}.
\end{aligned}$$

Here, we have used the evenness of the cosine:

$$\mathfrak{Re}\left(a e^{i\omega t}\right) = |a| \cos\left(\omega t + \operatorname{Arg} a\right) = |a| \cos\left(-(\omega t + \operatorname{Arg} a)\right) = \mathfrak{Re}\left(a^* e^{-i\omega t}\right),$$

which is the same as the identity $\mathfrak{Re}(z) = \mathfrak{Re}(z^*)$, which holds for all complex z.

Combining these results yields

$$B_1 = \boldsymbol{D}_1 \cdot \mathfrak{Re}\left(\boldsymbol{U}_{0b}^1\right) + \frac{1}{2}(\boldsymbol{D}_1)^* \cdot \boldsymbol{U}_{2b}^1 + \frac{1}{2}\boldsymbol{D}_3 \cdot \left(\boldsymbol{U}_{2b}^1\right)^*. \tag{B.9.1}$$

Our goal is now to determine the Fourier coefficients $\boldsymbol{D}_1$ and $\boldsymbol{D}_3$.

Using the same method as before for each component, we find that the Fourier coefficients of the unit vector $\boldsymbol{n}_b^0$ are given by

$$\boldsymbol{D}_n = \xi_n \frac{1}{T}\int_0^T \frac{\boldsymbol{u}_b^0}{\left|\boldsymbol{u}_b^0\right|} e^{-in\omega t}\, dt.$$

We introduce the nondimensional coordinate $\theta = \omega t$. Using this coordinate transformation, we obtain the integral

$$\boldsymbol{D}_n = \xi_n \frac{1}{2\pi}\int_0^{2\pi} \frac{\mathfrak{Re}\left(\boldsymbol{U}_b^0 e^{i\theta}\right)}{\left|\mathfrak{Re}\left(\boldsymbol{U}_b^0 e^{i\theta}\right)\right|} e^{-in\theta}\, d\theta.$$

We define the complex coordinate $z = e^{i\theta}$, which traces out an unit circle in the complex z-plane for $0 \le \theta \le 2\pi$. We obtain the contour integral

$$\boldsymbol{D}_n = \oint_{|z|=1} \boldsymbol{f}_n(z)\, dz,$$

where we have defined the integrand:

$$\boldsymbol{f}_n(z) = \xi_n \frac{1}{2\pi i} \frac{\mathfrak{Re}\left(\boldsymbol{U}_b^0 z\right)}{\left|\mathfrak{Re}\left(\boldsymbol{U}_b^0 z\right)\right|} \frac{1}{z^{n+1}}.$$

We compute

$$\begin{aligned}
\boldsymbol{f}_n(-z) &= \xi_n \frac{1}{2\pi i} \frac{\mathfrak{Re}\left(\boldsymbol{U}_b^0(-z)\right)}{\left|\mathfrak{Re}\left(\boldsymbol{U}_b^0(-z)\right)\right|} \frac{1}{(-z)^{n+1}}, \\
&= (-1)^{n+1}\xi_n \frac{1}{2\pi i} \frac{(-1)\,\mathfrak{Re}\left(\boldsymbol{U}_b^0 z\right)}{\left|\mathfrak{Re}\left(\boldsymbol{U}_b^0 z\right)\right|} \frac{1}{z^{n+1}}, \\
&= (-1)^n \boldsymbol{f}_n(z).
\end{aligned}$$

Thus for even n, it follows that $(-1)^n = 1$ and, therefore, $\boldsymbol{f}_n(-z) = \boldsymbol{f}_n(z)$. Hence for n even, the function $\boldsymbol{f}_n(z)$ is even. Using that the contour is symmetric around the origin, it follows that the contour integral vanishes for even n (using the same symmetry argument as for the leading-order erosion flux). This confirms our earlier claim that the even Fourier coefficients of $\boldsymbol{D}_n$ vanish. Hence, $\boldsymbol{D}_n$ consists of only the odd harmonics of the M_2 tide. Thus the first non-zero contribution occurs for $n=1$, corresponding to the M_2 signal.

Expanding the real part and norm for $|z|=1$ shows that

$$\boldsymbol{D}_n = \xi_n \frac{1}{2\pi i} \oint_{|z|=1} \frac{\boldsymbol{\alpha} z + \boldsymbol{\alpha}^* \frac{1}{z}}{\sqrt{a z^2 + 2 + a^* \frac{1}{z^2}}} \frac{1}{z^{n+1}}\, dz.$$

We parametrise $a = r\, e^{i\theta}$ and apply the same rotation of the complex plane as before. We define the rotated complex coordinate $w = e^{i\theta/2} z$, to obtain

$$\boldsymbol{D}_n = \xi_n \frac{1}{2\pi i} e^{i n\theta/2} \oint_{|w|=1} \frac{\boldsymbol{\alpha} e^{-i\theta/2} w + \boldsymbol{\alpha}^* e^{i\theta/2} \frac{1}{w}}{\sqrt{2 + r\left(w^2 + \frac{1}{w^2}\right)}} \frac{1}{w^{n+1}}\, dw.$$

This contour integral can be decomposed into two parts

$$\boldsymbol{D}_n = \xi_n \frac{1}{\pi} \left(I_{n-1}\, \boldsymbol{\alpha} e^{i\theta/2(n-1)} + I_{n+1}\, \boldsymbol{\alpha}^* e^{i\theta/2(n+1)} \right),$$

where, we have defined

$$I_n = \frac{1}{2i} \oint_{|w|=1} \frac{1}{\sqrt{2 + r\left(w^2 + \frac{1}{w^2}\right)}} \frac{1}{w^{n+1}}\, dw.$$

For $n=1$ for $\boldsymbol{D}_n$, we get $n=0,2$ for I_n. For $n=3$ for $\boldsymbol{D}_n$, we get $n=2,4$ for I_n.

We have two integrals with a single bounded parameter. We go to the real domain again. Define the coordinate transformation $w = e^{i\theta}$ for dummy variable θ in $[-\pi, \pi]$. We obtain

$$I_n = \frac{1}{2} \int_{-\pi}^{\pi} \frac{1}{\sqrt{2 + 2r\cos 2\theta}} e^{-i n\theta}\, d\theta.$$

For even n for $\boldsymbol{I}_n$, we can use the period, and the even and oddness of the integrand to obtain the formula

$$I_n = 2 \int_0^{\pi/2} \frac{1}{\sqrt{2 + 2r\cos 2\theta}} \cos n\theta\, d\theta.$$

For $n=0$, we get using the double angle formula:

$$I_0 = \frac{2}{\sqrt{2+2r}} K(k),$$

with the same complete elliptic integral of the first kind $K(k)$ and k as before.

For $n=2$, we get

$$I_2 = \frac{2}{r\sqrt{2+2r}} \left[(1+r)E(k) - K(k)\right].$$

Combining, we obtain

$$\begin{aligned} \boldsymbol{D}_1 &= \frac{2}{\pi} \left(I_0\, \boldsymbol{\alpha} + I_2\, \boldsymbol{\alpha}^* e^{i\theta} \right), \\ &= \frac{4}{\pi} \left(\frac{1}{\sqrt{2+2r}} K(k)\, \boldsymbol{\alpha} + \frac{1}{r\sqrt{2+2r}} \left[(1+r)E(k) - K(k)\right] \boldsymbol{\alpha}^* e^{i\theta} \right). \end{aligned}$$

This calculation can also be performed for horizontal flow consisting of a single velocity component. For example, $U_b^0 = |U_b^0| \exp i\varphi \neq 0$ and $V_b^0 = 0$. The exact Fourier coefficient reads

$$\hat{E}_1 = \frac{4}{\pi} e^{i\varphi},$$

For $r = 1$, we found that the phase of the two components of $\boldsymbol{\alpha}$ must be equal, call it $\varphi = \operatorname{Arg} U_b^0$, and we also found that $\theta = 2\varphi$, see Eq. (B.8.6). Expanding yields

$$\boldsymbol{\alpha}^* e^{i\theta} = \begin{bmatrix} r_1 e^{i\varphi} \\ r_2 e^{i\varphi} \end{bmatrix}^* e^{2\varphi} = \begin{bmatrix} r_1 e^{i\varphi} \\ r_2 e^{i\varphi} \end{bmatrix} = \boldsymbol{\alpha}.$$

We get the following limit for $r \to 1$:

$$\boldsymbol{D}_1 = \frac{4}{\pi} \boldsymbol{\alpha}.$$

This reduces exactly to a single flow component case since when considering a single component, we get

$$\alpha_1 = \frac{U_b^0}{|U_b^0|} = e^{i\varphi}.$$

For $n = 4$, we get the following exact solution

$$\begin{aligned} I_4 &= 2\int_0^{\pi/2} \frac{1}{\sqrt{2+2r\cos 2\theta}} \cos 4\theta \, d\theta, \\ &= -\frac{2}{3} \frac{1}{r^2\sqrt{2+2r}} \left[4(1+r)E(k) + \left(r^2-4\right)K(k)\right]. \end{aligned}$$

Combining, we find

$$\begin{aligned} \boldsymbol{D}_3 &= \frac{2}{\pi}\left(I_2\, \boldsymbol{\alpha} e^{i\theta} + I_4\, \boldsymbol{\alpha}^* e^{i2\theta}\right), \\ &= \frac{4}{\pi}\left(\frac{1}{r\sqrt{2+2r}}\left[(1+r)E(k) - K(k)\right] \boldsymbol{\alpha} e^{i\theta} - \frac{1}{3}\frac{1}{r^2\sqrt{2+2r}}\left[4(1+r)E(k) + \left(r^2-4\right)K(k)\right] \boldsymbol{\alpha}^* e^{i2\theta}\right). \end{aligned}$$

For horizontal flow consisting of a single velocity component, e.g., $U_b^0 = |U_b^0| \exp i\varphi \neq 0$ and $V_b^0 = 0$, the exact Fourier coefficient reads

$$\hat{E}_3 = -\frac{4}{3\pi} e^{i3\varphi},$$

In the $r = 1$ limit, we get

$$\boldsymbol{D}_3 = -\frac{4}{3\pi} \boldsymbol{\alpha} e^{i\theta}.$$

Considering a single component yields $\alpha_1 = \exp i\varphi$ and $\theta = 2\varphi$. Thus, we obtain the same result as for a flow consisting of a single velocity component:

$$E_3 = -\frac{4}{3\pi} e^{i3\varphi}.$$

B.9.1 Practical approximations

To summarise, we have derived the following equations for Fourier coefficients B_n using equation (B.9.1):

$$\begin{aligned} B_0 &= 0, \\ B_1 &= \boldsymbol{D}_1 \cdot \Re\mathfrak{e}\left(\boldsymbol{U}_{0b}^1\right) + \frac{1}{2}\left(\boldsymbol{D}_1\right)^* \cdot \boldsymbol{U}_{2b}^1 + \frac{1}{2}\boldsymbol{D}_3 \cdot \left(\boldsymbol{U}_{2b}^1\right)^*, \\ B_2 &= 0. \end{aligned}$$

The corresponding Fourier coefficients $\boldsymbol{D}_n$ read

$$\begin{aligned} \boldsymbol{D}_0 &= 0, \\ \boldsymbol{D}_1 &= \frac{2}{\pi}\left(I_0(r)\, \boldsymbol{\alpha} + I_2(r)\, \boldsymbol{\alpha}^* e^{i\theta}\right), \\ \boldsymbol{D}_2 &= 0, \\ \boldsymbol{D}_3 &= \frac{2}{\pi}\left(I_2\, \boldsymbol{\alpha} e^{i\theta} + I_4\, \boldsymbol{\alpha}^* e^{i2\theta}\right), \\ \boldsymbol{D}_4 &= 0. \end{aligned}$$

The integrals I_n can be expressed as sole functions of r. However, these integrals become singular for r close to 1, with a log singularity. We separately include the singularity, we obtain the following Padé approximants:

$$\begin{aligned}
I_0(r) &\approx \frac{3.694249569 + (-3.343402152 + 0.1256704315r)\,r}{1.663642695 + (-1.148513254 - 0.2403747084r)\,r} - \frac{1}{2}\ln(1 - r + \varepsilon_n),\\
I_2(r) &\approx \frac{-0.00060244784 + (-0.0837643764 + (0.4442844276 - 0.3240069772r)\,r)\,r}{1.927203145 + (-2.111941818 + 0.3216217540r)\,r} + \frac{1}{2}\ln(1 - r + \varepsilon_n),\\
I_4(r) &\approx \frac{-0.00059672002 + (-1.175876043 + (1.790378347 - 0.6310292261r)\,r)\,r}{2.397004301 + (-4.101506231 + 1.722929722r)\,r} - \frac{1}{2}\ln(1 - r + \varepsilon_n).
\end{aligned}$$

The max absolute error of the non-singular parts of $I_0(r)$, $I_2(r)$ and $I_4(r)$ on the interval $0 \le r \le 1$ is given by, respectively, 0.000865877, 0.0003135757 and 0.0002497163. Here, we have added a small numerical parameter ε_n to make sure that for $r = 1$, the singular parts remain bounded such that the situation '0/0' is avoided numerically.

B.10 Derivatives of the coefficients of the forced water motion

To compute some higher-order moments of the forced water motion, horizontal and vertical derivatives of the corresponding coefficients are required. These terms are computed and summarised here.

B.10.1 Horizontal derivatives of $\mathrm{C}^0_{n,ii}(z)$

We need to explicitly compute the horizontal derivatives of $\mathrm{C}^0_{n,ii}(z)$ in order to construct the matrix $\hat{\nabla}\mathbf{C}^0_n(z)$. Denote the horizontal coordinates as $x_1 = x$ and $x_2 = y$, such that we can denote them using a single subscript, i.e., x_j for $j = 1,2$. The horizontal derivatives of $\mathrm{C}^0_{n,ii}(z)$ can then be denoted as $\mathrm{C}^0_{n,ii,x_j}(z)$ for $j = 1,2$, $i = 1,2$ and $n \in \mathbb{N}_0$.

Using the chain rule and matrix calculus notation, we can expand the horizontal derivate of $\mathrm{C}^0_{n,ii}(z)$ with respect to x_j as

$$\mathrm{C}^0_{n,ii,x_j}(z) = \frac{d\mathrm{C}^0_{n,ii}}{d\boldsymbol{\phi}^0}(z)\,\frac{\partial\boldsymbol{\phi}^0}{\partial x_j},$$

with

$$\frac{d\mathrm{C}^0_{n,ii}}{d\boldsymbol{\phi}^0}(z) = \begin{bmatrix} \frac{d\mathrm{C}^0_{n,ii}}{dA^0_\nu}(z) & \frac{d\mathrm{C}^0_{n,ii}}{ds^0_f}(z) & \frac{d\mathrm{C}^0_{n,ii}}{dH}(z) & \frac{d\mathrm{C}^0_{n,ii}}{dR}(z) \end{bmatrix},$$

and

$$\frac{\partial\boldsymbol{\phi}^0}{\partial x_j} = \begin{bmatrix} A^0_{\nu,x_j} & s^0_{f,x_j} & H_{x_j} & R_{x_j} \end{bmatrix}^T.$$

It turns out that directly calculating derivative with respect to these components already leads to quite involved expressions. To make the resulting expressions a little more readable, we use the chain rule a second time. This yields

$$\frac{d\mathrm{C}^0_{n,ii}}{d\boldsymbol{\phi}^0}(z) = \frac{\partial\mathrm{C}^0_{n,ii}}{\partial\boldsymbol{\phi}^0}(z) + \frac{\partial\mathrm{C}^0_{n,ii}}{\partial\boldsymbol{\vartheta}^0_{n,i}}(z)\frac{d\boldsymbol{\vartheta}^0_{n,i}}{d\boldsymbol{\phi}^0},$$

where we have defined the vectors

$$\frac{\partial\mathrm{C}^0_{n,ii}}{\partial\boldsymbol{\phi}^0}(z) = \begin{bmatrix} \frac{\partial\mathrm{C}^0_{n,ii}}{\partial A^0_\nu}(z) & \frac{\partial\mathrm{C}^0_{n,ii}}{\partial s^0_f}(z) & \frac{\partial\mathrm{C}^0_{n,ii}}{\partial H} & \frac{\partial\mathrm{C}^0_{n,ii}}{\partial R}(z) \end{bmatrix},$$

$$\boldsymbol{\vartheta}^0_{n,i} = \begin{bmatrix} \alpha^0_{n,ii} & \beta^0_{n,ii} \end{bmatrix}^T,$$

$$\frac{\partial\mathrm{C}^0_{n,ii}}{\partial\boldsymbol{\vartheta}^0_{n,i}}(z) = \begin{bmatrix} \frac{\partial\mathrm{C}^0_{n,ii}}{\partial\alpha^0_{n,ii}}(z) & \frac{\partial\mathrm{C}^0_{n,ii}}{\partial\beta^0_{n,ii}}(z) \end{bmatrix},$$

and the matrix

$$\frac{d\boldsymbol{\vartheta}^0_{n,i}}{d\boldsymbol{\phi}^0} = \begin{bmatrix} \frac{\partial\alpha^0_{n,ii}}{\partial A^0_\nu} & \frac{\partial\alpha^0_{n,ii}}{\partial s^0_f} & \frac{\partial\alpha^0_{n,ii}}{\partial H} & \frac{\partial\alpha^0_{n,ii}}{\partial R} \\ \frac{d\beta^0_{n,ii}}{dA^0_\nu} & \frac{\partial\beta^0_{n,ii}}{\partial s^0_f} & \frac{\partial\beta^0_{n,ii}}{\partial H} & \frac{\partial\beta^0_{n,ii}}{\partial R} \end{bmatrix}.$$

Here, the derivative of $\beta^0_{n,ii}$ w.r.t. A^0_ν remains the total derivative as it still depends on A^0_ν through $\alpha^0_{n,ii}$.

Thus, we can compute the horizontal derivative of $\mathrm{C}^0_{n,ii}(z)$ with respect to x_j as

$$\mathrm{C}^0_{n,ii,x_j}(z) = \left(\frac{\partial\mathrm{C}^0_{n,ii}}{\partial\boldsymbol{\phi}^0}(z) + \frac{\partial\mathrm{C}^0_{n,ii}}{\partial\boldsymbol{\vartheta}^0_{n,i}}(z)\frac{d\boldsymbol{\vartheta}^0_{n,i}}{d\boldsymbol{\phi}^0}\right)\frac{\partial\boldsymbol{\phi}^0}{\partial x_j}.$$

Next, we consider each vector separately and explicitly compute the stated derivatives.

Consider $\partial \mathrm{C}^0_{n,ii}/\partial \boldsymbol{\phi}^0(z)$ We have

$$\frac{\partial \mathrm{C}^0_{n,ii}}{\partial \boldsymbol{\phi}^0}(z) = \begin{bmatrix} -\dfrac{1}{A^0_v}\mathrm{C}^0_{n,ii}(z) \\ \dfrac{g\beta^0_{n,ii}}{A^0_v\left(\alpha^0_{n,ii}\right)^3}\left[\sinh\left(\alpha^0_{n,ii}(z-R)\right)+\sinh\left(\alpha^0_{n,ii}D\right)\right] \\ \dfrac{g}{A^0_v\left(\alpha^0_{n,ii}\right)^2}\left\{s^0_f\beta^0_{n,ii}\cosh\left(\alpha^0_{n,ii}D\right)-1\right\} \\ \dfrac{g s^0_f\beta^0_{n,ii}}{A^0_v\left(\alpha^0_{n,ii}\right)^2}\left\{-\cosh\left(\alpha^0_{n,ii}(z-R)\right)+\cosh\left(\alpha^0_{n,ii}D\right)\right\} \end{bmatrix}^T.$$

Consider $\partial \mathrm{C}^0_{n,ii}/\partial \boldsymbol{\vartheta}^0_{n,i}(z)$ It follows that

$$\frac{\partial \mathrm{C}^0_{n,ii}}{\partial \boldsymbol{\vartheta}^0_{n,i}}(z) = \begin{bmatrix} -\dfrac{2}{\alpha^0_{n,ii}}\mathrm{C}^0_{n,ii}(z)+\dfrac{g s^0_f\beta^0_{n,ii}}{A^0_v\left(\alpha^0_{n,ii}\right)^3}\left\{-\dfrac{1}{\alpha^0_{n,ii}}\left[\sinh\left(\alpha^0_{n,ii}(z-R)\right)+\sinh\left(\alpha^0_{n,ii}D\right)\right]\right. \\ \qquad\qquad \left.+(z-R)\cosh\left(\alpha^0_{n,ii}(z-R)\right)+D\cosh\left(\alpha^0_{n,ii}D\right)\right\} \\ \dfrac{g s^0_f}{A^0_v\left(\alpha^0_{n,ii}\right)^3}\left[\sinh\left(\alpha^0_{n,ii}(z-R)\right)+\sinh\left(\alpha^0_{n,ii}D\right)\right] \end{bmatrix}^T.$$

Here, the first component of the vector is too large to be displayed on a single line. Thus, we have chosen to put the remaining part on the next line.

Consider $d\boldsymbol{\vartheta}^0_{n,i}/d\boldsymbol{\phi}^0$ This matrix reads

$$\frac{d\boldsymbol{\vartheta}^0_{n,i}}{d\boldsymbol{\phi}^0} = \begin{bmatrix} -\dfrac{1}{2A^0_v}\alpha^0_{n,ii} & \dfrac{d\beta^0_{n,ii}}{dA^0_v} \\ 0 & -\left(\beta^0_{n,ii}\right)^2\cosh\left(\alpha^0_{n,ii}D\right) \\ 0 & -\alpha^0_{n,ii}\left(\beta^0_{n,ii}\right)^2\left[A^0_v\alpha^0_{n,ii}\cosh\left(\alpha^0_{n,ii}D\right)+s^0_f\sinh\left(\alpha^0_{n,ii}D\right)\right] \\ 0 & -\alpha^0_{n,ii}\left(\beta^0_{n,ii}\right)^2\left[A^0_v\alpha^0_{n,ii}\cosh\left(\alpha^0_{n,ii}D\right)+s^0_f\sinh\left(\alpha^0_{n,ii}D\right)\right] \end{bmatrix}^T,$$

where

$$\frac{d\beta^0_{n,ii}}{dA^0_v} = \frac{\partial\beta^0_{n,ii}}{\partial A^0_v}+\frac{\partial\beta^0_{n,ii}}{\partial\alpha^0_{n,ii}}\frac{\partial\alpha^0_{n,ii}}{\partial A^0_v},$$

with

$$\frac{\partial\beta^0_{n,ii}}{\partial A^0_v} = -\alpha^0_{n,ii}\left(\beta^0_{n,ii}\right)^2\sinh\left(\alpha^0_{n,ii}D\right),$$

and

$$\frac{\partial\beta^0_{n,ii}}{\partial\alpha^0_{n,ii}} = -\left(\beta^0_{n,ii}\right)^2\left\{A^0_v\left[\sinh\left(\alpha^0_{n,ii}D\right)+D\alpha^0_{n,ii}\cosh\left(\alpha^0_{n,ii}D\right)\right]+s^0_f D\sinh\left(\alpha^0_{n,ii}D\right)\right\}.$$

The term $\partial\alpha^0_{n,ii}/\partial A^0_v$ can be found in the matrix.

Depth-integration of $\mathrm{C}^0_{n,ii}(z)$ and $\hat{\nabla}\mathbf{C}^0_n(z)$

We compute the depth-integrals of $\mathrm{C}^0_{n,ii}(z)$ and $\hat{\nabla}\mathbf{C}^0_n(z)$ in order to construct the matrix $\hat{\boldsymbol{\mathcal{K}}}\mathbf{C}^0_n(z)$.

The depth-integral of $\mathrm{C}^0_{n,ii}(z)$ reads

$$\int_{-H}^{z} \mathrm{C}^0_{n,ii}(\tilde{z})\,d\tilde{z} = \frac{g}{A^0_v\left(\alpha^0_{n,ii}\right)^2}\left\{\frac{s^0_f\beta^0_{n,ii}}{\alpha^0_{n,ii}}\left[\frac{1}{\alpha^0_{n,ii}}\Big(\cosh\big(\alpha^0_{n,ii}(z-R)\big)-\cosh\big(\alpha^0_{n,ii}D\big)\Big)+(z+H)\sinh\big(\alpha^0_{n,ii}D\big)\right]\right.$$
$$\left.-\frac{1}{2}(z+H)^2\right\}.$$

For the depth-integral of $\hat{\nabla}\mathbf{C}^0_n(z)$, we may separately consider the depth integral of the horizontal derivative of $\mathrm{C}^0_{n,ii}(z)$ with respect to x_j for $i=1,2$ and $j=1,2$. We have for the depth-integral of the horizontal derivative of $\mathrm{C}^0_{n,ii}(z)$ to x_j that

$$\int_{-H}^{z} \mathrm{C}^0_{n,ii,x_j}(\tilde{z})\,d\tilde{z} = \left(\int_{-H}^{z}\frac{\partial \mathrm{C}^0_{n,ii}}{\partial \boldsymbol{\phi}^0}(\tilde{z})\,d\tilde{z} + \int_{-H}^{z}\frac{\partial \mathrm{C}^0_{n,ii}}{\partial \boldsymbol{\vartheta}^0_{n,i}}(\tilde{z})\,d\tilde{z}\,\frac{d\boldsymbol{\vartheta}^0_{n,i}}{d\boldsymbol{\phi}^0}\right)\frac{\partial \boldsymbol{\phi}^0}{\partial x_j}.$$

Thus using the chain rule twice, we find that we only need to consider the depth-integral of the vectors $\partial\mathrm{C}^0_{n,ii}/\partial\boldsymbol{\phi}^0(z)$ and $\partial\mathrm{C}^0_{n,ii}/\partial\boldsymbol{\vartheta}^0_{n,i}(z)$ since the other vectors do not depend on z. We consider the first z-dependent vector:

$$\int_{-H}^{z}\frac{\partial \mathrm{C}^0_{n,ii}}{\partial \boldsymbol{\phi}^0}(\tilde{z})\,d\tilde{z} = \begin{bmatrix} -\dfrac{1}{A^0_v}\displaystyle\int_{-H}^{z}\mathrm{C}^0_{n,ii}(\tilde{z})\,d\tilde{z} \\ \dfrac{g\beta^0_{n,ii}}{A^0_v\left(\alpha^0_{n,ii}\right)^3}\left\{\dfrac{1}{\alpha^0_{n,ii}}\Big[\cosh\big(\alpha^0_{n,ii}(z-R)\big)-\cosh\big(\alpha^0_{n,ii}D\big)\Big]+(z+H)\sinh\big(\alpha^0_{n,ii}D\big)\right\} \\ (z+H)\dfrac{\partial \mathrm{C}^0_{n,ii}}{\partial H} \\ \dfrac{gs^0_f\beta^0_{n,ii}}{A^0_v\left(\alpha^0_{n,ii}\right)^2}\left\{-\dfrac{1}{\alpha^0_{n,ii}}\Big[\sinh\big(\alpha^0_{n,ii}(z-R)\big)+\sinh\big(\alpha^0_{n,ii}D\big)\Big]+(z+H)\cosh\big(\alpha^0_{n,ii}D\big)\right\}\end{bmatrix}^T.$$

Next, we consider the depth-integral of the second z-dependent vector:

$$\int_{-H}^{z}\frac{\partial \mathrm{C}^0_{n,ii}}{\partial \boldsymbol{\vartheta}^0_{n,i}}(\tilde{z})\,d\tilde{z} = \begin{bmatrix} -\dfrac{2}{\alpha^0_{n,ii}}\displaystyle\int_{-H}^{z}\mathrm{C}^0_{n,ii}(\tilde{z})\,d\tilde{z} \\ +\dfrac{gs^0_f\beta^0_{n,ii}}{A^0_v\left(\alpha^0_{n,ii}\right)^3}\left\{-\dfrac{2}{\left(\alpha^0_{n,ii}\right)^2}\Big[\cosh\big(\alpha^0_{n,ii}(z-R)\big)-\cosh\big(\alpha^0_{n,ii}D\big)\Big]\right. \\ +\dfrac{1}{\alpha^0_{n,ii}}\Big[(z-R)\sinh\big(\alpha^0_{n,ii}(z-R)\big)-(z+H+D)\sinh\big(\alpha^0_{n,ii}D\big)\Big] \\ \left.+(z+H)D\cosh\big(\alpha^0_{n,ii}D\big)\right\} \\ \dfrac{gs^0_f}{A^0_v\left(\alpha^0_{n,ii}\right)^3}\left\{\dfrac{1}{\alpha^0_{n,ii}}\Big[\cosh\big(\alpha^0_{n,ii}(z-R)\big)-\cosh\big(\alpha^0_{n,ii}D\big)\Big]+(z+H)\sinh\big(\alpha^0_{n,ii}D\big)\right\}\end{bmatrix}^T.$$

This concludes the horizontal derivatives and depth-integration of $\mathrm{C}^0_{n,ii}(z)$. Thus the vertical velocity W and the depth-integrated vertical velocity $\mathcal{W}$ can be now be computed.

It turns out that when deriving the first-order advective analytical solution, we also need the horizontal derivatives of $\mathrm{c}^0_{n,ii}(z)$ and for the first-order no-stress analytical solution, we need the second-order vertical derivative of $\mathrm{c}^0_{n,ii}(z)$. Computing these derivatives is the subject of the next two sections.

Horizontal derivatives of $\mathrm{c}^0_{n,ii}(z)$

In this section, the horizontal derivatives of $\mathrm{c}^0_{n,ii}(z)$ are computed. Again, using the chain rule and matrix calculus notation, we can expand the horizontal derivate of $\mathrm{c}^0_{n,ii}$ with respect to x_j as

$$\mathrm{c}^0_{n,ii,x_j}(z) = \frac{d\mathrm{c}^0_{n,ii}}{d\boldsymbol{\phi}^0}(z)\,\frac{\partial \boldsymbol{\phi}^0}{\partial x_j},$$

with

$$\frac{d\mathrm{c}^0_{n,ii}}{d\boldsymbol{\phi}^0}(z) = \begin{bmatrix} \frac{d\mathrm{c}^0_{n,ii}}{dA^0_v}(z) & \frac{d\mathrm{c}^0_{n,ii}}{ds^0_f}(z) & \frac{d\mathrm{c}^0_{n,ii}}{dH}(z) & \frac{d\mathrm{c}^0_{n,ii}}{dR}(z) \end{bmatrix},$$

and

$$\frac{\partial\boldsymbol{\phi}^0}{\partial x_j} = \begin{bmatrix} A^0_{v,x_j} & s^0_{f,x_j} & H_{x_j} & R_{x_j} \end{bmatrix}^T.$$

Again, directly calculating the derivative with respect to these components already leads to quite involved expressions. To make the resulting expressions more readable, we use the chain rule a second time. This yields

$$\frac{d\mathrm{c}^0_{n,ii}}{d\boldsymbol{\phi}^0}(z) = \frac{\partial\mathrm{c}^0_{n,ii}}{\partial\boldsymbol{\phi}^0}(z) + \frac{\partial\mathrm{c}^0_{n,ii}}{\partial\boldsymbol{\vartheta}^0_{n,i}}(z)\frac{d\boldsymbol{\vartheta}^0_{n,i}}{d\boldsymbol{\phi}^0},$$

where we have defined the vectors

$$\begin{aligned} \frac{\partial\mathrm{c}^0_{n,ii}}{\partial\boldsymbol{\phi}^0}(z) &= \begin{bmatrix} \frac{\partial\mathrm{c}^0_{n,ii}}{\partial A^0_v}(z) & \frac{\partial\mathrm{c}^0_{n,ii}}{\partial s^0_f}(z) & \frac{\partial\mathrm{c}^0_{n,ii}}{\partial H}(z) & \frac{\partial\mathrm{c}^0_{n,ii}}{\partial R}(z) \end{bmatrix}, \\ \boldsymbol{\vartheta}^0_{n,i} &= \begin{bmatrix} \alpha^0_{n,ii} & \beta^0_{n,ii} \end{bmatrix}^T, \\ \frac{\partial\mathrm{c}^0_{n,ii}}{\partial\boldsymbol{\vartheta}^0_{n,i}}(z) &= \begin{bmatrix} \frac{\partial\mathrm{c}^0_{n,ii}}{\partial\alpha^0_{n,ii}}(z) & \frac{\partial\mathrm{c}^0_{n,ii}}{\partial\beta^0_{n,ii}}(z) \end{bmatrix}, \end{aligned}$$

and the matrix

$$\frac{d\boldsymbol{\vartheta}^0_{n,i}}{d\boldsymbol{\phi}^0} = \begin{bmatrix} \frac{\partial\alpha^0_{n,ii}}{\partial A^0_v} & \frac{\partial\alpha^0_{n,ii}}{\partial s^0_f} & \frac{\partial\alpha^0_{n,ii}}{\partial H} & \frac{\partial\alpha^0_{n,ii}}{\partial R} \\ \frac{d\beta^0_{n,ii}}{dA^0_v} & \frac{\partial\beta^0_{n,ii}}{\partial s^0_f} & \frac{\partial\beta^0_{n,ii}}{\partial H} & \frac{\partial\beta^0_{n,ii}}{\partial R} \end{bmatrix}.$$

Here, the derivative of $\beta^0_{n,ii}$ w.r.t. A^0_v remains the total derivative as it still depends on A^0_v through $\alpha^0_{n,ii}$.

Thus, we can compute the horizontal derivative of $\mathrm{c}^0_{n,ii}(z)$ with respect to x_j as

$$\mathrm{c}^0_{n,ii,x_j}(z) = \left(\frac{\partial\mathrm{c}^0_{n,ii}}{\partial\boldsymbol{\phi}^0}(z) + \frac{\partial\mathrm{c}^0_{n,ii}}{\partial\boldsymbol{\vartheta}^0_{n,i}}(z)\frac{d\boldsymbol{\vartheta}^0_{n,i}}{d\boldsymbol{\phi}^0}\right)\frac{\partial\boldsymbol{\phi}^0}{\partial x_j},$$

which is completely analogous to the horizontal derivative of $\mathrm{C}^0_{n,ii}(z)$ with respect to x_j.

Next, we consider the vectors $\partial\mathrm{c}^0_{n,ii}/\partial\boldsymbol{\phi}^0(z)$ and $\partial\mathrm{c}^0_{n,ii}/\partial\boldsymbol{\vartheta}^0_{n,i}(z)$ separately and compute the stated derivatives. The matrix $d\boldsymbol{\vartheta}^0_{n,i}/d\boldsymbol{\phi}^0$ has already been computed for the horizontal derivative of $\mathrm{C}^0_{n,ii}(z)$.

Consider $\partial\mathrm{c}^0_{n,ii}/\partial\boldsymbol{\phi}^0(z)$ We have

$$\frac{\partial\mathrm{c}^0_{n,ii}}{\partial\boldsymbol{\phi}^0}(z) = \begin{bmatrix} -\frac{1}{A^0_v}\mathrm{c}^0_{n,ii}(z) \\ \frac{g\beta^0_{n,ii}}{A^0_v(\alpha^0_{n,ii})^2}\cosh\big(\alpha^0_{n,ii}(z-R)\big) \\ 0 \\ -\frac{gs^0_f\beta^0_{n,ii}}{A^0_v\alpha^0_{n,ii}}\sinh\big(\alpha^0_{n,ii}(z-R)\big) \end{bmatrix}^T.$$

Here, we have used that $\mathrm{c}^0_{n,ii}(z)$ does not depend on H such that this partial derivative vanishes.

Consider $\partial \mathrm{c}^0_{n,ii} / \partial \boldsymbol{\vartheta}^0_{n,i}(z)$ It follows that

$$\frac{\partial \mathrm{c}^0_{n,ii}}{\partial \boldsymbol{\vartheta}^0_{n,i}}(z) = \begin{bmatrix} -\frac{2}{\alpha^0_{n,ii}} \mathrm{c}^0_{n,ii}(z) + \frac{g s^0_f \beta^0_{n,ii}}{A^0_v \left(\alpha^0_{n,ii}\right)^2}(z-R)\sinh\left(\alpha^0_{n,ii}(z-R)\right) \\ \frac{g s^0_f}{A^0_v \left(\alpha^0_{n,ii}\right)^2}\cosh\left(\alpha^0_{n,ii}(z-R)\right) \end{bmatrix}^T.$$

Vertical derivatives of $\mathrm{c}^0_{n,ii}(z)$

The no-stress analytic solution depends on the forcing $\boldsymbol{\chi}^1_n$. This forcing in turn depends on the second-order derivative of $\boldsymbol{U}$ with respect to the vertical coordinate z. We start by computing the first-order vertical derivative:

$$\boldsymbol{U}^0_{n,z}(z) = \mathbf{P}\,\mathbf{c}^0_{n,z}(z)\,\mathbf{P}^* \nabla Z^0_n,$$

since the vertical derivative is just a scalar and the matrix $\mathbf{c}^0_n(z)$ is the only z dependent quantity.

Similarly for the second-order vertical derivative:

$$\boldsymbol{U}^0_{n,zz}(z) = \mathbf{P}\,\mathbf{c}^0_{n,zz}(z)\,\mathbf{P}^* \nabla Z^0_n.$$

Next, we calculate the entries of matrices $\mathbf{c}^0_{n,z}(z)$ and $\mathbf{c}^0_{n,zz}(z)$. We first calculate $\mathrm{c}^0_{n,ii,z}(z)$ for $i = 1, 2$:

$$\mathrm{c}^0_{n,ii,z}(z) = \frac{g s^0_f \beta^0_{n,ii}}{A^0_v \alpha^0_{n,ii}} \sinh\left(\alpha^0_{n,ii}(z-R)\right),$$

and $\mathrm{c}^0_{n,ii,zz}(z)$ follows analogously

$$\mathrm{c}^0_{n,ii,zz}(z) = \frac{g s^0_f \beta^0_{n,ii}}{A^0_v} \cosh\left(\alpha^0_{n,ii}(z-R)\right).$$

B.11 Deriving the advective analytic solution

We consider the advective forcing $f = \eta$ separately under the standard forcing conditions, see Section 1.7. For $n = 0, 2$, the differential equation reads

$$\check{\boldsymbol{R}}^{1,\eta}_{n,zz}(z) - \left(\boldsymbol{\alpha}^0_n\right)^2 \check{\boldsymbol{R}}^{1,\eta}_n(z) = \frac{1}{A^0_v}\, \mathbf{P}^* \boldsymbol{\eta}^1_n(z),$$

with boundary conditions

$$\begin{aligned} A^0_v \check{\boldsymbol{R}}^{1,\eta}_{n,z}(z) &= \mathbf{0}, && \text{at} \quad z = R, \\ A^0_v \check{\boldsymbol{R}}^{1,\eta}_{n,z}(z) &= s^0_f \check{\boldsymbol{R}}^{1,\eta}_n(z), && \text{at} \quad z = -H. \end{aligned}$$

We decompose the advective forcing into a *horizontal* and a *vertical* advective component:

$$\boldsymbol{\eta}^1_n(z) = \boldsymbol{\eta}^{1,u}_n(z) + \boldsymbol{\eta}^{1,w}_n(z),$$

where we have defined the components

$$\boldsymbol{\eta}^{1,u}_n = \frac{1}{2}\, \boldsymbol{U}^{0,\overline{n}}_1(z) \cdot \nabla \boldsymbol{U}^0_1(z), \qquad \boldsymbol{\eta}^{1,w}_n = \frac{1}{2}\, W^0_1(z)\, \boldsymbol{U}^{0,\overline{n}}_{1,z}(z).$$

Here, we have defined a new type of index $\overline{n}$. This index is a compact notation to indicate whether a quantity should be complex conjugated based on the value of n. For $n = 0$, the superscript $\overline{0}$ indicates applying the complex conjugate and for $n = 2$, the superscript $\overline{2}$ indicates applying the identity operator, i.e., doing nothing. In equation form, this can be expressed as

$$[\,\cdot\,]^{\overline{0}} = \overline{[\,\cdot\,]}, \qquad [\,\cdot\,]^{\overline{2}} = [\,\cdot\,].$$

Similar to the construction of the advective forcing, the forcing rotating flow variables can be decomposed into a horizontal and vertical component:

$$\check{\boldsymbol{R}}^{1,\eta}_n(z) = \check{\boldsymbol{R}}^{1,\eta,u}_n(z) + \check{\boldsymbol{R}}^{1,\eta,w}_n(z).$$

Both of which can be further divided into a particular and homogenous solution:

$$\check{\boldsymbol{R}}^{1,\eta,u}_n(z) = \check{\boldsymbol{R}}^{1,\eta,u,p}_n(z) + \check{\boldsymbol{R}}^{1,\eta,u,h}_n(z), \qquad \check{\boldsymbol{R}}^{1,\eta,w}_n(z) = \check{\boldsymbol{R}}^{1,\eta,w,p}_n(z) + \check{\boldsymbol{R}}^{1,\eta,w,h}_n(z).$$

For $n = 0, 2$ and $v = u, w$, the particular solution satisfies the inhomogeneous differential equation,

$$\check{\boldsymbol{R}}^{1,\eta,v,p}_{n,zz}(z) - \left(\boldsymbol{\alpha}^0_n\right)^2 \check{\boldsymbol{R}}^{1,\eta,v,p}_n(z) = \boldsymbol{F}^{1,\eta,v}_n(z),$$

and does not satisfy any boundary conditions. Here, we have defined the advective forcing vector

$$\boldsymbol{F}^{1,\eta,v}_n(z) = \frac{1}{A^0_v}\, \mathbf{P}^* \boldsymbol{\eta}^{1,v}_n(z).$$

The homogenous solution, on the other hand, satisfies the homogenous differential equation with inhomogeneous boundary conditions. These boundary conditions are constructed such that the sum of the particular and the homogenous solution satisfy the original boundary conditions.

We first construct the particular solutions. Then, we construct the homogeneous solutions because they depend on the particular solutions through the boundary conditions.

Deriving particular analytic solutions for the advective forcing components turns out te be quite involved endeavour. We therefore start by considering the vertical advective forcing $\boldsymbol{\eta}^{1,w}_n(z)$ because this derivation is slightly simpler. Then, we consider the slightly more complicated horizontal advective forcing $\boldsymbol{\eta}^{1,u}_n(z)$. Both derivations are quite similar and follow an analogous solution procedure.

B.11.1 Constructing a particular solution for the vertical advective forcing

We consider the vertical advective forcing for $n = 0, 2$. This forcing is given by

$$\boldsymbol{\eta}_n^{1,w} = \frac{1}{2}\, W_1^0(z)\, \boldsymbol{U}_{1,z}^{0,\overline{n}}(z).$$

The vertical advective forcing depends on the vector $\boldsymbol{U}_{1,z}^{0,\overline{n}}(z)$. This vector can be expanded as

$$\boldsymbol{U}_{1,z}^{0,\overline{n}}(z) = \mathbf{P}^{\overline{n}}\, \mathbf{c}_{1,z}^{0,\overline{n}}(z)\, \mathbf{P}^{*,\overline{n}}\, \nabla Z_1^{0,\overline{n}},$$

where we have used that $\boldsymbol{U}_{1,z}^{0}(z) = \mathbf{P}\,\mathbf{c}_{1,z}^{0}(z)\,\mathbf{P}^*\nabla Z_1^0$ and that the index operator $\overline{n}$ is distributive over multiplication since the underlying complex conjugate and identity operators are distributive over multiplication.

The matrices $\mathbf{P}^{\overline{n}}$, $\mathbf{P}^{*,\overline{n}}$ and the vector $\nabla Z_1^{0,\overline{n}}$ may be simplified by considering the operator $\overline{n}$ element wise. This yields new quantities that can be indexed by the superscript n. Thus, define the matrices $\mathbf{P}^n = \mathbf{P}^{\overline{n}}$, $\mathbf{P}^{*,n} = \mathbf{P}^{*,\overline{n}}$ and the vector $\nabla Z_1^{0,n} = \nabla Z_1^{0,\overline{n}}$. It follows that these indexed quantities can be expressed as

$$\mathbf{P}^n = \frac{1}{\sqrt{2}}\begin{bmatrix} 1 & 1 \\ -i^{n+3} & i^{n+3}\end{bmatrix}, \qquad \mathbf{P}^{*,n} = \frac{1}{\sqrt{2}}\begin{bmatrix} 1 & i^{n+3} \\ 1 & -i^{n+3}\end{bmatrix}, \qquad \nabla Z_1^{0,n} = \mathfrak{Re}\{\nabla Z_1^0\} + i^{n+3}\,\mathfrak{Im}\{\nabla Z_1^0\}.$$

We note that the powers of i in these expressions are not unique since $i^4 = 1$, so we can always add or subtract any multiple of 4 to the power of i^{n+3}. Furthermore, $i^2 = -1$, hence we can always add or subtract 2 to the power of i^{n+3} at the expense of a minus sign. Finally, one could consider changing the index to $-n$.

Thus, define the indexed vector as $\boldsymbol{U}_{1,z}^{0,n}(z) = \boldsymbol{U}_{1,z}^{0,\overline{n}}(z)$, then it follows that we have derived that

$$\boldsymbol{U}_{1,z}^{0,n}(z) = \mathbf{P}^{n}\, \mathbf{c}_{1,z}^{0,\overline{n}}(z)\, \mathbf{P}^{*,n}\, \nabla Z_1^{0,n}.$$

We want to stress that the superscript n without the bar is just a regular superscript.

To construct a particular solution for this differential equation, the exact z-dependency of right-hand side forcing needs to be known. Therefore, we want to isolate this z-dependency. In principle, one could write out all matrix multiplications element wise. However, this would result in expressions that are not very insightful and very complex. Instead, we work with the z-dependent matrices directly.

The advective forcing related to W can be expanded as

$$\begin{aligned}
\boldsymbol{F}_n^{1,\eta,w}(z) &= \frac{1}{A_v^0}\,\mathbf{P}^*\boldsymbol{\eta}_n^{1,w}(z), \\
&= \frac{1}{2A_v^0}\,\mathbf{P}^*\boldsymbol{U}_{1,z}^{0,n}(z)\, W_1^0(z), \\
&= \frac{1}{2A_v^0}\,\mathbf{P}^*\Big(\mathbf{P}^n\,\mathbf{c}_{1,z}^{0,\overline{n}}(z)\,\mathbf{P}^{*,n}\,\nabla Z_1^{0,n}\Big)\Big(-\frac{1}{2}\,\mathrm{tr}\big(\mathbf{C}_1^0(z)\big)\Delta Z_1^0 - \check{\boldsymbol{P}}^*\hat{\nabla}\mathbf{C}_1^0(z)\,\mathbf{P}^*\nabla Z_1^0\Big), \\
&= -\frac{1}{2A_v^0}\,(\mathbf{P}^*\mathbf{P}^n)\left[\mathbf{c}_{1,z}^{0,\overline{n}}(z)\,\mathrm{tr}\big(\mathbf{C}_1^0(z)\big)\frac{1}{2}\Delta Z_1^0\,\mathbf{P}^{*,n}\,\nabla Z_1^{0,n} + \mathbf{c}_{1,z}^{0,\overline{n}}(z)\,(\mathbf{P}^{*,n}\,\nabla Z_1^{0,n}\,\check{\boldsymbol{P}}^*)\hat{\nabla}\mathbf{C}_1^0(z)\,\mathbf{P}^*\nabla Z_1^0\right], \\
&= -\frac{1}{2A_v^0}\,\mathscr{I}_2^n\left[\mathbf{c}_{1,z}^{0,\overline{n}}(z)\,\mathrm{tr}\big(\mathbf{C}_1^0(z)\big)\Big(\frac{1}{2}\Delta Z_1^0\,\mathbf{P}^{*,n}\,\nabla Z_1^{0,n}\Big) + \mathbf{c}_{1,z}^{0,\overline{n}}(z)\,\hat{\mathbf{G}}_n^1\hat{\nabla}\mathbf{C}_1^0(z)\,\big(\mathbf{P}^*\nabla Z_1^0\big)\right], \\
&= -\frac{1}{2A_v^0}\,\mathscr{I}_2^n\begin{bmatrix}\mathbf{c}_{1,z}^{0,\overline{n}}(z)\,\mathrm{tr}\big(\mathbf{C}_1^0(z)\big) & \mathbf{c}_{1,z}^{0,\overline{n}}(z)\,\hat{\mathbf{G}}_n^1\hat{\nabla}\mathbf{C}_1^0(z)\end{bmatrix}\begin{bmatrix}\frac{1}{2}\Delta Z_1^0\,\mathbf{P}^{*,n}\,\nabla Z_1^{0,n} \\ \mathbf{P}^*\nabla Z_1^0\end{bmatrix}, \\
&= -\frac{1}{2A_v^0}\,\mathscr{I}_2^n\,\hat{\mathcal{C}}_n^1(z)\,\boldsymbol{H}_n^1.
\end{aligned}$$

Here, we have used that

$$W_1^0(z) = -\frac{1}{2}\,\mathrm{tr}\big(\mathbf{C}_1^0(z)\big)\Delta Z_1^0 - \check{\boldsymbol{P}}^*\hat{\nabla}\mathbf{C}_1^0(z)\,\mathbf{P}^*\nabla Z_1^0.$$

and grouped matrices that are similar using the brackets. Lastly, we have defined the constant, z-dependent and independent matrices and vector:

$$\mathscr{I}_2^n = \mathbf{P}^*\mathbf{P}^n, \qquad \hat{\mathcal{C}}_n^1(z) = \begin{bmatrix}\mathbf{c}_{1,z}^{0,\overline{n}}(z)\mathrm{C}_{1,11}^0(z) + \mathbf{c}_{1,z}^{0,\overline{n}}(z)\mathrm{C}_{1,22}^0(z) & \mathbf{c}_{1,z}^{0,\overline{n}}(z)\,\hat{\mathbf{G}}_n^1\hat{\nabla}\mathbf{C}_1^0(z)\end{bmatrix},$$

$$\hat{\mathbf{G}}^1_n = \begin{bmatrix} \hat{\mathrm{G}}^1_{n,11} & \hat{\mathrm{G}}^1_{n,12} \\ \hat{\mathrm{G}}^1_{n,21} & \hat{\mathrm{G}}^1_{n,22} \end{bmatrix} = \mathbf{P}^{*,n} \nabla Z^{0,n}_1 \check{\boldsymbol{P}}^*, \qquad \boldsymbol{H}^1_n = \begin{bmatrix} \frac{1}{2}\Delta Z^0_1 \mathbf{P}^{*,n} \nabla Z^{0,n}_1 \\ \mathbf{P}^* \nabla Z^0_1 \end{bmatrix}.$$

The constant prefactor matrix is given by

$$\mathscr{J}^n_2 = \frac{1}{2} \begin{bmatrix} 1 - i^n & 1 + i^n \\ 1 + i^n & 1 - i^n \end{bmatrix}.$$

This matrix simplifies if we evaluate the index n:

$$\mathscr{J}^n_2 = \begin{cases} \mathbf{J}_2, & \text{if } n = 0, \\ \mathbf{I}_2, & \text{if } n = 2, \end{cases}$$

where we have defined the 2×2 exchange and identity matrix as

$$\mathbf{J}_2 = \begin{bmatrix} 0 & 1 \\ 1 & 0 \end{bmatrix}, \qquad \mathbf{I}_2 = \begin{bmatrix} 1 & 0 \\ 0 & 1 \end{bmatrix}.$$

In the exchange matrix, the anti-diagonal is populated with ones in contrast to the identity matrix where the main diagonal is populated with ones. Furthermore, the exchange matrix has a period of 2, i.e., $\mathbf{J}_2^2 = \mathbf{I}_2$. As a consequence, the matrix $\mathscr{J}^n_2$ has a period of 2 for $n = 0$ and 1 for $n = 2$. So, in general, we have that $(\mathscr{J}^n_2)^2 = \mathbf{I}_2$.

The reason for defining the matrix $\hat{\mathbf{G}}^1_n$ is as follows. We want to explicitly express the z dependence such that particular solution can be constructed. This matrix is precisely the matrix that is multiplied form both the left and right by z-dependent matrices. This matrix does not depend on z and as such only acts as to 'scale' the z-dependent behaviour.

The z-dependent behaviour can be identified by decomposing the z-dependent matrix into two submatrices:

$$\widehat{\mathcal{C}}^1_n(z) = \begin{bmatrix} \widehat{\mathcal{C}}^{1,1}_n(z) & \hat{\mathbf{G}}^{1,2}_n \widehat{\mathcal{C}}^{1,2}_n(z) \end{bmatrix}.$$

The z-dependent matrices $\widehat{\mathcal{C}}^{1,1}_n(z)$ and $\widehat{\mathcal{C}}^{1,2}_n(z)$ can be further decomposed into four z-dependent submatrices

$$\widehat{\mathcal{C}}^{1,1}_n(z) = \widehat{\mathcal{C}}^{1,1,1}_n(z) + \widehat{\mathcal{C}}^{1,1,2}_n(z), \qquad \widehat{\mathcal{C}}^{1,2}_n(z) = \begin{bmatrix} \widehat{\mathcal{C}}^{1,2,1}_n(z) \\ \widehat{\mathcal{C}}^{1,2,2}_n(z) \end{bmatrix}.$$

The four z-dependent *combination* submatrices are given by

$$\widehat{\mathcal{C}}^{1,1,1}_n(z) = \mathbf{c}^{0,\overline{n}}_{1,z}(z)\, \mathrm{C}^0_{1,11}(z) = \begin{bmatrix} \mathrm{c}^{0,\overline{n}}_{1,11,z}(z)\, \mathrm{C}^0_{1,11}(z) & 0 \\ 0 & \mathrm{c}^{0,\overline{n}}_{1,22,z}(z)\, \mathrm{C}^0_{1,11}(z) \end{bmatrix},$$

$$\widehat{\mathcal{C}}^{1,1,2}_n(z) = \mathbf{c}^{0,\overline{n}}_{1,z}(z)\, \mathrm{C}^0_{1,22}(z) = \begin{bmatrix} \mathrm{c}^{0,\overline{n}}_{1,11,z}(z)\, \mathrm{C}^0_{1,22}(z) & 0 \\ 0 & \mathrm{c}^{0,\overline{n}}_{1,22,z}(z)\, \mathrm{C}^0_{1,22}(z) \end{bmatrix},$$

$$\widehat{\mathcal{C}}^{1,2,1}_n(z) = \mathrm{c}^{0,\overline{n}}_{1,11,z}(z)\, \hat{\nabla}\mathbf{C}^0_1(z) = \begin{bmatrix} \mathrm{c}^{0,\overline{n}}_{1,11,z}(z)\, \mathrm{C}^0_{1,11,x}(z) & \mathrm{c}^{0,\overline{n}}_{1,11,z}(z)\, \mathrm{C}^0_{1,22,x}(z) \\ \mathrm{c}^{0,\overline{n}}_{1,11,z}(z)\, \mathrm{C}^0_{1,11,y}(z) & -\mathrm{c}^{0,\overline{n}}_{1,11,z}(z)\, \mathrm{C}^0_{1,22,y}(z) \end{bmatrix},$$

$$\widehat{\mathcal{C}}^{1,2,2}_n(z) = \mathrm{c}^{0,\overline{n}}_{1,22,z}(z)\, \hat{\nabla}\mathbf{C}^0_1(z) = \begin{bmatrix} \mathrm{c}^{0,\overline{n}}_{1,22,z}(z)\, \mathrm{C}^0_{1,11,x}(z) & \mathrm{c}^{0,\overline{n}}_{1,22,z}(z)\, \mathrm{C}^0_{1,22,x}(z) \\ \mathrm{c}^{0,\overline{n}}_{1,22,z}(z)\, \mathrm{C}^0_{1,11,y}(z) & -\mathrm{c}^{0,\overline{n}}_{1,22,z}(z)\, \mathrm{C}^0_{1,22,y}(z) \end{bmatrix}.$$

Here, we have also defined the z-independent matrix

$$\hat{\mathbf{G}}^{1,2}_n = \begin{bmatrix} \hat{\mathrm{G}}^1_{n,11} & \hat{\mathrm{G}}^1_{n,12} & 0 & 0 \\ 0 & 0 & \hat{\mathrm{G}}^1_{n,21} & \hat{\mathrm{G}}^1_{n,22} \end{bmatrix}.$$

The four z-dependent submatrices are also referred to as combination submatrices because the first two contain all four combinations of elements of the z-dependent matrices $\mathbf{c}^{0,\overline{n}}_{1,z}(z)$ and $\mathbf{C}^0_1(z)$, whereas the last two contain all eight combinations of the z-dependent matrices $\mathbf{c}^{0,\overline{n}}_{1,z}(z)$ and $\hat{\nabla}\mathbf{C}^0_1(z)$.

The reason we have we gone through this matrix derivation is that it allows us to individually solve for the particular solution of each combination submatrix $\widehat{\mathcal{C}}_n^{1,m,j}(z)$ for $m = 1,2$ and $j = 1,2$ and once we have those solutions then we can use the derived matrices to construct the total particular solution. Thus, the matrices are mostly used for bookkeeping purposes.

This observation can be made precise by a change of variables. The change of variables follows from the factorisation of the vertical advective forcing $\boldsymbol{F}_n^{1,\eta,w}(z)$. Introduce the solution matrix $\widehat{\mathbf{E}}_n^1(z)$ as

$$\check{\boldsymbol{R}}_n^{1,\eta,w,p}(z) = -\frac{1}{2A_v^0}\mathscr{I}_2^n\,\widehat{\mathbf{E}}_n^1(z)\,\boldsymbol{H}_n^1,$$

which consists of two solution submatrices $\widehat{\mathbf{E}}_n^{1,1}(z)$ and $\widehat{\mathbf{E}}_n^{1,2}(z)$ as

$$\widehat{\mathbf{E}}_n^1(z) = \begin{bmatrix}\widehat{\mathbf{E}}_n^{1,1}(z) & \widehat{\mathbf{G}}_n^{1,2}\,\widehat{\mathbf{E}}_n^{1,2}(z)\end{bmatrix}.$$

The solution matrices $\widehat{\mathbf{E}}_n^{1,1}(z)$ and $\widehat{\mathbf{E}}_n^{1,2}(z)$ consist of the four solution submatrices

$$\widehat{\mathbf{E}}_n^{1,1}(z) = \widehat{\mathbf{E}}_n^{1,1,1}(z) + \widehat{\mathbf{E}}_n^{1,1,2}(z), \qquad \widehat{\mathbf{E}}_n^{1,2}(z) = \begin{bmatrix}\widehat{\mathbf{E}}_n^{1,2,1}(z)\\ \widehat{\mathbf{E}}_n^{1,2,2}(z)\end{bmatrix}.$$

Here, $\widehat{\mathbf{E}}_n^1(z)$ is a 2×4 matrix, $\widehat{\mathbf{E}}_n^{1,1}(z)$ is a 2×2 matrix, $\widehat{\mathbf{E}}_n^{1,2}(z)$ is a 4×2 matrix and $\widehat{\mathbf{E}}_n^{1,1,1}(z)$, $\widehat{\mathbf{E}}_n^{1,1,2}(z)$, $\widehat{\mathbf{E}}_n^{1,2,1}(z)$ and $\widehat{\mathbf{E}}_n^{1,2,2}(z)$ are 2×2 matrices. These solution matrices are constructed the same way as the combination matrices. Hence, each combination matrix has a corresponding solution matrix and visa versa.

By introducing this new variable in the rotating flow differential equation, we obtain

$$-\frac{1}{2A_v^0}\mathscr{I}_2^n\left(\widehat{\mathbf{E}}_{n,zz}^1(z) - \left(\hat{\boldsymbol{\alpha}}_n^0\right)^2\widehat{\mathbf{E}}_n^1(z) - \widehat{\mathcal{C}}_n^1(z)\right)\boldsymbol{H}_n^1 = \mathbf{0},$$

where we have defined

$$\hat{\boldsymbol{\alpha}}_n^0 = \mathscr{I}_2^n\,\boldsymbol{\alpha}_n^0\,\mathscr{I}_2^n = \begin{cases}\mathbf{J}_2\,\boldsymbol{\alpha}_0^0\,\mathbf{J}_2, & \text{if } n = 0,\\ \boldsymbol{\alpha}_2^0, & \text{if } n = 2,\end{cases}$$

with

$$\mathbf{J}_2\,\boldsymbol{\alpha}_0^0\,\mathbf{J}_2 = \begin{bmatrix}\alpha_{0,22}^0 & 0\\ 0 & \alpha_{0,11}^0\end{bmatrix}, \qquad \boldsymbol{\alpha}_2^0 = \begin{bmatrix}\alpha_{2,11}^0 & 0\\ 0 & \alpha_{2,22}^0\end{bmatrix}.$$

The matrix $(\boldsymbol{\alpha}_n^0)^2$ and the matrix $\mathscr{I}_2^n$ do not commute for $n = 0$. To factor out the matrix $\mathscr{I}_2^n$ on the left-hand side of the expression, we have used the property that $(\mathscr{I}_2^n)^2 = \mathbf{I}_2$.

Since $A_v < \infty$, the matrix $\mathscr{I}_2^n$ unequal to the zero matrix and since this equation has to hold for any column vector $\boldsymbol{H}_n^1$, it follows that the term in the large parenthesis must be equal to the zero matrix. We obtain the following equivalent system of equations

$$\widehat{\mathbf{E}}_{n,zz}^1(z) - \left(\hat{\boldsymbol{\alpha}}_n^0\right)^2\widehat{\mathbf{E}}_n^1(z) = \widehat{\mathcal{C}}_n^1(z),$$

which can be further divided into two separate families of differential equations:

$$\widehat{\mathbf{E}}_{n,zz}^{1,1}(z) - \left(\hat{\boldsymbol{\alpha}}_n^0\right)^2\widehat{\mathbf{E}}_n^{1,1}(z) = \widehat{\mathcal{C}}_n^{1,1}(z), \qquad \widehat{\mathbf{E}}_{n,zz}^{1,2}(z) - \left(\check{\boldsymbol{\alpha}}_n^0\right)^2\widehat{\mathbf{E}}_n^{1,2}(z) = \widehat{\mathcal{C}}_n^{1,2}(z),$$

where we have defined

$$\check{\boldsymbol{\alpha}}_n^0 = \hat{\boldsymbol{\alpha}}_n^0 \otimes \mathbf{I}_2 = \begin{bmatrix}\hat{\alpha}_{n,11}^0 & 0 & 0 & 0\\ 0 & \hat{\alpha}_{n,11}^0 & 0 & 0\\ 0 & 0 & \hat{\alpha}_{n,22}^0 & 0\\ 0 & 0 & 0 & \hat{\alpha}_{n,22}^0\end{bmatrix},$$

with $\cdot\otimes\cdot$ the Kronecker product.

In the next sections, the differential equations for $\widehat{\mathbf{E}}_n^{1,m}(z)$ are solved for $m = 1$ and $m = 2$.

Constructing particular solutions for m=1 We construct a particular solution for the combination matrix $\widehat{\boldsymbol{\mathcal{C}}}_n^{1,1}(z)$. This combination matrix depends on the submatrices $\widehat{\boldsymbol{\mathcal{C}}}_n^{1,1,1}(z)$ and $\widehat{\boldsymbol{\mathcal{C}}}_n^{1,1,2}(z)$. Furthermore, the corresponding solution matrix $\widehat{\mathbf{E}}_n^{1,1}(z)$ depends on the solution submatrices $\widehat{\mathbf{E}}_n^{1,1,1}(z)$ and $\widehat{\mathbf{E}}_n^{1,1,2}(z)$. Using this decomposition, we can write the first family of differential equations for the submatrices as

$$\widehat{\mathbf{E}}_{n,zz}^{1,1,j}(z) - \left(\hat{\boldsymbol{\alpha}}_n^0\right)^2 \widehat{\mathbf{E}}_n^{1,1,j}(z) = \widehat{\boldsymbol{\mathcal{C}}}_n^{1,1,j}(z),$$

for $j = 1,2$. Here, the index j corresponds to the respective submatrix.

We focus on constructing particular solutions. Since both $\hat{\boldsymbol{\alpha}}_n^0$ and the forcing $\widehat{\boldsymbol{\mathcal{C}}}_n^{1,1,j}(z)$ are diagonal matrices, it follows that the solution matrices $\widehat{\mathbf{E}}_n^{1,1,j}(z)$ are diagonal matrices too. Strictly speaking, the off-diagonal terms yield the homogenous differential equation with homogeneous solution which is considered later. Hence, these terms are set to zero. It then follows that we want to solve element wise

$$\widehat{\mathrm{E}}_{n,ii,zz}^{1,1,j}(z) - \left(\alpha_{n,rr}^0\right)^2 \widehat{\mathrm{E}}_{n,ii}^{1,1,j}(z) = \widehat{\mathcal{C}}_{n,ii}^{1,1,j}(z),$$

for $i = 1,2$ and $j = 1,2$. Here, the index i corresponds to the diagonal entries of the solution matrix. Furthermore, we have introduced the auxiliary index r that depends on the indices i and n as follows

$$r(i,n) = \begin{cases} 3-i, & \text{if } n = 0, \\ i, & \text{if } n = 2. \end{cases}$$

For $n = 0$, the index r is essentially the complement of the index i, it is 2 whenever $i = 1$ and 1 whenever $i = 2$.

The elements of the combination submatrices $\widehat{\mathcal{C}}_{n,ii}^{1,1,j}(z)$ are highly regular. Compare, for example, the elements of the first two combination matrices $\widehat{\boldsymbol{\mathcal{C}}}_n^{1,1,j}(z)$ for $j = 1,2$. We can index their entries parametrically as follows

$$\widehat{\mathcal{C}}_{n,ii}^{1,1,j}(z) = \mathrm{c}_{1,ii,z}^{0,\overline{n}}(z)\,\mathrm{C}_{1,jj}^0(z),$$

for $i = 1,2$ and $j = 1,2$.

The next step in constructing particular solutions is to factor out the explicit z-dependent behaviour of the elements of the combination matrices. The factored form is given by

$$\widehat{\mathcal{C}}_{n,ii}^{1,1,j}(z) = \breve{\gamma}_{n,i}^{0,j}\,\widehat{\boldsymbol{T}}^{1,1,j}\,\widehat{\boldsymbol{Q}}_{n,i}^{1,1,j}(z).$$

Here, we have defined the scaling factors

$$\breve{\gamma}_{n,i}^{0,j} = \left(\frac{g}{A_v^0 \alpha_{1,jj}^0}\right)^2 \hat{\gamma}_{n,i}^0, \qquad \hat{\gamma}_{n,i}^0 = \frac{s_f^0 \beta_{1,ii}^{0,n}}{\alpha_{1,ii}^{0,n}}, \qquad \hat{\gamma}_j^0 = \frac{s_f^0 \beta_{1,jj}^0}{\alpha_{1,jj}^0}.$$

With the z-independent coefficient vector given by

$$\widehat{\boldsymbol{T}}^{1,1,j} = \begin{bmatrix} \hat{\gamma}_j^0 \sinh\left(\alpha_{1,jj}^0 D\right) - H & -1 & \hat{\gamma}_j^0 \end{bmatrix},$$

and the z-dependent vector reads

$$\widehat{\boldsymbol{Q}}_{n,i}^{1,1,j}(z) = \sinh\left(\alpha_{1,ii}^{0,n}(z-R)\right) \begin{bmatrix} 1 & z & \sinh\left(\alpha_{1,jj}^0(z-R)\right) \end{bmatrix}^T.$$

Furthermore, we have introduced explicit expressions for the parameters

$$\alpha_{1,\ell\ell}^{0,n}(x,y) = \sqrt{i^{n+3}\left(\omega + (-1)^{\ell+1} f\right)/A_v^0}, \qquad \beta_{1,ii}^{0,n}(x,y) = \frac{1}{A_v^0 \alpha_{1,ii}^{0,n} \sinh\left(\alpha_{1,ii}^{0,n} D\right) + s_f^0 \cosh\left(\alpha_{1,ii}^{0,n} D\right)},$$

which are defined as $\alpha^{0,n}_{1,\ell\ell}(x,y)=\alpha^{0,\overline{n}}_{1,\ell\ell}(x,y)$ and $\beta^{0,n}_{1,ii}(x,y)=\beta^{0,\overline{n}}_{1,ii}(x,y)$.[1]

We can again define a new solution variable such that the system of differential equations simplifies. We define the solution vector $\widehat{\boldsymbol{S}}^{1,1,j}_{n,i}(z)$ as

$$\widehat{\mathrm{E}}^{1,1,j}_{n,ii}(z)=\breve{\gamma}^{0,j}_{n,i}\,\widehat{\boldsymbol{T}}^{1,1,j}\,\widehat{\boldsymbol{S}}^{1,1,j}_{n,i}(z).$$

Substituting this expression into the differential equation and using similar arguments as before, we get a system of differential equations

$$\widehat{\boldsymbol{S}}^{1,1,j}_{n,zz,i}(z)-\left(\alpha^{0}_{n,rr}\right)^2\widehat{\boldsymbol{S}}^{1,1,j}_{n,i}(z)=\widehat{\boldsymbol{Q}}^{1,1,j}_{n,i}(z),$$

for $i=1,2$ and $j=1,2$. Since this system is decoupled we can solve for each component of the vector $\widehat{\boldsymbol{S}}^{1,1,j}_{n,i}(z)$ separately.

We want to emphasize that under the standard forcing conditions, the α's of the forcing, $\alpha^{0,n}_{1,ii}$, are not equal to plus or minus the α's of the differential equation, $\alpha^{0}_{n,rr}$, provided that $\omega\neq 0$. That is to say $\alpha^{0,n}_{1,ii}\neq\pm\alpha^{0}_{n,rr}$ for $i=1,2$ and $n=0,2$. This implies that the first forcing does not excite the normal frequency of the first-order rotating flow variables. Similar assumptions are made for the other forcing mechanisms. These assumptions are important when deriving analytic solutions for these differential equations.

The solution of the differential equation reads

$$\widehat{\boldsymbol{S}}^{1,1,j}_{n,i}(z)=\begin{bmatrix}\delta^{0,n}_{r,i}\sinh\!\left(\alpha^{0,n}_{1,ii}(z-R)\right)\\ \delta^{0,n}_{r,i}\left[z\sinh\!\left(\alpha^{0,n}_{1,ii}(z-R)\right)-2\delta^{0,n}_{r,i}\alpha^{0,n}_{1,ii}\cosh\!\left(\alpha^{0,n}_{1,ii}(z-R)\right)\right]\\ \breve{\delta}^{0,j,n}_{r,i}\Big[\;\hat{\delta}^{0,j,n}_{r,i}\sinh\!\left(\alpha^{0,n}_{1,ii}(z-R)\right)\sinh\!\left(\alpha^{0}_{1,jj}(z-R)\right)\\ \qquad+\tilde{\delta}^{0,j,n}_{i}\cosh\!\left(\alpha^{0,n}_{1,ii}(z-R)\right)\cosh\!\left(\alpha^{0}_{1,jj}(z-R)\right)\Big]\end{bmatrix},$$

where we have defined the coefficients

$$\delta^{0,n}_{r,i}=-\frac{1}{\left(\alpha^{0}_{n,rr}\right)^2-\left(\alpha^{0,n}_{1,ii}\right)^2},\qquad \hat{\delta}^{0,j,n}_{r,i}=\left(\alpha^{0}_{n,rr}\right)^2-\left(\alpha^{0,n}_{1,ii}\right)^2-\left(\alpha^{0}_{1,jj}\right)^2,\qquad \tilde{\delta}^{0,j,n}_{i}=2\alpha^{0,n}_{1,ii}\alpha^{0}_{1,jj},$$

and

$$\breve{\delta}^{0,j,n}_{r,i}=-\frac{1}{\left(\alpha^{0}_{n,rr}+\alpha^{0,n}_{1,ii}+\alpha^{0}_{1,jj}\right)\left(\alpha^{0}_{n,rr}-\alpha^{0,n}_{1,ii}+\alpha^{0}_{1,jj}\right)\left(\alpha^{0}_{n,rr}+\alpha^{0,n}_{1,ii}-\alpha^{0}_{1,jj}\right)\left(\alpha^{0}_{n,rr}-\alpha^{0,n}_{1,ii}-\alpha^{0}_{1,jj}\right)}.$$

Constructing particular solutions for m=2 We want to construct a particular solution for the combination matrix $\widehat{\boldsymbol{\mathcal{C}}}^{1,2}_{n}(z)$, which depends on the submatrices $\widehat{\boldsymbol{\mathcal{C}}}^{1,2,j}_{n}(z)$ for $j=1,2$. Similarly, the corresponding solution matrix $\widehat{\mathbf{E}}^{1,2}_{n}(z)$ depends on the solution submatrices $\widehat{\mathbf{E}}^{1,2,j}_{n}(z)$ for $j=1,2$. For these submatrices, multiplication with the square matrix $(\breve{\boldsymbol{\alpha}}^{0}_{n})^2$ becomes multiplication with the scalar $(\hat{\alpha}^{0}_{n,jj})^2$. The second family of differential equations can be written for the submatrices as

$$\widehat{\mathbf{E}}^{1,2,j}_{n,zz}(z)-\left(\hat{\alpha}^{0}_{n,jj}\right)^2\widehat{\mathbf{E}}^{1,2,j}_{n}(z)=\widehat{\boldsymbol{\mathcal{C}}}^{1,2,j}_{n}(z),$$

for $j=1,2$. Again, the index j specifies the submatrix.

[1] To derive these explicit expressions, we have used that the operator $\overline{n}$ is commutative under composition with the exponential function. That is, for any complex number $z\in\mathbb{C}$, it holds that $\exp(z)^{\overline{n}}=\exp\!\left(z^{\overline{n}}\right)$ and as a result $\sinh(z)^{\overline{n}}=\sinh\!\left(z^{\overline{n}}\right)$ and $\cosh(z)^{\overline{n}}=\cosh\!\left(z^{\overline{n}}\right)$. In addition, the operator $\overline{n}$ is commutative under composition with the principal square root function for any complex number not laying on the negative real axis. That is, for any complex number not on the negative real axis $z\in\mathbb{C}\backslash\mathbb{R}^-$, it holds that $\sqrt{z}^{\overline{n}}=\sqrt{z^{\overline{n}}}$. Thus, if we want to use this identity we need to check whether the argument of the square root is not on the negative real axis. We have

$$\alpha^{0}_{1,\ell\ell}(x,y)=\sqrt{i\left(\omega+(-1)^{\ell+1}f\right)/A^{0}_{\nu}}.$$

The physical parameters are real-valued such that for any parameter value, we have $\left(\omega+(-1)^{\ell+1}f\right)/A^{0}_{\nu}\in\mathbb{R}$ and, therefore, $i\left(\omega+(-1)^{\ell+1}f\right)/A^{0}_{\nu}\in i\mathbb{R}$. This shows that the argument of the square root is strictly imaginary. Hence, it is not on the negative real axis and we can use the stated identity.

This equation can also be formulated element wise and reads

$$\widehat{\mathrm{E}}^{1,2,j}_{n,k\ell,zz}(z) - \left(\alpha^0_{n,dd}\right)^2 \widehat{\mathrm{E}}^{1,2,j}_{n,k\ell}(z) = \widehat{\mathcal{C}}^{1,2,j}_{n,k\ell}(z),$$

for $j = 1,2$, $k = 1,2$ and $\ell = 1,2$. The indices k and ℓ indicate which element of the solution matrix is considered. Here, we have defined the index

$$d(j,n) = \begin{cases} 3-j, & \text{if } n = 0, \\ j, & \text{if } n = 2. \end{cases}$$

The structure of the combination submatrices $\widehat{\mathcal{C}}^{1,2,j}_{n,k\ell}(z)$ for $j = 1,2$ is highly similar. We can index their entries parametrically as

$$\widehat{\mathcal{C}}^{1,2,j}_{n,k\ell}(z) = \mathrm{c}^{0,\overline{n}}_{1,jj,z}(z) \left(\hat{\nabla}\mathrm{C}^0_1\right)_{k\ell}(z).$$

The quantity $\left(\hat{\nabla}\mathrm{C}^0_1\right)_{k\ell}(z)$ consists of the elements $\mathrm{C}^0_{1,\ell\ell,x_k}(z)$ for $k = 1,2$ and $\ell = 1,2$, where we have used the notation $x_1 = x$ and $x_2 = y$. Using this notation, we have

$$\widehat{\mathcal{C}}^{1,2,j}_{n,k\ell}(z) = (-1)^{\delta_{k\ell 2}}\, \mathrm{c}^{0,\overline{n}}_{1,jj,z}(z)\, \mathrm{C}^0_{1,\ell\ell,x_k}(z).$$

Here, $\delta_{k\ell 2}$ is the Kronecker delta of three arguments. It is only one if all of its arguments match.

Using the matrices defined in a previous section, we can expand this forcing as follows

$$\begin{aligned}
\widehat{\mathcal{C}}^{1,2,j}_{n,k\ell}(z) &= (-1)^{\delta_{k\ell 2}}\, \mathrm{c}^{0,\overline{n}}_{1,jj,z}(z)\, \frac{d\mathrm{C}^0_{1,\ell\ell}}{d\boldsymbol{\phi}^0}(z)\, \frac{\partial \boldsymbol{\phi}^0}{\partial x_k}, \\
&= (-1)^{\delta_{k\ell 2}}\, \mathrm{c}^{0,\overline{n}}_{1,jj,z}(z) \left(\frac{\partial \mathrm{C}^0_{1,\ell\ell}}{\partial \boldsymbol{\phi}^0}(z) + \frac{\partial \mathrm{C}^0_{1,\ell\ell}}{\partial \boldsymbol{\vartheta}^0_{1,\ell}}(z)\, \frac{d\boldsymbol{\vartheta}^0_{1,\ell}}{d\boldsymbol{\phi}^0} \right) \frac{\partial \boldsymbol{\phi}^0}{\partial x_k}, \\
&= (-1)^{\delta_{k\ell 2}} \left(\widehat{\mathfrak{C}}^{1,2,j,1}_{n,\ell}(z) + \widehat{\mathfrak{C}}^{1,2,j,2}_{n,\ell}(z)\, \frac{d\boldsymbol{\vartheta}^0_{1,\ell}}{d\boldsymbol{\phi}^0} \right) \frac{\partial \boldsymbol{\phi}^0}{\partial x_k},
\end{aligned}$$

where we have defined the vectors

$$\widehat{\mathfrak{C}}^{1,2,j,1}_{n,\ell}(z) = \mathrm{c}^{0,\overline{n}}_{1,jj,z}(z)\, \frac{\partial \mathrm{C}^0_{1,\ell\ell}}{\partial \boldsymbol{\phi}^0}(z), \qquad \widehat{\mathfrak{C}}^{1,2,j,2}_{n,\ell}(z) = \mathrm{c}^{0,\overline{n}}_{1,jj,z}(z)\, \frac{\partial \mathrm{C}^0_{1,\ell\ell}}{\partial \boldsymbol{\vartheta}^0_{1,\ell}}(z).$$

We focus on each z-dependent row vector separately.

Consider $\widehat{\mathfrak{C}}^{1,2,j,1}_{n,\ell}(z)$ We can write this expression as a product between a scaling factor, a z-dependent vector, a z-independent coefficient and a scaling matrix. This yields

$$\widehat{\mathfrak{C}}^{1,2,j,1}_{n,\ell}(z) = \breve{\gamma}^{0,\ell}_{n,j}\, \widehat{\boldsymbol{Q}}^{1,2,j}_{n,\ell}(z)\, \widehat{\mathbf{T}}^{1,2,\cdot,1}_{\ell}\, \boldsymbol{\mathcal{S}}^1_{\ell},$$

where we have defined the z-dependent vector

$$\widehat{\boldsymbol{Q}}^{1,2,j}_{n,\ell}(z) = \sinh\!\left(\alpha^{0,n}_{1,jj}(z-R)\right) \begin{bmatrix} 1 & z & \sinh\!\left(\alpha^0_{1,\ell\ell}(z-R)\right) & \cosh\!\left(\alpha^0_{1,\ell\ell}(z-R)\right) & z\cosh\!\left(\alpha^0_{1,\ell\ell}(z-R)\right) \end{bmatrix},$$

the z-independent coefficient matrix

$$\widehat{\mathbf{T}}^{1,2,\cdot,1}_{\ell} = \begin{bmatrix} H - \hat{\gamma}^0_\ell \sinh\!\left(\alpha^0_{1,\ell\ell}D\right) & \sinh\!\left(\alpha^0_{1,\ell\ell}D\right) & s^0_f \beta^0_{1,\ell\ell} \cosh\!\left(\alpha^0_{1,\ell\ell}D\right) - 1 & \cosh\!\left(\alpha^0_{1,\ell\ell}D\right) \\ 1 & 0 & 0 & 0 \\ -\hat{\gamma}^0_\ell & 1 & 0 & 0 \\ 0 & 0 & 0 & -1 \\ 0 & 0 & 0 & 0 \end{bmatrix},$$

and the scaling matrix

$$\boldsymbol{\mathcal{S}}^1_\ell = \begin{bmatrix} 1/A^0_v & 0 & 0 & 0 \\ 0 & \beta^0_{1,\ell\ell}/\alpha^0_{1,\ell\ell} & 0 & 0 \\ 0 & 0 & 1 & 0 \\ 0 & 0 & 0 & s^0_f\beta^0_{1,\ell\ell} \end{bmatrix}.$$

Here, the dot in the matrix $\widehat{\mathbf{T}}^{1,2,\cdot,1}_\ell$ indicates that this matrix is at the same index level as $\widehat{\mathfrak{C}}^{1,2,j,1}_{n,\ell}(z)$ while being independent of the index j. Furthermore, we have included the z-dependent element $z\sinh\big(\alpha^{0,n}_{1,jj}(z-R)\big)\cosh\big(\alpha^0_{1,\ell\ell}(z-R)\big)$ in the z-dependent vector, even though this forcing does not depend on this component as can be seen by the zero row in the matrix $\widehat{\mathbf{T}}^{1,2,\cdot,1}_\ell$. This choice turns out to be convenient later when factoring terms.

Consider $\widehat{\mathfrak{C}}^{1,2,j,2}_{n,\ell}(z)$ We write this forcing as a scaling factor times a z-dependent vector times a z-independent coefficient matrix. We have

$$\widehat{\mathfrak{C}}^{1,2,j,2}_{n,\ell}(z) = \frac{1}{\alpha^0_{1,\ell\ell}}\breve{\gamma}^{0,\ell}_{n,j}\,\widehat{\boldsymbol{Q}}^{1,2,j}_{n,\ell}(z)\,\widehat{\mathbf{T}}^{1,2,\cdot,2}_\ell,$$

where we have defined the z-dependent vector

$$\widehat{\boldsymbol{Q}}^{1,2,j}_{n,\ell}(z) = \sinh\big(\alpha^{0,n}_{1,jj}(z-R)\big)\begin{bmatrix}1 & z & \sinh\big(\alpha^0_{1,\ell\ell}(z-R)\big) & \cosh\big(\alpha^0_{1,\ell\ell}(z-R)\big) & z\cosh\big(\alpha^0_{1,\ell\ell}(z-R)\big)\end{bmatrix},$$

and the z-independent coefficient matrix

$$\widehat{\mathbf{T}}^{1,2,\cdot,2}_\ell = \begin{bmatrix} -3\hat{\gamma}^0_\ell\sinh\big(\alpha^0_{1,\ell\ell}D\big) + s^0_f\beta^0_{1,\ell\ell}D\cosh\big(\alpha^0_{1,\ell\ell}D\big) + 2H & s^0_f\sinh\big(\alpha^0_{1,\ell\ell}D\big) \\ 2 & 0 \\ -3\hat{\gamma}^0_\ell & s^0_f \\ -s^0_f\beta^0_{1,\ell\ell}R & 0 \\ s^0_f\beta^0_{1,\ell\ell} & 0 \end{bmatrix}.$$

Continuing the derivation We have written $\widehat{\mathfrak{C}}^{1,2,j,1}_{n,\ell}(z)$ and $\widehat{\mathfrak{C}}^{1,2,j,2}_{n,\ell}(z)$ as a product between a z-dependent vector and z-independent coefficient matrices. Using this notation, we obtain

$$\widehat{C}^{1,2,j}_{n,k\ell}(z) = (-1)^{\delta_{k\ell 2}}\,\breve{\gamma}^{0,\ell}_{n,j}\,\widehat{\boldsymbol{Q}}^{1,2,j}_{n,\ell}(z)\,\widehat{\boldsymbol{\Gamma}}^1_\ell\,\boldsymbol{\phi}^0_{x_k},$$

where we have defined the z-independent coefficient matrix and used the subscript notation:

$$\widehat{\boldsymbol{\Gamma}}^1_\ell = \widehat{\mathbf{T}}^{1,2,\cdot,1}_\ell\boldsymbol{\mathcal{S}}^1_\ell + \frac{1}{\alpha^0_{1,\ell\ell}}\widehat{\mathbf{T}}^{1,2,\cdot,2}_\ell\frac{d\boldsymbol{\vartheta}^0_{1,\ell}}{d\boldsymbol{\phi}^0}, \qquad \boldsymbol{\phi}^0_{x_k} = \frac{\partial\boldsymbol{\phi}^0}{\partial x_k}.$$

We can define a new solution variable such that the differential equation simplifies. We define the solution row vector $\widehat{\mathbf{S}}^{1,2,j}_{n,\ell}(z)$ as

$$\widehat{\mathrm{E}}^{1,2,j}_{n,k\ell}(z) = (-1)^{\delta_{k\ell 2}}\,\breve{\gamma}^{0,\ell}_{n,j}\,\widehat{\mathbf{S}}^{1,2,j}_{n,\ell}(z)\,\widehat{\boldsymbol{\Gamma}}^1_\ell\,\boldsymbol{\phi}^0_{x_k}.$$

The differential equation becomes

$$\widehat{\mathbf{S}}^{1,2,j}_{n,zz,\ell}(z) - \big(\alpha^0_{n,dd}\big)^2\,\widehat{\mathbf{S}}^{1,2,j}_{n,\ell}(z) = \widehat{\boldsymbol{Q}}^{1,2,j}_{n,\ell}(z),$$

for $\ell = 1,2$ and $j = 1,2$. Interestingly, this differential equation has become independent of the index k.

We notice that the first three-components of the forcing $\widehat{\boldsymbol{Q}}_{n,\ell}^{1,2,j}(z)$ are the same as before. This implies we can re-use the corresponding solutions. Assuming that no eigenfrequencies are exited, we obtain the solution

$$\widehat{\boldsymbol{S}}_{n,\ell}^{1,2,j}(z) = \begin{bmatrix} \delta_{d,j}^{0,n} \sinh\big(\alpha_{1,jj}^{0,n}(z-R)\big) \\[2ex] \delta_{d,j}^{0,n}\Big[z \sinh\big(\alpha_{1,jj}^{0,n}(z-R)\big) - 2\delta_{d,j}^{0,n}\alpha_{1,jj}^{0,n} \cosh\big(\alpha_{1,jj}^{0,n}(z-R)\big)\Big] \\[2ex] \begin{aligned} \breve{\delta}_{d,j}^{0,\ell,n}\Big[\; & \hat{\delta}_{d,j}^{0,\ell,n} \sinh\big(\alpha_{1,jj}^{0,n}(z-R)\big) \sinh\big(\alpha_{1,\ell\ell}^{0}(z-R)\big) \\ & + \tilde{\delta}_{j}^{0,\ell,n} \cosh\big(\alpha_{1,jj}^{0,n}(z-R)\big) \cosh\big(\alpha_{1,\ell\ell}^{0}(z-R)\big)\Big] \end{aligned} \\[4ex] \begin{aligned} \breve{\delta}_{d,j}^{0,\ell,n}\Big[\; & \hat{\delta}_{d,j}^{0,\ell,n} \sinh\big(\alpha_{1,jj}^{0,n}(z-R)\big) \cosh\big(\alpha_{1,\ell\ell}^{0}(z-R)\big) \\ & + \tilde{\delta}_{j}^{0,\ell,n} \cosh\big(\alpha_{1,jj}^{0,n}(z-R)\big) \sinh\big(\alpha_{1,\ell\ell}^{0}(z-R)\big)\Big] \end{aligned} \\[4ex] \begin{aligned} \breve{\delta}_{d,j}^{0,\ell,n}\Big\{ \; & \hat{\delta}_{d,j}^{0,\ell,n} z \sinh\big(\alpha_{1,jj}^{0,n}(z-R)\big) \cosh\big(\alpha_{1,\ell\ell}^{0}(z-R)\big) \\ & + \tilde{\delta}_{j}^{0,\ell,n} z \cosh\big(\alpha_{1,jj}^{0,n}(z-R)\big) \sinh\big(\alpha_{1,\ell\ell}^{0}(z-R)\big) \\ & + \breve{\delta}_{d,j}^{0,\ell,n}\Big[\; \check{\delta}_{d,j}^{0,\ell,n} \sinh\big(\alpha_{1,jj}^{0,n}(z-R)\big) \sinh\big(\alpha_{1,\ell\ell}^{0}(z-R)\big) \\ & \qquad + \dot{\delta}_{d,j}^{0,\ell,n} \cosh\big(\alpha_{1,jj}^{0,n}(z-R)\big) \cosh\big(\alpha_{1,\ell\ell}^{0}(z-R)\big)\Big]\Big\} \end{aligned} \end{bmatrix}^{T},$$

where we have defined the coefficients

$$\delta_{d,j}^{0,n} = -\frac{1}{\big(\alpha_{n,dd}^{0}\big)^2 - \big(\alpha_{1,jj}^{0,n}\big)^2}, \qquad \hat{\delta}_{d,j}^{0,\ell,n} = \big(\alpha_{n,dd}^{0}\big)^2 - \big(\alpha_{1,jj}^{0,n}\big)^2 - \big(\alpha_{1,\ell\ell}^{0}\big)^2, \qquad \tilde{\delta}_{j}^{0,\ell,n} = 2\alpha_{1,jj}^{0,n}\alpha_{1,\ell\ell}^{0},$$

$$\check{\delta}_{d,j}^{0,\ell,n} = -2\alpha_{1,\ell\ell}^{0}\Big\{\big(\alpha_{1,\ell\ell}^{0}\big)^4 + \Big[\big(\alpha_{n,dd}^{0}\big)^2 - \big(\alpha_{1,jj}^{0,n}\big)^2\Big]\Big[\big(\alpha_{n,dd}^{0}\big)^2 + 3\big(\alpha_{1,jj}^{0,n}\big)^2 - 2\big(\alpha_{1,\ell\ell}^{0}\big)^2\Big]\Big\},$$

$$\dot{\delta}_{d,j}^{0,\ell,n} = -2\alpha_{1,jj}^{0,n}\Big\{\big(\alpha_{1,\ell\ell}^{0}\big)^2\Big[2\big(\alpha_{n,dd}^{0}\big)^2 + 2\big(\alpha_{1,jj}^{0,n}\big)^2 - 3\big(\alpha_{1,\ell\ell}^{0}\big)^2\Big] + \Big[\big(\alpha_{n,dd}^{0}\big)^2 - \big(\alpha_{1,jj}^{0,n}\big)^2\Big]^2\Big\},$$

and

$$\breve{\delta}_{d,j}^{0,\ell,n} = -\frac{1}{\big(\alpha_{n,dd}^{0} + \alpha_{1,jj}^{0,n} + \alpha_{1,\ell\ell}^{0}\big)\big(\alpha_{n,dd}^{0} - \alpha_{1,jj}^{0,n} + \alpha_{1,\ell\ell}^{0}\big)\big(\alpha_{n,dd}^{0} + \alpha_{1,jj}^{0,n} - \alpha_{1,\ell\ell}^{0}\big)\big(\alpha_{n,dd}^{0} - \alpha_{1,jj}^{0,n} - \alpha_{1,\ell\ell}^{0}\big)}.$$

B.11.2 Constructing a particular solution for the horizontal advective forcing

We consider the horizontal advective forcing for $n = 0, 2$. This forcing is given by

$$\boldsymbol{\eta}_n^{1,u} = \frac{1}{2}\boldsymbol{U}_1^{0,\overline{n}}(z) \cdot \nabla \boldsymbol{U}_1^0(z).$$

The horizontal advective derivative acting on $\boldsymbol{U}_1^0(z)$ can be written in several equivalent forms. We consider three cases:

1. The first case is the closest in notation to the usual notation of the advective derivative acting on U. It reads
$$\boldsymbol{U}_1^{0,\overline{n}}(z) \cdot \nabla \boldsymbol{U}_1^0(z) = \left(\boldsymbol{U}_1^{0,\overline{n}}(z)^T \breve{\nabla}\left[\boldsymbol{\mathcal{D}}\{\boldsymbol{U}_1^0(z)\}\right]\right)^T.$$
2. In the second formulation the transpose operator is expanded once, to obtain
$$\boldsymbol{U}_1^{0,\overline{n}}(z) \cdot \nabla \boldsymbol{U}_1^0(z) = \left(\breve{\nabla}\left[\boldsymbol{\mathcal{D}}\{\boldsymbol{U}_1^0(z)\}\right]\right)^T \boldsymbol{U}_1^{0,\overline{n}}(z).$$
3. In the third formulation, the transpose operator is expanded a second time. This leads to the left-derivative formulation:
$$\boldsymbol{U}_1^{0,\overline{n}}(z) \cdot \nabla \boldsymbol{U}_1^0(z) = \left[\boldsymbol{\mathcal{D}}\{\boldsymbol{U}_1^0(z)\}\right] \overleftarrow{\breve{\nabla}}^T \boldsymbol{U}_1^{0,\overline{n}}(z).$$

Here, the diagonal operator $\boldsymbol{\mathcal{D}}\{\cdot\}$ creates a diagonal matrix from a vector argument and the arrow indicates that the operator acts in the indicated direction. Thus, in the third case, the differential operator acts to the left instead of the more customary right. This is also indicated by the square brackets in front of the operator. Lastly, we have defined the operators

$$\breve{\nabla} = \begin{bmatrix} \partial_x & \partial_x \\ \partial_y & \partial_y \end{bmatrix}, \qquad \overleftarrow{\breve{\nabla}}^T = \begin{bmatrix} \overleftarrow{\partial_x} & \overleftarrow{\partial_y} \\ \overleftarrow{\partial_x} & \overleftarrow{\partial_y} \end{bmatrix}.$$

We have chosen to use the *third form* of the advective operator because it simplifies the notation considerably. This is the case because it expands the transpose operator most, removing unnecessary transpose operations in the rest of the derivation. It does, however, introduce a more cumbersome left-derivative operator. This is not a problem because it can be considered once, after which its components become regular derivatives.

The left-derivative operator in the third formulation can be expanded as

$$\left[\boldsymbol{\mathcal{D}}\{\boldsymbol{U}_1^0(z)\}\right] \overleftarrow{\breve{\nabla}}^T = \mathbf{P}\left[\mathbf{c}_1^0(z)\,\mathbf{P}^*\boldsymbol{\mathcal{D}}\{\nabla Z_1^0\}\right] \overleftarrow{\breve{\nabla}}^T,$$

which can be further expanded as follows

$$\left[\mathbf{c}_1^0(z)\,\mathbf{P}^*\boldsymbol{\mathcal{D}}\{\nabla Z_1^0\}\right] \overleftarrow{\breve{\nabla}}^T = \mathbf{c}_1^0(z)\,\mathbf{P}^*\mathbf{H}Z_1^0 + \boldsymbol{\mathcal{D}}\{\mathbf{P}^*\nabla Z_1^0\}\,\mathbf{c}_1^0 \overleftarrow{\breve{\nabla}}^T(z).$$

Here, we have used that $\boldsymbol{U}_1^0(z) = \mathbf{P}\,\mathbf{c}_1^0(z)\,\mathbf{P}^*\nabla Z_1^0$ and defined the matrix

$$\mathbf{c}_1^0 \overleftarrow{\breve{\nabla}}^T(z) = \begin{bmatrix} \mathrm{c}_{1,11,x}^0(z) & \mathrm{c}_{1,11,y}^0(z) \\ \mathrm{c}_{1,22,x}^0(z) & \mathrm{c}_{1,22,y}^0(z) \end{bmatrix}.$$

Similar as before, we define the indexed vector as $\boldsymbol{U}_1^{0,n}(z) = \boldsymbol{U}_1^{0,\overline{n}}(z)$. It then follows that

$$\boldsymbol{U}_1^{0,n}(z) = \mathbf{P}^n\,\mathbf{c}_1^{0,\overline{n}}(z)\,\mathbf{P}^{*,n}\,\nabla Z_1^{0,n}.$$

Here, we have used that the index operator $\overline{n}$ is distributive over multiplication.

We expand the advective forcing related to U using the derived expressions:

$$
\begin{aligned}
\boldsymbol{F}_n^{1,\eta,u}(z) &= \frac{1}{A_v^0}\,\mathbf{P}^*\boldsymbol{\eta}_n^{1,u},\\
&= \frac{1}{2A_v^0}\,\mathbf{P}^*\boldsymbol{U}_1^{0,n}(z)\cdot\nabla\boldsymbol{U}_1^0(z),\\
&= \frac{1}{2A_v^0}\,\mathbf{P}^*\left[\boldsymbol{\mathcal{D}}\{\boldsymbol{U}_1^0(z)\}\right]\overleftarrow{\breve{\nabla}}^T\boldsymbol{U}_1^{0,n}(z),\\
&= \frac{1}{2A_v^0}\left\{\mathbf{c}_1^0(z)\,\mathbf{P}^*\mathbf{H}Z_1^0+\boldsymbol{\mathcal{D}}\{\mathbf{P}^*\nabla Z_1^0\}\,\mathbf{c}_1^0\,\overleftarrow{\breve{\nabla}}^T(z)\right\}\mathbf{P}^n\,\mathbf{c}_1^{0,\overline{n}}(z)\left(\mathbf{P}^{*,n}\nabla Z_1^{0,n}\right),\\
&= \frac{1}{2A_v^0}\left\{\mathbf{I}_2\left(\mathbf{c}_1^0(z)\,\mathbf{P}^*\mathbf{H}Z_1^0\,\mathbf{P}^n\,\mathbf{c}_1^{0,\overline{n}}(z)\right)+\boldsymbol{\mathcal{D}}\{\mathbf{P}^*\nabla Z_1^0\}\left(\mathbf{c}_1^0\,\overleftarrow{\breve{\nabla}}^T(z)\,\mathbf{P}^n\,\mathbf{c}_1^{0,\overline{n}}(z)\right)\right\}\left(\mathbf{P}^{*,n}\nabla Z_1^{0,n}\right),\\
&= \frac{1}{2A_v^0}\begin{bmatrix}\mathbf{I}_2 & \boldsymbol{\mathcal{D}}\{\mathbf{P}^*\nabla Z_1^0\}\end{bmatrix}\begin{bmatrix}\mathbf{c}_1^0(z)\,\mathbf{P}^*\mathbf{H}Z_1^0\,\mathbf{P}^n\,\mathbf{c}_1^{0,\overline{n}}(z)\\ \mathbf{c}_1^0\,\overleftarrow{\breve{\nabla}}^T(z)\,\mathbf{P}^n\,\mathbf{c}_1^{0,\overline{n}}(z)\end{bmatrix}\left(\mathbf{P}^{*,n}\nabla Z_1^{0,n}\right),\\
&= \frac{1}{2A_v^0}\,\mathbf{K}^1\,\widetilde{\boldsymbol{\mathcal{C}}}_n^1(z)\left(\mathbf{P}^{*,n}\nabla Z_1^{0,n}\right).
\end{aligned}
$$

Here, we have grouped similar matrices using the brackets and defined the z-independent and dependent matrices

$$
\mathbf{K}^1=\begin{bmatrix}\mathbf{I}_2 & \boldsymbol{\mathcal{D}}\{\mathbf{P}^*\nabla Z_1^0\}\end{bmatrix},\qquad \widetilde{\boldsymbol{\mathcal{C}}}_n^1(z)=\begin{bmatrix}\mathbf{c}_1^0(z)\,\mathbf{P}^*\mathbf{H}Z_1^0\,\mathbf{P}^n\,\mathbf{c}_1^{0,\overline{n}}(z)\\ \mathbf{c}_1^0\,\overleftarrow{\breve{\nabla}}^T(z)\,\mathbf{P}^n\,\mathbf{c}_1^{0,\overline{n}}(z)\end{bmatrix}.
$$

The next step in the derivation is to further isolate the z-dependent behaviour. The z-dependent behaviour can be identified by decomposing the z-dependent matrix into two parts:

$$
\widetilde{\boldsymbol{\mathcal{C}}}_n^1(z)=\begin{bmatrix}\widetilde{\boldsymbol{\mathcal{C}}}_n^{1,1}(z)\,\tilde{\mathbf{G}}_n^{1,1}\\ \widetilde{\boldsymbol{\mathcal{C}}}_n^{1,2}(z)\,\tilde{\mathbf{G}}_n^{1,2}\end{bmatrix}.
$$

The two z-dependent matrices can be further decomposed into four z-dependent submatrices

$$
\widetilde{\boldsymbol{\mathcal{C}}}_n^{1,1}(z)=\begin{bmatrix}\widetilde{\boldsymbol{\mathcal{C}}}_n^{1,1,1}(z) & \widetilde{\boldsymbol{\mathcal{C}}}_n^{1,1,2}(z)\end{bmatrix},\qquad \widetilde{\boldsymbol{\mathcal{C}}}_n^{1,2}(z)=\begin{bmatrix}\widetilde{\boldsymbol{\mathcal{C}}}_n^{1,2,1}(z) & \widetilde{\boldsymbol{\mathcal{C}}}_n^{1,2,2}(z)\end{bmatrix},
$$

with the four z-dependent, combination submatrices given by

$$
\begin{aligned}
\widetilde{\boldsymbol{\mathcal{C}}}_n^{1,1,1}(z) &= \mathbf{c}_1^0(z)\,\mathbf{c}_1^{0,\overline{n}}(z)=\begin{bmatrix}\mathrm{c}_{1,11}^0(z)\mathrm{c}_{1,11}^{0,\overline{n}}(z) & 0\\ 0 & \mathrm{c}_{1,22}^0(z)\mathrm{c}_{1,22}^{0,\overline{n}}(z)\end{bmatrix},\\
\widetilde{\boldsymbol{\mathcal{C}}}_n^{1,1,2}(z) &= \mathbf{c}_1^0(z)\,\mathbf{J}_2\,\mathbf{c}_1^{0,\overline{n}}(z)\,\mathbf{J}_2=\begin{bmatrix}\mathrm{c}_{1,11}^0(z)\,\mathrm{c}_{1,22}^{0,\overline{n}}(z) & 0\\ 0 & \mathrm{c}_{1,22}^0(z)\,\mathrm{c}_{1,11}^{0,\overline{n}}(z)\end{bmatrix},\\
\widetilde{\boldsymbol{\mathcal{C}}}_n^{1,2,1}(z) &= \mathbf{c}_{1,x}^0(z)\,\mathbf{1}\,\mathbf{c}_1^{0,\overline{n}}(z)=\begin{bmatrix}\mathrm{c}_{1,11,x}^0(z)\,\mathrm{c}_{1,11}^{0,\overline{n}}(z) & \mathrm{c}_{1,11,x}^0(z)\,\mathrm{c}_{1,22}^{0,\overline{n}}(z)\\ \mathrm{c}_{1,22,x}^0(z)\,\mathrm{c}_{1,11}^{0,\overline{n}}(z) & \mathrm{c}_{1,22,x}^0(z)\,\mathrm{c}_{1,22}^{0,\overline{n}}(z)\end{bmatrix},\\
\widetilde{\boldsymbol{\mathcal{C}}}_n^{1,2,2}(z) &= \mathbf{c}_{1,y}^0(z)\,\mathbf{1}\,\mathbf{c}_1^{0,\overline{n}}(z)=\begin{bmatrix}\mathrm{c}_{1,11,y}^0(z)\,\mathrm{c}_{1,11}^{0,\overline{n}}(z) & \mathrm{c}_{1,11,y}^0(z)\,\mathrm{c}_{1,22}^{0,\overline{n}}(z)\\ \mathrm{c}_{1,22,y}^0(z)\,\mathrm{c}_{1,11}^{0,\overline{n}}(z) & \mathrm{c}_{1,22,y}^0(z)\,\mathrm{c}_{1,22}^{0,\overline{n}}(z)\end{bmatrix}.
\end{aligned}
$$

Here, we have also defined the two z-independent matrices

$$
\tilde{\mathbf{G}}_n^{1,1}=\frac{1}{2}\begin{bmatrix}\boldsymbol{\mathcal{G}}_n^1 Z_1^0\\ \boldsymbol{\mathcal{G}}_n^2 Z_1^0\end{bmatrix},\qquad \tilde{\mathbf{G}}_n^{1,2}=\frac{1}{\sqrt{2}}\begin{bmatrix}\mathbf{I}_2\\ \tilde{\mathbf{I}}_2^n\end{bmatrix},
$$

with the two matrix operators given by

$$
\begin{aligned}
\boldsymbol{\mathcal{G}}_n^1 &= \begin{bmatrix}\partial_{xx}+i\left(1+i^n\right)\partial_{xy}-i^n\partial_{yy} & 0\\ 0 & \partial_{xx}-i\left(1+i^n\right)\partial_{xy}-i^n\partial_{yy}\end{bmatrix},\\
\boldsymbol{\mathcal{G}}_n^2 &= \begin{bmatrix}0 & \partial_{xx}+i\left(1-i^n\right)\partial_{xy}+i^n\partial_{yy}\\ \partial_{xx}-i\left(1-i^n\right)\partial_{xy}+i^n\partial_{yy} & 0\end{bmatrix},
\end{aligned}
$$

and constant matrices

$$\mathbf{1} = \begin{bmatrix} 1 & 1 \\ 1 & 1 \end{bmatrix}, \qquad \tilde{\mathbf{I}}_2^n = i^{n+3} \begin{bmatrix} -1 & 0 \\ 0 & 1 \end{bmatrix}.$$

We note that we can write the second operator $\boldsymbol{\mathcal{G}}_n^2$ in terms of the first operator $\boldsymbol{\mathcal{G}}_n^1$ as follows $\boldsymbol{\mathcal{G}}_n^2 = \boldsymbol{\mathcal{G}}_{n+2}^1 \mathbf{J}_2$, showing that defining the operator $\boldsymbol{\mathcal{G}}_n^2$ is not strictly necessary.

The matrix operators simplify if we evaluate the index n:

$$\boldsymbol{\mathcal{G}}_n^1 = \begin{cases} \begin{bmatrix} \partial_{xx} + 2i\partial_{xy} - \partial_{yy} & 0 \\ 0 & \partial_{xx} - 2i\partial_{xy} - \partial_{yy} \end{bmatrix}, & \text{if } n = 0, \\ \Delta \mathbf{I}_2, & \text{if } n = 2, \end{cases}$$

$$\boldsymbol{\mathcal{G}}_n^2 = \begin{cases} \Delta \mathbf{J}_2, & \text{if } n = 0, \\ \begin{bmatrix} 0 & \partial_{xx} + 2i\partial_{xy} - \partial_{yy} \\ \partial_{xx} - 2i\partial_{xy} - \partial_{yy} & 0 \end{bmatrix}, & \text{if } n = 2, \end{cases}$$

where we have defined the Laplacian $\Delta = \partial_{xx} + \partial_{yy}$.

The next step in the construction of a particular solution is a change of basis to simply the differential equations. This transformation separates the z-independent multiplications from the z-dependent matrix part. Define the solution matrix $\widetilde{\mathbf{E}}_n^1(z)$ as follows

$$\check{\boldsymbol{R}}_n^{1,\eta,u,p}(z) = \frac{1}{2A_v^0} \mathbf{K}^1 \, \widetilde{\mathbf{E}}_n^1(z) \left(\mathbf{P}^{*,n} \nabla Z_1^{0,n} \right),$$

where we have defined the two solution matrices $\widetilde{\mathbf{E}}_n^{1,1}(z)$ and $\widetilde{\mathbf{E}}_n^{1,2}(z)$ as

$$\widetilde{\mathbf{E}}_n^1(z) = \begin{bmatrix} \widetilde{\mathbf{E}}_n^{1,1}(z) \, \tilde{\mathbf{G}}_n^{1,1} \\ \widetilde{\mathbf{E}}_n^{1,2}(z) \, \tilde{\mathbf{G}}_n^{1,2} \end{bmatrix},$$

and the four solution submatrices as

$$\widetilde{\mathbf{E}}_n^{1,1}(z) = \begin{bmatrix} \widetilde{\mathbf{E}}_n^{1,1,1}(z) & \widetilde{\mathbf{E}}_n^{1,1,2}(z) \end{bmatrix}, \qquad \widetilde{\mathbf{E}}_n^{1,2}(z) = \begin{bmatrix} \widetilde{\mathbf{E}}_n^{1,2,1}(z) & \widetilde{\mathbf{E}}_n^{1,2,2}(z) \end{bmatrix}.$$

Here, $\widetilde{\mathbf{E}}_n^1(z)$ is a 4×2 matrix, $\widetilde{\mathbf{E}}_n^{1,1}(z)$ and $\widetilde{\mathbf{E}}_n^{1,2}(z)$ are 2×4 matrices and $\widetilde{\mathbf{E}}_n^{1,1,1}(z)$, $\widetilde{\mathbf{E}}_n^{1,1,2}(z)$, $\widetilde{\mathbf{E}}_n^{1,2,1}(z)$, $\widetilde{\mathbf{E}}_n^{1,2,2}(z)$ are 2×2 matrices. Again, each combination (sub)matrix has, by construction, a corresponding solution (sub)matrix.

Using this transformation, we obtain the following differential equation for the solution matrix

$$\widetilde{\mathbf{E}}_{n,zz}^1(z) - \left(\tilde{\boldsymbol{\alpha}}_n^0 \right)^2 \widetilde{\mathbf{E}}_n^1(z) = \widetilde{\boldsymbol{\mathcal{C}}}_n^1(z),$$

where we have defined the matrix

$$\tilde{\boldsymbol{\alpha}}_n^0 = \mathbf{I}_2 \otimes \boldsymbol{\alpha}_n^0 = \begin{bmatrix} \boldsymbol{\alpha}_n^0 & 0 \\ 0 & \boldsymbol{\alpha}_n^0 \end{bmatrix} = \begin{bmatrix} \alpha_{n,11}^0 & 0 & 0 & 0 \\ 0 & \alpha_{n,22}^0 & 0 & 0 \\ 0 & 0 & \alpha_{n,11}^0 & 0 \\ 0 & 0 & 0 & \alpha_{n,22}^0 \end{bmatrix}.$$

This differential equation separates in to two families of differential equations

$$\widetilde{\mathbf{E}}_{n,zz}^{1,1}(z) - \left(\boldsymbol{\alpha}_n^0 \right)^2 \widetilde{\mathbf{E}}_n^{1,1}(z) = \widetilde{\boldsymbol{\mathcal{C}}}_n^{1,1}(z), \qquad \widetilde{\mathbf{E}}_{n,zz}^{1,2}(z) - \left(\boldsymbol{\alpha}_n^0 \right)^2 \widetilde{\mathbf{E}}_n^{1,2}(z) = \widetilde{\boldsymbol{\mathcal{C}}}_n^{1,2}(z).$$

In the next sections, the differential equations for $\widetilde{\mathbf{E}}_n^{1,m}(z)$ are solved for $m = 1$ and $m = 2$.

Constructing particular solutions for m=1 We construct a particular solution of the solution matrix $\widetilde{\mathbf{E}}_n^{1,1}(z)$ for the forcing $\widetilde{\boldsymbol{\mathcal{C}}}_n^{1,1}(z)$. These matrices depend on the submatrices $\widetilde{\mathbf{E}}_n^{1,1,j}(z)$ and $\widetilde{\boldsymbol{\mathcal{C}}}_n^{1,1,j}(z)$ for $j = 1,2$. The first family of differential equations can be written for the submatrices as

$$\widetilde{\mathbf{E}}_{n,zz}^{1,1,j}(z) - \left(\boldsymbol{\alpha}_n^0\right)^2 \widetilde{\mathbf{E}}_n^{1,1,j}(z) = \widetilde{\boldsymbol{\mathcal{C}}}_n^{1,1,j}(z),$$

for $j = 1,2$. Here, the index j corresponds to the respective submatrix.

We are interested in constructing particular solutions. Under this condition, it again follows that the solution matrices $\widetilde{\mathbf{E}}_n^{1,1,j}(z)$ are diagonal as we set the off-diagonal elements, corresponding to the homogeneous equation, to zero. Thus, we want to solve element wise

$$\widetilde{\mathrm{E}}_{n,ii,zz}^{1,1,j}(z) - \left(\alpha_{n,ii}^0\right)^2 \widetilde{\mathrm{E}}_{n,ii}^{1,1,j}(z) = \widetilde{\mathcal{C}}_{n,ii}^{1,1,j}(z),$$

for $i = 1,2$ and $j = 1,2$. Here, the index i corresponds to the diagonal entries of the solution matrix.

The structure of the combination submatrices $\widetilde{\mathcal{C}}_{n,ii}^{1,1,j}(z)$ is highly similar. We can index their entries parametrically as follows

$$\widetilde{\mathcal{C}}_{n,ii}^{1,1,j}(z) = \mathrm{c}_{1,ii}^{0}(z)\, \mathrm{c}_{1,ll}^{0,\overline{n}}(z),$$

for $i = 1,2$ and $j = 1,2$. Here, we have defined the index l which depends on the indices i and j as

$$l(i,j) = \begin{cases} i, & \text{if } j = 1, \\ 3 - i, & \text{if } j = 2. \end{cases}$$

The forcing can be written as a scaling factor times a z-independent vector times a z-dependent vector as follows

$$\widetilde{\mathcal{C}}_{n,ii}^{1,1,j}(z) = \check{\gamma}_{n,i}^{0,j}\, \widetilde{\boldsymbol{T}}_{n,i}^{1,1,j}\, \widetilde{\boldsymbol{Q}}_{n,i}^{1,1,j}(z),$$

where we have defined the scaling factor

$$\check{\gamma}_{n,i}^{0,j} = \left(\frac{g}{A_v^0 \alpha_{1,ii}^0 \alpha_{1,ll}^{0,n}}\right)^2,$$

the z-independent coefficient vector

$$\widetilde{\boldsymbol{T}}_{n,i}^{1,1,j} = \begin{bmatrix} 1 & -s_f^0 \beta_{1,ii}^0 & -s_f^0 \beta_{1,ll}^{0,n} & \left(s_f^0\right)^2 \beta_{1,ii}^0 \beta_{1,ll}^{0,n} \end{bmatrix},$$

and the z-dependent vector

$$\widetilde{\boldsymbol{Q}}_{n,i}^{1,1,j}(z) = \begin{bmatrix} 1 & \cosh\!\left(\alpha_{1,ii}^0 (z-R)\right) & \cosh\!\left(\alpha_{1,ll}^{0,n}(z-R)\right) & \cosh\!\left(\alpha_{1,ii}^0 (z-R)\right)\cosh\!\left(\alpha_{1,ll}^{0,n}(z-R)\right) \end{bmatrix}^T.$$

We can again define a new solution variable such that the system of differential equations simplifies. We define the solution vector $\widetilde{\boldsymbol{S}}_{n,i}^{1,1,j}(z)$ as

$$\widetilde{\mathrm{E}}_{n,ii}^{1,1,j}(z) = \check{\gamma}_{n,i}^{0,j}\, \widetilde{\boldsymbol{T}}_{n,i}^{1,1,j}\, \widetilde{\boldsymbol{S}}_{n,i}^{1,1,j}(z).$$

Substituting this expression into the differential equation and using similar arguments as before, we get a system of differential equations

$$\widetilde{\boldsymbol{S}}_{n,zz,i}^{1,1,j}(z) - \left(\alpha_{n,ii}^0\right)^2 \widetilde{\boldsymbol{S}}_{n,i}^{1,1,j}(z) = \widetilde{\boldsymbol{Q}}_{n,i}^{1,1,j}(z),$$

for $i = 1,2$ and $j = 1,2$. Since this system is decoupled we can solve for each component of the vector $\widetilde{\boldsymbol{S}}_{n,i}^{1,1,j}(z)$ separately.

Assuming that no eigenfrequencies are exited, we obtain the solution

$$\tilde{\mathbf{S}}^{1,1,j}_{n,i}(z) = \begin{bmatrix} \ddot{\Delta}^{0,n}_{i} \\ \Delta^{0,n}_{i,i}\cosh\big(\alpha^{0}_{1,ii}(z-R)\big) \\ \acute{\Delta}^{0,l,n}_{i}\cosh\big(\alpha^{0,n}_{1,ll}(z-R)\big) \\ \begin{aligned}\check{\Delta}^{0,l,n}_{i,i}\Big[& \tilde{\Delta}^{0,l,n}_{i}\sinh\big(\alpha^{0}_{1,ii}(z-R)\big)\sinh\big(\alpha^{0,n}_{1,ll}(z-R)\big) \\ & +\hat{\Delta}^{0,l,n}_{i,i}\cosh\big(\alpha^{0}_{1,ii}(z-R)\big)\cosh\big(\alpha^{0,n}_{1,ll}(z-R)\big)\Big]\end{aligned} \end{bmatrix},$$

where we have defined the coefficients

$$\ddot{\Delta}^{0,n}_{i} = -\frac{1}{\big(\alpha^{0}_{n,ii}\big)^2}, \qquad \Delta^{0,n}_{i,i} = -\frac{1}{\big(\alpha^{0}_{n,ii}\big)^2-\big(\alpha^{0}_{1,ii}\big)^2}, \qquad \acute{\Delta}^{0,l,n}_{i} = -\frac{1}{\big(\alpha^{0}_{n,ii}\big)^2-\big(\alpha^{0,n}_{1,ll}\big)^2},$$

$$\hat{\Delta}^{0,l,n}_{i,i} = \big(\alpha^{0}_{n,ii}\big)^2-\big(\alpha^{0}_{1,ii}\big)^2-\big(\alpha^{0,n}_{1,ll}\big)^2, \qquad \tilde{\Delta}^{0,l,n}_{i} = 2\alpha^{0}_{1,ii}\alpha^{0,n}_{1,ll},$$

and

$$\check{\Delta}^{0,l,n}_{i,i} = -\frac{1}{\big(\alpha^{0}_{n,ii}+\alpha^{0}_{1,ii}+\alpha^{0,n}_{1,ll}\big)\big(\alpha^{0}_{n,ii}-\alpha^{0}_{1,ii}+\alpha^{0,n}_{1,ll}\big)\big(\alpha^{0}_{n,ii}+\alpha^{0}_{1,ii}-\alpha^{0,n}_{1,ll}\big)\big(\alpha^{0}_{n,ii}-\alpha^{0}_{1,ii}-\alpha^{0,n}_{1,ll}\big)}.$$

Constructing particular solutions for m=2 In this section, we construct a particular solution of the solution matrix $\tilde{\mathbf{E}}^{1,2}_{n}(z)$ for the forcing $\tilde{\boldsymbol{\mathcal{C}}}^{1,2}_{n}(z)$. These matrices depend on the submatrices $\tilde{\mathbf{E}}^{1,2,j}_{n}(z)$ and $\tilde{\boldsymbol{\mathcal{C}}}^{1,2,j}_{n}(z)$ for $j=1,2$. The second family of differential equations for the submatrices becomes

$$\tilde{\mathbf{E}}^{1,2,j}_{n,zz}(z) - \big(\boldsymbol{\alpha}^{0}_{n}\big)^2\tilde{\mathbf{E}}^{1,2,j}_{n}(z) = \tilde{\boldsymbol{\mathcal{C}}}^{1,2,j}_{n}(z),$$

for $j=1,2$. Here, the index j corresponds to the respective submatrix.

This equation can also be formulated element wise and this yields

$$\tilde{\mathrm{E}}^{1,2,j}_{n,k\ell,zz}(z) - \big(\alpha^{0}_{n,kk}\big)^2\tilde{\mathrm{E}}^{1,2,j}_{n,k\ell}(z) = \tilde{\mathcal{C}}^{1,2,j}_{n,k\ell}(z),$$

for $j=1,2$, $k=1,2$ and $\ell=1,2$. The indices k and ℓ indicate which element of the solution matrix is considered.

Once again, the structure of the combination submatrices $\tilde{\mathcal{C}}^{1,2,j}_{n,k\ell}(z)$ is highly similar. We can index their entries parametrically as

$$\tilde{\mathcal{C}}^{1,2,j}_{n,k\ell}(z) = \mathrm{c}^{0}_{1,kk,x_j}(z)\,\mathrm{c}^{0,\overline{n}}_{1,\ell\ell}(z).$$

Using the chain rule twice, we can expand this forcing as

$$\begin{aligned}\tilde{\mathcal{C}}^{1,2,j}_{n,k\ell}(z) &= \frac{d\mathrm{c}^{0}_{1,kk}}{d\boldsymbol{\phi}^{0}}(z)\,\frac{\partial\boldsymbol{\phi}^{0}}{\partial x_j}\,\mathrm{c}^{0,\overline{n}}_{1,\ell\ell}(z), \\ &= \left(\frac{\partial\mathrm{c}^{0}_{1,kk}}{\partial\boldsymbol{\phi}^{0}}(z) + \frac{\partial\mathrm{c}^{0}_{1,kk}}{\partial\boldsymbol{\vartheta}^{0}_{1,k}}(z)\,\frac{d\boldsymbol{\vartheta}^{0}_{1,k}}{d\boldsymbol{\phi}^{0}}\right)\mathrm{c}^{0,\overline{n}}_{1,\ell\ell}(z)\,\frac{\partial\boldsymbol{\phi}^{0}}{\partial x_j}, \\ &= \left(\tilde{\mathfrak{C}}^{1,2,\cdot,1}_{n,\ell,k}(z) + \tilde{\mathfrak{C}}^{1,2,\cdot,2}_{n,\ell,k}(z)\,\frac{d\boldsymbol{\vartheta}^{0}_{1,k}}{d\boldsymbol{\phi}^{0}}\right)\frac{\partial\boldsymbol{\phi}^{0}}{\partial x_j},\end{aligned}$$

where we have defined the vectors

$$\tilde{\mathfrak{C}}^{1,2,\cdot,1}_{n,\ell,k}(z) = \frac{\partial\mathrm{c}^{0}_{1,kk}}{\partial\boldsymbol{\phi}^{0}}(z)\,\mathrm{c}^{0,\overline{n}}_{1,\ell\ell}(z), \qquad \tilde{\mathfrak{C}}^{1,2,\cdot,2}_{n,\ell,k}(z) = \frac{\partial\mathrm{c}^{0}_{1,kk}}{\partial\boldsymbol{\vartheta}^{0}_{1,k}}(z)\,\mathrm{c}^{0,\overline{n}}_{1,\ell\ell}(z).$$

We focus on each z-dependent vector separately.

Consider $\widetilde{\mathfrak{C}}^{1,2,\cdot,1}_{n,\ell,k}(z)$ We can write this expression as a product between a scaling factor, z-dependent vector, z-independent coefficient matrix and scaling matrix. This yields

$$\widetilde{\mathfrak{C}}^{1,2,\cdot,1}_{n,\ell,k}(z) = \tilde{\gamma}^0_{n,\ell,k}\,\widetilde{\boldsymbol{Q}}^{1,2}_{n,\ell,k}(z)\,\widetilde{\mathbf{T}}^{1,2,\cdot,1}_{n,\ell,k}\,\boldsymbol{\mathcal{S}}^1_k,$$

where we have defined the scaling factor

$$\tilde{\gamma}^0_{n,\ell,k} = \frac{1}{\alpha^0_{1,kk}}\left(\frac{g}{A^0_v\alpha^{0,n}_{1,\ell\ell}}\right)^2,$$

the z-dependent vector and the z-independent coefficient matrix

$$\widetilde{\boldsymbol{Q}}^{1,2}_{n,\ell,k}(z) = \begin{bmatrix} 1 \\ \sinh\big(\alpha^0_{1,kk}(z-R)\big) \\ \cosh\big(\alpha^0_{1,kk}(z-R)\big) \\ \cosh\big(\alpha^{0,n}_{1,\ell\ell}(z-R)\big) \\ z\sinh\big(\alpha^0_{1,kk}(z-R)\big) \\ \cosh\big(\alpha^0_{1,kk}(z-R)\big)\cosh\big(\alpha^{0,n}_{1,\ell\ell}(z-R)\big) \\ \sinh\big(\alpha^0_{1,kk}(z-R)\big)\cosh\big(\alpha^{0,n}_{1,\ell\ell}(z-R)\big) \\ z\sinh\big(\alpha^0_{1,kk}(z-R)\big)\cosh\big(\alpha^{0,n}_{1,\ell\ell}(z-R)\big) \end{bmatrix}^T, \quad \widetilde{\mathbf{T}}^{1,2,\cdot,1}_{n,\ell,k} = \begin{bmatrix} -1/\alpha^0_{1,kk} & 0 & 0 & 0 \\ 0 & 0 & 0 & 1 \\ \hat{\gamma}^0_k & -1 & 0 & 0 \\ s^0_f\beta^{0,n}_{1,\ell\ell}/\alpha^0_{1,kk} & 0 & 0 & 0 \\ 0 & 0 & 0 & 0 \\ -s^0_f\beta^{0,n}_{1,\ell\ell}\hat{\gamma}^0_k & s^0_f\beta^{0,n}_{1,\ell\ell} & 0 & 0 \\ 0 & 0 & 0 & -s^0_f\beta^{0,n}_{1,\ell\ell} \\ 0 & 0 & 0 & 0 \end{bmatrix},$$

and the z-independent scaling matrix

$$\boldsymbol{\mathcal{S}}^1_k = \begin{bmatrix} 1/A^0_v & 0 & 0 & 0 \\ 0 & \beta^0_{1,kk}/\alpha^0_{1,kk} & 0 & 0 \\ 0 & 0 & 1 & 0 \\ 0 & 0 & 0 & s^0_f\beta^0_{1,kk} \end{bmatrix}.$$

Consider $\widetilde{\mathfrak{C}}^{1,2,\cdot,2}_{n,\ell,k}(z)$ We write this forcing as a scaling factor times a z-dependent vector times a z-independent coefficient matrix. We have

$$\widetilde{\mathfrak{C}}^{1,2,\cdot,2}_{n,\ell,k}(z) = \frac{1}{\alpha^0_{1,kk}}\tilde{\gamma}^0_{n,\ell,k}\,\widetilde{\boldsymbol{Q}}^{1,2}_{n,\ell,k}(z)\,\widetilde{\mathbf{T}}^{1,2,\cdot,2}_{n,\ell,k},$$

where we have defined the z-dependent vector and the z-independent coefficient matrix

$$\widetilde{\boldsymbol{Q}}^{1,2}_{n,\ell,k}(z) = \begin{bmatrix} 1 \\ \sinh\big(\alpha^0_{1,kk}(z-R)\big) \\ \cosh\big(\alpha^0_{1,kk}(z-R)\big) \\ \cosh\big(\alpha^{0,n}_{1,\ell\ell}(z-R)\big) \\ z\sinh\big(\alpha^0_{1,kk}(z-R)\big) \\ \cosh\big(\alpha^0_{1,kk}(z-R)\big)\cosh\big(\alpha^{0,n}_{1,\ell\ell}(z-R)\big) \\ \sinh\big(\alpha^0_{1,kk}(z-R)\big)\cosh\big(\alpha^{0,n}_{1,\ell\ell}(z-R)\big) \\ z\sinh\big(\alpha^0_{1,kk}(z-R)\big)\cosh\big(\alpha^{0,n}_{1,\ell\ell}(z-R)\big) \end{bmatrix}^T, \quad \widetilde{\mathbf{T}}^{1,2,\cdot,2}_{n,\ell,k} = \begin{bmatrix} -2/\alpha^0_{1,kk} & 0 \\ s^0_f\beta^0_{1,kk}R & 0 \\ 2\hat{\gamma}^0_k & -s^0_f \\ 2s^0_f\beta^{0,n}_{1,\ell\ell}/\alpha^0_{1,kk} & 0 \\ -s^0_f\beta^0_{1,kk} & 0 \\ -2s^0_f\beta^{0,n}_{1,\ell\ell}\hat{\gamma}^0_k & \big(s^0_f\big)^2\beta^{0,n}_{1,\ell\ell} \\ -\big(s^0_f\big)^2\beta^0_{1,kk}\beta^{0,n}_{1,\ell\ell}R & 0 \\ \big(s^0_f\big)^2\beta^0_{1,kk}\beta^{0,n}_{1,\ell\ell} & 0 \end{bmatrix}.$$

Continuing the derivation We have written $\widetilde{\mathfrak{C}}^{1,2,\cdot,1}_{n,\ell,k}(z)$ and $\widetilde{\mathfrak{C}}^{1,2,\cdot,2}_{n,\ell,k}(z)$ as a product between a z-dependent vector and z-independent coefficient matrices. The forcing can then be expanded as

$$\widetilde{\mathcal{C}}^{1,2,j}_{n,k\ell}(z) = \tilde{\gamma}^0_{n,\ell,k}\,\widetilde{\boldsymbol{Q}}^{1,2}_{n,\ell,k}(z)\,\widetilde{\boldsymbol{\Gamma}}^1_{n,\ell,k}\,\boldsymbol{\phi}^0_{x_j}.$$

where we have defined the z-independent coefficient matrix and used the subscript notation:

$$\widetilde{\boldsymbol{\Gamma}}^1_{n,\ell,k} = \widetilde{\mathbf{T}}^{1,2,\cdot,1}_{n,\ell,k}\,\boldsymbol{\mathcal{S}}^1_k + \frac{1}{\alpha^0_{1,kk}}\widetilde{\mathbf{T}}^{1,2,\cdot,2}_{n,\ell,k}\,\frac{d\boldsymbol{\vartheta}^0_{1,k}}{d\boldsymbol{\phi}^0}, \qquad \boldsymbol{\phi}^0_{x_j} = \frac{\partial\boldsymbol{\phi}^0}{\partial x_j}.$$

We define a new solution variable such that the differential equation simplifies. We define the solution row vector $\widetilde{\mathbf{S}}^{1,2}_{n,\ell,k}(z)$ as

$$\widetilde{\mathrm{E}}^{1,2,j}_{n,k\ell}(z) = \tilde{\gamma}^{0}_{n,\ell,k}\,\widetilde{\mathbf{S}}^{1,2}_{n,\ell,k}(z)\,\widetilde{\boldsymbol{\Gamma}}^{1}_{n,\ell,k}\,\boldsymbol{\phi}^{0}_{x_j}.$$

Using this transformation, the differential equation becomes

$$\widetilde{\mathbf{S}}^{1,2}_{n,zz,k,\ell}(z) - \left(\alpha^{0}_{n,kk}\right)^2 \widetilde{\mathbf{S}}^{1,2}_{n,\ell,k}(z) = \widetilde{\boldsymbol{Q}}^{1,2}_{n,\ell,k}(z),$$

for $k = 1,2$ and $\ell = 1,2$. It is interesting to note that this differential equation has become independent of the index j.

Assuming no eigenfrequencies are exited, we obtain the solution

$$\widetilde{\mathbf{S}}^{1,2}_{n,\ell,k}(z) = \begin{bmatrix} \ddot{\Delta}^{0,n}_{k} \\[1ex] \Delta^{0,n}_{k,k}\sinh\!\left(\alpha^{0}_{1,kk}(z-R)\right) \\[1ex] \Delta^{0,n}_{k,k}\cosh\!\left(\alpha^{0}_{1,kk}(z-R)\right) \\[1ex] \acute{\Delta}^{0,\ell,n}_{k}\cosh\!\left(\alpha^{0,n}_{1,\ell\ell}(z-R)\right) \\[1ex] \Delta^{0,n}_{k,k}\left[z\sinh\!\left(\alpha^{0}_{1,kk}(z-R)\right) - 2\Delta^{0,n}_{k,k}\alpha^{0}_{1,kk}\cosh\!\left(\alpha^{0}_{1,kk}(z-R)\right)\right] \\[1ex] \begin{aligned} \check{\Delta}^{0,\ell,n}_{k,k}\Big[\;& \tilde{\Delta}^{0,\ell,n}_{k}\sinh\!\left(\alpha^{0}_{1,kk}(z-R)\right)\sinh\!\left(\alpha^{0,n}_{1,\ell\ell}(z-R)\right) \\ &+ \hat{\Delta}^{0,\ell,n}_{k,k}\cosh\!\left(\alpha^{0}_{1,kk}(z-R)\right)\cosh\!\left(\alpha^{0,n}_{1,\ell\ell}(z-R)\right)\Big] \end{aligned} \\[1ex] \begin{aligned} \check{\Delta}^{0,\ell,n}_{k,k}\Big[\;& \hat{\Delta}^{0,\ell,n}_{k,k}\sinh\!\left(\alpha^{0}_{1,kk}(z-R)\right)\cosh\!\left(\alpha^{0,n}_{1,\ell\ell}(z-R)\right) \\ &+ \tilde{\Delta}^{0,\ell,n}_{k}\cosh\!\left(\alpha^{0}_{1,kk}(z-R)\right)\sinh\!\left(\alpha^{0,n}_{1,\ell\ell}(z-R)\right)\Big] \end{aligned} \\[1ex] \begin{aligned} \check{\Delta}^{0,\ell,n}_{k,k}\Big\{\;& \hat{\Delta}^{0,\ell,n}_{k,k}\,z\sinh\!\left(\alpha^{0}_{1,kk}(z-R)\right)\cosh\!\left(\alpha^{0,n}_{1,\ell\ell}(z-R)\right) \\ &+ \tilde{\Delta}^{0,\ell,n}_{k}\,z\cosh\!\left(\alpha^{0}_{1,kk}(z-R)\right)\sinh\!\left(\alpha^{0,n}_{1,\ell\ell}(z-R)\right) \\ &+ \check{\Delta}^{0,\ell,n}_{k,k}\Big[\; \check{\Delta}^{0,\ell,n}_{k,k}\sinh\!\left(\alpha^{0}_{1,kk}(z-R)\right)\sinh\!\left(\alpha^{0,n}_{1,\ell\ell}(z-R)\right) \\ &\qquad + \dot{\Delta}^{0,\ell,n}_{k,k}\cosh\!\left(\alpha^{0}_{1,kk}(z-R)\right)\cosh\!\left(\alpha^{0,n}_{1,\ell\ell}(z-R)\right)\Big]\Big\} \end{aligned} \end{bmatrix}^{T},$$

where we have defined the coefficients

$$\ddot{\Delta}^{0,n}_{k} = -\frac{1}{\left(\alpha^{0}_{n,kk}\right)^2}, \qquad \Delta^{0,n}_{k,k} = -\frac{1}{\left(\alpha^{0}_{n,kk}\right)^2 - \left(\alpha^{0}_{1,kk}\right)^2}, \qquad \acute{\Delta}^{0,\ell,n}_{k} = -\frac{1}{\left(\alpha^{0}_{n,kk}\right)^2 - \left(\alpha^{0,n}_{1,\ell\ell}\right)^2},$$

$$\hat{\Delta}^{0,\ell,n}_{k,k} = \left(\alpha^{0}_{n,kk}\right)^2 - \left(\alpha^{0}_{1,kk}\right)^2 - \left(\alpha^{0,n}_{1,\ell\ell}\right)^2, \qquad \tilde{\Delta}^{0,\ell,n}_{k} = 2\alpha^{0}_{1,kk}\alpha^{0,n}_{1,\ell\ell},$$

$$\check{\Delta}^{0,\ell,n}_{k,k} = -2\alpha^{0,n}_{1,\ell\ell}\left\{\left(\alpha^{0,n}_{1,\ell\ell}\right)^4 + \left[\left(\alpha^{0}_{n,kk}\right)^2 - \left(\alpha^{0}_{1,kk}\right)^2\right]\left[\left(\alpha^{0}_{n,kk}\right)^2 + 3\left(\alpha^{0}_{1,kk}\right)^2 - 2\left(\alpha^{0,n}_{1,\ell\ell}\right)^2\right]\right\},$$

$$\dot{\Delta}^{0,\ell,n}_{k,k} = -2\alpha^{0}_{1,kk}\left\{\left(\alpha^{0,n}_{1,\ell\ell}\right)^2\left[2\left(\alpha^{0}_{n,kk}\right)^2 + 2\left(\alpha^{0}_{1,kk}\right)^2 - 3\left(\alpha^{0,n}_{1,\ell\ell}\right)^2\right] + \left[\left(\alpha^{0}_{n,kk}\right)^2 - \left(\alpha^{0}_{1,kk}\right)^2\right]^2\right\},$$

and

$$\check{\Delta}^{0,\ell,n}_{k,k} = -\frac{1}{\left(\alpha^{0}_{n,kk} + \alpha^{0}_{1,kk} + \alpha^{0,n}_{1,\ell\ell}\right)\left(\alpha^{0}_{n,kk} - \alpha^{0}_{1,kk} + \alpha^{0,n}_{1,\ell\ell}\right)\left(\alpha^{0}_{n,kk} + \alpha^{0}_{1,kk} - \alpha^{0,n}_{1,\ell\ell}\right)\left(\alpha^{0}_{n,kk} - \alpha^{0}_{1,kk} - \alpha^{0,n}_{1,\ell\ell}\right)}.$$

B.11.3 Summary of the advective particular solutions

The derivation of the advective particular solution has become quite elaborate. Nonetheless, the construction of the particular solution of the horizontal and vertical advective forcing components can be described quite concisely. In this section, an overview of the construction of these particular solutions is given.

The particular advective solution consists of a horizontal and vertical part:

$$\check{\boldsymbol{R}}_n^{1,\eta,p}(z) = \check{\boldsymbol{R}}_n^{1,\eta,u,p}(z) + \check{\boldsymbol{R}}_n^{1,\eta,w,p}(z),$$

which are defined in terms of their respective solution matrix $\mathbf{E}_n^1(z)$ as

$$\check{\boldsymbol{R}}_n^{1,\eta,u,p}(z) = \frac{1}{2A_v^0}\,\mathbf{K}^1\,\widetilde{\mathbf{E}}_n^1(z)\left(\mathbf{P}^{*,n}\,\nabla Z_1^{0,n}\right), \qquad \check{\boldsymbol{R}}_n^{1,\eta,w,p}(z) = -\frac{1}{2A_v^0}\,\mathscr{I}_2^n\,\widehat{\mathbf{E}}_n^1(z)\,\boldsymbol{H}_n^1.$$

The solution matrices can be decomposed into their respective solution submatrices $\mathbf{E}_n^{1,1}(z)$ and $\mathbf{E}_n^{1,2}(z)$ as

$$\widetilde{\mathbf{E}}_n^1(z) = \begin{bmatrix} \widetilde{\mathbf{E}}_n^{1,1}(z)\,\tilde{\mathbf{G}}_n^{1,1} \\ \widetilde{\mathbf{E}}_n^{1,2}(z)\,\tilde{\mathbf{G}}_n^{1,2} \end{bmatrix}, \qquad \widehat{\mathbf{E}}_n^1(z) = \begin{bmatrix} \widehat{\mathbf{E}}_n^{1,1}(z) & \hat{\mathbf{G}}_n^{1,2}\,\widehat{\mathbf{E}}_n^{1,2}(z) \end{bmatrix}.$$

The solution submatrices in turn depend on the 2×2 solution submatrices:

$$\widetilde{\mathbf{E}}_n^{1,1}(z) = \begin{bmatrix} \widetilde{\mathbf{E}}_n^{1,1,1}(z) & \widetilde{\mathbf{E}}_n^{1,1,2}(z) \end{bmatrix}, \qquad \widehat{\mathbf{E}}_n^{1,1}(z) = \widehat{\mathbf{E}}_n^{1,1,1}(z) + \widehat{\mathbf{E}}_n^{1,1,2}(z),$$

$$\widetilde{\mathbf{E}}_n^{1,2}(z) = \begin{bmatrix} \widetilde{\mathbf{E}}_n^{1,2,1}(z) & \widetilde{\mathbf{E}}_n^{1,2,2}(z) \end{bmatrix}, \qquad \widehat{\mathbf{E}}_n^{1,2}(z) = \begin{bmatrix} \widehat{\mathbf{E}}_n^{1,2,1}(z) \\ \widehat{\mathbf{E}}_n^{1,2,2}(z) \end{bmatrix}.$$

The entries of the 2×2 solution submatrices are given by the inner product between the coefficient vectors $\boldsymbol{T}^{1,1,j}$, $\boldsymbol{\Gamma}_\ell^1\,\boldsymbol{\phi}_x^0$ and the explicit z-dependent solution vectors $\boldsymbol{S}_n^1(z)$:

$$\begin{aligned} \widetilde{\mathrm{E}}_{n,ii}^{1,1,j}(z) &= \check{\gamma}_{n,i}^{0,j}\,\widetilde{\boldsymbol{T}}_{n,i}^{1,1,j}\,\widetilde{\boldsymbol{S}}_{n,i}^{1,1,j}(z), & \widehat{\mathrm{E}}_{n,ii}^{1,1,j}(z) &= \check{\gamma}_{n,i}^{0,j}\,\widehat{\boldsymbol{T}}^{1,1,j}\,\widehat{\boldsymbol{S}}_{n,i}^{1,1,j}(z), \\ \widetilde{\mathrm{E}}_{n,k\ell}^{1,2,j}(z) &= \check{\gamma}_{n,\ell,k}^{0}\,\widetilde{\boldsymbol{S}}_{n,\ell,k}^{1,2}(z)\,\widetilde{\boldsymbol{\Gamma}}_{n,\ell,k}^{1}\,\boldsymbol{\phi}_{x_j}^0, & \widehat{\mathrm{E}}_{n,k\ell}^{1,2,j}(z) &= (-1)^{\delta_{k\ell 2}}\,\check{\gamma}_{n,j}^{0,\ell}\,\widehat{\boldsymbol{S}}_{n,\ell}^{1,2,j}(z)\,\widehat{\boldsymbol{\Gamma}}_\ell^1\,\boldsymbol{\phi}_{x_k}^0. \end{aligned}$$

Here, we have set the off-diagonal terms in the 2×2 solution submatrices $\mathbf{E}_n^{1,1,j}(z)$ to zero. The structure of these particular solutions is based on the structure of the z-dependent advective forcing mechanisms.

B.11.4 The homogenous solution

We have constructed particular solutions for U and W. Hence, the particular solutions are known. A particular solution does, in general, not satisfy the boundary conditions. For this purpose the homogenous solution is used. The degrees of freedom of the homogenous conditions are chosen such that the sum of the particular solution and the homogenous solution satisfy the imposed boundary conditions.

For $n = 0, 2$ and $v = u, w$, the homogenous solution satisfies the homogeneous differential equation

$$\check{\boldsymbol{R}}_{n,zz}^{1,\eta,v,h}(z) - \left(\boldsymbol{\alpha}_n^0\right)^2\check{\boldsymbol{R}}_n^{1,\eta,v,h}(z) = \mathbf{0},$$

with inhomogeneous boundary conditions

$$\begin{aligned} A_v^0\,\check{\boldsymbol{R}}_{n,z}^{1,\eta,v,h}(z) &= -\boldsymbol{g}_n^{1,v}, && \text{at} \quad z = R, \\ A_v^0\,\check{\boldsymbol{R}}_{n,z}^{1,\eta,v,h}(z) - s_f^0\,\check{\boldsymbol{R}}_n^{1,\eta,v,h}(z) &= -\boldsymbol{g}_n^{2,v}, && \text{at} \quad z = -H. \end{aligned}$$

Here, we have defined

$$\boldsymbol{g}_n^{1,v} = A_v^0\,\check{\boldsymbol{R}}_{n,z}^{1,\eta,v,p}(z)\Big|_{z=R}, \qquad \boldsymbol{g}_n^{2,v} = \left(A_v^0\,\check{\boldsymbol{R}}_{n,z}^{1,\eta,v,p}(z) - s_f^0\,\check{\boldsymbol{R}}_n^{1,\eta,v,p}(z)\right)\Big|_{z=-H}.$$

These boundary conditions show that the vertical derivative of the particular solutions of the rotating flow variables must be calculated. These particular solutions can, through the transformation matrices (see the previous section), be expressed in terms of the explicit z-dependent solution vectors $\boldsymbol{S}_n^1(z)$. Thus the vertical derivative of the particular solution translates into the vertical derivative of the explicit z-dependent solution vectors. The vertical derivative of the explicit z-dependent solution vectors $\boldsymbol{S}_n^1(z)$ are included at the end of the advective derivation.

Construction of the homogenous solutions The homogeneous solution is forced at the free surface and at the bed. The homogenous solution can be written as

$$\check{\boldsymbol{R}}_n^{1,\eta,\nu,h}(z) = \mathbf{c}_n^{0,\chi}(z)\,\boldsymbol{g}_n^{1,\nu} - \mathbf{c}_n^{0,\mu}(z)\,\boldsymbol{g}_n^{2,\nu}.$$

B.11.5 The total advective solution

The total forcing advective solution consists of two parts

$$\check{\boldsymbol{R}}_n^{1,\eta}(z) = \check{\boldsymbol{R}}_n^{1,\eta,u}(z) + \check{\boldsymbol{R}}_n^{1,\eta,w}(z),$$

with

$$\check{\boldsymbol{R}}_n^{1,\eta,u}(z) = \check{\boldsymbol{R}}_n^{1,\eta,u,p}(z) + \check{\boldsymbol{R}}_n^{1,\eta,u,h}(z), \qquad \check{\boldsymbol{R}}_n^{1,\eta,w}(z) = \check{\boldsymbol{R}}_n^{1,\eta,w,p}(z) + \check{\boldsymbol{R}}_n^{1,\eta,w,h}(z).$$

We depth-integrate the forcing advective solution to obtain the depth-integrated forcing rotating flow variables of the advective forcing:

$$\check{\boldsymbol{\mathcal{R}}}_n^{1,\eta}(z) = \int_{-H}^{z} \check{\boldsymbol{R}}_n^{1,\eta}(\tilde{z})\,d\tilde{z}.$$

The homogeneous solution has already been integrated over the depth and is not considered here. The particular solution, on the other hand, has not. Similar to the vertical derivative of the particular solution, the explicit z-dependent solution vectors $\boldsymbol{S}_n^1(z)$ must be integrated over the depth when integrating the particular solutions. The integration over depth is included after the vertical derivate section.

Vertical derivatives The vertical derivative of the explicit z-dependent solution vectors is calculated here.

For $\widehat{\boldsymbol{S}}^{1,1,j}_{n,i}(z)$, we have

$$\widehat{\boldsymbol{S}}^{1,1,j}_{n,z,i}(z) = \begin{bmatrix} \delta^{0,n}_{r,i}\alpha^{0,n}_{1,ii}\cosh\big(\alpha^{0,n}_{1,ii}(z-R)\big) \\[1ex] \delta^{0,n}_{r,i}\Big[\alpha^{0,n}_{1,ii}\,z\cosh\big(\alpha^{0,n}_{1,ii}(z-R)\big)+\big\{1-2\delta^{0,n}_{r,i}\big(\alpha^{0,n}_{1,ii}\big)^2\big\}\sinh\big(\alpha^{0,n}_{1,ii}(z-R)\big)\Big] \\[1ex] \begin{aligned} \breve{\delta}^{0,j,n}_{r,i}\Big[& \big(\tilde{\delta}^{0,j,n}_{i}\alpha^{0,n}_{1,ii}+\hat{\delta}^{0,j,n}_{r,i}\alpha^{0}_{1,jj}\big)\sinh\big(\alpha^{0,n}_{1,ii}(z-R)\big)\cosh\big(\alpha^{0}_{1,jj}(z-R)\big) \\ & +\big(\hat{\delta}^{0,j,n}_{r,i}\alpha^{0,n}_{1,ii}+\tilde{\delta}^{0,j,n}_{i}\alpha^{0}_{1,jj}\big)\cosh\big(\alpha^{0,n}_{1,ii}(z-R)\big)\sinh\big(\alpha^{0}_{1,jj}(z-R)\big)\Big] \end{aligned} \end{bmatrix}.$$

The vertical derivative of $\widehat{\boldsymbol{S}}^{1,2,j}_{n,\ell}(z)$ is given by

$$\widehat{\boldsymbol{S}}^{1,2,j}_{n,z,\ell}(z) = \begin{bmatrix} \delta^{0,n}_{d,j}\alpha^{0,n}_{1,jj}\cosh\big(\alpha^{0,n}_{1,jj}(z-R)\big) \\[1ex] \delta^{0,n}_{d,j}\Big[\alpha^{0,n}_{1,jj}\,z\cosh\big(\alpha^{0,n}_{1,jj}(z-R)\big)+\big\{1-2\delta^{0,n}_{d,j}\big(\alpha^{0,n}_{1,jj}\big)^2\big\}\sinh\big(\alpha^{0,n}_{1,jj}(z-R)\big)\Big] \\[1ex] \begin{aligned} \breve{\delta}^{0,\ell,n}_{d,j}\Big[& \big(\tilde{\delta}^{0,\ell,n}_{j}\alpha^{0,n}_{1,jj}+\hat{\delta}^{0,\ell,n}_{d,j}\alpha^{0}_{1,\ell\ell}\big)\sinh\big(\alpha^{0,n}_{1,jj}(z-R)\big)\cosh\big(\alpha^{0}_{1,\ell\ell}(z-R)\big) \\ & +\big(\hat{\delta}^{0,\ell,n}_{d,j}\alpha^{0,n}_{1,jj}+\tilde{\delta}^{0,\ell,n}_{j}\alpha^{0}_{1,\ell\ell}\big)\cosh\big(\alpha^{0,n}_{1,jj}(z-R)\big)\sinh\big(\alpha^{0}_{1,\ell\ell}(z-R)\big)\Big] \end{aligned} \\[1ex] \begin{aligned} \breve{\delta}^{0,\ell,n}_{d,j}\Big[& \big(\tilde{\delta}^{0,\ell,n}_{j}\alpha^{0,n}_{1,jj}+\hat{\delta}^{0,\ell,n}_{d,j}\alpha^{0}_{1,\ell\ell}\big)\sinh\big(\alpha^{0,n}_{1,jj}(z-R)\big)\sinh\big(\alpha^{0}_{1,\ell\ell}(z-R)\big) \\ & +\big(\hat{\delta}^{0,\ell,n}_{d,j}\alpha^{0,n}_{1,jj}+\tilde{\delta}^{0,\ell,n}_{j}\alpha^{0}_{1,\ell\ell}\big)\cosh\big(\alpha^{0,n}_{1,jj}(z-R)\big)\cosh\big(\alpha^{0}_{1,\ell\ell}(z-R)\big)\Big] \end{aligned} \\[1ex] \begin{aligned} \breve{\delta}^{0,\ell,n}_{d,j}\Big\{ & \big(\tilde{\delta}^{0,\ell,n}_{j}\alpha^{0,n}_{1,jj}+\hat{\delta}^{0,\ell,n}_{d,j}\alpha^{0}_{1,\ell\ell}\big)\,z\sinh\big(\alpha^{0,n}_{1,jj}(z-R)\big)\sinh\big(\alpha^{0}_{1,\ell\ell}(z-R)\big) \\ & +\big(\hat{\delta}^{0,\ell,n}_{d,j}\alpha^{0,n}_{1,jj}+\tilde{\delta}^{0,\ell,n}_{j}\alpha^{0}_{1,\ell\ell}\big)\,z\cosh\big(\alpha^{0,n}_{1,jj}(z-R)\big)\cosh\big(\alpha^{0}_{1,\ell\ell}(z-R)\big) \\ & +\Big[\hat{\delta}^{0,\ell,n}_{d,j}+\breve{\delta}^{0,\ell,n}_{d,j}\big(\dot{\delta}^{0,\ell,n}_{d,j}\alpha^{0,n}_{1,jj}+\check{\delta}^{0,\ell,n}_{d,j}\alpha^{0}_{1,\ell\ell}\big)\Big]\sinh\big(\alpha^{0,n}_{1,jj}(z-R)\big)\cosh\big(\alpha^{0}_{1,\ell\ell}(z-R)\big) \\ & +\Big[\tilde{\delta}^{0,\ell,n}_{j}+\breve{\delta}^{0,\ell,n}_{d,j}\big(\check{\delta}^{0,\ell,n}_{d,j}\alpha^{0,n}_{1,jj}+\dot{\delta}^{0,\ell,n}_{d,j}\alpha^{0}_{1,\ell\ell}\big)\Big]\cosh\big(\alpha^{0,n}_{1,jj}(z-R)\big)\sinh\big(\alpha^{0}_{1,\ell\ell}(z-R)\big)\Big\} \end{aligned} \end{bmatrix}^{T}.$$

The last two vertical derivatives of $\widetilde{\boldsymbol{S}}^{1,1,j}_{n,i}(z)$ and $\widetilde{\boldsymbol{S}}^{1,2}_{n,\ell,k}(z)$ read, respectively

$$\widetilde{\boldsymbol{S}}^{1,1,j}_{n,z,i}(z) = \begin{bmatrix} 0 \\[1ex] \Delta^{0,n}_{i,i}\alpha^{0}_{1,ii}\sinh\big(\alpha^{0}_{1,ii}(z-R)\big) \\[1ex] \acute{\Delta}^{0,l,n}_{i}\alpha^{0,n}_{1,ll}\sinh\big(\alpha^{0,n}_{1,ll}(z-R)\big) \\[1ex] \begin{aligned} \check{\Delta}^{0,l,n}_{i,i}\Big[& \big(\hat{\Delta}^{0,l,n}_{i,i}\alpha^{0}_{1,ii}+\tilde{\Delta}^{0,l,n}_{i}\alpha^{0,n}_{1,ll}\big)\sinh\big(\alpha^{0}_{1,ii}(z-R)\big)\cosh\big(\alpha^{0,n}_{1,ll}(z-R)\big) \\ & +\big(\tilde{\Delta}^{0,l,n}_{i}\alpha^{0}_{1,ii}+\hat{\Delta}^{0,l,n}_{i,i}\alpha^{0,n}_{1,ll}\big)\cosh\big(\alpha^{0}_{1,ii}(z-R)\big)\sinh\big(\alpha^{0,n}_{1,ll}(z-R)\big)\Big] \end{aligned} \end{bmatrix},$$

and

$$
\widetilde{\mathbf{S}}^{1,2}_{n,k,\ell,z}(z) = \begin{bmatrix}
0 \\[1ex]
\Delta^{0,n}_{k,k}\alpha^{0}_{1,kk}\cosh\big(\alpha^{0}_{1,kk}(z-R)\big) \\[1ex]
\Delta^{0,n}_{k,k}\alpha^{0}_{1,kk}\sinh\big(\alpha^{0}_{1,kk}(z-R)\big) \\[1ex]
\acute{\Delta}^{0,\ell,n}_{k}\alpha^{0,n}_{1,\ell\ell}\sinh\big(\alpha^{0,n}_{1,\ell\ell}(z-R)\big) \\[1ex]
\Delta^{0,n}_{k,k}\Big[\alpha^{0}_{1,kk}\,z\cosh\big(\alpha^{0}_{1,kk}(z-R)\big)+\big\{1-2\Delta^{0,n}_{k,k}\big(\alpha^{0}_{1,kk}\big)^{2}\big\}\sinh\big(\alpha^{0}_{1,kk}(z-R)\big)\Big] \\[1ex]
\begin{aligned}
\breve{\Delta}^{0,\ell,n}_{k,k}\Big[\quad &\big(\hat{\Delta}^{0,\ell,n}_{k,k}\alpha^{0}_{1,kk}+\tilde{\Delta}^{0,\ell,n}_{k}\alpha^{0,n}_{1,\ell\ell}\big)\sinh\big(\alpha^{0}_{1,kk}(z-R)\big)\cosh\big(\alpha^{0,n}_{1,\ell\ell}(z-R)\big) \\
&+\big(\tilde{\Delta}^{0,\ell,n}_{k}\alpha^{0}_{1,kk}+\hat{\Delta}^{0,\ell,n}_{k,k}\alpha^{0,n}_{1,\ell\ell}\big)\cosh\big(\alpha^{0}_{1,kk}(z-R)\big)\sinh\big(\alpha^{0,n}_{1,\ell\ell}(z-R)\big)\Big]
\end{aligned} \\[1ex]
\begin{aligned}
\breve{\Delta}^{0,\ell,n}_{k,k}\Big[\quad &\big(\tilde{\Delta}^{0,\ell,n}_{k}\alpha^{0}_{1,kk}+\hat{\Delta}^{0,\ell,n}_{k,k}\alpha^{0,n}_{1,\ell\ell}\big)\sinh\big(\alpha^{0}_{1,kk}(z-R)\big)\sinh\big(\alpha^{0,n}_{1,\ell\ell}(z-R)\big) \\
&+\big(\hat{\Delta}^{0,\ell,n}_{k,k}\alpha^{0}_{1,kk}+\tilde{\Delta}^{0,\ell,n}_{k}\alpha^{0,n}_{1,\ell\ell}\big)\cosh\big(\alpha^{0}_{1,kk}(z-R)\big)\cosh\big(\alpha^{0,n}_{1,\ell\ell}(z-R)\big)\Big]
\end{aligned} \\[1ex]
\begin{aligned}
\breve{\Delta}^{0,\ell,n}_{k,k}\Big\{\quad &\big(\tilde{\Delta}^{0,\ell,n}_{k}\alpha^{0}_{1,kk}+\hat{\Delta}^{0,\ell,n}_{k,k}\alpha^{0,n}_{1,\ell\ell}\big)\,z\sinh\big(\alpha^{0}_{1,kk}(z-R)\big)\sinh\big(\alpha^{0,n}_{1,\ell\ell}(z-R)\big) \\
&+\big(\hat{\Delta}^{0,\ell,n}_{k,k}\alpha^{0}_{1,kk}+\tilde{\Delta}^{0,\ell,n}_{k}\alpha^{0,n}_{1,\ell\ell}\big)\,z\cosh\big(\alpha^{0}_{1,kk}(z-R)\big)\cosh\big(\alpha^{0,n}_{1,\ell\ell}(z-R)\big) \\
&+\Big[\hat{\Delta}^{0,\ell,n}_{k,k}+\breve{\Delta}^{0,\ell,n}_{k,k}\big(\dot{\Delta}^{0,\ell,n}_{k,k}\alpha^{0}_{1,kk}+\breve{\Delta}^{0,\ell,n}_{k,k}\alpha^{0,n}_{1,\ell\ell}\big)\Big]\sinh\big(\alpha^{0}_{1,kk}(z-R)\big)\cosh\big(\alpha^{0,n}_{1,\ell\ell}(z-R)\big) \\
&+\Big[\tilde{\Delta}^{0,\ell,n}_{k}+\breve{\Delta}^{0,\ell,n}_{k,k}\big(\breve{\Delta}^{0,\ell,n}_{k,k}\alpha^{0}_{1,kk}+\dot{\Delta}^{0,\ell,n}_{k,k}\alpha^{0,n}_{1,\ell\ell}\big)\Big]\cosh\big(\alpha^{0}_{1,kk}(z-R)\big)\sinh\big(\alpha^{0,n}_{1,\ell\ell}(z-R)\big)\Big\}
\end{aligned}
\end{bmatrix}^{T}.
$$

Integration over depth The explicit z-dependent solution vectors are integrated over depth.

We keep the usual basis consisting of the products of hyperbolic sine and cosine. However, it may be beneficial to first express the integrands as a sum of hyperbolic sines and cosines using the hyperbolic product-to-sum formulas, because a single hyperbolic sine or cosine is easier to integrate than their product.

For $\widehat{\mathbf{S}}^{1,1,j}_{n,i}(z)$, we obtain

$$\int_{-H}^{z} \widehat{\mathbf{S}}^{1,1,j}_{n,i}(\tilde{z})\,d\tilde{z} = \begin{bmatrix} \dfrac{\delta^{0,n}_{r,i}}{\alpha^{0,n}_{1,ii}}\Big[\cosh\big(\alpha^{0,n}_{1,ii}(z-R)\big) - \cosh\big(\alpha^{0,n}_{1,ii}D\big)\Big] \\ \delta^{0,n}_{r,i}\Big\{ \quad \big(\alpha^{0,n}_{1,ii}\big)^{-1}\Big[z\cosh\big(\alpha^{0,n}_{1,ii}(z-R)\big) + H\cosh\big(\alpha^{0,n}_{1,ii}D\big)\Big] \\ \qquad - \Big(2\delta^{0,n}_{r,i} + \big(\alpha^{0,n}_{1,ii}\big)^{-2}\Big)\Big[\sinh\big(\alpha^{0,n}_{1,ii}(z-R)\big) + \sinh\big(\alpha^{0,n}_{1,ii}D\big)\Big]\Big\} \\ \displaystyle\int_{-H}^{z} \widehat{S}^{1,1,j}_{n,3,i}(\tilde{z})\,d\tilde{z} \end{bmatrix},$$

where we have defined

$$\begin{aligned} &\int_{-H}^{z} \widehat{S}^{1,1,j}_{n,3,i}(\tilde{z})\,d\tilde{z} \\ &= \begin{cases} \frac{1}{4}\breve{\delta}^{0,j,n}_{r,i}\Big\{ \quad \big(\alpha^{0}_{1,jj}\big)^{-1}\big(\hat{\delta}^{0,j,n}_{r,i} + \tilde{\delta}^{0,j,n}_{i}\big)\Big[\sinh\big(2\alpha^{0}_{1,jj}(z-R)\big) + \sinh\big(2\alpha^{0}_{1,jj}D\big)\Big] & \text{if } n=2 \text{ and } i=j, \\ \qquad + 2\big(\tilde{\delta}^{0,j,n}_{i} - \hat{\delta}^{0,j,n}_{r,i}\big)(z+H)\Big\}, & \\ \breve{\delta}^{0,j,n}_{r,i}\grave{\delta}^{0,j,n}_{i}\Big\{ \quad \big(\tilde{\delta}^{0,j,n}_{i}\alpha^{0,n}_{1,ii} - \hat{\delta}^{0,j,n}_{r,i}\alpha^{0}_{1,jj}\big) & \\ \qquad \times\Big[\sinh\big(\alpha^{0,n}_{1,ii}(z-R)\big)\cosh\big(\alpha^{0}_{1,jj}(z-R)\big) + \sinh\big(\alpha^{0,n}_{1,ii}D\big)\cosh\big(\alpha^{0}_{1,jj}D\big)\Big] & \text{else.} \\ \qquad + \big(\hat{\delta}^{0,j,n}_{r,i}\alpha^{0,n}_{1,ii} - \tilde{\delta}^{0,j,n}_{i}\alpha^{0}_{1,jj}\big) & \\ \qquad \times\Big[\cosh\big(\alpha^{0,n}_{1,ii}(z-R)\big)\sinh\big(\alpha^{0}_{1,jj}(z-R)\big) + \cosh\big(\alpha^{0,n}_{1,ii}D\big)\sinh\big(\alpha^{0}_{1,jj}D\big)\Big]\Big\}, & \end{cases} \end{aligned}$$

The conditional statement has been derived from the condition that

$$\big(\alpha^{0,n}_{1,ii}\big)^2 = \big(\alpha^{0}_{1,jj}\big)^2,$$

and we have defined the coefficient

$$\grave{\delta}^{0,j,n}_{i} = \frac{1}{\big(\alpha^{0,n}_{1,ii}\big)^2 - \big(\alpha^{0}_{1,jj}\big)^2}.$$

We consider $\widehat{\mathbf{S}}^{1,2,j}_{n,\ell}(z)$. Integration over depth yields

$$\int_{-H}^{z} \widehat{\mathbf{S}}^{1,2,j}_{n,\ell}(\tilde{z})\,d\tilde{z} = \begin{bmatrix} \dfrac{\delta^{0,n}_{d,j}}{\alpha^{0,n}_{1,jj}}\Big[\cosh\big(\alpha^{0,n}_{1,jj}(z-R)\big) - \cosh\big(\alpha^{0,n}_{1,jj}D\big)\Big] \\ \delta^{0,n}_{d,j}\Big\{ \quad \big(\alpha^{0,n}_{1,jj}\big)^{-1}\Big[z\cosh\big(\alpha^{0,n}_{1,jj}(z-R)\big) + H\cosh\big(\alpha^{0,n}_{1,jj}D\big)\Big] \\ \qquad - \Big(2\delta^{0,n}_{d,j} + \big(\alpha^{0,n}_{1,jj}\big)^{-2}\Big)\Big[\sinh\big(\alpha^{0,n}_{1,jj}(z-R)\big) + \sinh\big(\alpha^{0,n}_{1,jj}D\big)\Big]\Big\} \\ \displaystyle\int_{-H}^{z} \widehat{S}^{1,2,j}_{n,3,\ell}(\tilde{z})\,d\tilde{z} \\ \displaystyle\int_{-H}^{z} \widehat{S}^{1,2,j}_{n,4,\ell}(\tilde{z})\,d\tilde{z} \\ \displaystyle\int_{-H}^{z} \widehat{S}^{1,2,j}_{n,5,\ell}(\tilde{z})\,d\tilde{z} \end{bmatrix}^{T}.$$

Here, we have defined

$$
\begin{aligned}
&\int_{-H}^{z} \widehat{S}^{1,2,j}_{n,3,\ell}(\tilde{z})\, d\tilde{z} \\
&= \begin{cases}
\begin{aligned}\frac{1}{4}\breve{\delta}^{0,\ell,n}_{d,j}\Big\{ & \big(\alpha^{0}_{1,\ell\ell}\big)^{-1}\big(\hat{\delta}^{0,\ell,n}_{d,j}+\tilde{\delta}^{0,\ell,n}_{j}\big)\Big[\sinh\big(2\alpha^{0}_{1,\ell\ell}(z-R)\big)+\sinh\big(2\alpha^{0}_{1,\ell\ell}D\big)\Big] \\
&+2\big(\tilde{\delta}^{0,\ell,n}_{j}-\hat{\delta}^{0,\ell,n}_{d,j}\big)(z+H)\Big\},\end{aligned} & \text{if } n=2 \text{ and } \ell=j, \\
\begin{aligned}\breve{\delta}^{0,\ell,n}_{d,j}\grave{\delta}^{0,\ell,n}_{j}\Big\{ & \big(\tilde{\delta}^{0,\ell,n}_{j}\alpha^{0,n}_{1,jj}-\hat{\delta}^{0,\ell,n}_{d,j}\alpha^{0}_{1,\ell\ell}\big) \\
&\times\Big[\sinh\big(\alpha^{0,n}_{1,jj}(z-R)\big)\cosh\big(\alpha^{0}_{1,\ell\ell}(z-R)\big)+\sinh\big(\alpha^{0,n}_{1,jj}D\big)\cosh\big(\alpha^{0}_{1,\ell\ell}D\big)\Big] \\
&+\big(\hat{\delta}^{0,\ell,n}_{d,j}\alpha^{0,n}_{1,jj}-\tilde{\delta}^{0,\ell,n}_{j}\alpha^{0}_{1,\ell\ell}\big) \\
&\times\Big[\cosh\big(\alpha^{0,n}_{1,jj}(z-R)\big)\sinh\big(\alpha^{0}_{1,\ell\ell}(z-R)\big)+\cosh\big(\alpha^{0,n}_{1,jj}D\big)\sinh\big(\alpha^{0}_{1,\ell\ell}D\big)\Big]\Big\},\end{aligned} & \text{else,}
\end{cases}
\end{aligned}
$$

and

$$
\begin{aligned}
&\int_{-H}^{z} \widehat{S}^{1,2,j}_{n,4,\ell}(\tilde{z})\, d\tilde{z} \\
&= \begin{cases}
\begin{aligned}\frac{1}{4}\breve{\delta}^{0,\ell,n}_{d,j}\big(\alpha^{0}_{1,\ell\ell}\big)^{-1}\Big\{ & \big(\hat{\delta}^{0,\ell,n}_{d,j}+\tilde{\delta}^{0,\ell,n}_{j}\big)\Big[\cosh\big(2\alpha^{0}_{1,\ell\ell}(z-R)\big)+\cosh\big(2\alpha^{0}_{1,\ell\ell}D\big)\Big] \\
&-2\big(\hat{\delta}^{0,\ell,n}_{d,j}+\tilde{\delta}^{0,\ell,n}_{j}\big)\cosh\big(2\alpha^{0}_{1,\ell\ell}D\big)\Big\},\end{aligned} & \text{if } n=2 \text{ and } \ell=j, \\
\begin{aligned}\breve{\delta}^{0,\ell,n}_{d,j}\grave{\delta}^{0,\ell,n}_{j}\Big\{ & \big(\tilde{\delta}^{0,\ell,n}_{j}\alpha^{0,n}_{1,jj}-\hat{\delta}^{0,\ell,n}_{d,j}\alpha^{0}_{1,\ell\ell}\big) \\
&\times\Big[\sinh\big(\alpha^{0,n}_{1,jj}(z-R)\big)\sinh\big(\alpha^{0}_{1,\ell\ell}(z-R)\big)-\sinh\big(\alpha^{0,n}_{1,jj}D\big)\sinh\big(\alpha^{0}_{1,\ell\ell}D\big)\Big] \\
&+\big(\hat{\delta}^{0,\ell,n}_{d,j}\alpha^{0,n}_{1,jj}-\tilde{\delta}^{0,\ell,n}_{j}\alpha^{0}_{1,\ell\ell}\big) \\
&\times\Big[\cosh\big(\alpha^{0,n}_{1,jj}(z-R)\big)\cosh\big(\alpha^{0}_{1,\ell\ell}(z-R)\big)-\cosh\big(\alpha^{0,n}_{1,jj}D\big)\cosh\big(\alpha^{0}_{1,\ell\ell}D\big)\Big]\Big\},\end{aligned} & \text{else,}
\end{cases}
\end{aligned}
$$

and

$$
\begin{aligned}
&\int_{-H}^{z} \widehat{S}^{1,2,j}_{n,5,\ell}(\tilde{z})\, d\tilde{z} \\
&= \begin{cases}
\begin{aligned}\frac{1}{8}\breve{\delta}^{0,\ell,n}_{d,j}\Big\{ & 2\big(\alpha^{0}_{1,\ell\ell}\big)^{-1}\big(\hat{\delta}^{0,\ell,n}_{d,j}+\tilde{\delta}^{0,\ell,n}_{j}\big)\Big[z\cosh\big(2\alpha^{0}_{1,\ell\ell}(z-R)\big)+H\cosh\big(2\alpha^{0}_{1,\ell\ell}D\big)\Big] \\
&+\big(\alpha^{0}_{1,\ell\ell}\big)^{-1}\Big[2\breve{\delta}^{0,\ell,n}_{d,j}\big(\breve{\delta}^{0,\ell,n}_{d,j}+\dot{\delta}^{0,\ell,n}_{d,j}\big)-\big(\alpha^{0}_{1,\ell\ell}\big)^{-1}\big(\hat{\delta}^{0,\ell,n}_{d,j}+\tilde{\delta}^{0,\ell,n}_{j}\big)\Big] \\
&\times\Big[\sinh\big(2\alpha^{0}_{1,\ell\ell}(z-R)\big)+\sinh\big(2\alpha^{0}_{1,\ell\ell}D\big)\Big] \\
&+4\breve{\delta}^{0,\ell,n}_{d,j}\big(\dot{\delta}^{0,\ell,n}_{d,j}-\breve{\delta}^{0,\ell,n}_{d,j}\big)(z+H)\Big\},\end{aligned} & \text{if } n=2 \text{ and } \ell=j, \\
\begin{aligned}\breve{\delta}^{0,\ell,n}_{d,j}\grave{\delta}^{0,\ell,n}_{j}\Big\{ & \big(\tilde{\delta}^{0,\ell,n}_{j}\alpha^{0,n}_{1,jj}-\hat{\delta}^{0,\ell,n}_{d,j}\alpha^{0}_{1,\ell\ell}\big) \\
&\times\Big[z\sinh\big(\alpha^{0,n}_{1,jj}(z-R)\big)\sinh\big(\alpha^{0}_{1,\ell\ell}(z-R)\big)+H\sinh\big(\alpha^{0,n}_{1,jj}D\big)\sinh\big(\alpha^{0}_{1,\ell\ell}D\big)\Big] \\
&+\big(\hat{\delta}^{0,\ell,n}_{d,j}\alpha^{0,n}_{1,jj}-\tilde{\delta}^{0,\ell,n}_{j}\alpha^{0}_{1,\ell\ell}\big) \\
&\times\Big[z\cosh\big(\alpha^{0,n}_{1,jj}(z-R)\big)\cosh\big(\alpha^{0}_{1,\ell\ell}(z-R)\big)+H\cosh\big(\alpha^{0,n}_{1,jj}D\big)\cosh\big(\alpha^{0}_{1,\ell\ell}D\big)\Big] \\
&+\hat{\kappa}^{0,\ell,n}_{d,j}\Big[\sinh\big(\alpha^{0,n}_{1,jj}(z-R)\big)\cosh\big(\alpha^{0}_{1,\ell\ell}(z-R)\big)+\sinh\big(\alpha^{0,n}_{1,jj}D\big)\cosh\big(\alpha^{0}_{1,\ell\ell}D\big)\Big] \\
&+\tilde{\kappa}^{0,\ell,n}_{d,j}\Big[\cosh\big(\alpha^{0,n}_{1,jj}(z-R)\big)\sinh\big(\alpha^{0}_{1,\ell\ell}(z-R)\big)+\cosh\big(\alpha^{0,n}_{1,jj}D\big)\sinh\big(\alpha^{0}_{1,\ell\ell}D\big)\Big]\Big\},\end{aligned} & \text{else.}
\end{cases}
\end{aligned}
$$

Here, we have defined

$$
\begin{aligned}
\hat{\kappa}^{0,\ell,n}_{d,j} &= \grave{\delta}^{0,\ell,n}_{j}\Big[2\tilde{\delta}^{0,\ell,n}_{j}\alpha^{0,n}_{1,jj}\alpha^{0}_{1,\ell\ell}-\hat{\delta}^{0,\ell,n}_{d,j}\Big(\big(\alpha^{0,n}_{1,jj}\big)^{2}+\big(\alpha^{0}_{1,\ell\ell}\big)^{2}\Big)\Big]+\breve{\delta}^{0,\ell,n}_{d,j}\big[\dot{\delta}^{0,\ell,n}_{d,j}\alpha^{0,n}_{1,jj}-\breve{\delta}^{0,\ell,n}_{d,j}\alpha^{0}_{1,\ell\ell}\big], \\
\tilde{\kappa}^{0,\ell,n}_{d,j} &= \grave{\delta}^{0,\ell,n}_{j}\Big[2\hat{\delta}^{0,\ell,n}_{d,j}\alpha^{0,n}_{1,jj}\alpha^{0}_{1,\ell\ell}-\tilde{\delta}^{0,\ell,n}_{j}\Big(\big(\alpha^{0,n}_{1,jj}\big)^{2}+\big(\alpha^{0}_{1,\ell\ell}\big)^{2}\Big)\Big]+\breve{\delta}^{0,\ell,n}_{d,j}\big[\breve{\delta}^{0,\ell,n}_{d,j}\alpha^{0,n}_{1,jj}-\dot{\delta}^{0,\ell,n}_{d,j}\alpha^{0}_{1,\ell\ell}\big],
\end{aligned}
$$

and the coefficient

$$\grave{\delta}_j^{0,\ell,n} = \frac{1}{\left(\alpha_{1,jj}^{0,n}\right)^2 - \left(\alpha_{1,\ell\ell}^{0}\right)^2}.$$

We consider the explicit z-dependent vectors related to U. For $\widetilde{\boldsymbol{S}}_{n,i}^{1,1,j}(z)$, the depth integral is given by

$$\int_{-H}^{z} \widetilde{\boldsymbol{S}}_{n,i}^{1,1,j}(\tilde{z})\,d\tilde{z} = \begin{bmatrix} \ddot{\Delta}_i^{0,n}(z+H) \\ \dfrac{\Delta_{i,i}^{0,n}}{\alpha_{1,ii}^{0}}\left[\sinh\!\left(\alpha_{1,ii}^{0}(z-R)\right) + \sinh\!\left(\alpha_{1,ii}^{0}D\right)\right] \\ \dfrac{\acute{\Delta}_i^{0,l,n}}{\alpha_{1,ll}^{0,n}}\left[\sinh\!\left(\alpha_{1,ll}^{0,n}(z-R)\right) + \sinh\!\left(\alpha_{1,ll}^{0,n}D\right)\right] \\ \displaystyle\int_{-H}^{z} \widetilde{S}_{n,3,i}^{1,1,j}(\tilde{z})\,d\tilde{z} \end{bmatrix},$$

where we have defined

$$\begin{aligned} &\int_{-H}^{z} \widetilde{S}_{n,3,i}^{1,1,j}(\tilde{z})\,d\tilde{z} \\ &= \begin{cases} \dfrac{1}{4}\breve{\Delta}_{i,i}^{0,l,n}\Big\{ \left(\alpha_{1,ii}^{0}\right)^{-1}\left(\tilde{\Delta}_i^{0,l,n} + \hat{\Delta}_{i,i}^{0,l,n}\right)\left[\sinh\!\left(2\alpha_{1,ii}^{0}(z-R)\right) + \sinh\!\left(2\alpha_{1,ii}^{0}D\right)\right] \\ \qquad + 2\left(\hat{\Delta}_{i,i}^{0,l,n} - \tilde{\Delta}_i^{0,l,n}\right)(z+H)\Big\}, & \text{if } n=2 \text{ and } i=l, \\ \breve{\Delta}_{i,i}^{0,l,n}\grave{\Delta}_i^{0,l,n}\Big\{ \left(\hat{\Delta}_{i,i}^{0,l,n}\alpha_{1,ii}^{0} - \tilde{\Delta}_i^{0,l,n}\alpha_{1,ll}^{0,n}\right) \\ \qquad \times\left[\sinh\!\left(\alpha_{1,ii}^{0}(z-R)\right)\cosh\!\left(\alpha_{1,ll}^{0,n}(z-R)\right) + \sinh\!\left(\alpha_{1,ii}^{0}D\right)\cosh\!\left(\alpha_{1,ll}^{0,n}D\right)\right] \\ \qquad + \left(\tilde{\Delta}_i^{0,l,n}\alpha_{1,ii}^{0} - \hat{\Delta}_{i,i}^{0,l,n}\alpha_{1,ll}^{0,n}\right) & \text{else,} \\ \qquad \times\left[\cosh\!\left(\alpha_{1,ii}^{0}(z-R)\right)\sinh\!\left(\alpha_{1,ll}^{0,n}(z-R)\right) + \cosh\!\left(\alpha_{1,ii}^{0}D\right)\sinh\!\left(\alpha_{1,ll}^{0,n}D\right)\right]\Big\}, \end{cases} \end{aligned}$$

with

$$\grave{\Delta}_i^{0,l,n} = \frac{1}{\left(\alpha_{1,ii}^{0}\right)^2 - \left(\alpha_{1,ll}^{0,n}\right)^2}.$$

Lastly, the explicit z-dependent solution vector $\widetilde{\boldsymbol{S}}_{n,\ell,k}^{1,2}(z)$ is depth integrated:

$$\int_{-H}^{z} \widetilde{\boldsymbol{S}}_{n,\ell,k}^{1,2}(\tilde{z})\,d\tilde{z} = \begin{bmatrix} \ddot{\Delta}_k^{0,n}(z+H) \\ \dfrac{\Delta_{k,k}^{0,n}}{\alpha_{1,kk}^{0}}\left[\cosh\!\left(\alpha_{1,kk}^{0}(z-R)\right) - \cosh\!\left(\alpha_{1,kk}^{0}D\right)\right] \\ \dfrac{\Delta_{k,k}^{0,n}}{\alpha_{1,kk}^{0}}\left[\sinh\!\left(\alpha_{1,kk}^{0}(z-R)\right) + \sinh\!\left(\alpha_{1,kk}^{0}D\right)\right] \\ \dfrac{\acute{\Delta}_k^{0,\ell,n}}{\alpha_{1,\ell\ell}^{0,n}}\left[\sinh\!\left(\alpha_{1,\ell\ell}^{0,n}(z-R)\right) + \sinh\!\left(\alpha_{1,\ell\ell}^{0,n}D\right)\right] \\ \Delta_{k,k}^{0,n}\Big\{ \left(\alpha_{1,kk}^{0}\right)^{-1}\left[z\cosh\!\left(\alpha_{1,kk}^{0}(z-R)\right) + H\cosh\!\left(\alpha_{1,kk}^{0}D\right)\right] \\ \quad - \left(2\Delta_{k,k}^{0,n} + \left(\alpha_{1,kk}^{0}\right)^{-2}\right)\left[\sinh\!\left(\alpha_{1,kk}^{0}(z-R)\right) + \sinh\!\left(\alpha_{1,kk}^{0}D\right)\right]\Big\} \\ \displaystyle\int_{-H}^{z} \widetilde{S}_{n,k,\ell,6}^{1,2}(\tilde{z})\,d\tilde{z} \\ \displaystyle\int_{-H}^{z} \widetilde{S}_{n,k,\ell,7}^{1,2}(\tilde{z})\,d\tilde{z} \\ \displaystyle\int_{-H}^{z} \widetilde{S}_{n,k,\ell,8}^{1,2}(\tilde{z})\,d\tilde{z} \end{bmatrix}^T.$$

Here, we have defined

$$
\begin{aligned}
&\int_{-H}^{z} \widetilde{S}^{1,2}_{n,k,\ell,6}(\tilde{z})\, d\tilde{z} \\
&= \begin{cases}
\begin{aligned}
\frac{1}{4}\check{\Delta}^{0,\ell,n}_{k,k}\Big\{ & \left(\alpha^{0}_{1,kk}\right)^{-1}\left(\tilde{\Delta}^{0,\ell,n}_{k} + \hat{\Delta}^{0,\ell,n}_{k,k}\right)\Big[\sinh\!\big(2\alpha^{0}_{1,kk}(z-R)\big) + \sinh\!\big(2\alpha^{0}_{1,kk}D\big)\Big] \\
& + 2\left(\hat{\Delta}^{0,\ell,n}_{k,k} - \tilde{\Delta}^{0,\ell,n}_{k}\right)(z+H)\Big\},
\end{aligned} & \text{if } n=2 \text{ and } \ell = k, \\[2ex]
\begin{aligned}
\check{\Delta}^{0,\ell,n}_{k,k}\grave{\Delta}^{0,\ell,n}_{k}\Big\{ & \left(\hat{\Delta}^{0,\ell,n}_{k,k}\alpha^{0}_{1,kk} - \tilde{\Delta}^{0,\ell,n}_{k}\alpha^{0,n}_{1,\ell\ell}\right) \\
& \times \Big[\sinh\!\big(\alpha^{0}_{1,kk}(z-R)\big)\cosh\!\big(\alpha^{0,n}_{1,\ell\ell}(z-R)\big) + \sinh\!\big(\alpha^{0}_{1,kk}D\big)\cosh\!\big(\alpha^{0,n}_{1,\ell\ell}D\big)\Big] \\
& + \left(\tilde{\Delta}^{0,\ell,n}_{k}\alpha^{0}_{1,kk} - \hat{\Delta}^{0,\ell,n}_{k,k}\alpha^{0,n}_{1,\ell\ell}\right) \\
& \times \Big[\cosh\!\big(\alpha^{0}_{1,kk}(z-R)\big)\sinh\!\big(\alpha^{0,n}_{1,\ell\ell}(z-R)\big) + \cosh\!\big(\alpha^{0}_{1,kk}D\big)\sinh\!\big(\alpha^{0,n}_{1,\ell\ell}D\big)\Big]\Big\},
\end{aligned} & \text{else,}
\end{cases}
\end{aligned}
$$

and

$$
\begin{aligned}
&\int_{-H}^{z} \widetilde{S}^{1,2}_{n,k,\ell,7}(\tilde{z})\, d\tilde{z} \\
&= \begin{cases}
\begin{aligned}
\frac{1}{4}\check{\Delta}^{0,\ell,n}_{k,k}\left(\alpha^{0}_{1,kk}\right)^{-1}\Big\{ & \left(\hat{\Delta}^{0,\ell,n}_{k,k} + \tilde{\Delta}^{0,\ell,n}_{k}\right)\Big[\cosh\!\big(2\alpha^{0}_{1,kk}(z-R)\big) + \cosh\!\big(2\alpha^{0}_{1,kk}D\big)\Big] \\
& - 2\left(\hat{\Delta}^{0,\ell,n}_{k,k} + \tilde{\Delta}^{0,\ell,n}_{k}\right)\cosh\!\big(2\alpha^{0}_{1,kk}D\big)\Big\},
\end{aligned} & \text{if } n=2 \text{ and } \ell = k, \\[2ex]
\begin{aligned}
\check{\Delta}^{0,\ell,n}_{k,k}\grave{\Delta}^{0,\ell,n}_{k}\Big\{ & \left(\tilde{\Delta}^{0,\ell,n}_{k}\alpha^{0}_{1,kk} - \hat{\Delta}^{0,\ell,n}_{k,k}\alpha^{0,n}_{1,\ell\ell}\right) \\
& \times \Big[\sinh\!\big(\alpha^{0}_{1,kk}(z-R)\big)\sinh\!\big(\alpha^{0,n}_{1,\ell\ell}(z-R)\big) - \sinh\!\big(\alpha^{0}_{1,kk}D\big)\sinh\!\big(\alpha^{0,n}_{1,\ell\ell}D\big)\Big] \\
& + \left(\hat{\Delta}^{0,\ell,n}_{k,k}\alpha^{0}_{1,kk} - \tilde{\Delta}^{0,\ell,n}_{k}\alpha^{0,n}_{1,\ell\ell}\right) \\
& \times \Big[\cosh\!\big(\alpha^{0}_{1,kk}(z-R)\big)\cosh\!\big(\alpha^{0,n}_{1,\ell\ell}(z-R)\big) - \cosh\!\big(\alpha^{0}_{1,kk}D\big)\cosh\!\big(\alpha^{0,n}_{1,\ell\ell}D\big)\Big]\Big\},
\end{aligned} & \text{else,}
\end{cases}
\end{aligned}
$$

and

$$
\begin{aligned}
&\int_{-H}^{z} \widetilde{S}^{1,2}_{n,k,\ell,8}(\tilde{z})\, d\tilde{z} \\
&= \begin{cases}
\begin{aligned}
\frac{1}{8}\check{\Delta}^{0,\ell,n}_{k,k}\Big\{ & 2\left(\alpha^{0}_{1,kk}\right)^{-1}\left(\hat{\Delta}^{0,\ell,n}_{k,k} + \tilde{\Delta}^{0,\ell,n}_{k}\right)\Big[z\cosh\!\big(2\alpha^{0}_{1,kk}(z-R)\big) + H\cosh\!\big(2\alpha^{0}_{1,kk}D\big)\Big] \\
& + \left(\alpha^{0}_{1,kk}\right)^{-1}\Big[2\check{\Delta}^{0,\ell,n}_{k,k}\left(\check{\Delta}^{0,\ell,n}_{k,k} + \dot{\Delta}^{0,\ell,n}_{k,k}\right) - \left(\alpha^{0}_{1,kk}\right)^{-1}\left(\hat{\Delta}^{0,\ell,n}_{k,k} + \tilde{\Delta}^{0,\ell,n}_{k}\right)\Big] \\
& \times \Big[\sinh\!\big(2\alpha^{0}_{1,kk}(z-R)\big) + \sinh\!\big(2\alpha^{0}_{1,kk}D\big)\Big] \\
& + 4\check{\Delta}^{0,\ell,n}_{k,k}\left(\dot{\Delta}^{0,\ell,n}_{k,k} - \check{\Delta}^{0,\ell,n}_{k,k}\right)(z+H)\Big\},
\end{aligned} & \text{if } n=2 \text{ and } \ell = k, \\[2ex]
\begin{aligned}
\check{\Delta}^{0,\ell,n}_{k,k}\grave{\Delta}^{0,\ell,n}_{k}\Big\{ & \left(\tilde{\Delta}^{0,\ell,n}_{k}\alpha^{0}_{1,kk} - \hat{\Delta}^{0,\ell,n}_{k,k}\alpha^{0,n}_{1,\ell\ell}\right) \\
& \times \Big[z\sinh\!\big(\alpha^{0}_{1,kk}(z-R)\big)\sinh\!\big(\alpha^{0,n}_{1,\ell\ell}(z-R)\big) + H\sinh\!\big(\alpha^{0}_{1,kk}D\big)\sinh\!\big(\alpha^{0,n}_{1,\ell\ell}D\big)\Big] \\
& + \left(\hat{\Delta}^{0,\ell,n}_{k,k}\alpha^{0}_{1,kk} - \tilde{\Delta}^{0,\ell,n}_{k}\alpha^{0,n}_{1,\ell\ell}\right) \\
& \times \Big[z\cosh\!\big(\alpha^{0}_{1,kk}(z-R)\big)\cosh\!\big(\alpha^{0,n}_{1,\ell\ell}(z-R)\big) + H\cosh\!\big(\alpha^{0}_{1,kk}D\big)\cosh\!\big(\alpha^{0,n}_{1,\ell\ell}D\big)\Big] \\
& + \dot{\kappa}^{0,\ell,n}_{k,k}\Big[\sinh\!\big(\alpha^{0}_{1,kk}(z-R)\big)\cosh\!\big(\alpha^{0,n}_{1,\ell\ell}(z-R)\big) + \sinh\!\big(\alpha^{0}_{1,kk}D\big)\cosh\!\big(\alpha^{0,n}_{1,\ell\ell}D\big)\Big] \\
& + \check{\kappa}^{0,\ell,n}_{k,k}\Big[\cosh\!\big(\alpha^{0}_{1,kk}(z-R)\big)\sinh\!\big(\alpha^{0,n}_{1,\ell\ell}(z-R)\big) + \cosh\!\big(\alpha^{0}_{1,kk}D\big)\sinh\!\big(\alpha^{0,n}_{1,\ell\ell}D\big)\Big]\Big\},
\end{aligned} & \text{else.}
\end{cases}
\end{aligned}
$$

Here, we have defined

$$
\begin{aligned}
\dot{\kappa}^{0,\ell,n}_{k,k} &= \grave{\Delta}^{0,\ell,n}_{k}\Big[2\tilde{\Delta}^{0,\ell,n}_{k}\alpha^{0}_{1,kk}\alpha^{0,n}_{1,\ell\ell} - \hat{\Delta}^{0,\ell,n}_{k,k}\Big(\left(\alpha^{0}_{1,kk}\right)^{2} + \left(\alpha^{0,n}_{1,\ell\ell}\right)^{2}\Big)\Big] + \check{\Delta}^{0,\ell,n}_{k,k}\left[\dot{\Delta}^{0,\ell,n}_{k,k}\alpha^{0}_{1,kk} - \check{\Delta}^{0,\ell,n}_{k,k}\alpha^{0,n}_{1,\ell\ell}\right], \\
\check{\kappa}^{0,\ell,n}_{k,k} &= \grave{\Delta}^{0,\ell,n}_{k}\Big[2\hat{\Delta}^{0,\ell,n}_{k,k}\alpha^{0}_{1,kk}\alpha^{0,n}_{1,\ell\ell} - \tilde{\Delta}^{0,\ell,n}_{k}\Big(\left(\alpha^{0}_{1,kk}\right)^{2} + \left(\alpha^{0,n}_{1,\ell\ell}\right)^{2}\Big)\Big] + \check{\Delta}^{0,\ell,n}_{k,k}\left[\check{\Delta}^{0,\ell,n}_{k,k}\alpha^{0}_{1,kk} - \dot{\Delta}^{0,\ell,n}_{k,k}\alpha^{0,n}_{1,\ell\ell}\right],
\end{aligned}
$$

and the coefficient

$$
\grave{\Delta}^{0,\ell,n}_{k} = \frac{1}{\left(\alpha^{0}_{1,kk}\right)^{2} - \left(\alpha^{0,n}_{1,\ell\ell}\right)^{2}}.
$$

Bibliography

G. K. Batchelor. *An introduction to fluid dynamics*. Cambridge University Press, Cambridge, 1967. ISBN O 521 66396 2.

R. L. Brouwer, G. P. Schramkowski, Y. M. Dijkstra, and H. M. Schuttelaars. Time Evolution of Estuarine Turbidity Maxima in Well-Mixed, Tidally Dominated Estuaries: The Role of Availability- and Erosion-Limited Conditions. *Journal of Physical Oceanography*, 48(8):1629–1650, 2018. doi:10.1175/JPO-D-17-0183.1.

H. Burchard. *Applied Turbulence Modelling in Marine Waters*. Springer-Verlag, Germany, 2002. ISBN 3-540-43795-9.

H. Burchard and H. Baumert. The formation of estuarine turbidity maxima due to density effects in the salt wedge. A hydrodynamic process study. *Journal of Physical Oceanography*, 28(2):309–321, 1998. doi:10.1175/1520-0485(1998)028<0309:TFOETM>2.0.CO;2.

B. Butman. *On the dynamics of shallow water currents in Massachusetts Bay and on the New England continental shelf*. PhD thesis, Massachusetts Institute of Technology, 1975.

P. Cheng, A. Valle-Levinson, and H. E. De Swart. Residual currents induced by asymmetric tidal mixing in weakly stratified narrow estuaries. *Journal of Physical Oceanography*, 40(9):2135–2147, 2010. doi:10.1175/2010JPO4314.1.

A. S. Chernetsky. *Trapping of sediment in tidal estuaries*. PhD thesis, TU Delft, 2012. URL `http://resolver.tudelft.nl/uuid:c4e993ce-75f5-4136-96c3-f0f902799fb0`.

B. Cushman-Roisin and J.-M. Beckers. *Introduction to Geophysical Fluid Dynamics: Physical and Numerical Aspects*. Academic Press, 2009. ISBN 9780120887590.

Y. Dijkstra. *Regime shifts in sediment concentrations in tide-dominated estuaries*. PhD thesis, Delft University of Technology, 2019.

Y. M. Dijkstra, H. M. Schuttelaars, and H. Burchard. Generation of exchange flows in estuaries by tidal and gravitational eddy viscosity-shear covariance (ESCO). *Journal of Geophysical Research: Oceans*, 122(5):4217–4237, may 2017. doi:10.1002/2016JC012379.

J. L. DiLorenzo. The overtide and filtering response of small inlet/bay systems. In D. G. Aubrey and L. Weishar, editors, *Hydrodynamics and Sediment Dynamics of Tidal Inlets, Coastal and Estuarine studies*, pages 22–53. Springer-Verlag, New York, 1988.

P. Dyke. *Coastal and shelf sea modelling*. Springer, 2001. ISBN 978-1-4419-5013-0. doi:10.1007/978-1-4757-4786-7.

E. Ensing, H. E. de Swart, and H. M. Schuttelaars. Sensitivity of tidal motion in well-mixed estuaries to cross-sectional shape, deepening, and sea level rise: An analytical study. *Ocean Dynamics*, 65(7):933–950, 2015. doi:10.1007/s10236-015-0844-8.

C. Friedrichs, B. Armbrust, and H. de Swart. Hydrodynamics and equilibrium sediment dynamics of shallow, funnel-shaped tidal estuaries. In J. Dronkers and M. Scheffers, editors, *Physics of Estuaries and Coastal Seas*, pages 315–328. Balkema, Rotterdam, 1998. ISBN 90 5410 965 3. URL `http://web.vims.edu/{~}cfried/cv/1998/Friedrichs{_}etal{_}1998{_}PECS{_}Volume.pdf`.

B. S. Gallagher and W. H. Munk. Tides in shallow water: Spectroscopy. *Tellus*, 23(4-5):346–363, 1971. doi:10.3402/tellusa.v23i4-5.10515.

A. E. Gill. *Atmosphere-ocean dynamics*. 1982.

P. Henrici. *Applied and computational complex analysis, Volume 3: Discrete Fourier analysis, Cauchy integrals, construction of conformal maps, univalent functions*. John Wiley & Sons, 1987.

E. Hinch. *Perturbation methods*. Cambridge University Press, 1991.

M. H. Holmes. *Introduction to Perturbation Methods*. Springer, 2nd edition, 2013. ISBN 978-1-4614-5476-2.

K. M. Huijts, H. M. Schuttelaars, H. E. de Swart, and A. Valle-Levinson. Lateral entrapment of sediment in tidal estuaries: An idealized model study. *Journal of Geophysical Research: Oceans*, 111(12):1–14, 2006. doi:10.1029/2006JC003615.

K. M. Huijts, H. E. De Swart, G. P. Schramkowski, and H. M. Schuttelaars. Transverse structure of tidal and residual flow and sediment concentration in estuaries: Sensitivity to tidal forcing and water depth. *Ocean Dynamics*, 61(8):1067–1091, 2011. doi:10.1007/s10236-011-0414-7.

J. P. Ianniello. Tidally induced residual currents in estuaries of constant breadth and depth. *Journal of Physical Oceanography*, 35(4):755–786, sep 1977.

J. P. Ianniello. Tidally Induced Residual Currents in Estuaries of Variable Breadth and Depth. *Journal of Physical Oceanography*, 9(5):962–974, sep 1979. doi:10.1175/1520-0485(1979)009<0962:TIRCIE>2.0.CO;2.

A. Kabbaj and C. Le Provost. Nonlinear tidal waves in channels. *Tellus*, 32(2):143–163, 1980. doi:10.3402/tellusa.v32i2.10490.

H. Kreiss. Some Remarks About Nonlinear Oscillations In Tidal Channels. *Tellus*, 9(1):53–68, 1957. doi:10.3402/tellusa.v9i1.9068.

K. Kreutz-Delgado. The Complex Gradient Operator and the CR-Calculus. 2009.

M. Kumar. *Three-Dimensional Model For Estuarine Turbidity Maxima In Tidally Dominated Estuaries*. PhD thesis, Delft University of Technology, 2018.

H. Lamb. *Hydrodynamics*. Cambridge University Press, London, 6th edition, 1932.

P. H. LeBlond and L. A. Mysak. *Waves in the Ocean*. Elsevier Science, 1978. ISBN 0-444-41926-8.

S. Lee, S.-K. Ryi, and H. Lim. Solutions of Navier-Stokes Equation with Coriolis Force. *Advances in Mathematical Physics*, 2017, 2017. doi:10.1155/2017/7042686.

W. H. Li. Well-Mixed Estuaries With Nonlinear Resistance. *Journal of Hydraulic Research*, 12(1):83–98, 1974. doi:10.1080/00221687409499759.

L. R. Maas and J. J. van Haren. Observations on the vertical structure of tidal and inertial currents in the central North Sea. *Journal of Marine Research*, 45(2):293–318, 1987. doi:10.1357/002224087788401106.

R. K. McCarthy. Residual currents in tidally dominated, well-mixed estuaries. *Tellus*, 45 A(4):325–340, 1993. doi:10.3402/tellusa.v45i4.14896.

H. O. Mofjeld. Effects of Vertical Viscosity on Kelvin Waves. *Journal of Physical Oceanography*, 10(7):1039–1050, 1980. doi:10.1175/1520-0485(1980)010<1039:eovvok>2.0.co;2.

A. B. Murray. Contrasting the goals, strategies, and predictions associated with simplified numerical models and detailed simulations. *Geophysical Monograph Series*, 135:151–165, 2003. doi:10.1029/135GM11.

J. Pedlosky. *Geophysical Fluid Dynamics*. R. R. Donnelley & Sons, 2nd edition, 1987. ISBN 0387963871.

D. T. Pugh. *Tides, surges and mean sea-level*. 1996.

M. P. Rozendaal. An Idealised Morphodynamic Model of a Tidal Inlet and the Adjacent Sea. Technical report, TU Delft, 2019. URL `http://resolver.tudelft.nl/uuid:edc2ffd6-00fd-4cd6-883b-13b14528cb72`.

G. P. Schramkowski and H. E. De Swart. Morphodynamic equilibrium in straight tidal channels: Combined effects of Coriolis force and external overtides. *Journal of Geophysical Research: Oceans*, 107(12), 2002. doi:10.1029/2000jc000693.

H. M. Schuttelaars. *Evolution and stability analysis of bottom patterns in a tidal embayment.* Phd dissertation, Utrecht University, 1997.

H. M. Schuttelaars and T. J. Zitman. Morphodynamic Modelling in Marine Environments: Model Formulation and Solution Techniques. In H. Schuttelaars, A. Heemink, and E. Deleersnijder, editors, *The Mathematics of Marine Modelling*, pages 243–285. Springer, Cham, 2022. ISBN 9783031095580. doi:10.1007/978-3-031-09559-7_10. URL `https://link.springer.com/10.1007/978-3-031-09559-7{_}10`.

S. Shetye and A. Gouviea. On the role of geometry of cross-section in generating flood-dominance in shallow estuaries. *Estuarine, Coastal and Shelf Science*, 35(2):113–126, aug 1992. doi:10.1016/S0272-7714(05)80107-6.

R. L. Soulsby. The bottom boundary layer of shelf seas. In B. Johns, editor, *Physical Oceanography of Coastal and Shelf Seas.* Elsevier, Amsterdam, 1983. ISBN 0-444-41623-4.

A. J. Souza and J. H. Simpson. The modification of tidal ellipses by stratification in the Rhine ROFI. *Continental Shelf Research*, 16(8):997–1007, 1996. doi:10.1016/0278-4343(95)00042-9.

R. W. Sternberg. Friction factors in tidal channels with differing bed roughness. *Marine Geology*, 6(3):243–260, 1968. doi:10.1016/0025-3227(68)90033-9.

H. U. Sverdrup. Dynamic of Tides on the North Siberian Shelf. *Geofysiske publikasjoner*, 4(5):2–75, 1926.

R. J. Uncles. A note on tidal asymmetry in the severn estuary. *Estuarine, Coastal and Shelf Science*, 13(4): 419–432, 1981. doi:10.1016/S0302-3524(81)80038-2.

A. W. Visser, A. J. Souza, K. Hessner, and J. H. Simpson. The effect of stratification on tidal current profiles in a region of freshwater influence. *Oceanologica Acta*, 17(4), 1994.

C. B. Vreugdenhil. *Numerical methods for shallow-water flow.* Kluwer Academic Publishers, Dordrecht, 1994. ISBN 978-90-481-4472-3. doi:10.1007/978-94-015-8354-1.

A. F. Waterhouse, A. Valle-Levinson, and C. D. Winant. Tides in a System of Connected Estuaries. *Journal of Physical Oceanography*, 41(5):946–959, 2011. doi:10.1175/2010JPO4504.1.

X. Wei. *A process-based, idealized study of salt and sediment dynamics in well-mixed estuaries.* PhD thesis, TU Delft, 2017.

S. Wiggins. *Introduction to Applied Nonlinear Dynamical Systems and Chaos.* Springer, New York, 2nd edition, 2003. ISBN 0387001778. doi:10.1007/b97481.

C. D. Winant. Three-dimensional tidal flow in an elongated, rotating basin. *Journal of Physical Oceanography*, 37(9):2345–2362, 2007. doi:10.1175/JPO3122.1.

C. D. Winant. Three-dimensional residual tidal circulation in an elongated, rotating basin. *Journal of Physical Oceanography*, 38(6):1278–1295, 2008. doi:10.1175/2007JPO3819.1.